



# **The role of MIF in melanoma progression**

**Camila Salum de Oliveira**

BSc in Biological Sciences and Master in Neuroscience

**Thesis submitted in fulfilment of the requirements for obtain the degree of Doctor  
of Philosophy in Medical Biochemistry**

**School of Biomedical Sciences and Pharmacy  
University of Newcastle**

**November 2012**

## Statement of Originality

The thesis contains no material which has been accepted for the award of any other degree or diploma in any university or other tertiary institution and, to the best of my knowledge and belief, contains no material previously published or written by another person, except where due reference has been made in the text. I give consent to this copy of my thesis, when deposited in the University Library, being made available for loan and photocopying subject to the provision of the Copyright Act 1968.

---

Camila Salum de Oliveira

## Acknowledgements

Firstly I would like to express my sincerest gratitude to my supervisor, Dr Rick Thorne, who has given me all the assistance I could have hoped for since the beginning of this journey. I cannot thank him enough for his guidance, patience and support in every possible aspect of this PhD experience. Without him this thesis would not have been completed. I would also like to thank my first co-supervisor, Prof Gordon Burns, whose knowledge and experience provided valuable advice and insight throughout the progress of this project. I am also very grateful to Dr Charles de Bock whose enthusiasm and energy has always created a vibrant and fun atmosphere to the lab. I also thank him for the patience teaching lab techniques and the invaluable help in reviewing the manuscript. I wish to acknowledge Prof Xu Dong Zhang for providing the cell lines and for offering his laboratory and advices for the intracellular signalling analysis that is part of this thesis.

Dr Tim Molloy from Garvan Institute (Sydney) was of essential help to perform the survival analysis and his collaboration was greatly appreciated. Thanks to Ms Xu Guang Yan for her invaluable assistance with the immunohistochemistry and immunofluorescence staining, up to the last minute, and for all the technical support in the lab. To all the other members of Cancer Research Unit, past and present, thanks for always being available to help whenever I needed, for sharing knowledge and some good laughs. To my office mates and office neighbours, thanks for the much needed pauses and distractions from work.

I am very grateful to my beloved partner, João, for always being by my side, for joining me in this adventure and for making it all much more fun. Finally, I want to express my gratitude to the loved ones back home. Thanks to my brothers and sisters, the blood ones and the chosen ones, for being so present even when physically distant. To my parents, who taught me the real values in life that made me who I am, thanks for being my foundation and my haven. A special thanks to my mum for always “looking after” me even when I was half a planet away from home. This thesis is dedicated to my dad, who passed away recently. I am proud of everything I learned from him and I would not have come so far if it wasn't for his enormous support. Words cannot describe my love and gratitude.

# Table of Contents

<b>ABSTRACT</b> .....	<b>XVI</b>
<b>CHAPTER 1</b> .....	<b>1</b>
1.1 MELANOMA .....	2
1.1.1 <i>Epidemiology</i> .....	2
1.1.2 <i>Etiology and Risk Factors</i> .....	5
1.1.3 <i>Pathology of Melanocytic Tumours</i> .....	7
1.1.4 <i>Staging and Prognosis</i> .....	9
1.1.5 <i>Treatment</i> .....	11
1.2 SIGNALLING NETWORKS IN MELANOMA .....	12
1.2.1 <i>BRAF and MAPK/ERK signalling pathway</i> .....	12
1.2.2 <i>PTEN and the Akt signalling pathway</i> .....	16
1.2.3 <i>NRAS mutations</i> .....	17
1.2.4 <i>Autocrine signalling</i> .....	20
1.3 MIF .....	21
1.3.1 <i>MIF in Melanoma</i> .....	22
1.3.2 <i>MIF signalling</i> .....	23
1.4 CD74 .....	23
1.5 CD44 .....	25
1.5.1 <i>CD44 in cancer</i> .....	27

1.5.2	<i>The dual nuclear signalling roles of CD44</i> .....	29
1.6	CHEMOKINE RECEPTORS AND MIF SIGNALLING .....	32
1.7	HYPOTHESIS AND AIMS .....	35
	<b>CHAPTER 2</b> .....	<b>37</b>
2.1	CELL CULTURE .....	38
2.1.1	<i>Cell lines and culture conditions</i> .....	38
2.1.2	<i>Cryostorage of cells</i> .....	39
2.1.3	<i>Revival of cells from liquid nitrogen storage</i> .....	39
2.1.4	<i>Cell culture in hypoxic conditions</i> .....	39
2.2	IMMUNOHISTOCHEMISTRY .....	40
2.3	<i>IN SILICO</i> ANALYSIS OF MICROARRAY DATASETS .....	40
2.4	WHOLE CELL PROTEIN EXTRACTION .....	41
2.5	BCA PROTEIN ASSAY .....	42
2.6	SDS-PAGE ELECTROPHORESIS .....	43
2.7	WESTERN BLOT ANALYSIS .....	44
2.8	QUANTIFICATION OF WESTERN BLOT USING DENSITOMETRY .....	46
2.9	FLOW CYTOMETRY .....	46
2.10	SMALL INTERFERING RNA (siRNA) KNOCKDOWN OF GENE EXPRESSION .....	47
2.11	ASSESSMENT OF CELL NUMBER AND VIABILITY .....	49
2.12	CLICK-IT™ EDU FLOW CYTOMETRY ASSAY .....	49
2.13	SOFT AGAR COLONY FORMATION ASSAY .....	50

2.14	CELL PROLIFERATION AND VIABILITY MEASUREMENTS USING MTS REDUCTION.....	51
2.15	SUB-CELLULAR FRACTIONATION TECHNIQUES.....	51
2.15.1	<i>Detergent lysis method</i> .....	51
2.15.2	<i>Nitrogen decompression method</i> .....	52
2.16	IMMUNOFLUORESCENCE MICROSCOPY .....	53
<b>CHAPTER 3.....</b>		<b>54</b>
3.1	INTRODUCTION .....	55
3.1.1	<i>MIF as a cancer biomarker</i> .....	55
3.1.2	<i>MIF and melanoma</i> .....	57
3.2	RESULTS.....	59
3.2.1	<i>MIF mRNA and protein expression in melanocytic tumours</i> .....	59
3.2.2	<i>MIF expression levels in melanoma metastases are prognostic for disease progression</i> .....	64
3.2.3	<i>Analysis of MIF receptor expression and association with disease-specific survival in melanoma clinical samples</i> .....	67
3.3	DISCUSSION.....	69
<b>CHAPTER 4.....</b>		<b>75</b>
4.1	INTRODUCTION .....	76
4.2	RESULTS.....	78
4.2.1	<i>Characterisation of MIF expression and MIF receptors in human melanoma cell lines</i>	78
4.2.2	<i>Small interfering RNA knockdown of MIF decreases melanoma cell proliferation and viability</i> .....	81

4.2.3	<i>MIF Knockdown reduces the number of cells entering S phase</i> .....	82
4.2.4	<i>MIF knockdown decreases anchorage-independent colony formation</i> .....	86
4.2.5	<i>MIF expression modulates Akt signalling pathway in melanoma cell lines</i> .....	88
4.2.6	<i>MIF expression is upregulated under hypoxic conditions in melanoma cell lines</i> .....	90
4.3	DISCUSSION .....	93
<b>CHAPTER 5</b> .....		<b>99</b>
5.1	INTRODUCTION .....	100
5.2	RESULTS.....	102
5.2.1	<i>The subcellular localisation of MIF in cultured melanoma cells</i> .....	102
5.2.2	<i>The cellular distribution of CD44 in cultured human melanoma cells</i> .....	104
5.2.3	<i>Characterization of CD44 sub-cellular localization in HT-29 and MCF10A cells</i> .....	106
5.2.4	<i>Characterisation of antibodies against the extracellular and intracellular domain of CD44 in Western blotting</i> .....	111
5.2.5	<i>Biochemical determination of the subcellular localization of CD44 using a detergent-based lysis method</i> .....	113
5.2.6	<i>Determination of CD44 sub-cellular localization using nitrogen decompression lysis and fractionation by differential centrifugation</i> .....	116
5.3	DISCUSSION .....	118
<b>CHAPTER 6</b> .....		<b>121</b>
6.1	GENERAL CONCLUSIONS.....	122
6.1.1	<i>Recent facts on melanoma</i> .....	122
6.1.2	<i>MIF expression in melanoma progression</i> .....	124

6.1.3	<i>The functional role of MIF in melanoma cell lines</i> .....	125
6.1.4	<i>CD44 translocation to the nucleus: a potential mechanism for delivering the MIF signal?</i> .....	127
6.2	FUTURE DIRECTIONS .....	129
	<b>APPENDIX 1</b> .....	<b>131</b>
	<b>APPENDIX 2</b> .....	<b>147</b>
	<b>APPENDIX 3</b> .....	<b>152</b>
	<b>REFERENCES</b> .....	<b>155</b>

# List of Figures

**Figure 1.1 – Melanoma incidence and mortality rates in Australia** –Melanoma incidence and mortality from 1982 to 2007. The rates were age-standardised to the Australian population as at 30 June 2001 and are expressed per 100,000 population (top panel). Melanoma incidence and mortality by age at diagnosis. The rates shown are age-specific rates (bottom panel). Adapted from “Cancer in Australia: an overview, 2010” (5). ..... 3

**Figure 1.2 – Melanoma progression model showing the five stages of melanoma progression.** Benign lesions originate within normal skin and include common acquired or congenital naevi [1] and dysplastic naevi [2]. Both are considered to be precursors of melanoma and can further progress to *in situ* melanoma, which grows laterally and remain largely confined to the epidermis. This stage is known as radial-growth phase (RGP) melanoma [3]. The next stage, vertical growth phase (VGP) [4], is characterised by the vertical growth of a new population of cells within the melanoma, which may invade the dermis and form expansive nodules. In the latter phase of progression metastatic melanoma [5] dissociates from the primary tumour, and colonises distant sites (Adapted from Chin, 2003 (7))...... 8

**Figure 1.3 – Schematic representation of the activation of MAPK/ERK signalling pathway in mammalian cells.** A simplified MAPK signalling module is illustrated here with the RAS-RAF-MEK-ERK pathway. Extracellular stimuli lead to activation of ERK pathway via consecutive phosphorylations initiated by RAS (HRAS, NRAS and KRAS) which phosphorylates the MKKK RAF (ARAF, BRAF and CRAF). RAF, in turn, phosphorylates MEK (MEK1 and MEK2), which then phosphorylates ERK MAPK (ERK1 and ERK2) leading to activation of transcription factors and regulation of several cellular processes (Modified from Chin 2003 (7)). ..... 15

**Figure 1.4 – Altered signalling pathways in melanoma.** Representative diagram showing the major molecular pathways involved in melanoma tumorigenesis, survival and senescence. NRAS pathway, in green, includes ERK and Akt pathways and is involved in melanoma proliferation, survival and progression. The CDKN2A locus encodes for tumour suppressors which are thought to contribute to senescence. The p53/Bcl-2 pathway regulates melanoma apoptosis and is modulated by many of the known oncogenic pathways (Adapted from Hocker *et al.*, 2008 (6))...... 19

**Figure 1.5 – CD44 Structure.** Graphic representative of CD44 molecule showing potential N- and O-linked sugar residues and CS (chondroitin sulfate side chains) incorporated into the

extracellular domain and serine phosphorylation sites in its intracellular domain (Modified from Martegani *et al.*, 1999 (1))...... 26

**Figure 1.6 – Model of the MIF-CD74-CD44 signalling complex.** MIF binds to its receptor CD74 with activation of downstream pathways occurring through CD44. MIF can activate both the MAPK/ERK and the PI3K/Akt pathways in immunological systems but the details of MIF-signalling are poorly defined in cancers (Modified from Shi *et al.*, 2006 (2))...... 28

**Figure 1.7 – CD44 proteolytic cleavage.** Extracellular region of CD44 is cleaved by ADAM10, ADAM17 and MMP14, which triggers the intramembranous cleavage by presenilin- $\gamma$ -secretase. These sequential cleavages result in the release of the soluble ectodomain of CD44 and the release of an intracellular domain (ICD) fragment, which has been shown to be involved in nuclear signalling (Adapted from Thorne *et al.*, 2004 (3)). ..... 31

**Figure 3.1 – MIF and MIF-signalling receptor expression in melanocytic lesions measured using microarray data.** Levels of *MIF* (A), *CXCR4* (B), *CD44* (C) and *CD74* (D) expression in the two normal skin tissue samples (NS1; NS2), benign naevi (BN1; BN2), atypical naevi (AN1; AN2), melanomas in situ (in situ1; in situ2), VGP melanomas (VGP1; VGP2), MGP melanomas (MGP1; MGP2), and the three MGP melanoma-positive lymph nodes (LN1; LN2; LN3) were obtained from the microarray dataset GSE4587 as described in Chapter 2. Insets show the distribution of expression in the same samples divided in (E) early- and (A) advanced-stage. MIF and CXCR4 expression were higher on the “advanced-stage” samples compared to the “early-stage” samples. Distribution of transcript levels are summarised as box plots (n=8 early stage; n=9 advanced stage. Mann-Whitney test \*\*p<0.01; \*p<0.05)...... 60

**Figure 3.2 – MIF immunohistochemistry staining in ex-vivo sections of different stages of melanocytic lesions.** Representative micrographs (40x magnification) showing examples of MIF positive staining as detailed in Table 3.1. Tissue sections representing: (A) benign naevus, (B) dysplastic naevus, (C) primary melanoma and (D) metastatic melanoma. Sections were prepared from archival paraffin embedded tissues and processed for antigen retrieval using Citrate buffer (0.05M, pH 6.0). Sections were incubated with anti-human MIF antibody with detection using Vectastain ABC and VIP substrate (purple colour). Slides were then counterstained with Methyl Green. .... 62

**Figure 3.3 – MIF expression and association with survival in primary and metastatic melanoma clinical samples using microarrays (GEO dataset GSE8401).** (A) *MIF* expression is ~30% higher in metastatic melanoma compared to primary melanoma samples from GEO dataset GSE8401. Values are mean + SEM (t-test, n=31 primary tumour n=52 metastatic melanoma. \*\*p<0.01) (B) Kaplan-Meier survival analysis showed no difference in disease-

specific survival between high *MIF* (dotted line, upper 50%) and low *MIF* (solid line) expression groups (hazard ratio = 1.091, 95% confidence interval 0.312-3.809;  $p = 0.8911$ ). (C) Kaplan-Meier survival analysis indicate that patients with metastatic melanoma expressing high *MIF* had significantly poorer outcome (hazard ratio = 2.946, 95% confidence interval 1.440-6.029;  $p = 0.0045$ ,  $n=52$ ) compared to those with low *MIF* expression. .... 65

**Figure 3.4 - Association between *MIF* expression and survival in melanoma clinical samples (GEO datasets GSE22153 and GSE22154).** (A) Kaplan-Meier survival curves were generated for patients with lymph node and subcutaneous melanoma metastases according to the level of *MIF* expression ( $p = 0.319$ ,  $n=57$ ). (B) Kaplan-Meier survival curves for melanoma patients with liver and lymph nodemetastases ( $p= 0.117$ ,  $n=20$ )..... 66

**Figure 3.5 – CD74, CD44 and CXCR4 expression and survival in primary and metastatic melanoma clinical samples using GEO dataset GSE8401.** Kaplan-Meier survival curves were generated based on association between the survival data of 52 patients with metastatic melanoma or 31 patients with primary melanoma and the level of CD74, CD44 and CXCR4 expression. No difference in disease-specific survival was measured between high and low expressors for any of the receptors analysed (A-C) for the cases of primary melanoma. Metastatic melanoma patients expressing high CD44 (dotted line, upper 50%) showed significantly poorer outcome ( $p = 0.025$ ) compared to the low CD44 expression patients (solid line) (E). Conversely, high expression CD74 and CXCR4 was associated with significantly better survival in metastatic disease ( $p = 0.002$  and  $0.005$ , respectively) (D and F). .... 68

**Figure 4.1– MIF and MIF receptor expression in the human melanoma cell line panel.** (A) Representative Western blots showing MIF (~12.5KDa), CD44 (~85-150KDa), CD74 (~34KDa) and GAPDH (~36Kda) immunoreactive bands for all cell lines used throughout this study. MIF receptor, CD74, was detected in 10 out of 20 cell lines, while the co-receptor CD44 was ubiquitously expressed. Receptor expression was confirmed by cell surface staining and flow cytometry analysis (B and C). Specific antibody staining (open histogram) is shown overlaid over staining using a control antibody (solid histogram). (B) Consistent with the Western blotting results, all the cell lines stained positively for CD44. (C) CD74 was present at the surface of 10 out of 20 cells analysed (6 representative cell lines are displayed for the flow cytometric analyses)..... 79

**Figure 4.2– Chemokine receptor expression in the human melanoma cell line panel.** CXCR4 and CXCR2 expression was assessed by cell surface staining and flow cytometry analysis. The cells were stained with specific antibodies compared to control antibodies (open histogram versus solid histogram respectively). (A) CXCR4 was present in all the cell lines

analysed while (B) CXCR2 expression was absent in all the 20 cell lines (6 representative cell lines shown for each analysis). ..... 80

**Figure 4.3 – Small interfering RNA (siRNA) knockdown of MIF decreases melanoma cell proliferation and viability.** The indicated melanoma cell lines were transfected with MIF siRNA (siMIF; 50nM), and the knockdown was confirmed by Western blotting against MIF (~12.5KDa) or GAPDH(~36KDa) as a loading control. As a transfection control, a scrambled siRNA was used at the same concentration (siNC). MIF protein expression was reduced 1 day after transfection, and the knockdown was sustained for 5 days in both (A) MelCV and (B) Me1007 cell lines. The cell number and viability were determined using an automated cell counter using the propidium iodide (PI) exclusion method. (C, D) The results for both MelCV and Me1007 showed a significant reduction in the cell number starting from day 3 after transfection (E, F) and the viability was also reduced in a time-dependent manner. Values are mean + SEM of 3 experiments performed in triplicate (t-test, n=3, compared to siNC transfected cells. \*\*\*\* p<0.0001; \*\*\* p<0.001; \*\*p<0.01; \*p<0.05) ..... 82

**Figure 4.4– Effects of MIF knockdown on the proportion of melanoma cells in S phase analysed using the Click-IT assay.** Cell proliferation was determined using Click-iT™ EdU flow cytometry assay as described in Section 2.11. Briefly, cells were transfected with MIF and NC siRNA and after 3 days, 10nM EdU was added to the media for 3h. Analysis of the samples was then conducted on a FACS Calibur flow cytometer. (A, B) Analysis of MelCV and Me1007 cells using the Click-iT™ assay allows accurate determination of the populations of cells entering S phase (box). The results show a clear reduction of number of cells in S phase after MIF knockdown for both MelCV and Me1007 cell lines. (C, D) The bar graphs show the percentage of cells in S phase after MIF knockdown. (E) The analysis was repeated for additional melanoma cell lines and MIF expression significantly reduced the number of cells entering S-phase for 4/6 cell lines. Values are means + SEM (t-test, n = 5, compared to siNC transfected cells. \*\*\* p<0.001 \*\*p<0.01 \*p<0.05). ..... 85

**Figure 4.5- MIF knockdown decreases anchorage-independent colony formation.** Three days after MIF knockdown, the indicated melanoma cells were harvested and seeded in plates within soft agar. Cells were allowed to grow and form colonies for 3-4 weeks. (A, B) Colonies were stained with Crystal Violet. Photos show a representative field from one of the wells at 5X magnification and the insets show the colonies in detail seen under 40X magnification. (C-F) Colonies from 10 different fields in were counted and 25 colonies measured for each experiment using the Axiovision software package. Analysis showed there was a significant reduction in colony numbers and size after MIF knockdown for both MelCV and Me1007. Values

are means + SEM of 3 experiments performed in triplicate (t-test, n = 3, compared to siNC transfected cells. \*\*\*\* p<0.0001) ..... 87

**Figure 4.6 - MIF expression modulates Akt signalling in melanoma cell lines.**

Representative Western blots showing specific immunoreactive bands for MIF, Akt and key cell cycle regulators in the 6 indicated melanoma cell lines. Cells were transfected with MIF and NC siRNA and after 3 days, cells were lysed and submitted to Western blotting. (A) Inhibition of MIF expression 3 days after knockdown was confirmed for all the cell lines analysed. The normalised ratio of expression comparing MIF to control NC knockdown was determined by dividing the optical density of the MIF specific band (~12.5KDa) by GAPDH(~36KDa) using the Multi Gauge software package, as described in Section 2.8. (B) Phosphorylation of Akt (Ser 473) was reduced with MIF knockdown in different levels across the cell lines. In this case, the ratio shows the optical density of the phospho-Akt (~60KDa) band divided by the total Akt (~60KDa). (C) Cell cycle regulators Cyclin D1 (~37KDa) and CDK4 (~34KDa) were also reduced after MIF knockdown in all cell lines, while the cyclin-dependent kinase inhibitor p27 (27KDa) was also increased in most cell lines. The ratio was determined by dividing the optical density of the specific band by that of GAPDH. The ratios shown are the means of 3 independent experiments..... 89

**Figure 4.7 - MIF is upregulated in melanoma cell lines under hypoxia.**

Representative Western blot showing MIF immunoreactive bands (~12.5KDa) for Me1007 and MeICV cell lines after 3 days under normoxia (N; atmospheric O<sub>2</sub> and 5% CO<sub>2</sub>) or hypoxia (H; 0.1% O<sub>2</sub> and 5% CO<sub>2</sub>). The bar graph reports the optical density (OD) values of MIF relative to GAPDH (~36KDa) with data normalised to control cells kept under normoxic conditions. Values are mean + SEM (t-test, n=3, compared to normoxia; \*p<0.05). ..... 91

**Figure 4.8 – Effects of MIF depletion on melanoma cell viability under conditions of hypoxia.**

(A) Representative Western blot showing MIF immunoreactive bands (~12.5KDa) and GAPDH (~36KDa) for Me1007 and MeICV cell lines 3 days after transfection with MIF or NC siRNA under normoxia (N) or hypoxia (H). (B) Cell viability measured by MTS reduction represented as percentage of cells transfected with NC siRNA under normoxia for each cell line. Values are mean + SEM (t-test, n=3, compared to normoxia; \*p<0.05 and \*\*p<0.01). ..... 92

**Figure 5.1 – Cellular distribution of MIF in human melanoma cell lines.**

The indicated cell lines were grown on glass coverslips, fixed, permeabilised and immunostained with MIF mAb antibody and a fluorescent secondary conjugate (Alexa488 anti-mouse IgG). The cells were imaged using epifluorescence microscopy. The left panels are standard immunofluorescence (IF) microphotographs whereas the middle and right panels are optical sections of cells showing MIF staining or the nuclear marker DAPI as indicated. Scale bar = 20µm ..... 103

**Figure 5.2– Cellular distribution of CD44 in human melanoma cell lines.** The indicated cell lines grown on glass coverslips were fixed, permeabilised and immunostained with CD44 mAb antibody (Hermes3) and a fluorescent secondary conjugate (Alexa488 anti-mouse IgG). The left panels are immunofluorescence (IF) microphotographs whereas the middle and the right panels are optical sections of cells showing CD44 staining or the nuclear marker DAPI as indicated. Scale bar = 20µm..... 105

**Figure 5.3- Distribution of CD44 in HT-29 cells.** Cells grown on glass coverslips were fixed, permeabilised and immunostained with (i) detection reagents alone (anti-mouse IgG Alexa488 conjugate) or (ii - ix) mAb directed against the extracellular domain of CD44. The clones used were: (ii) Hermes-3 (in house); (iii) E1/2 (in house); (iv) Bu52 (Serotec); (v) F10-44-2 (SouthernBiothech); (vi) 2F10 (RD); (vii) 3E8 (in house); (viii) 5F12 (NeoMarkers); (ix) Bu52 (Ansell). The cells were analysed using confocal microscopy. The images are optical sections of cells stained with each CD44 antibody against the extracellular domain in combination with a fluorescent secondary conjugate (Alexa488 anti-mouse IgG). Scale bar = 20µm ..... 108

**Figure 5.4 – Immunofluorescence analysis showing the distribution of CD44 in MCF10A cells.** The photomicrographs represent optical sections of cells stained with the CD44 antibody (clone E1/2) against the extracellular domain in combination with the secondary antibody Alexa555<sup>®</sup> anti-mouse IgG or other indicated markers. Cell nuclei were counterstained using DAPI. (A) Immunofluorescence analysis of MCF10A cultured under different conditions (low density, high density and acini) showing CD44 staining (red; left panel), nuclear staining by DAPI (blue; middle panel) and the merged images (right panel). No co-localization of CD44 and the nuclear marker is observed. (B; next page) Immunofluorescence analysis of MCF10A cells under low magnification showing filamentous actin staining (Green; Top left panel) using Alexa488<sup>®</sup> phalloidin probe (Life Technologies); CD44 staining (Red; Top right panel); DAPI nuclear staining (Blue; Bottom left panel) and the merged images (Bottom right panel). A large number of cells can be observed in the small magnification images but no co-localization of CD44 and the nuclear marker is observed. (C, next page) MCF10A cells stained with anti-cytochrome C antibody as a mitochondrial marker (Green; top left panel), CD44 staining (Red; top right panel), DAPI (Blue, bottom left panel) or the merged images (bottom right panel). The Zenon<sup>®</sup> labelling kit was used to prepare direct fluorophore labelled-primary antibodies as described in Section 2.16 Some intracellular CD44 appears within the cytosol but no CD44 is seen in the cell nucleus..... 109

**Figure 5.5– Detection of CD44 by Western blotting using antibodies against extracellular and intracellular domain.** (A) HT-29 cells were transfected with siRNA against CD44 (siCD44) or scrambled siRNA (siNC) and after 3 days, were harvested and submitted to Western blotting

with an antibody against the extracellular domain of CD44 (Hermes-3). The immunoreactive bands detected correspond to the different isoforms of CD44 with molecular weights ranging from ~90-150kDa (FL CD44). (B) Blotting with an antibody against the cytoplasmic tail of CD44 (CD44 ICD). Besides the full length molecule (90kDa), two additional specific bands were observed. The 25KDa band corresponds to the membrane bound cleaved CD44 containing the cytoplasmic domain (CD44 CTF). The CD44 intracytoplasmic domain (ICD) was also detected (~16kDa). (C) HT-29 cells were treated with 100 or 500ng/mL of PMA for 30 minutes. PMA treatment caused the appearance of bands at ~25 and ~16kDa representing the cleavage products of CD44. Note that different percentages of acrylamide were used to optimally detect FL CD44 (7.5%, A) and the cleaved products (12%, B and C) and therefore the migration patterns of markers appear different..... 112

**Figure 5.6 - Subcellular localization of CD44 after cell fractionation using detergent-based lysis.** Nuclear and cytoplasmic fractions prepared from the HT-29 cell line were analysed by Western blotting using antibodies against CD44 extracellular domain (Hermes-3; A); CD44 ICD (B); GAPDH (C); Lamin A/C (D) and CD9 (E). Specific CD44 bands are highlighted as per Figure 5.3: full-length CD44 (FL CD44), intracytoplasmic domain (CD44 ICD) and membrane-bound C-terminal fragment (CD44-CTF). Numbers on the left are Molecular Weights (KDa). 115

**Figure 5.7- Sub-cellular localization of CD44 in HT-29 cells after nitrogen decompression lysis and cell fractionation.** Cells were disrupted by nitrogen decompression and the subcellular fractions were separated by differential centrifugation. Fraction 1 is the nuclear fraction (Nuc), pelleted at 1000 x g; fraction 2 is the mitochondrial fraction (Mito) pelleted at 20,000 x g; Fraction 3 contains light cell membranes (Mem) pelleted at 100,000 x g and the supernatant is the cytosolic fraction (Cyto; fraction 4). The different fractions were analysed by Western blotting using antibodies against CD44 extracellular domain (Hermes-3; A); GAPDH (B); Lamin A/C (C) or CD9 (D). ..... 117

## Abstract

There is currently no effective treatment for melanoma once the tumour has spread beyond the primary site. Unlike many other cancers, metastatic melanoma is frequently resistant to all conventional forms of anti-cancer treatment. This inherent resistance of melanoma cells is in large part due to their hyper-activation of survival signalling pathways, most notably ERK and Akt. This often results from mutations of key proteins such as in BRAF, NRAS and PTEN, and consequently these molecules have been the subject of intensive investigation. These efforts have led to the revolutionary new treatments such as those targeting mutated BRAF that occurs in ~50% of melanomas. However, while these agents demonstrate a high initial response rate, their clinical benefit has been plagued by the development of acquired drug resistance. In any case this treatment is not applicable to those patients not presenting with the BRAF mutation and finding other therapeutic targets is urgent.

Another important mechanism driving survival signalling pathways in melanoma is the aberrant production of growth factors that act in an autocrine manner. The work presented in this thesis fits within this area with studies focused on the role of macrophage migration inhibitory factor (MIF). MIF is an atypical cytokine for which a number of diverse roles have been described including those of both hormone and enzyme. In the context of cancer, MIF is believed act as the autocrine factor driving activation of survival pathways. MIF signalling is known to be initiated by binding to the cell surface CD74/CD44 receptor complex or to the chemokine receptors CXCR2 and CXCR4. Although MIF signalling has been implicated in several tumours, the role of MIF in melanoma had not been previously studied in great detail.

This thesis first investigated the expression of MIF in melanocytic tumours *in vivo* using a combination of *in silico* analysis of microarray data and immunocytochemistry staining of *ex vivo* tumour sections. The results presented herein show that MIF expression generally increases with disease progression and in advanced tumours it preferentially localises to the nucleus of cancer cells. Analysing the available survival data it was shown that MIF was a significant prognostic factor for patients with metastatic melanoma, with higher expression levels predicting poorer outcome since patients underwent faster relapse. MIF expression was only important in the context of secondary tumours since the analysis of MIF levels in primary

melanoma samples failed to show outcome differences. Similar prognostic analyses of the known MIF receptors, CD74, CD44 that acts as a co-receptor, and CXCR2 and CXCR4 were also performed. Only CD44 expression appeared to be associated with prognosis since high CD44 levels in tumours were also predictive of shorter survival in metastatic disease. The conclusion from these data suggested that high levels of MIF expression in metastatic melanoma are associated with tumour aggressiveness.

Further experiments undertaken in a large panel of 20 human melanoma cell lines showed that MIF, CD44 and CXCR4 were ubiquitously expressed. CD74 was only expressed in 50% of cell lines and CXCR2 in none. The function of MIF was then examined in six of these cell lines using siRNA to deplete MIF. With respect to control treated cells, MIF siRNA significantly decreased cell proliferation in 4 out of 6 cell lines. Further analysis showed that MIF also influenced cell survival and anchorage-independent growth. The sensitivity of cells to MIF depletion appear to be associated with the presence of MIF in the cell nucleus, but it was independent of BRAF mutational status. Analysis of signalling pathways showed that MIF acts to regulate the Akt pathway in a high proportion of melanoma cell lines and this finding is highly significant with respect to targeting survival signalling in this disease.

The receptor systems that MIF likely utilises in melanoma were also investigated. It was noticeable that MIF effects on melanoma cell lines were independent of CD74 expression since cells not expressing CD74 were also sensitive to MIF knockdown. Analyses focussed on the nuclear localisation of MIF and the presumed involvement of CD44 in this process, since CD44 had been previously shown to translocate to the nucleus. Extensive imaging and biochemical analyses failed to demonstrate this was the mechanism of MIF nuclear translocation in melanoma.

In conclusion, the work presented here implicates MIF in melanoma progression and reveals MIF as a potential prognostic factor for metastatic melanoma. MIF actions are likely to involve the activation of Akt signalling pathway to regulate the cell-cycle, a key finding that has implications for melanoma proliferation and progression. Taken together, these results indicate MIF as a potential new therapeutic target for melanoma and one that is potentially independent of - and complementary to - current therapies.

# **Chapter 1**

## **General Introduction**

## **1.1 Melanoma**

### **1.1.1 Epidemiology**

Skin cancers are an increasing problem in Western societies, of which melanoma is the most aggressive and treatment-resistant form (8). The occurrence of melanoma is less common than other types of skin cancer like basal cell carcinoma and squamous cell carcinoma. Nevertheless melanoma is definitely the most life-threatening, being responsible for near 75% of skin-cancer associated deaths. To compound this problem, the incidence of melanoma has been steadily rising worldwide for the last 50 years, especially among fair-skinned populations (9). This rise in melanoma incidence has been particularly rapid in Australia, where it is a significant health issue, and despite prevention campaigns being implemented, the incidence rates are the highest in the world.

The areas with the highest incidence begin in the northern regions of Queensland and decrease moving south away from the equator to the southern coastal regions of Victoria. Indeed, melanoma is the fourth most frequent cancer in Australia, with more than 11,000 new cases diagnosed every year. Worryingly, Australian melanoma rates have doubled in the 20 years from 1986-2006 and are still on the rise with an estimated 392 extra cases per year (Figure 1.1). Among young Australians aged 15-44 years old, melanoma is the most common cancer, making up 20% of all cancer cases and being responsible for 8% of all cancer deaths. In 15-29 year-olds, melanoma kills more young Australians than any other cancer (Table 1.1). Overall as many as 1 in 19 Australians will be diagnosed with melanoma before age 85 (4, 5, 9-11). On the basis of these statistics, research into better ways to treat melanoma once it has formed and spread remains a high priority for Australian biomedical research.

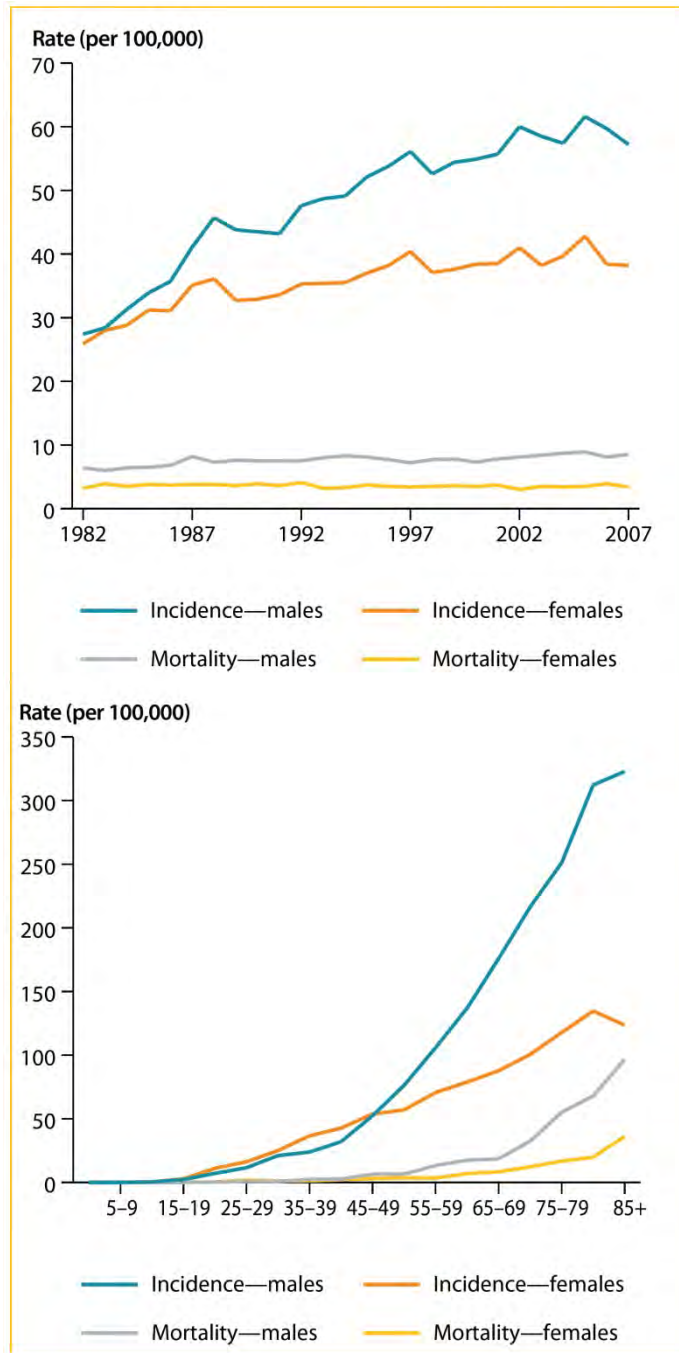


**Figure 1.1 – Melanoma incidence and mortality rates in Australia** –Melanoma incidence and mortality from 1982 to 2007. The rates were age-standardised to the Australian population as at 30 June 2001 and are expressed per 100,000 population (top panel). Melanoma incidence and mortality by age at diagnosis. The rates shown are age-specific rates (bottom panel). Adapted from “Cancer in Australia: an overview, 2010” (5).

**Table 1.1– Incidence of the 10 most common cancers in young Australians (15-29 year-olds), 2003-2007.** Adapted from “Cancer in adolescents and young adults in Australia.” (4).

<b>Cancer type/site</b>	<b>No. of cases</b>	<b>% of all cancers</b>
Melanoma	2,251	25.6
Gonadal germ cell cancer	1,127	12.8
Hodgkin lymphoma	851	9.7
Thyroid carcinoma	685	7.8
Other carcinoma	673	7.7
Non-Hodgkin lymphoma	494	5.6
Colorectal carcinoma (including anus)	315	3.6
Breast carcinoma (females only)	299	3.4
Other soft-tissue sarcoma	279	3.2
Cervical carcinoma	253	2.9
<b>All cancers</b>	<b>8,783</b>	<b>100.0</b>

### 1.1.2 Etiology and Risk Factors

Melanoma arises from the malignant transformation of melanocytes, which are cells located mainly in the basal layer of the epidermis. However, it can also be found in the eyes and other epithelial surfaces. In the skin, melanocytes are normally long-lived, nonproliferative cells and they are responsible for the production and distribution of melanin to the neighbouring keratinocytes. This distribution is achieved through specialized organelles called melanosomes, where the melanin synthesis occurs. It is widely accepted that lesions in melanocytes lead to melanoma, with the majority occurring in the skin (cutaneous melanoma), and less commonly in the eye (uveal melanoma) and internal mucosal membranes (mucous membrane melanoma) (12). There are a number of risk factors in developing melanoma and include both genetic predisposition and environmental factors, with the combination of both influencing the onset of the disease.

At the genetic level, approximately 5-10 % of all cutaneous melanomas occur in families with melanoma predisposition (13). In familial melanoma, a number of different genes have been associated with increased melanoma risk, with the most widely studied mutations involving the loci *CDKN2A* (cyclin-dependent kinase inhibitor 2A) and *CDK4* (cyclin-dependent kinase 4) (12-14). The *CDKN2A* locus is particularly intriguing as it encodes two distinct tumour suppressor proteins that play essential regulatory roles in cell growth as well as apoptosis. The first is p16<sup>INK4A</sup> (cell-cycle inhibitor of kinase 4A) and the second is p14<sup>ARF</sup> (arising from an alternate reading frame) (15, 16). During cell cycle progression, p16<sup>INK4A</sup> inhibits cyclin-dependent protein kinases (Cdks)-4 and -6. The p16/CDK complex further prevents phosphorylation of pRb, blocking the G1-S transition of the cell cycle. The alternative gene product p14<sup>ARF</sup> directly affects p53 expression by sequestration of the protein mdm2, which promotes p53 degradation (17). Thus, in the context of familial melanoma, the loss of p16<sup>INK4A</sup> leads to Rb hyperphosphorylation allowing the cells to go from G1 to S-phase and begin to proliferate, while the loss of p14<sup>ARF</sup> results in an indirect loss of p53 function and deregulation of cell cycling and DNA damage signalling (14, 16, 17). Mutations within the *CDK4* locus have also

been implicated in melanoma risk, although affecting a smaller number of melanoma-prone families. Primarily, mutations in the *CDK4* gene found in melanoma cells result in the expression of a protein resistant to inhibitory regulation by p16<sup>INK4A</sup>. Because the two proteins directly interact, carriers of *CDK4* mutations share a similar phenotype to those affected by loss of the *CDKN2A* locus (14, 18, 19).

In addition to genetic factors, environmental factors also play an important role in melanoma risk. The most important environmental risk factor for melanoma is ultraviolet radiation (UVR) exposure, from the sun or artificial tanning beds. UVR is believed to promote malignant changes in the skin by direct mutagenic effects on DNA, by stimulating the cells to produce growth factors, by reducing cutaneous immune defences and by promoting reactive oxygen species (20, 21). It is also important to consider the genetic-environmental interaction in melanoma etiology. For example, sensitivity to UVR is associated with polymorphisms in particular genes that affect both the defensive response of the skin and the risk of melanoma. Therefore, the synergism between two or more possible etiologic factors may contribute as a cause to melanoma development (20, 22).

### 1.1.3 Pathology of Melanocytic Tumours

The malignant transformation of melanocytes is characterised by progressive histological changes that are outlined in Figure 1.2. Five distinct stages have been proposed in the evolution of melanoma on the basis of location and stage of progression: [1] common acquired and congenital naevi without dysplastic changes; [2] dysplastic naevi with structural and architectural atypia; [3] radial-growth phase (RGP) melanoma; [4] vertical-growth phase (VGP) melanoma; and [5] metastatic melanoma (23).

Even though in most cases of malignant melanoma there is no evidence of a precursor naevus, it is generally believed that the onset of malignant transformation is preceded by different degrees of dysplasia arising within a benign melanocytic lesion. Although it is normally considered a precursor to melanoma, a benign naevus rarely progresses to cancer, probably due to oncogene-induced cell senescence (24). The dysplastic naevus is considered a pre-malignant lesion, which can still regress but the probability to become malignant is increased. Both benign and dysplastic naevi are characterised by disruption of the epidermal melanin unit, leading to increased numbers of melanocytes in relation to keratinocytes. These precursor lesions may progress to *in situ* melanoma, which grow laterally and remain largely confined to the epidermis, and this stage is defined as the radial-growth phase (RGP). In this phase, lesions tend to be oval or circular and have no ability to metastasise. As mentioned above, the primary tumour may also arise from melanocytes that do not pass through the naevus stage, a fact that can confound strategies aimed at early diagnosis.

Independent of the origin of the melanoma, the next critical phase is vertical growth phase (VGP), where melanoma acquires competence for metastasis. The VGP is characterised by the vertical growth of a new population of cells within the melanoma, perpendicularly to the directional growth of RGP, and cells may invade the dermis and form expansive nodules. In the latter phase of progression, metastatic melanoma dissociates from primary tumour, and grows at distant sites. It may lodge into regional lymph nodes and spread by the bloodstream to further areas such as the lung, brain or liver (7, 22-25).

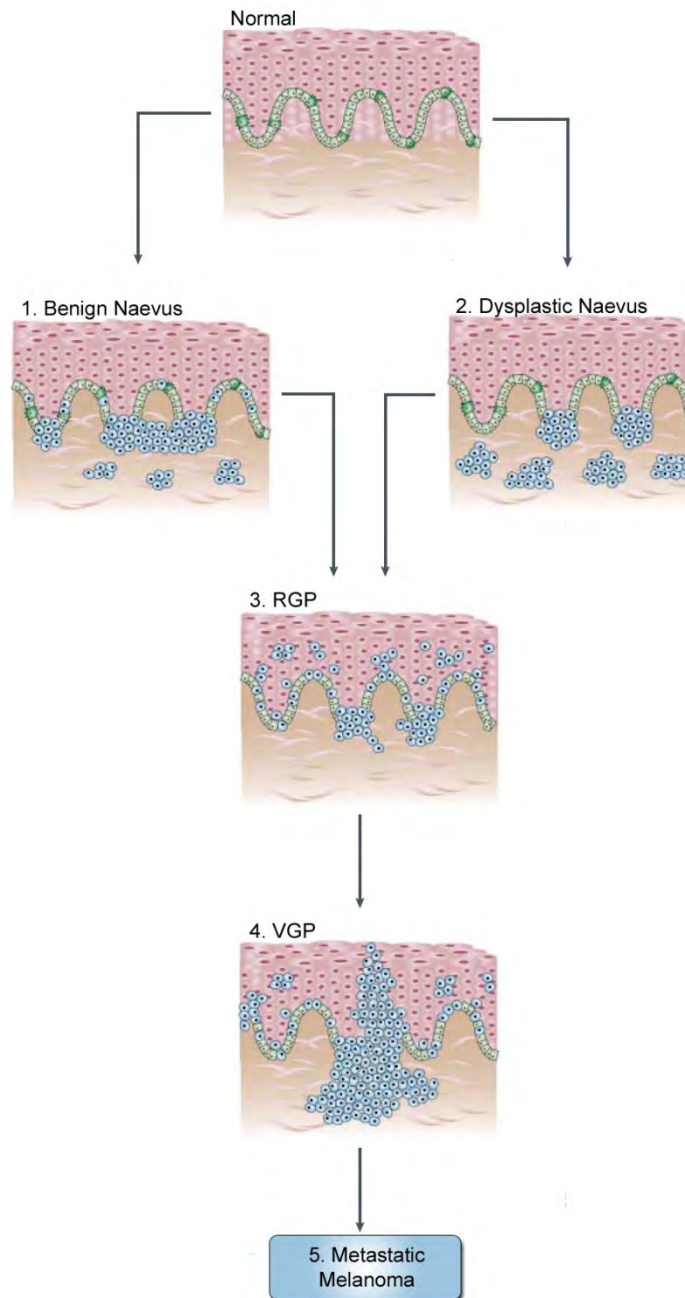


**Figure 1.2 – Melanoma progression model showing the five stages of melanoma progression.** Benign lesions originate within normal skin and include common acquired or congenital naevi [1] and dysplastic naevi [2]. Both are considered to be precursors of melanoma and can further progress to *in situ* melanoma, which grows laterally and remain largely confined to the epidermis. This stage is known as radial-growth phase (RGP) melanoma [3]. The next stage, vertical growth phase (VGP) [4], is characterised by the vertical growth of a new population of cells within the melanoma, which may invade the dermis and form expansive nodules. In the latter phase of progression metastatic melanoma [5] dissociates from the primary tumour, and colonises distant sites (Adapted from Chin, 2003 (7)).

#### **1.1.4 Staging and Prognosis**

Metastatic melanoma has a well-known predilection for distant spread and patients with advanced disease have a median survival time of 6 to 9 months (26). The prognosis depends mainly on two factors: the thickness of the primary tumour and the presence or absence of metastasis to regional lymph nodes. However, other prognostic factors are very important, including tumour ulceration, mitotic rate and presence of regression, as well as sex and age of the patient and tumour site (27). In advanced regional disease, melanoma commonly metastasises to other skin regions, soft tissues, the lung, the liver, and the brain. The brain is the most common site of metastases and is associated with poorer prognosis compared with other visceral sites (28). Lungs are the second most common sites of metastatic disease, after lymph node involvement (29). In patients who have visceral metastatic disease, the liver is the most common site involved (30).

The melanoma staging system is based on the tumour-node-metastasis (TNM) staging criteria described by the American Joint Committee on Cancer (AJCC) Melanoma Staging and Classification, which was recently revised in 2009. The TNM staging categories consider histopathologic factors such as primary tumour thickness, ulceration status, and rate of mitosis. In addition, the number of metastatic nodes and presence of metastases are also important (31, 32). The classification scheme detailing the different stages is shown in Table 1.2.

**Table 1.2 – TNM Staging Categories for Cutaneous Melanoma (reproduced from Balch *et al.*, 2009 (31)).**

Classification	Thickness (mm)	Ulceration Status/Mitoses
<b>T</b>		
Tis	NA	NA
T1	≤ 1.00	a: Without ulceration and mitosis < 1/mm <sup>2</sup> b: With ulceration or mitoses ≥ 1/mm <sup>2</sup>
T2	1.01-2.00	a: Without ulceration b: With ulceration
T3	2.01-4.00	a: Without ulceration b: With ulceration
T4	> 4.00	a: Without ulceration b: With ulceration
<b>N</b>		
	No. of Metastatic Nodes	Nodal Metastatic Burden
N0	0	NA
N1	1	a: Micrometastasis* b: Macrometastasis†
N2	2-3	a: Micrometastasis* b: Macrometastasis† c: In transit metastases/satellites without metastatic nodes
N3	4+ metastatic nodes, or matted nodes, or in transit metastases/satellites with metastatic nodes	
<b>M</b>		
	Site	Serum LDH
M0	No distant metastases	NA
M1a	Distant skin, subcutaneous, or nodal metastases	Normal
M1b	Lung metastases	Normal
M1c	All other visceral metastases	Normal
	Any distant metastasis	Elevated
Abbreviations: NA, not applicable; LDH, lactate dehydrogenase. *Micrometastases are diagnosed after sentinel lymph node biopsy. †Macrometastases are defined as clinically detectable nodal metastases confirmed pathologically.		

### 1.1.5 Treatment

At the time of diagnosis, most patients with melanoma have disease that is confined to the primary site on the skin, and surgical excision of primary melanoma normally results in a complete cure. For patients with thick melanoma (>2mm), surgery is followed by adjuvant therapy or clinical trial enrolment. The only effective adjuvant treatment is Interferon- $\alpha$  (INF- $\alpha$ ), a cytokine that has been shown to have anti-angiogenic activity in metastatic melanoma. However, because of the limited benefit upon disease-free survival and the smaller potential improvement of overall survival, the indication for INF- $\alpha$  treatment remains controversial (33).

The malignancy of melanoma is in part due to its ability to give rise to metastasis in virtually every tissue, with distant metastases commonly causing death. Once a melanoma has spread beyond the skin and regional lymph nodes, it is largely incurable by currently available chemotherapeutic and other agents. Among patients with metastatic melanoma, only ~10% survive >5 years from diagnosis (31). The most widely used single chemotherapeutic agent for the treatment of metastatic melanoma is dacarbazine, which is an alkylating agent that methylates nucleic acids and inhibits DNA, RNA, and protein synthesis. Unfortunately, most responses to this agent and its oral analogue temozolomide are transient; only 1%-2% of patients achieve a durable long-term response to chemotherapy (33).

Another option for patients with metastatic melanoma is immunotherapy. Interleukin 2 (IL-2) is an immunotherapeutic agent that was approved by the US Food and Drug Administration (FDA) for the treatment of metastatic melanoma. However the overall response rate for IL-2 is low (16%) and systemic toxicity is high, restricting this treatment to highly specific patients and institutions (12). In 2011, the FDA approved ipilimumab for the treatment of advanced-stage melanoma. Ipilimumab is a monoclonal antibody against cytotoxic T-lymphocyte-associated antigen 4 that incites a T-cell-mediated response against the tumour. In clinical trials, ipilimumab was found to improve patient survival by 4 months in patients with advanced-stage melanoma (12).

Radiotherapy is used as a treatment in 90% of all cancer patients but plays a limited role in the treatment of melanoma because it is radioresistant compared to other cancers. Indeed radiotherapy responses rates are dose dependent and because very high doses of radiation are needed to eradicate melanocytic tumours, radiotherapy is less optimal as primary treatment of melanoma because of its associated adverse effects. However, radiotherapy has been used as an adjuvant therapy when adequate surgical margins cannot be achieved, such as with lesions on the head and neck (34).

Overall, melanoma is highly curable when diagnosed in the early stages but there is currently no effective treatment once it becomes metastatic. Since conventional treatments often fail, novel strategies are needed and the knowledge of signal transduction pathways may provide novel targets for melanoma therapeutics (6, 35-37).

## **1.2 Signalling Networks in Melanoma**

### **1.2.1 BRAF and MAPK/ERK signalling pathway**

During the transformation into aggressive melanomas, melanocytes undergo extensive genetic changes. These changes deregulate genes whose aberrant activity promotes the development of this disease. Familial melanoma is associated with highly penetrant germline mutations and represents approximately 10% of new cases. As mentioned above, germline mutations of *CDKN2A* were identified in 25-50% of familial melanoma kindreds (6). In addition to germline mutations, somatic *CDKN2A* alterations have also been reported in up to 30-70% of sporadic melanomas (6, 38).

In sporadic melanoma, the gene most commonly known to be mutated is *BRAF*, a serine-threonine kinase that plays a central role in regulating mitogen activated protein kinase (MAPK) signalling (Figure 1.3). Activating mutations of the MAPK pathway enable cancer cells to become self-sufficient in growth signals, one of the hallmarks of cancer (39). Several studies

have shown that *BRAF* is mutated in 50-70% of melanoma, from primary to metastatic stages (Figure 1.4) (40-42). Mutations in *BRAF* have also been reported in benign naevi, but in these cells it appears to cause cell senescence, preventing hyperplastic melanocytes to progress to melanoma by increasing the expression of *p16<sup>INK4A</sup>*. This oncogene-induced senescence has been suggested to be a protective physiological process. Because *BRAF* mutation induces senescence in benign naevi and uncontrolled proliferation in melanoma, it was hypothesised that mutation of *BRAF* alone is unable to cause the malignant transformation of melanocytes. Hence, a second oncogenic lesion would be needed to inactivate the BRAF-senescence pathway, and this may be by mutations in *p16<sup>INK4A</sup>* itself or mutations in other genes residing in the same signal transduction pathway (22, 40, 43, 44).

*BRAF* mutation results in abnormal activation of ERK (extracellular-signal regulated kinase) pathways, known to be an early event in melanoma progression, and to be involved in a variety of cellular processes such as proliferation, migration and survival (45, 46). Normal ERK signalling plays a critical role in signal transduction from the cell surface to the nucleus. Extracellular signals interact with their respective receptor tyrosine kinase leading to the activation of the ras-family GTPases followed by a series of specific phosphorylations of RAF, MEK and ERK proteins. Once activated, ERK phosphorylates a wide range of nuclear and cytoplasmic targets, including a variety of transcription factors which lead to a variety of cellular responses from proliferation to differentiation and also senescence and cell death. The cellular response depends upon multiple inputs including the intensity and duration of the signal, what other pathways are active in the cell, and on additional intrinsic and extrinsic cell factors that enable this pathway to participate in such apparently contradictory cellular outcomes (47-49) (Figure 1.4). What is clear is that hyperactivation of ERK pathway is present in virtually all melanomas, normally as a consequence of mutations in *BRAF* or other upstream proteins.

Since the initial discovery of the subset of melanoma patients harbouring *BRAF* mutations, the development of therapeutic interventions to inhibit the function of this protein is

revolutionising the standard of care for patients with *BRAF* mutation-bearing tumours. Although over 50 different mutations have been identified in *BRAF* gene, more than 90% of the mutations occur at codon 600 in exon 15, which results in an amino acid change from valine to glutamic acid ( $BRAF^{V600E}$ ), and increases its catalytic activity by a factor of 500 (50-52). The first therapeutic approach to block this protein was the use of multikinase inhibitor sorafenib, as a monotherapy agent (53) or combined with traditional agents like dacarbazine (54), temozolomide (55), carboplatin plus paclitaxel (56) and temsirolimus (57). However all these trials failed to significantly increase patient survival.

Since these trials, other inhibitors of mutant *BRAF* have been developed which are more potent and selective than sorafenib (50-52, 58). The first selective *BRAF* inhibitor to be developed in the clinical setting was vemurafenib (PLX4032). Vemurafenib is an orally available inhibitor with an approximately 30-fold selectivity for  $BRAF^{V600E}$  compared with wild-type *BRAF* (59). It produced major responses in phase I and II testing and showed an overall survival advantage as single agent against dacarbazine in a recent phase III trial (60). In addition to vemurafenib, several other *BRAF* inhibitors are also in clinical development. GSK21118436 is a second higher potency *BRAF* inhibitor with a >100-fold selectivity for cell lines that harbour  $BRAF^{V600E}$  mutation. It is currently being evaluated and showing promising responses in clinical trials (50, 51). However, for most patients, the clinical benefit of receiving vemurafenib as a single agent is limited and it appears that the great majority of patients treated eventually exhibit disease progression due to acquired resistance to treatment. The mechanisms related to resistance to *BRAF* inhibition are under intensive research and at least four mechanisms of resistance have been described to date. These include upstream mutation of *NRAS*, activation of membrane bound receptor tyrosine kinases (61), with subsequent signalling through other growth pathways, overexpression of the Ser/Thr MAPK kinase kinase (MAP3K), *COT*, which activates ERK through MEK-dependent mechanisms that do not require RAF signalling (62), and downstream mutation of MEK (63). In an attempt to overcome these resistance mechanisms, novel combination regimens are currently being evaluated in clinical trials.

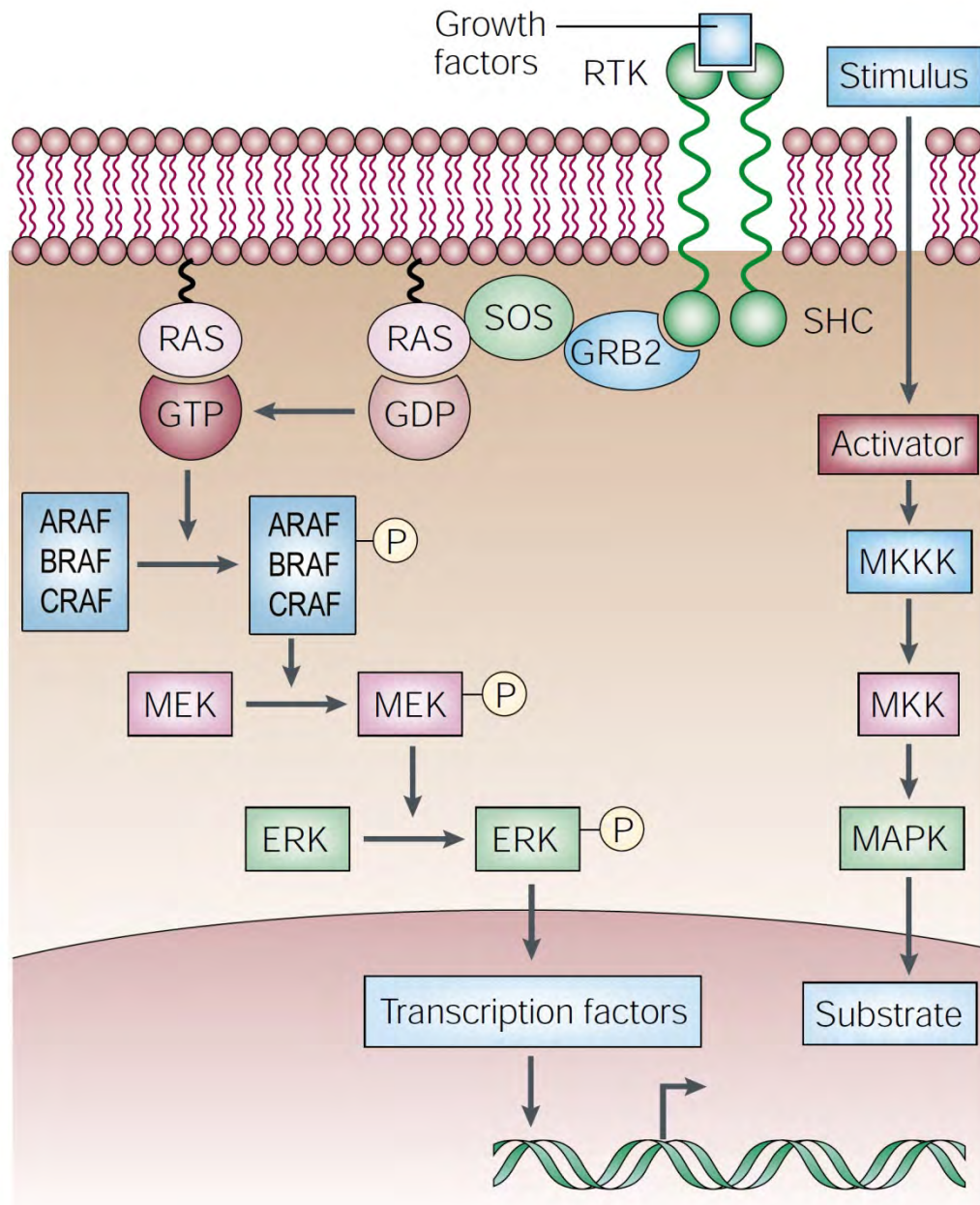


**Figure 1.3 – Schematic representation of the activation of MAPK/ERK signalling pathway in mammalian cells.** A simplified MAPK signalling module is illustrated here with the RAS-RAF-MEK-ERK pathway. Extracellular stimuli lead to activation of ERK pathway via consecutive phosphorylations initiated by RAS (HRAS, NRAS and KRAS) which phosphorylates the MKKK RAF (ARAF, BRAF and CRAF). RAF, in turn, phosphorylates MEK (MEK1 and MEK2), which then phosphorylates ERK MAPK (ERK1 and ERK2) leading to activation of transcription factors and regulation of several cellular processes (Modified from Chin 2003 (7)).

### 1.2.2 PTEN and the Akt signalling pathway

Another frequent genetic alteration in melanoma and other cancers is the loss or inactivation of PTEN (phosphatase and tensin homolog), which is well known by its role as a tumour suppressor (64, 65). The *PTEN* gene encodes a phosphatase whose primary function is to degrade the products of PI3K by dephosphorylating PIP3 (66). Loss of functional PTEN from tumour cells causes accumulation of PIP3, which is a critical second messenger lipid, and in turn this increases Akt phosphorylation and activity (67, 68). Because PTEN functions as an antagonist of PI3K-mediated signalling, a consequence of PTEN loss is constitutive activation of the Akt pathway in melanoma (69).

Akt plays a critical role in normal cells, controlling several cellular processes, including inhibition of apoptosis, cell survival and cell cycle regulation (Figure 1.4). Akt has been postulated to phosphorylate over 9,000 proteins and several studies have shown that Akt activates the transcription of a wide range of genes, especially those involved in immune activation, cell proliferation, apoptosis and cell survival (70, 71).

The Akt kinase family consists of three protein kinases Akt1, Akt2 and Akt3. Akt isoforms share >80% amino acid homology and their activity is regulated through similar mechanisms, but activity of a particular isoform is cell type dependent (70, 72). Although all three isoforms are expressed in melanoma, Akt3 is the predominantly active isoform. Increased Akt3 expression/activity occurs in 60–70% of sporadic melanomas demonstrating a key role in melanoma development (69, 73). It is unknown why Akt3 and not the other isoforms are activated in melanomas, however, it is known that loss of functional PTEN preferentially regulates Akt3 activity in this malignancy (73).

Akt3 has been shown to act as a pro-survival kinase in melanoma (73). Activated Akt3 has several different important enzymatic substrates including Mdm2, procaspase 9, NF- $\kappa$ B, mammalian target of rapamycin (mTOR), and p27<sup>Kip1</sup>, many of which contribute to tumour

proliferation and survival (Figure 1.4) (6). Decreased sensitivity to apoptosis makes melanoma cells less sensitive to chemotherapeutic agents functioning through this mechanism (74).

It has been shown that mutations in BRAF and loss of PTEN may interact to induce melanoma malignancy (75). Mutation in BRAF alone is not able to induce melanoma development in mice, but when BRAF mutation is combined with gene silencing of PTEN, it causes melanoma development with 100% penetrance, being able to metastasise into lungs and lymph nodes (75). These data are consistent with the fact that *BRAF* mutation often happens together with the loss of PTEN in human melanoma and this could be the second mutation necessary to overcome BRAF-induced senescence (44).

### 1.2.3 *NRAS* mutations

Constitutive activation of ERK and Akt pathways can also be achieved by mutations in *NRAS*, present in 15-30% of melanoma cases (42, 76). As both pathways are included in the *NRAS* signalling network (Figure 1.4), additional mutations in downstream targets would be redundant. Indeed, mutations in *NRAS* are almost invariably mutually exclusive with alterations in other genes, such as *PTEN* and *BRAF* (77). As such, in spite of the high frequency of mutated *BRAF* or *NRAS* in human melanoma, simultaneous presence of *BRAF* and *NRAS* mutations in the same tumour are rare (78). Previous studies of melanoma cell lines show that cell lines that harbor *BRAF* mutations do not have *NRAS* mutations (41, 79), and in the few exceptional cases in which a *BRAF* mutation was found together with a transforming *NRAS* mutation, the *BRAF* mutation did not include the V600E change (80). More recently, Ellerhorst *et al.* (81) examined a series of 223 primary human cutaneous melanomas for alterations in the same genes. The results showed that 109 patients (48.9%) had *BRAF* mutations, 31 patients (13.9%) had mutated *NRAS*, and only 3 patients (1.3%) showed a double mutation (81). Although complete reciprocity is not universal, these findings suggest that activation is required

at only one point in the RAS/RAF/MAPK pathway to activate the downstream targets and initiate cell proliferation and/or tumourigenesis (40, 82). Although in rare cases *NRAS* and *BRAF* activating mutations can co-exist in the same melanoma, they are mutually exclusive at the single-cell level, suggesting that such neoplastic cells may either lack a survival advantage, or may even be selected against during tumourigenesis (83).

Interestingly, as is true for *NRAS* and *BRAF*, studies on cell lines have shown that *PTEN* loss is also reciprocal in at least a subset of melanoma cell lines (79). Analysis of primary melanoma tumours by Goel *et al.*, 2006 (84) revealed that 13 out of 69 tumours showed *PTEN* reduction or absence but none of those had mutated *NRAS*. None of the 10 tumours with *NRAS* mutations had reduced expression of *PTEN*, strongly suggesting that in most cases, mutations in *NRAS* and *PTEN* are also mutually exclusive (84).

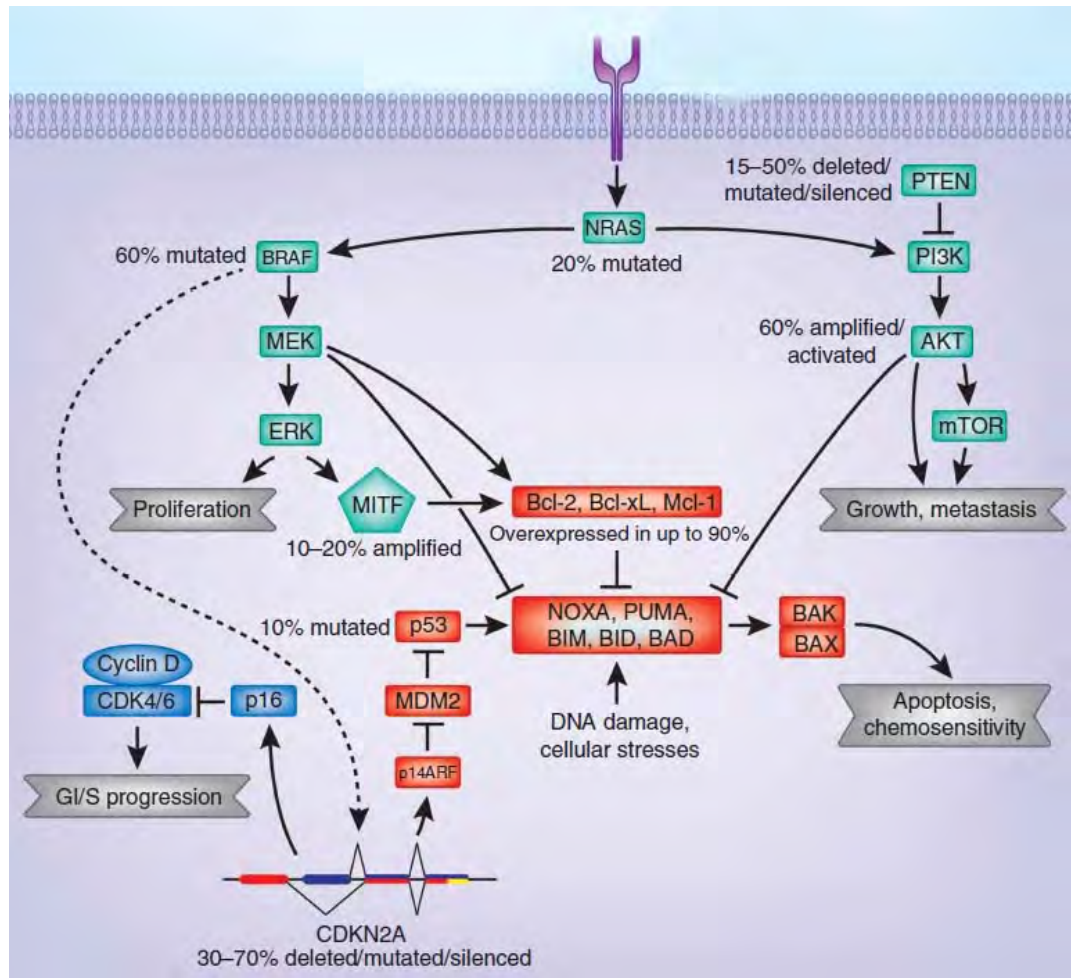


**Figure 1.4 – Altered signalling pathways in melanoma.** Representative diagram showing the major molecular pathways involved in melanoma tumorigenesis, survival and senescence. NRAS pathway, in green, includes ERK and Akt pathways and is involved in melanoma proliferation, survival and progression. The CDKN2A locus encodes for tumour suppressors which are thought to contribute to senescence. The p53/Bcl-2 pathway regulates melanoma apoptosis and is modulated by many of the known oncogenic pathways (Adapted from Hocker *et al.*, 2008 (6)).

#### 1.2.4 Autocrine signalling

Both ERK and Akt signalling cascades have a central role in melanoma development and they are believed to contribute to the inherent chemotherapeutic resistance of melanoma cells. The ideal therapeutic agent should therefore target both pathways in order to be an effective treatment for melanoma patients in advanced stages (49, 69, 85). Although BRAF inhibition is showing promise in melanoma treatment, these advances are only available to around 60% of the patients, that is, those who have the BRAF mutation, and to date, responses have been transitory in these patients. For those not presenting this mutation, finding other targets is urgent (52). While in some cases activation of ERK and Akt pathways can clearly be associated with gene mutations in components of these pathways, melanoma cells with non-mutated NRAS and BRAF can also exhibit hyperactivation. Since these tumours without obvious mutant genotypes are neither rare nor have improved treatment outcomes for patients, they must be considered in the overall approach to address melanoma.

One area that deserves further research efforts involves the autocrine production of growth factors that serve to drive ERK and Akt activation in melanoma (86, 87). Unlike normal melanocytes, melanoma cells usually use autocrine mechanisms to control their proliferation, survival and migration, becoming autonomous. Indeed, one of the early characteristics of the melanocytes transformation is the production and secretion of growth factors, creating autocrine stimulatory loops (88). In this context, one potentially attractive target is the macrophage migration inhibition factor (MIF), since MIF binding activates both the MAPK/ERK and the PI3K/Akt pathways.

### 1.3 MIF

Macrophage migration inhibitory factor (MIF) was first reported in 1966 for its ability to inhibit random migration of macrophages and to recruit them at inflammatory sites (89). Although it was the first cytokine discovered, it is atypical of the conventional classes of cytokines, since functions for MIF extend to include roles as both hormone and enzyme (90, 91). Besides its well-studied role in inflammation and immunity, MIF has recently been shown to play a role in cell proliferation and it is suggested to be involved in the development and progression of cancer, acting as an extracellular, pro-tumourigenic factor (92-94). Over the past few years, the role of MIF in a variety of tumours has been examined (95, 96). MIF influences tumour growth and development in several ways, including induction of angiogenesis (97, 98), promotion of cell cycle progression (99, 100), inhibition of apoptosis (101) and inhibition of the lysing of tumour cells by natural killer (NK) cells (100, 102).

MIF expression was found to be upregulated in a variety of different tumour cells and the work of several groups points to a correlation between MIF expression and cancer prognosis (92, 103, 104). Targeting of MIF signalling in tumours producing autocrine MIF is already showing promise in prostate, breast, bladder and pancreatic cancers (105-108). For example, Meyer-Siegler and collaborators (106) showed that treatment of human bladder cancer cells with anti-MIF antibody or MIF anti-sense RNA reduced proliferation and decreased secretion of a wide range of inflammatory cytokines, including TNF- $\alpha$  and IL-1 $\beta$ , suggesting that neutralising MIF may serve as a therapeutic treatment for bladder carcinoma (106). More recently, the same group also demonstrated that inhibition of MIF or its receptor CD74 decreased proliferation, MIF secretion and invasion of aggressive prostate cancer cells (DU-145). Thus, blocking MIF or its receptor (CD74) may also provide new targeted therapies for prostate cancer (105).

### 1.3.1 MIF in Melanoma

In the context of melanoma, a small number of studies suggest that MIF is widely expressed and may function as a growth factor that stimulates growth and invasion. Shimizu *et al.* (1999) showed that human melanoma cell lines have a higher degree of MIF expression than normal melanocytes. They also showed that inhibition of MIF expression in one melanoma cell line (G361) resulted in inhibition of proliferation, migration and tumour-induced angiogenesis (98). MIF production was also shown in human uveal melanoma cell lines, in which MIF prevents lysis by NK cells (109). In a study of differentially expressed genes in models of melanoma progression, MIF was one of the transcripts identified as being associated with increased aggressiveness (110). Another work by Culp *et al.* (2007) demonstrated that MIF inhibition in a mouse melanoma cell line (B16-F10) significantly delayed tumour establishment when injected into mice (111).

MIF expression has not been extensively studied in melanocytic tumours *in vivo*. In the largest reported study to date, Miracco *et al.* (112) evaluated the expression of MIF at both mRNA (55 cases) and protein levels (126 cases) in a range of cutaneous melanocytic tumours, including benign and atypical naevi, melanoma and melanoma metastases. These authors found that MIF transcript levels measured by qRT-PCR were significantly higher in all types of melanocytic lesions compared to skin margins, with the highest expression occurring in atypical naevi and malignant melanoma. MIF protein was highly expressed in all lesions, although limited to the cytoplasm in most benign naevi with nuclear MIF reported in addition to cytoplasmic protein in both atypical naevi and melanomas. Notably they found MIF protein expression was frequently heterogeneous, particularly in malignant tumours. However, despite the evidence that MIF levels are variable and often increased in malignant disease (112), there have been no published articles investigating whether the expression levels of MIF has prognostic significance for outcomes in melanoma patients.

### 1.3.2 MIF signalling

The pleiotropic actions of MIF can be achieved through its unique signalling properties, including activation of the ERK and Akt pathways and the regulation of Jab1, p53, SCF ubiquitin ligases and HIF-1 (113). How MIF can transduce these signals has only recently been revealed when the widely expressed Type II transmembrane protein CD74 was cloned and identified as the cell surface receptor for MIF (114). The CD74 cytoplasmic tail appears to lack intracellular signalling domains (115) and in 2006, CD44, the major cell surface receptor for hyaluronic acid, was identified as its co-receptor responsible for transducing MIF signals (2). More recently, the CXC chemokine receptors CXCR2 and CXCR4 were also identified as receptors for MIF (116).

## 1.4 CD74

CD74 was first identified as the invariant chain (Ii) of the major histocompatibility factor class II (MHCII) complex. In humans, the predominant subset of MHCII molecules is the human leucocyte antigen (HLA)-DR. Before its characterisation as a receptor for MIF, the main function of CD74 (Ii) was thought to be as a chaperone, stabilizing HLA-DR  $\alpha\beta$ -heterodimers and targeting HLA-DR molecules to endocytic compartments. Thus, CD74 influences multiple aspects in antigen presentation via MHC class II molecules (117). More recently, CD74 expression has been examined in cell types other than antigen presenting cells, such as epithelial cells (118). In addition, some reports suggest that CD74 might be expressed independently of class II MHC, indicating additional functions (119).

The CD74 intracellular domain is only 46 amino acids long and has no homology with tyrosine or serine/threonine kinases, or interaction domains for nonreceptor kinases or nucleotide binding proteins (115). Nevertheless, the intracytoplasmic tail may be phosphorylated (120), and there is work suggesting a pathway for the intramembranous proteolytic release of the cytosolic domain (121). As introduced above, another additional cell surface molecule, CD44, was shown to be associated with CD74 forming a receptor complex (2,

122). While CD74 is sufficient for MIF binding to the cell surface, CD44 association was found to be the means whereby this complex can achieve intracellular signalling (2).

The discovery that CD74 functions as a high-affinity receptor for MIF indicated an entirely new role for this molecule in signal transduction pathways (114). Indeed, it has been demonstrated that MIF-CD74 can induce a signalling pathway that leads to activation of NF- $\kappa$ B and increases DNA synthesis and cell entry in S phase, as well as Bcl-X<sub>L</sub> expression, suggesting a role for CD74 in survival (115). Several authors have shown that the ability of MIF/CD74 to activate ERK and Akt signalling pathways can induce proliferation and inhibit apoptosis (2, 105, 107, 114, 123, 124).

CD44 is a cell surface transmembrane protein but during its life cycle it remains on the cell surface for a very short time, since it is rapidly internalised and replenished by newly synthesised CD74 molecules (125, 126). The rapid internalisation of CD74, together with other factors like its expression by a range of cancer cell lines and its restricted expression by normal tissues, makes CD74 a potential target for cancer therapies. Indeed, CD74 expression is linked with several forms of cancers and it has been correlated with poor prognosis (105, 123, 127-133). Although there are few reports on CD74 expression in melanoma, surface CD74 has been identified in primary melanoma, but not in benign melanocytes (134, 135). The specific role of surface CD74 in melanoma remains to be elucidated.

## 1.5 CD44

CD44 is a transmembrane cell adhesion molecule that acts as the major cell surface receptor for hyaluronic acid (HA), a ubiquitous component of the extracellular matrix (136). The ability to bind hyaluronan provides CD44 with a role in cell-cell and cell-substrate interaction, and this interaction appears to have a role in different physiological and pathophysiological cell processes, including migration and metastasis (137-139).

The role of CD44 in a variety of cell functions may be attributed to its complex structure (Figure 1.5). Even though it is a product of a single gene, it appears to have extensive size heterogeneity, ranging from the standard form (sCD44; 85-95kDa) to the larger variants (vCD44; up to 200kDa). The observed size variation can be partially due to differential glycosylation, since all the CD44 isoforms are highly glycosylated, but most of the variation in size is generated by alternative splicing of up to 12 exons, ten of which are present in the proximal extracellular region, and the other two in the cytoplasmic extension (140, 141).

The HA binding ability is common to all CD44 isoforms, however, the structural differences that result from N- or O-glycosylations can significantly alter the ability to bind hyaluronan, as well as influence cell behaviour and motility (142, 143). In addition, the expression of certain variant isoforms has been associated with tumour progression and metastasis (138, 143, 144). There is ample evidence for the importance of CD44 expression in the progression of many tumour types (145), as well as for its expression on cancer-initiating cells (CICs; also known as cancer stem cells) (146, 147).

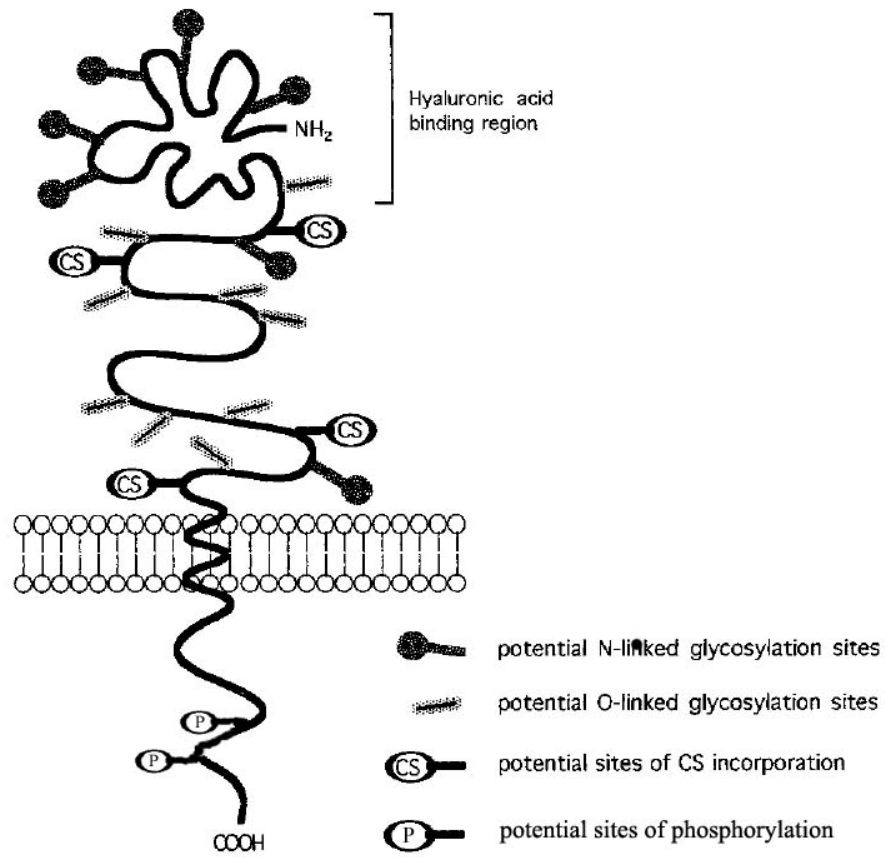


**Figure 1.5 – CD44 Structure.** Graphic representative of CD44 molecule showing potential N- and O-linked sugar residues and CS (chondroitin sulfate side chains) incorporated into the extracellular domain and serine phosphorylation sites in its intracellular domain (Modified from Martegani *et al.*, 1999 (1)).

### 1.5.1 CD44 in cancer

How CD44 promotes tumour growth and metastasis still remains poorly understood. Although roles for alternative splicing and variable glycosylation have been extensively investigated, the mechanism by which CD44 coordinates structural and signalling events to elicit complex cellular responses remains unclear. In melanoma, CD44 is widely expressed and it has been suggested to play a role in tumorigenicity and metastasis formation (148, 149). It appears that different variant isoforms have distinct expression patterns in melanocytes, naevi and primary and metastatic malignant melanoma, but the role of each isoform in melanoma progression needs further investigation (150, 151).

Work from our group and others has shown that CD44 can signal through proteins associated with its cytoplasmic tail that include members of the Src family of kinases (3, 143, 152). Several known serine phosphorylation sites present within the cytoplasmic tail are likely to regulate these events (Figure 1.5). Indeed, upon cell activation, the phosphorylation state of CD44 undergoes complex changes. Two specific serine residues (Ser291 and Ser316) have been shown to regulate CD44-dependent chemotaxis in response to phorbol ester (153). Additionally CD44 is known to be cysteine palmitoylated on two known sites in its cytoplasmic tail, which has implications for targeting to lipid rafts and signalling (3).

Investigating a functional association between CD74 and CD44 was first prompted by the studies of Naujokas *et al.* (1993) in T-cell activation, prior to the identification of MIF as an extracellular ligand for CD74 (122). In 2006, Shi *et al.* identified CD44 as a co-receptor responsible for providing the signalling arm for the complex. They utilised COS-7/M6 cell lines engineered to stably express CD74 or CD44, their combination, or CD74 together with a truncated CD44 lacking its cytoplasmic signalling domain. Their results led to the conclusion that CD74 alone mediated MIF binding; however, MIF-induced signalling required the coexpression of full-length CD44. Furthermore, MIF binding was associated with the serine phosphorylation of CD74 and CD44. This work established CD44 as an integral member of the

CD74 receptor complex leading to MIF signal transduction (2) (Figure 1.6). In addition, the MIF/CD74/CD44 complex was shown by several authors to induce ERK phosphorylation via a Ras-Raf-MEK pathway and also Akt activation (downstream of Src and PI3K). Such activation has important consequences such as enhancing proliferation and preventing apoptosis (2, 107, 154, 155).

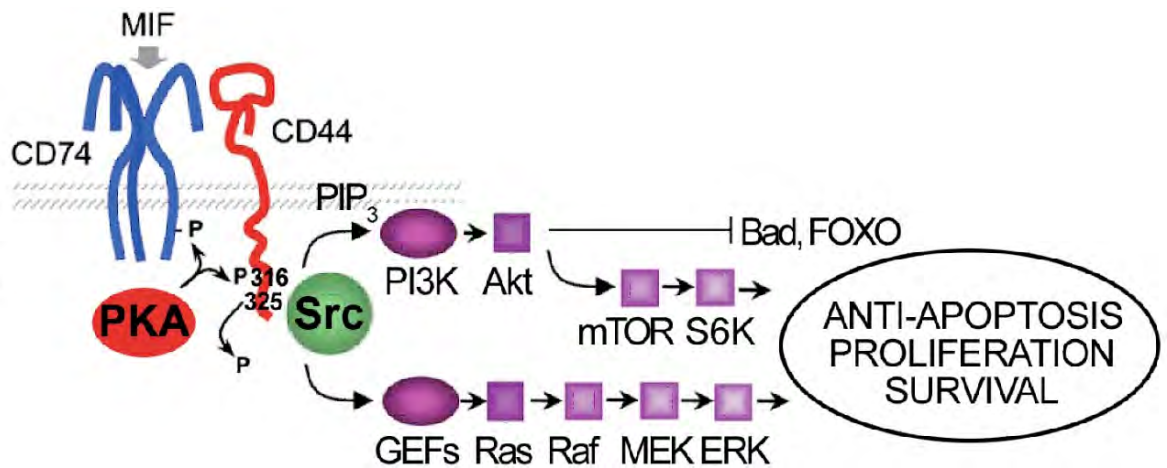


**Figure 1.6 – Model of the MIF-CD74-CD44 signalling complex.** MIF binds to its receptor CD74 with activation of downstream pathways occurring through CD44. MIF can activate both the MAPK/ERK and the PI3K/Akt pathways in immunological systems but the details of MIF-signalling are poorly defined in cancers (Modified from Shi *et al.*, 2006 (2)).

### 1.5.2 The dual nuclear signalling roles of CD44

In addition to the engagement of signalling molecules such as the Src-family kinase, understanding the signalling function of CD44 is further complicated by the occurrence of two discrete signalling mechanisms involving the translocation of CD44 to the cell nucleus. One involves proteolytic cleavage of the molecule prior to the translocation; the other involves the intact CD44 molecule.

First, CD44 is known to undergo sequential proteolytic cleavages in the extracellular domain and intramembranous domains. This process results in the release of the soluble ectodomain of CD44 from the membrane-bound C-terminal fragment (CD44EXT), and the release of an intracellular domain (ICD) fragment (Figure 1.7) (156-158). The ectodomain cleavage of CD44 contributes to the regulation of cell attachment to and migration on HA matrices (156, 157). The proteolytic cleavage of CD44's ectodomain has also been implicated in the malignancy of several tumours, including melanoma (159), with soluble CD44 levels in the serum correlating with tumour burden for non-Hodgkin's lymphoma, and gastric and colon carcinoma (160-162).

The cleavage of CD44 is regulated by a number of extrinsic and intrinsic mechanisms including extracellular Ca<sup>2+</sup> influx, the activation of protein kinase C (PKC), and the activation of Rho family small GTPases, Rac and Ras oncoproteins (163, 164). Furthermore, the metalloproteinases ADAM10, ADAM17 and MMP14 have been implicated in the shedding of CD44 from various tumour cells. Specifically in melanoma, ADAM10 is thought to be the constitutive functional sheddase of CD44 (156, 165).

After the extracellular cleavage and shedding of CD44 ectodomain, the protein further undergoes a regulated intramembrane proteolysis (RIP) by the presenilin- $\gamma$ -secretase complex. Proteolysis by this enzyme complex is a mechanism common to many transmembrane receptors. The most well-known substrate for the complex is the amyloid protein precursor

(APP), which undergoes successive proteolysis and generates amyloid  $\beta$ -protein ( $A\beta$ ) that characteristically deposits in the brain in Alzheimer disease (166). Similarly, CD44 transmembrane cleavage by the presenilin- $\gamma$ -secretase complex leads to the generation of a CD44 intracellular domain fragment (ICD) (3, 167). The ICD then translocates to the nucleus and promotes transcription of a number of genes mediated by the transcriptional co-activator CBP/p300. One of the target genes is CD44 itself, with the ICD increasing CD44 mRNA to provide a positive feedback mechanism for regulating CD44 expression (Figure 1.7) (156, 168). Furthermore, the CD44 ICD shows transforming activity, suggesting that CD44 shedding may not only affect metastasis, but also earlier events in tumourigenesis (168, 169). Thus translocation of the CD44 ICD can be viewed as an integral component of its signalling function.

The second CD44 nuclear signalling pathway comes from two recent reports suggesting that the whole CD44 molecule can be internalized and translocated to the nucleus to regulate transcription (170, 171). In the first report, Lee *et al.*, (2009) showed that full-length CD44 is internalised and translocated into the nucleus of colon (HT-29) and lung cancer (H1299) cell lines, where it forms a complex with STAT3 and p300, binds to the cyclin D1 promoter and enhances cell proliferation (171). In the second report in 2010, Janiszewska *et al.* showed full-length CD44 localises to the nucleus of several cell types, including prostate carcinoma (PC3), fetal fibroblasts (MRC5) and mammary epithelial cells (MCF10A) and suggested that the full-length protein is imported from the cytoplasm to the nucleus by the transportin1 carrier (170).

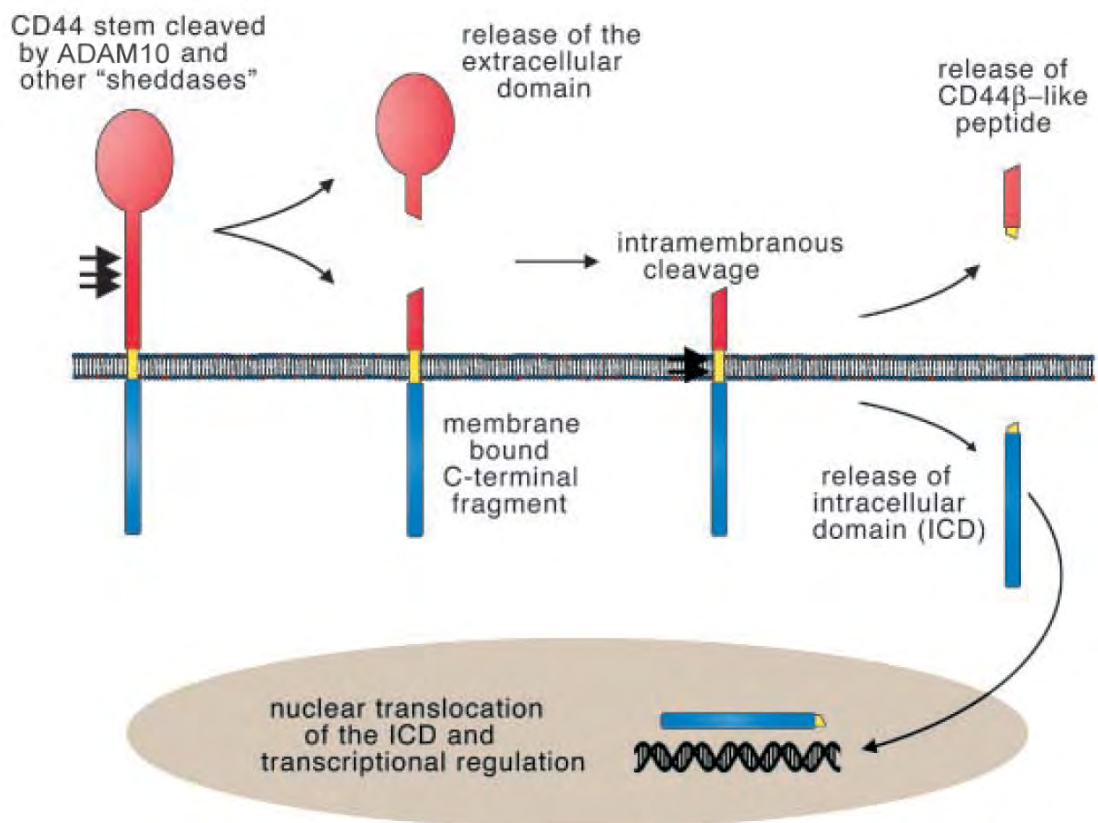


**Figure 1.7 – CD44 proteolytic cleavage.** Extracellular region of CD44 is cleaved by ADAM10, ADAM17 and MMP14, which triggers the intramembranous cleavage by presenilin- $\gamma$ -secretase. These sequential cleavages result in the release of the soluble ectodomain of CD44 and the release of an intracellular domain (ICD) fragment, which has been shown to be involved in nuclear signalling (Adapted from Thorne *et al.*, 2004 (3)).

## 1.6 Chemokine receptors and MIF signalling

Chemokines are the chemoattractant members of the cytokines, and their function is well known in inflammation, where they guide leucocytes to specific sites. Moreover, they have also been shown to be present on multiple cell types, including endothelial cells and tumour cells, and may affect proliferation and the promotion of angiogenesis. Indeed, specific chemokines and their receptors have been shown to play important roles in the metastatic process (172).

MIF is not a member of the chemokine family, but it has been recognised as having chemokine-like properties and is classified as a chemokine-like function (CLF) chemokine (116, 173). Similar to chemokines, MIF promotes directed migration and recruitment of leukocytes into infectious and inflammatory sites, and it is produced by a variety of cell types in addition to immune cells including endocrine, endothelial, and epithelial cells (96). Increasing evidence suggests that inflammation is closely associated with many types of cancer, with inflammatory pathways originally designed to defend against infection and injury, found to promote an environment favouring tumour growth and metastasis. MIF is therefore ideally placed in providing a direct link between the processes of inflammation and tumour growth (174).

It was recently demonstrated that, in addition to binding to CD74, MIF can also bind with high affinity to CXCR4 and CXCR2 (116, 175). Of these two receptors, melanomas rarely express CXCR2, and therefore the remainder of this section will focus on CXCR4. CXCR4 is one of the most studied chemokine receptors due to its role as a co-receptor for HIV entry (176). It is a seven transmembrane domain, G-protein-coupled receptor expressed by a wide spectrum of cells. CXCR4 was shown to be involved in a variety of migratory, proliferative and survival signalling cascades, including ERK and Akt pathways (177). Among the chemokine receptors, CXCR4 is by far the most commonly overexpressed in human cancers, being present

in more than 23 human malignancies and it appears to be associated with tumour progression and metastatic spread (178-182).

The MIF/CXCR4 axis has been shown to promote the atherogenic and inflammatory recruitment of leucocytes. The downstream signalling pathways activated by MIF/CXCR4 are largely unknown, but inhibitor studies implicate the Akt pathway in MIF-mediated monocyte chemotaxis and T cell activation (183). Receptor binding studies showed that MIF can individually bind to CD74 or CXCR4 with high affinity independent of whether the other receptor type was co-expressed; yet co-expression of CD74 with CXCR4 as it occurs on monocytes amplifies MIF-triggered responses (116). Schwartz *et al.* showed that CXCR4 and CD74 can form a complex under endogenous conditions in monocytes and T cells. This complex is responsive to MIF, as MIF-triggered CD74-dependent Akt activation in T cells was blocked by AMD3100, a small molecule inhibitor of CXCR4, as well as by CD74 and CXCR4 antibodies (183). Furthermore, the CD74/CXCR4 complex was recently shown to promote clathrin-dependent endocytosis of MIF in HEK293 and HeLa cells, and the use of inhibitors to reduce endocytosis reduced MIF-stimulated Akt signalling, suggesting that MIF signalling is in part due to endosomal signalling mechanisms (184).

The MIF/CXCR4 axis has also been described in cancer. The presence of an autocrine MIF-CXCR4 loop was described for the drug-resistant metastatic colon carcinoma cell line HT-29 cells. HT-29 do not express either CXCR2 or CD74, and the autocrine MIF-CXCR4 loop was shown to enhance the invasive potential of cancer cells and promote cell proliferation (185). In addition to HT-29 cells, rhabdomyosarcoma (RMS) cell lines also highly express and secrete MIF, which enhances adhesion of these cells through CXCR4 and CXCR7. In RMS cells MIF induces phosphorylation of MAPK and Akt, stimulates cell adhesion, enhances tumour vascularization, but surprisingly decreases recruitment of cancer-associated fibroblasts (CAF). Interestingly, when MIF is downregulated in RMS cells that are then injected *in vivo* into immunodeficient mice, the formation of larger tumours that displayed higher stromal-cell support

was observed. This *in vivo* observation suggests that the autocrine/paracrine MIF-CXCR4/CXCR7 axis plays an important pleiotropic role in RMS growth (179).

In melanoma cells, several chemokine receptors have been described, including CXCR4. The levels of CXCR4 expression are higher in melanoma compared to normal melanocytes and work from different groups points to a role for this receptor in promoting melanoma metastasis (186, 187). Indeed, CXCR4 is widely expressed and active in human melanoma metastasis, where it was shown to promote ERK activation, cell migration and cell growth (188). CXCR4 expression on tumour cells was also correlated with poor prognosis in patients with malignant melanoma (189-191). To date, a direct link between MIF and CXCR4 remains to be elucidated in melanoma.

## 1.7 Hypothesis and Aims

Despite intensive research over many years, malignant melanoma remains refractory to conventional therapy. Once the tumour progresses beyond the primary stage which can be removed surgically the prognosis is extremely dire. More recent work has pointed to the importance of autocrine cytokine production, and also of the Akt signalling pathways being important factors in driving melanoma growth and dissemination. However to date, this knowledge has not been exploited towards novel therapies.

Depending on the cellular context and stimulation status, MIF can bind to different receptor proteins and trigger several signalling pathways. MIF is known to bind to CD74 and it has also been identified as a non-cognate ligand of the chemokine receptor CXCR4. MIF signalling through CD74 requires the recruitment of a co-receptor, CD44, which provides the signalling arm to the complex. Furthermore, CD74 has also been shown to form active receptor complexes with CXCR4, but it is not known if CXCR4/CD74 complexes comprise CD44 or whether CD44 can be recruited to such complexes.

CD44 is the major adhesion molecule expressed in most human cell types and implicated in a wide variety of physiological and pathological processes, including the regulation of tumour cell growth and metastasis. The broad spectrum of functions suggests that CD44 can transduce multiple intracellular signals; however, it remains unclear how CD44 acts as a signal transduction molecule. CD44 undergoes sequential proteolytic cleavage in the ectodomain and intramembranous domain, resulting in the release of the soluble ectodomain of CD44 and the release of an intracellular domain (ICD) fragment. The ICD can directly interact with the transcriptional machinery, resulting in the regulation of several genes, including CD44 itself. Although the intramembranous cleavage of CD44 has been well described and characterised, followed by translocation of the CD44 ICD to the nucleus, there is also evidence suggesting that

the whole CD44 molecule is internalized and translocated to the nucleus where it can participate in signalling.

My overarching hypothesis is that autocrine MIF signalling plays an important role in melanoma growth, survival and metastasis; that this signalling is achieved through receptors complexes including CXCR4, CD74 and/or CD44, which are known to be present on the surface of a high proportion of human melanomas; furthermore these pathways present novel targets for the treatment of some cases of melanoma refractile to chemotherapy.

The three specific aims of this project were to:

- Define the expression of MIF and its known receptors (CD74, CD44 and CXCR4) in clinical samples of primary and metastatic melanoma and define any association with clinical outcome.
- Characterise the expression of MIF and its receptors in a panel of human melanoma cell lines and identify the functional outcome of MIF signalling *in vitro* and downstream pathways involved in this process.
- Investigate mechanisms of MIF signal transduction in melanoma, particularly the receptors employed in delivering the MIF signal.

## **Chapter 2**

### **Materials and Methods**

## **2.1 Cell culture**

### **2.1.1 Cell lines and culture conditions**

The melanoma cell lines utilised throughout this thesis have been described in previous studies (192-198). MM200, Me1007, Me4405 and IgR3 were derived from primary melanomas; MelFH, MelCV and MelRMu were derived from lymph node metastases; MelRM was derived from a bowel metastasis. Melanoma cell lines with the prefix Mel were isolated from fresh surgical biopsies from patients attending the Sydney and Newcastle Melanoma Units, and kindly provided by Prof. XD Zhang (University of Newcastle) and Prof. Peter Hersey (University of Sydney) (192). The C32 (ATCC #CRL1585) and WM-115 (ATCC #CRL-1675) cell lines were derived from primary melanoma. MSM-M1 and MSM-M2 were isolated from a sub-cutaneous nodule and lymph nodes, respectively, of two patients with disseminated melanoma (ATCC #CRL9822 and #CRL9823, respectively) (193). LiBr was a secondary malignant melanoma cell line (198). MV3 was established from a fresh human melanoma metastasis (196). SK-Mel-110 and SK-Mel-28 (ATCC #HTB-72) are two of a very extensive series of melanoma lines isolated by T. Takahashi and associates (197). MeWo was originally derived and established from a lymph node metastasis (ATCC #HTB-72) and 70W is a WGA (wheat germ agglutinin) mutant of MeWo, which was isolated by sequential, stepwise selection in increasing concentrations of WGA (195). LOX was established as a sub-cutaneous xenograft in nude mice from a lymph-node metastasis (194). All melanoma cells were cultured in Dulbecco's modified Eagle's medium (DMEM; Lonza) supplemented with 5% of heat-inactivated foetal bovine serum (FBS; Sigma-Aldrich) at 37°C in a humidified atmosphere of 5% CO<sub>2</sub>.

Non-melanoma cell lines used were the human colorectal adenocarcinoma cell line HT-29 (ATCC #HTB-38) and immortalised mammary epithelial cells MCF-10A (ATCC #CRL-10317). The MCF-10A cell line was cultured in DMEM:F12 (Lonza) supplemented with 5% horse serum, 20ng/mL epidermal growth factor (Sigma), 0.5µg/mL hydrocortisone (Sigma),

100ng/mL cholera toxin (Sigma) and 10µg/mL insulin (Sigma). The HT-29 cell line was maintained in DMEM supplemented with 10% of FCS. Both cell lines were similarly cultured at 37°C in a humidified atmosphere of 5%CO<sub>2</sub>. For the experiments involving MCF10A cells grown as acini (Chapter 5), slides were supplied by Dr. Rick Thorne (University of Newcastle).

### **2.1.2 Cryostorage of cells**

Cell lines designated for storage in liquid nitrogen for revival at a later date were gently harvested with trypsin (0.05%)/EDTA (200mg/L) and pelleted by centrifugation at 200 x g for 5 minutes. Cells were resuspended in freezing media (10% dimethyl sulfoxide (DMSO) in FCS) at ~1X10<sup>6</sup> cells/mL and aliquots taken into cryotubes before being cooled at -80°C for 2-4 hours and transferred to liquid nitrogen for storage.

### **2.1.3 Revival of cells from liquid nitrogen storage**

When required, preserved cells were removed from liquid nitrogen and thawed quickly in a 37°C water bath. Cells were then added to 10mL of warm complete medium, mixed gently and pelleted by brief centrifugation at 200 x g. The supernatant was removed; the cells were resuspended in complete medium and grown as described in Section 2.1.1.

### **2.1.4 Cell culture in hypoxic conditions**

When indicated, cells were grown under hypoxic conditions (0.1% O<sub>2</sub>; 5% CO<sub>2</sub>). An incubator insert chamber (BioSpherix, #C-274) was connected to a carbon dioxide and oxygen controller (PRO-OX C21, BioSpherix). The system uses compressed nitrogen and carbon dioxide injection and mixing to obtain oxygen levels of 0.1% and CO<sub>2</sub> levels of 5%. Control cells growing under normoxia conditions were placed in the same incubator, outside the hypoxia chamber (21% O<sub>2</sub>, 5% CO<sub>2</sub>).

## 2.2 Immunohistochemistry

Sections were prepared from archival paraffin tissue blocks from 40 different patients, consisting of 12 naevi, 13 primary melanoma and 15 metastatic melanoma samples. The sections were processed for antigen retrieval using the microwave method and citrate buffer (Sodium Citrate 0.05M in PBS, pH 6.0). Briefly, slides were placed into a jar and covered with citrate buffer. The jar was placed in a standard microwave at high power for 13 minutes until the solution started to boil and then kept at medium power for further 15 minutes. Sections were then allowed to cool for 10 minutes and washed with PBS for 5 minutes. Endogenous peroxidase was quenched by adding 0.3% hydrogen peroxide (H<sub>2</sub>O<sub>2</sub>) for 30 minutes. Next, sections were blocked with normal horse serum (15µL in 1mL of PBS; Vector; #PK6200) and incubated with anti-human MIF antibody (1:100 in PBS with 1% BSA; R&D Systems) for 30 minutes followed by a 5 minutes wash with PBS and incubation with anti-mouse biotinylated secondary antibody (15µL in 1mL PBS with 1% BSA; Vector; #BA-2001) for 30 minutes. After another wash with PBS for 5 minutes, detection was performed by incubating sections with avidin-biotin complex (ABC) reagent (Vector; #PK6200) for 30 minutes, washing for 5 minutes in PBS and incubating with VIP substrate (purple colour; Vector; #SK4600) until desired stain intensity developed (2-15 minutes). Sections were then rinsed in tap water, counterstained with Methyl Green (DAKO), and mounted into glass slides (Livingstone).

## 2.3 *In Silico* analysis of microarray datasets

The normalised data files from publically available microarray gene expression datasets from NCBI's gene expression omnibus (GEO) database (<http://www.ncbi.nlm.nih.gov/geo/>) were used to determine the pattern and level of expression of genes of interest. To study *MIF* and *MIF* receptor expression during melanoma progression, the GEO dataset GSE4587 was used because it contained melanocytic lesions of different stages, from normal skin to metastatic melanoma. Samples were separated in two groups based on hierarchical clustering performed

previously (199). Group 1 was denominated “early-stage” and contained the normal skin, benign naevi and in situ melanoma samples. Group 2 was the “advanced-stage” since it contained the VGP melanoma, RGP melanoma and melanoma-positive lymph nodes (199). Relative transcript levels of MIF, CD74, CD44 and CXCR4 were extracted from the dataset and displayed in bar graphs (Chapter 3). Statistical analysis was based on Mann-Whitney test comparing gene expression in “early-stage” and “advanced-stage” samples. The software used for generating the box plots and statistical analysis was GraphPad Prism 4.

To verify whether MIF and MIF receptor expression were prognostic in melanoma, microarray data with associated clinical outcomes was used. The main dataset used was GSE8401, consisting of samples from 31 patients with primary melanoma and 52 patients with metastatic melanoma and analysis were conducted on each classification group. The tumour biopsies were segregated into high and low expressors for each gene based on an upper 50% cut off of expression level and associated with the available survival data. The primary end point for the survival analyses was disease-specific survival, which was measured from the date of diagnosis to disease-specific death, or otherwise censored at the time of the last follow-up or at non-disease-related death. Time to disease-specific death was plotted as Kaplan-Meier survival curves followed by cox proportional hazards analyses. Two additional datasets, GSE22153 and GSE22154, containing only melanoma metastases were also used to complement the analysis. Survival analyses were carried on in collaboration with Dr. Tim Molloy (Garvan Institute Sydney).

## **2.4 Whole cell protein extraction**

Culture media were removed from cells and discarded. The cells were washed with phosphate-buffered saline (PBS) by gently rocking the flask, and were released from the culture flask by the addition of Trypsin/EDTA and incubation at 37°C until cells were completely dissociated from the substratum. Trypsin was neutralised by the addition of complete medium.

The cell suspension was then collected and cells were counted using an automatic cell counter (ADAM-MC, Digital Biosciences) as described in Section 2.11. The cell suspension was then centrifuged at 200 x g for 5 minutes. The supernatant was discarded and the cell pellet was washed with ice cold PBS and collected by centrifugation at 200 x g for 5 minutes. Cell pellets were then resuspended in ice-cold NDE lysis buffer (1% Nonidet P-40, 0.4% sodium deoxycholate, 66mM EDTA, 10mM Tris-HCl, pH 7.4) supplemented with protease and phosphatase inhibitors (Complete protease inhibitor mixture and PhosSTOP, respectively; Roche Applied Science) at  $\sim 10^7$  cells/mL, and kept on ice for 20 minutes to lyse. The lysate was then transferred to 1.5mL centrifuge tubes and centrifuged at 10,000 x g for 15 minutes at 4°C to pellet insoluble material. The supernatant was stored at -20°C for later analysis.

## **2.5 BCA Protein Assay**

As required, protein concentrations were determined using the colourimetric bicinchoninic acid (BCA) protein assay reagent (Pierce #23227) adapted to 96 well plates. This assay is compatible with detergents and can measure insoluble proteins. The unknown protein samples for concentration determination were usually diluted 1/10 with water. A 50µL aliquot of the diluted sample was then placed in triplicate into the wells of a transparent 96-well plate. To each sample volume, 200µL of the BCA reagent, which was prepared by mixing 50 parts of BCA reagent A with 1 part of BCA reagent B (1:50) was then added. The 96-well plate was then sealed with parafilm and incubated at 37°C for 30 minutes. The absorbance was then read at 562nm using the SpectraMAX 250 spectrophotometer and the accompanying SOFTmax™ software. Protein concentrations were determined by comparing to a BSA standard curve ranging from 0-1000 µg/mL and multiplying by the dilution factor used for the sample.

## 2.6 SDS-PAGE electrophoresis

In general, protein samples were separated by SDS-PAGE using the standard Tris-glycine system. Resolving gels were prepared using a 40% stock solution of acrylamide and bis-acrylamide at a ratio of 29:1 (BioRad #161-0146), which was mixed with 4X resolving gel buffer (1.5M Tris, pH 8.8 and 0.4% SDS), ammonium persulphate (APS) and N,N,N',N'-tetramethylethylenediamine (TEMED). The final solution (375mM Tris, pH 8.8, 0.1% SDS, 0.1% APS and 0.01% TEMED) was poured in the electrophoresis apparatus, gently covered with water and let to polymerize for ~30min at room temperature (RT). The final concentration of acrylamide was 10-15%, with resolving gels of higher acrylamide composition used to analyse proteins with lower molecular weight. Stacking gels were prepared using 40% acrylamide/bis-acrylamide solution, 4X stacking gel buffer (0.5M Tris, pH 6.8 and 0.4% SDS), APS and TEMED. The final solution (125mM Tris, pH 6.8, 0.1% SDS, 0.1% APS and 0.01% TEMED) was poured on top of the polymerized resolving gel and an appropriate multi-well comb was placed in the solution before polymerization. Stacking gel was left to polymerize for at least 90min at RT.

In preparation for electrophoresis separation, cell lysates were diluted in 6X Sample Buffer (final concentration 1.5% SDS and 10% glycerol, 62.5mM Tris-HCl, pH6.8, 0.0025% bromophenol blue and 0.5mM DTT) and heat denatured at 95°C for 5 minutes. A total of 30-50µg of protein was loaded on the gels in Tris-Glycine running buffer (25mM Tris, 192mM glycine and 0.1% SDS, pH approx. 8.6.) with one well containing 7µL of PageRuler Prestained Protein Ladder (Fermentas) as a molecular weight marker. Gels were electrophoresed at 120V until the dye front reached the bottom of the gel (60-90min).

For MIF detection, precast Tris-tricine 16% gels (Invitrogen #EC66955) were used for better resolution of low molecular weight proteins. Samples were diluted in 2x Tris-tricine sample buffer (Invitrogen #LC1675) and run in Tris-tricine running buffer (Invitrogen #LC1676) according to manufacturer's directions.

## 2.7 Western Blot Analysis

Proteins present within the polyacrylamide gels were transferred to nitrocellulose membranes (Amersham, #RPN303D) in cold transfer buffer (20mM Tris, 150mM Glycine, 10% methanol). Membranes were washed in TBST (50mM Tris, 150mM NaCl, 0.05% Tween 20, pH 7.6) and were blocked with blocking buffer (5% milk or 5% BSA in TBST) for at least 1 hour at room temperature. Membranes were then incubated with primary antibodies diluted in the blocking buffer at titred concentrations, as detailed in Table 2.1, at 4°C overnight. Primary antibodies used were: MIF (R&D #MAB289); CD74 (mAb clone FMC14 (200)); CD44 (mAb clone Hermes-3); CD44 ICD (TransGenic Inc., K0601); CXCR4 (Abcam #Ab2074); CXCR2 (BD Pharmingen™, #555932); pAkt and total Akt (Cell signalling technology, #9271 and #9272 respectively); Cyclin D1 and CDK4 (Santa Cruz Biotechnology, INC, #sc-20044 and #sc-23896 respectively); p27<sup>Kip1</sup> (BD Transduction Laboratories™ #610242) and GAPDH (Santa Cruz #sc-25778). After washing with TBST three times for 5 minutes, membranes were incubated with secondary antibodies diluted in blocking buffer (1/5000 dilution). Secondary antibodies used were horseradish peroxidase (HRP)-conjugated anti-mouse or anti-rabbit immunoglobulins (BioRad, #1706516 and #1706515 respectively). Detection was accomplished by incubation in luminol buffer (1.25mM 3-Aminophthalic acid hydrazide (luminol), 200µM (E)-3-(4-hydroxyphenyl)-2-propenoic acid, 4-hydroxycinnamic (p-coumaric) acid, 0.009% (w/v) H<sub>2</sub>O<sub>2</sub> in 100mM Tris-HCl, pH 8.5) and bands were visualized using a cooled charge-coupled device camera system (Fuji-LAS-4000, Fujifilm Life Science Systems).

**Table 2.1 – Antibodies and dilutions used for specific applications**

Specificity	Source/Clone	Dilution per application		
		Western Blot	Flow Cytometry	Immunofluorescence
MIF	R&D #MAB289	1/1000	N/A	N/A
CD74	Clone FMC14 * (culture supernatant)	1/100	1/2	N/A
CD44	Clone Hermes-3 * (2.15mg/mL)	1/2000	N/A	1/430
CD44	Clone 3E8* (1.7mg/mL)	N/A	1/170	1/340
CD44	Clone E1/2* (culture supernatant)	N/A	N/A	1/5
CD44 V6	Clone Bu52 (Serotec)	N/A	N/A	1/200
CD44	Clone F10-44-2 (SouthernBiotech)	N/A	N/A	1/200
CD44 V6	Clone 2F10 (RD)	N/A	N/A	1/200
CD44	Clone 5F12 (NeoMarkers)	N/A	N/A	1/50
CD44	Clone Bu52 (Ansell)	N/A	N/A	1/100
CD44 ICD	TransGenic Inc. #K0601	1/20	N/A	N/A
CXCR4	Abcam #Ab2074	N/A	1/100	N/A
CXCR2	BD Pharmingen™ #555932	N/A	1/50	N/A
pAkt	Cell Signalling, #9271	1/200	N/A	N/A
Akt	Cell Signalling, #9272	1/1000	N/A	N/A
Cyclin D1	Santa Cruz #sc-20044	1/200	N/A	N/A
CDK4	Santa Cruz #sc-23896	1/200	N/A	N/A
P27 <sup>Kip1</sup>	BD #610242	1/1000	N/A	N/A
GAPDH	Santa Cruz #sc-25778	1/5000	N/A	N/A
Cytochrome c	Clone 6H2.B4 BD Pharmingen	N/A	N/A	1/200

N/A: Not Applicable. \* In house antibodies

## **2.8 Quantification of Western blot using densitometry**

To quantitatively assess the different signals obtained in Western blot analysis, the intensity of the bands was quantified using the Multi Gauge software (Fujifilm). A window size was chosen to include one band for each measurement and the mean optical density (OD) obtained. The ratio was determined dividing the OD obtained for each protein immunoreactive band by the OD of a control band detected with the same sample. This was usually the housekeeping gene GAPDH, except for phosphorylated Akt (pAkt), for which the OD of the active phospho-protein was divided by the OD of total Akt, representing an index of Akt activation. The values obtained were then normalised against the respective control.

## **2.9 Flow Cytometry**

Cell surface expression of CD44, CD74, CXCR4 and CXCR2 on melanoma cell lines was analysed by flow cytometry. Briefly, cells were harvested using trypsin/EDTA, pelleted by centrifugation at 200 x g for 5 min, washed with PBS, resuspended in 100µL primary antibody diluted in PBS with 0.1% BSA to the required concentration (Table 2.1) and incubated for 30 min at room temperature. Cells were then washed with PBS, pelleted by centrifugation at 200 x g for 5 min and incubated with Alexa Fluor<sup>®</sup> 488 Goat anti-rabbit or anti-mouse secondary antibody diluted in PBS with 1% BSA (1/500; Invitrogen, #A31627 and #A11001 respectively) for 30 min at room temperature in the dark. After another wash with PBS, cells were resuspended in 300µL PBS for analysis on the FACS Calibur flow cytometer (BD Biosciences). Ten thousand cells were counted in each sample and data were analysed using the Cell Quest software package (BD Biosciences).

## 2.10 Small interfering RNA (siRNA) knockdown of gene expression

Melanoma cells were seeded in 6-well plates at  $1 \times 10^5$  cells per well and allowed to reach ~50% confluence before transfection. The siRNA sequences used are detailed on Table 2.2. On the day of transfection, for each well to be transfected, 5 $\mu$ L of Lipofectamine RNAiMAX (Invitrogen, #13778) was added to 250 $\mu$ L of Opti-MEM<sup>®</sup> reduced serum media (Invitrogen, #31985-070) and mixed gently. In a separate tube, 7.5 $\mu$ L of stock siRNA (20 $\mu$ M) was added to 250 $\mu$ L of Opti-MEM<sup>®</sup>. After 5 minutes, the siRNA and the lipofectamine RNAiMAX solutions were combined and incubated at room temperature for 20 minutes. After that, 500 $\mu$ L of the siRNA and lipofectamine complex was added to each well of a 6 well plate containing cells and 2.5mL of media, giving a final concentration of 50nM siRNA. After 18 hours the media were replaced and cells were incubated at 37°C in a 5% CO<sub>2</sub> incubator until the different assays were performed as indicated. The efficiency of protein knockdown by siRNA transfection was measured by Western blot analysis.

**Table 2.2– Small interfering RNA sequences**

<b>siRNA</b>	<b>Sequences</b>	<b>Source</b>
MIF 21	5'-UGGUGUUUACGAUGAACAUUTT-3'	Shanghai GenePharma Co.
	5'-AUGUUCAUCGUAAACACCATT-3'	
MIF 25	5'-UUGGUGUUUACGAUGAACAUUCGGCA-3'	Shanghai GenePharma Co.
	5'-UGCCGAUGUUCAUCGUAAACACCAA-3'	
MIF 36	5'-AUAGUUGAUGUAGACCCUGUCCGGG-3'	Invitrogen life technologies
	5'-CCCGGACAGGGUCUACAUCAACUUAU-3'	
MIF 37	5'-UUCCAGCCCACAUUGGCCGCGUUCA-3'	Invitrogen life technologies
	5'-UGAACGCGGCCAAUGUGGGCUGGAA-3'	
MIF 38	5'-UUGGUGUUUACGAUGAACAUUCGGCA-3'	Invitrogen life technologies
	5'-UGCCGAUGUUCAUCGUAAACACCAA-3'	
CD44 #1	5'-GUAUGACACAUAUUGCUUCTT-3'	Dharmacon
	5'-GAAGCAAUAUGUGUCAUACTT-3'	
CD44 #2	5'-CUGGACUCCAGAAGAACATT-3'	Shanghai GenePharma Co.
	5'-UGUUCUUCUGGAAGUCCAGTT-3'	
CD74 #1	5'-AAACUGACAGUCACCUCCAGTT-3'	Shanghai GenePharma Co.
	5'-CUGGGAGGUGACUGUCAGUUUTT-3'	
CD74 #2	5'-CAUGGGAUGAGGUACAGGGUTT-3'	Shanghai GenePharma Co.
	5'-ACCCUGUACCUCAUCCCAUGTT-3'	
CD74 #3	5'-GCGACCUUAUCUCCAACAATT-3'	Shanghai GenePharma Co.
	5'-UUGUUGGAGAUAAAGGUCGCTT-3'	
CD74 #4	5'-CACCUUGGACAAGACAAATT-3'	Shanghai GenePharma Co.
	5'-UUUGUCUUGUCCAAGGGUGTT-3'	
CD74 #5	5'-GGCCAUGGUUCACAUAUAGATT-3'	Shanghai GenePharma Co.
	5'-UCUAAUGUGAACCAUGGCCTT-3'	
CXCR4 #1	5'-CAGCUAACACAGAUGUAAATT-3'	Shanghai GenePharma Co.
	5'-UUUACAUCUGUGUUAGCUGGA-3'	
CXCR4 #2	5'-GAGUCUGAGUCUUCAAGUUTT-3'	Shanghai GenePharma Co.
	5'-AACUGAAGACUCAGACUCTT-3'	
CXCR4 #3	5'-GCAUGACGGACAAGUACAGTT-3'	Shanghai GenePharma Co.
	5'-CUGUACUUGUCCGUCAUGTT-3'	
NC	5'-UUCUCCGAACGUGUCACGUTT-3'	Shanghai GenePharma Co.
	5'-ACGUGACACGUUCGGAGAATT-3'	

## **2.11 Assessment of cell number and viability**

Cell number and viability were determined using an automatic cell counter (Digital Bio, ADAM-MC). For each analysis, a small sample of cell suspension was mixed with an equal volume of AccuStain Solution T or AccuStain Solution N (Digital Bio, ADR-1000) and pipetted on to a disposable plastic chip (Digital Bio, AD2K-200). The chip was loaded in the machine, and the cells that had been stained were recorded by a sensitive CCD camera. Both Solutions T and N contain the fluorescent dye propidium iodide (PI). In order to measure the total number of cells, Solution T contains a lysis solution to disrupt the plasma membranes of all cells because PI does not enter cells with intact cell membranes. Solution N is composed of the fluorescent dye (PI) and PBS, so when the cells were treated with this solution only the non-viable cells were stained and detected. The viability and total cell number was automatically calculated in the Adam-MC software after each measurement of the total cells and the non-viable cells.

## **2.12 Click-iT™ EdU flow cytometry assay**

The Click-It Assay was performed according to manufacturer's instructions (Invitrogen, #C35002). Briefly, 3 days after transfection with siRNA, cells were incubated with 5-ethynyl-2'-deoxyuridine (EdU; 10 $\mu$ M for 3 hours), a nucleoside analog to thymidine which is incorporated into DNA during active DNA synthesis. After 3 hours, cells were harvested with trypsin/EDTA, washed in 1% BSA in PBS, pelleted by centrifugation at 500 x g for 5 min and supernatant removed. Cells were then resuspended in 100 $\mu$ L of 1% BSA in PBS and transferred to suitable flow cytometer tubes (BD). Thereafter, 100 $\mu$ L of Click-iT™ fixative (Component D) was added to the flow tubes and mixed well to ensure a homogenous sample. The cells were incubated for 15 min at room temperature protected from light. After that, cells were washed with 3mL of 1% BSA in PBS and the supernatant removed. At this stage cells could be stored at 4°C for up to one week. On the day of analysis, the pellet was dislodged and 100 $\mu$ L of the saponin-based permeabilization and wash buffer (Component E) was added to the cells and mixed well. After

washing with the same buffer (Component E), cells were incubated for 30 minutes at RT with the Click-iT™ reaction cocktail containing the reaction buffer, CuSO<sub>4</sub>, fluorescent dye azide and reaction buffer additive. Cells were then washed one more time and incubated with Ribonuclease A (Component L) and CellCycle 488-red (7-AAD, Component K) at RT for 30 minutes for measuring DNA content and cell cycle distribution. EdU incorporation was detected using a FACS Calibur flow cytometer (BD Biosciences). Ten thousand cells were counted in each sample and the percentage of cells in S-phase was determined using the Cell Quest software (BD Biosciences).

### **2.13 Soft Agar Colony Formation Assay**

The ability of cells to grow under anchorage-independent conditions was measured by a soft agar colony formation assay. To prepare the base agar layer, a 1.2% solution of sterile agar with low melt temperature (MetaPhor® Agarose) was melted in a microwave, cooled in a 42°C water bath, and mixed with equal volume of 2X DMEM containing 10% FCS to give a final concentration of 0.6% agar in 1X medium with 5% FCS. The DMEM/agar medium was then added to each well of a 6 well plate and allowed to set. For the top agar layer, 0.6% agar was melted, cooled in a 42°C water bath and mixed with equal volume of 2X DMEM 10% FCS to give a final concentration of 0.3% agar in 1x media with 5% FCS. The media with agar was kept at 42°C. Cells were harvested with trypsin/EDTA, counted using ADAM-MC cell counter (Digital Bio), and resuspended at an appropriate concentration ( $1 \times 10^4$  cells/mL) in the media containing 0.3% agar. Then, 1mL of the cell suspension was carefully applied to the base agar layer on each well ( $1 \times 10^4$  cells per well). Plates were incubated at 37°C for 3–4 weeks until colonies were formed. Colonies were then stained with 0.005% Crystal Violet and the number of colonies was determined using Axiovert 200M microscope (Zeiss). The size (diameter) of each colony was measured using the AxioVision Software (Zeiss) using the length measurement tool.

## **2.14 Cell proliferation and viability measurements using MTS reduction**

The number of viable cells after MIF knockdown under hypoxia or normoxia was measured using the CellTiter 96<sup>®</sup> AQueous One Solution Cell Proliferation Assay (Promega, #G3580), which is based on the reduction of the tetrazolium compound MTS. MTS is bio-reduced by the cells mitochondria into a coloured formazan product that is soluble in tissue culture medium. The quantity of formazan product as measured by the absorbance at 490nm is directly proportional to the number of living cells in culture. The assay was performed according to manufacturer's instructions. Briefly, cells were seeded into 96-well plates, treated as indicated, and then 20µL of the CellTiter 96<sup>®</sup> AQueous One Solution Reagent was added to each well containing the cells and 100µL of medium. Cells were incubated for 4 hours and the absorbance at 490nm was recorded using the SpectraMAX 250 spectrophotometer. The data obtained were plotted as a percentage of values obtained using control cultures.

## **2.15 Sub-cellular fractionation techniques**

### **2.15.1 Detergent lysis method**

To prepare nuclear and cytoplasmic cell fractions using the detergent lysis method, cells were grown in 60mm petri dishes. Cells were washed with PBS to remove any remaining media, harvested using trypsin/EDTA and collected into a 15mL tube. The cells were then washed three times with 10mL PBS, with centrifugation at 500 x g for 5min at 4°C between each wash. After removing the supernatant, cell pellets were resuspended in 1mL PBS and transferred to 1.5mL microcentrifuge tubes before further centrifugation at 1,500 x g for 3 min at 4°C. The supernatant was removed and pellets were resuspended in 1mL of 1x RSB (10mM Tris, pH 7.4, 10mM NaCl, 3mM MgCl<sub>2</sub>). Cells were swollen on ice for 3 minutes and then centrifuged at 1,500 x g for 3 minutes as above. The cell pellet volume was approximated, and 3 times this volume of RSBG40 lysis buffer (10mM Tris, pH 7.4, 10mM NaCl, 3mM MgCl<sub>2</sub>, 10% glycerol, 0.1% NP40) with 0.5mM DTT and 1x Protease inhibitors (Roche; PI) was added for resuspension.

Nuclei were pelleted at 5,000 x g for 3 minutes at 4°C and the supernatant containing the cytoplasmic protein fraction added to a new 1.5mL microcentrifuge tube. To collect the remaining cytoplasmic fraction, pellets were resuspended in RSBG40 buffer supplemented with 0.5mM DTT, 1x PI and 1% v/v NP40 and incubated on ice for 5 minutes. Following incubation, cells were centrifuged at 5,000 x g and the supernatant then added to the tube containing the cytoplasmic fraction. The remaining cell nuclei were washed in 500µL RSBG40 with centrifugation at 10,000 x g for 5 minutes at 4°C to remove any contaminating cytoplasmic protein. To isolate the nuclear protein fraction, remaining cell pellets were resuspended in 50µL NDE lysis buffer containing 1% SDS and transferred to a new 1.5mL microcentrifuge tube. Pellets were sonicated three times for 5-10 seconds to remove any genomic contaminants and then both cytoplasmic and nuclear fractions were stored at -80°C.

#### **2.15.2 Nitrogen decompression method**

Cell disruption by nitrogen decompression using a pressurised vessel is a rapid and effective way to homogenize cells and tissues, to release intact organelles, and to prepare cell membranes. Cells are placed in a pressure vessel and large quantities of oxygen-free nitrogen are dissolved in the cells under high pressure. When the pressure is released suddenly, the nitrogen bubbles out of solution, rupturing the cell membrane and releasing the cell contents (201). Cells were washed with ice-cold PBS and 2mL of HB buffer (0.25M Sucrose, 1mM EDTA, 20mM HEPES, pH 7.4) supplemented with protease inhibitors (PI, Roche) was added to each sub-confluent T175 flask and left on ice for 1h. Cells were then scraped and transferred to a 15mL tube on ice. The cell disruption bomb (Parr Instrument Company) was cleaned with 70% ethanol and kept on ice for 30 minutes. The cell suspension, together with a small magnetic stirring bar, was transferred to the chilled chamber of the cell disruption bomb, which was then assembled and connected to the nitrogen tank. The cell disruption bomb was charged to 550psi and the cell suspension left stirring at 4°C for 20 minutes using a magnetic stirrer. After that, the sample was released dropwise from the bomb into a clean 50mL tube. For cell fractionation, the homogenate was centrifuged at 1,000 x g for 15 minutes to pellet nuclei. The supernatant was

then centrifuged again at 20,000 x g and the mitochondrial fraction was pelleted. The supernatant was collected and ultracentrifuged for 1h at 100,000 x g to pellet the light membrane fraction and the supernatant was kept as the cytosolic fraction.

## **2.16 Immunofluorescence Microscopy**

Cells grown and adhered to glass coverslips were stained by an indirect immunofluorescence method as described previously by our laboratory (202). Briefly, glass coverslips were sterilised by baking and then aseptically placed in 24 well culture plates. Cells were added ( $\sim 5 \times 10^4$ /well) and cultured overnight. Before immunostaining, the cells were fixed in situ with 4% formaldehyde/5% sucrose solution for 5min at RT. Cells were permeated with 0.5% Triton-X100 in PBS for 5 min, at RT and washed 5 times in PBS. Coverslips were incubated with 3% BSA in PBS for 30 min at RT to block non-specific binding, and then rinsed once with PBS. The primary antibodies were diluted as appropriate (Table 2.1) in 0.1%BSA/PBS and incubated for 30-45 min at RT before three washes in PBS. In some experiments where two mouse antibodies were used the Zenon® kit (Invitrogen) using Alexa Fluor® conjugates was used to prepare direct fluorophore labelled-primary antibodies accorded to the manufacturer's instructions. The secondary antibodies, Alexa Fluor® conjugates, were added for 30-45 min at RT, before three washes in PBS. A solution of 4',6-diamidino-2-phenylindole (DAPI; Life Tehcnologies) was used to counterstain the nuclei of the cells. Coverslips were mounted onto glass slides using the SlowFade® Gold mounting reagent (Invitrogen) and immunostaining recorded as described using one of two imaging systems. Either Zeiss Axioplan 2 epifluorescent microscope fitted with an Axiocam MRm(v3) and Apotome slider (Carl Zeiss, Thornwood, NY) capable of both wide-field fluorescence and optical sectioning as previously reported (203). Micrographs were obtained using a PlanApochromat 63X Oil objective and processed using the Axiovision software package (v4.5). Images were subsequently exported to Adobe Photoshop CS2 to compile the final figures. Alternatively, images as optical sections were collected using a Zeiss Axiovert 100M fitted with a LSM510 confocal scanning system using sequential scan for each channel as previously described (204).

## **Chapter 3**

**MIF is differentially expressed during melanoma progression and is a prognostic factor for metastatic disease**

### **3.1 Introduction**

Macrophage migration inhibitory factor (MIF) is a multi-functional cytokine, which has been associated with inflammation. Moreover, MIF overexpression has been shown to have a role in tumourigenesis (205) and over the past few years, the role of MIF in both solid and haematological tumours has been established (95, 96). MIF influences tumour growth and progression in several ways, including induction of angiogenesis (97, 98), promotion of cell cycle progression (99, 100), inhibition of apoptosis (101) and inhibition of the lysing of tumour cells by natural killer (NK) cells (100, 102). MIF expression is upregulated in a variety of different tumour cells and appears to be involved in chemoresistance and to influence the prognosis in various malignancies (104, 206-208). Consequently, as reviewed in the following Section, MIF has been considered as a potential biomarker for a number of cancer types, particularly prostate, gastrointestinal, ovarian and breast cancer.

#### **3.1.1 MIF as a cancer biomarker**

One of the first clinical studies that examined MIF expression in human malignancy was performed in the context of prostate cancer. In this initial report, the authors observed an association of high serum levels of MIF in patients with prostate carcinoma. In addition, they also found that *MIF* mRNA was significantly higher in invasive prostate carcinoma epithelial cells compared with matched normal prostate epithelial cells (206). Since then, two further studies have extended these findings, indicating MIF as a possible marker for prostate cancer detection and disease progression (209, 210).

In tumours of the gastrointestinal tract, MIF was found to be highly expressed and secreted by colorectal carcinoma cells, and one report suggests that MIF levels have a high diagnostic value, being more specific and sensitive than CEA (carcinoembryonic antigen), one of the most frequently used tumour markers in clinical practice in detecting colorectal cancer (93). MIF is also highly expressed and secreted by esophageal squamous carcinoma cells, and

has been shown to correlate with differentiation and lymph node spread (211). In gastric cancer patients, MIF was found to be elevated in the serum and it was associated with enhanced angiogenesis and advanced stage disease. In support, several subsequent studies also suggest that MIF may be useful as a biomarker, either alone or in combination with other markers, for diagnosing and monitoring gastric cancer (212-214).

A study by Agarwal *et al.* demonstrated that epithelial ovarian cancer (EOC) cell lines, but not normal cells, secrete high levels of MIF *in vitro* and high levels of MIF were observed in the serum of patients with EOC but not in normal controls. These findings suggest that abnormal MIF expression may be related to the pathogenesis of ovarian cancer and MIF expression may serve as a specific marker for this malignancy (215). Prompted by their findings, the same authors have recently developed a novel multiplex assay for a combination of six serum biomarkers, including MIF, which shows high sensitivity (95.3%) and specificity (99.4%) for the detection of ovarian cancer (216, 217) and holds promise for the early detection of recurrent tumours, which are exceedingly difficult to treat.

In breast cancer, the involvement of MIF remains controversial. Jesneck *et al.* screened breast cancer patients and controls for different serum proteins and reported that MIF can be a valuable biomarker for detecting the presence of a breast lesion. However, circulating levels of MIF could not distinguish benign from malignant lesions, suggesting that this protein was more indicative of secondary effects such as inflammation rather than tumour invasion *per se* (218). Bando *et al.* identified MIF overexpression in 93 primary breast cancer tissues and notably, MIF levels and circulating MIF inversely correlated with nodal status (219). Another study by Xu *et al.* confirmed MIF overexpression in primary human breast cancer tissue and in this case, positive MIF expression was associated with disease-free but not overall survival (220). Thus, while there is consensus from these reports that MIF is overexpressed in human breast cancer, its functional correlation with breast tumourigenesis has remained unclear. To this end, Verjans *et al.* have suggested that there is a dual role for MIF in breast cancer: intracellular expression

of MIF is beneficial and may be indicative of good prognosis, since it was found to be highly expressed in non-invasive breast cancer cell lines but not in invasive ones; whereas extracellular MIF may play a pro-oncogenic role and may be a marker for unfavourable prognosis (133). While this notion still needs to be addressed, it is intriguing that the significance of MIF overexpression in breast cancer appears to contrast with that of other cancers.

### **3.1.2 MIF and melanoma**

MIF expression has also been studied in skin lesions, including benign and atypical naevi, melanoma and melanoma metastases. In the largest reported study to date, Miracco and colleagues examined the expression of MIF at both mRNA (55 cases) and protein levels (126 cases) in a range of cutaneous melanocytic tumours. These authors found that MIF transcript levels measured by qRT-PCR were higher in all types of melanocytic lesions compared to skin margins, with the highest expression occurring in atypical naevi and malignant melanoma (112). They also determined the expression patterns of MIF protein and these were largely associated with the measured mRNA levels in each tissue type examined. Notably they found strong cytoplasmic MIF positivity in most samples, but it was frequently heterogeneous, particularly in malignant tumours. There were differences in MIF sub-cellular localisation with both nuclear and cytoplasmic MIF protein expression reported in both atypical naevi and melanomas (112). Although these data provide some insight on MIF expression patterns in melanocytic tumours, to date there has been no study on the association of MIF expression with patient outcomes.

On the basis of findings that MIF expression appears to increase during melanoma progression *in vivo*, it is reasonable to propose that the levels of MIF expressed by individual tumours may correlate with their proliferative capacity. Moreover, if MIF signalling is significantly driving melanoma proliferation, high levels of MIF, and also MIF signalling receptors, may be indicative of poor disease outcome. Based on these hypotheses, the aims of the present

Chapter were therefore to investigate expression of MIF and its receptors in different stages of melanomogenesis using *in silico* analysis of publically available expression microarray data. The analysis of patient follow-up data detailing clinical outcome also affords an assessment as to whether MIF expression is prognostic in these studies. In addition, MIF expression and subcellular localisation was further investigated in tissue sections from different stages of melanoma by immunohistochemistry.

## 3.2 Results

### 3.2.1 MIF mRNA and protein expression in melanocytic tumours

As described in the previous section, there has been only a single study of any depth conducted on the subject of MIF expression in melanocytic tumours (112). Consequently, to independently confirm and validate these results, MIF expression was further investigated in melanoma, at both the mRNA and protein level.

Firstly, *in silico* analysis of microarray data (GEO data set GSE4587 (199)) comparing the relative transcript levels of MIF in staged melanoma against normal skin and naevi was performed as shown in Figure 3.1. In addition, the level and pattern of mRNA expression of known MIF receptors CXCR4, CXCR2, CD74 and CD44 were also determined. In the paper where this dataset was originally described, the authors performed hierarchical clustering and separated the samples into two groups which were termed “early-stage” and “advanced-stage”. The “early-stage” group contained the normal skin, benign naevi and *in situ* melanoma samples, while the “advanced-stage” contained the VGP melanoma, RGP melanoma and the melanoma-positive lymph nodes (refer to Figure 1.2) (199). The analysis showed that the expression levels of MIF in normal skin, naevi and *in situ* melanoma were lower than in the “advanced-stage” samples. Particularly, the highest expression of MIF was found on the lymph-node metastases samples (Figure 3.1A). Collectively, MIF expression was significantly higher in “advanced-stage” samples compared to “early-stage” (Figure 3.1A inset). Similarly, the MIF receptor CXCR4 was expressed at low levels in “early-stage” samples compared to higher levels in “advanced-stage” samples (Figure 3.1B). Expression of CD74, CD44 and CXCR2 were also analysed but CD74 and CD44 expression showed no significant difference across the samples (Figure 3.1C and D) and CXCR2 expression was either very low or absent (data not shown).

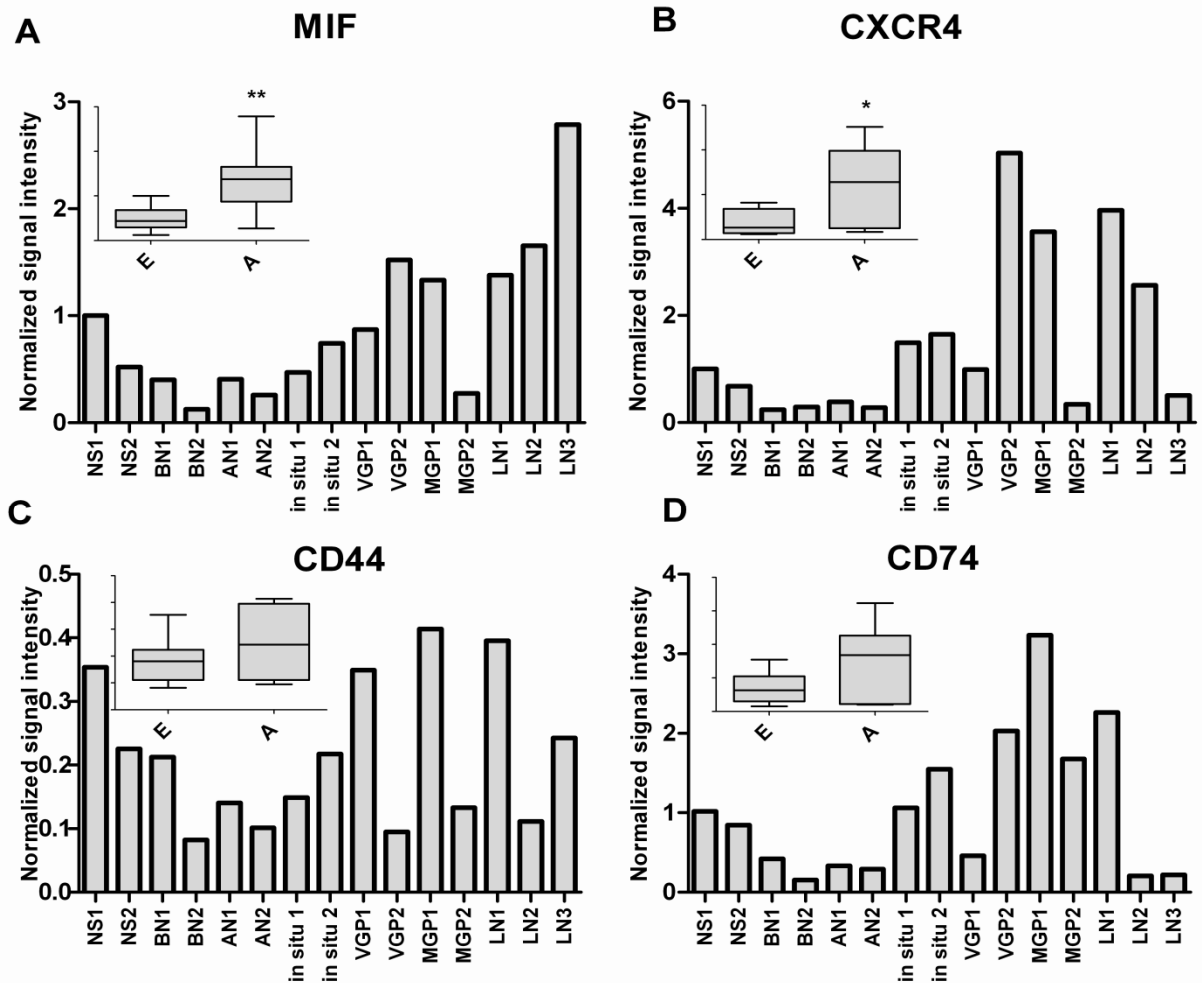


**Figure 3.1 – MIF and MIF-signalling receptor expression in melanocytic lesions measured using microarray data.** Levels of *MIF* (A), *CXCR4* (B), *CD44* (C) and *CD74* (D) expression in the two normal skin tissue samples (NS1; NS2), benign naevi (BN1; BN2), atypical naevi (AN1; AN2), melanomas in situ (in situ1; in situ2), VGP melanomas (VGP1; VGP2), MGP melanomas (MGP1; MGP2), and the three MGP melanoma-positive lymph nodes (LN1; LN2; LN3) were obtained from the microarray dataset GSE4587 as described in Chapter 2. Insets show the distribution of expression in the same samples divided in (E) early- and (A) advanced-stage. MIF and CXCR4 expression were higher on the “advanced-stage” samples compared to the “early-stage” samples. Distribution of transcript levels are summarised as box plots (n=8 early stage; n=9 advanced stage. Mann-Whitney test \*\*p<0.01; \*p<0.05).

Expression microarray data is a useful tool to study gene expression in a large number of samples; however the analysis of mRNA expression patterns by themselves can be insufficient for understanding the expression of protein products, since post-transcriptional mechanisms, including post-translational modification and degradation may influence the level of a given protein (221, 222). In the particular case of MIF expression in melanoma, it has been described that mRNA levels of *MIF* directly correlate with protein expression in different stages of melanocytic tumours (112). Nevertheless, to independently verify the results obtained from microarray data, a small cohort of surgical biopsies from patients attending the Sydney Melanoma Unit was used. The samples available for analysis consisted of 12 naevi, 13 primary melanoma and 15 metastatic melanoma samples and were submitted to immunohistochemistry using MIF monoclonal antibody.

In general the pattern of staining varied among the samples but it was mainly heterogenic nucleo-cytoplasmic staining (Figure 3.2 A-D). Only 3 out of 13 primary melanoma sections showed some MIF positivity, whereas metastatic melanoma sections showed positive MIF staining in 11 out of 15 cases (Table 3.1). Naevi tissue sections were positive for MIF in 8 out of 12 cases. MIF labelling intensity was visually determined, from - (no staining) to +++ (intense staining). The results confirmed that MIF is strongly expressed in metastatic melanoma but is expressed at significantly lower levels, or not detectable at all, in primary tumours (Table 3.1).

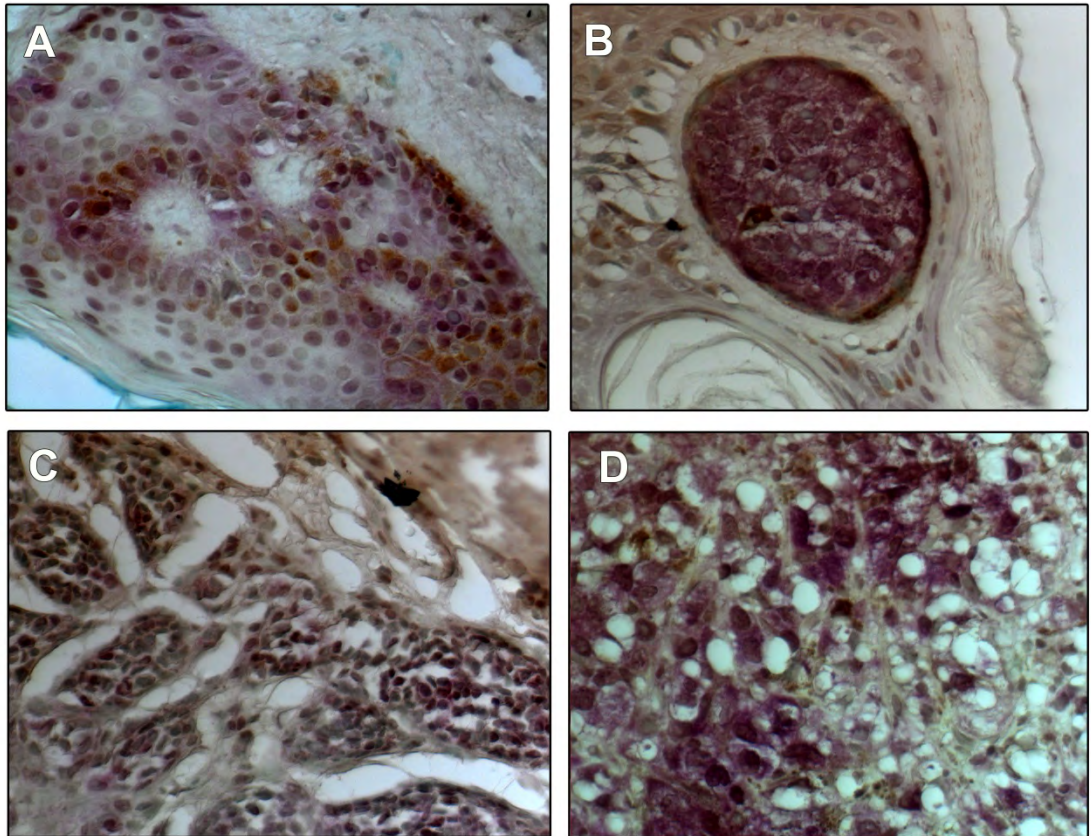


**Figure 3.2 – MIF immunohistochemistry staining in *ex-vivo* sections of different stages of melanocytic lesions.** Representative micrographs (40x magnification) showing examples of MIF positive staining as detailed in Table 3.1. Tissue sections representing: (A) benign naevus, (B) dysplastic naevus, (C) primary melanoma and (D) metastatic melanoma. Sections were prepared from archival paraffin embedded tissues and processed for antigen retrieval using Citrate buffer (0.05M, pH 6.0). Sections were incubated with anti-human MIF antibody with detection using Vectastain ABC and VIP substrate (purple colour). Slides were then counterstained with Methyl Green.

**Table 3.1** - MIF protein expression detected by immunohistochemistry in human naevi, primary melanoma and metastatic melanoma.

<b>MIF immunoreactivity</b> positive (total)	<b>-</b>	<b>+</b>	<b>++</b>	<b>+++</b>
<b>Naevi</b>	4(12)	4(12)	4(12)	0 (12)
<b>Primary Melanoma</b>	10(13)	2(13)	1(13)	0(13)
<b>Metastatic Melanoma</b>	4(15)	2(15)	2(15)	7(15)

\*MIF Immunoreactivity: intensity from (-) no staining to (+++) intense staining.

### 3.2.2 MIF expression levels in melanoma metastases are prognostic for disease progression

There are currently no published studies that have addressed whether the level of MIF expression in melanoma is prognostic for patient outcome. To investigate this point, an *in silico* analysis of microarray data associated with clinical outcomes was performed. Analyses were conducted on the data set generated by Xu *et al.* (223) consisting of eighty-three fresh melanoma patient biopsies profiled using the Affymetrix U133A microarray platform and deposited in the GEO (accession number GSE8401), as described in Chapter 2. Dividing the samples into primary melanoma (n=31) and metastatic melanoma (n=52) and comparing the MIF expression levels in each group showed a ~30% higher level of MIF in the metastatic melanoma compared to primary tumour samples (Figure 3.3A). The increase was significant ( $p<0.01$ ) and consistent with the notion that MIF expression is increased in metastatic disease.

The next step sought to establish whether the level of MIF mRNA expression in melanoma was predictive of patient outcome. Since the levels of MIF differed between primary and metastatic melanoma, analyses were conducted on each classification group. As described in Chapter 2, the tumour biopsies were segregated into high and low MIF based on a median cut-point of expression levels and associated with the available survival data. In the case of primary melanoma tumours there was no prognostic significance of MIF levels (Hazard ratio = 1.091; 95% confidence interval 0.312-3.809;  $p=0.8911$ ; Figure 3.3B). However, analysis of MIF expression in metastatic disease showed that high levels of MIF conferred significantly poorer outcome compared to those tumours expressing lower levels of MIF mRNA (Hazard ratio = 2.946; 95% confidence interval 1.440-6.029;  $p=0.0045$ ; Figure 3.3C). In particular, patients with the highest MIF levels succumbed much faster to their disease. To substantiate this finding, another two studies of metastatic melanoma were similarly analysed but did not provide statistically significant differences in outcome between high and low MIF expressing tumours (Figure 3.4). Nevertheless, the Kaplan-Meier plots of these data clearly delineate the same trend, suggesting that high MIF expression is associated with poorer outcome in melanoma patients.

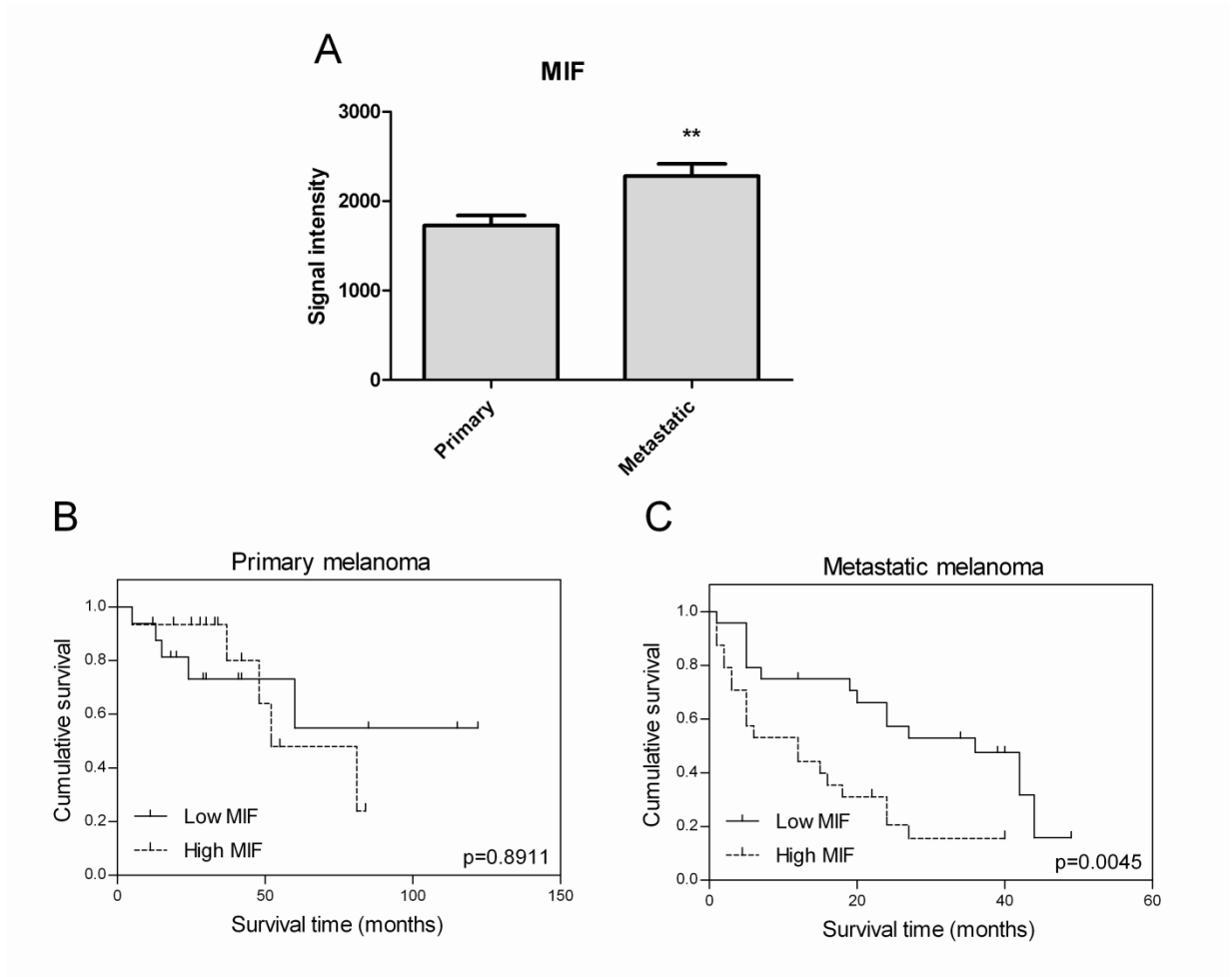


**Figure 3.3 – MIF expression and association with survival in primary and metastatic melanoma clinical samples using microarrays (GEO dataset GSE8401).** (A) *MIF* expression is ~30% higher in metastatic melanoma compared to primary melanoma samples from GEO dataset GSE8401. Values are mean + SEM (t-test, n=31 primary tumour n=52 metastatic melanoma. \*\*p<0.01) (B) Kaplan-Meier survival analysis showed no difference in disease-specific survival between high *MIF* (dotted line, upper 50%) and low *MIF* (solid line) expression groups (hazard ratio = 1.091, 95% confidence interval 0.312-3.809; p = 0.8911). (C) Kaplan-Meier survival analysis indicate that patients with metastatic melanoma expressing high *MIF* had significantly poorer outcome (hazard ratio = 2.946, 95% confidence interval 1.440-6.029; p = 0.0045, n=52) compared to those with low *MIF* expression.

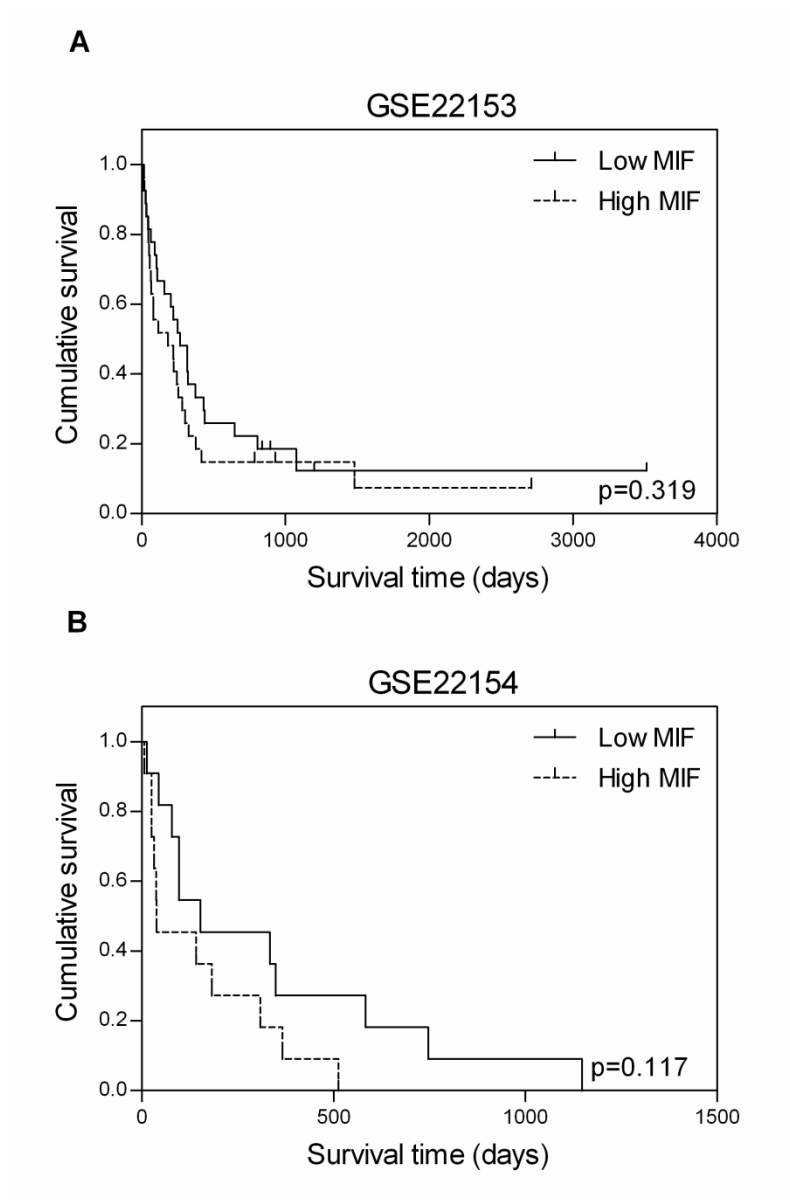


**Figure 3.4 - Association between *MIF* expression and survival in melanoma clinical samples (GEO datasets GSE22153 and GSE22154).** (A) Kaplan-Meier survival curves were generated for patients with lymph node and subcutaneous melanoma metastases according to the level of MIF expression ( $p = 0.319$ ,  $n=57$ ). (B) Kaplan-Meier survival curves for melanoma patients with liver and lymph node metastases ( $p = 0.117$ ,  $n=20$ ).

### **3.2.3 Analysis of MIF receptor expression and association with disease-specific survival in melanoma clinical samples**

MIF can activate several intracellular signalling cascades by binding to the receptor complex CD74/CD44 or to the chemokine receptor CXCR4 (2, 116, 122). These components of MIF signalling have also been independently shown to have prognostic significance in several malignancies. Therefore, it is possible that the effects of MIF on disease progression involve signalling through one or more of these receptors. For that reason, the expression of transcripts encoding MIF receptors was also extracted from the same clinical dataset (GSE8401) in order to investigate if these mRNA levels are also related to patient outcome. For CXCR4 and CD74, an upper quartile cut-point of expression levels was used and for CD44, the lower quartile cut-point was used as detailed in Appendix 2.

In the case of primary melanoma tumours, there was no predictive significance of any of the receptors expression level (Figure 3.5A-C). There was an apparent trend for both *CD74* and *CXCR4*, in that a percentage of patients with low receptor expression had a better outcome from those deemed high expressors. The analysis was repeated on the same dataset but this time using the patients diagnosed with metastatic melanoma. Surprisingly all of the analysis provided clear statistical distinctions between patients classified as high or low expressors of each receptors. Analysis of metastatic disease showed that higher level CD44 was predictive of faster disease-specific death compared to tumour samples expressing lower levels of this receptor (Figure 3.5E). Surprisingly, the opposite was observed for CD74 and CXCR4, for which higher expression was associated with longer disease-specific survival (Figure 3.5D and F).

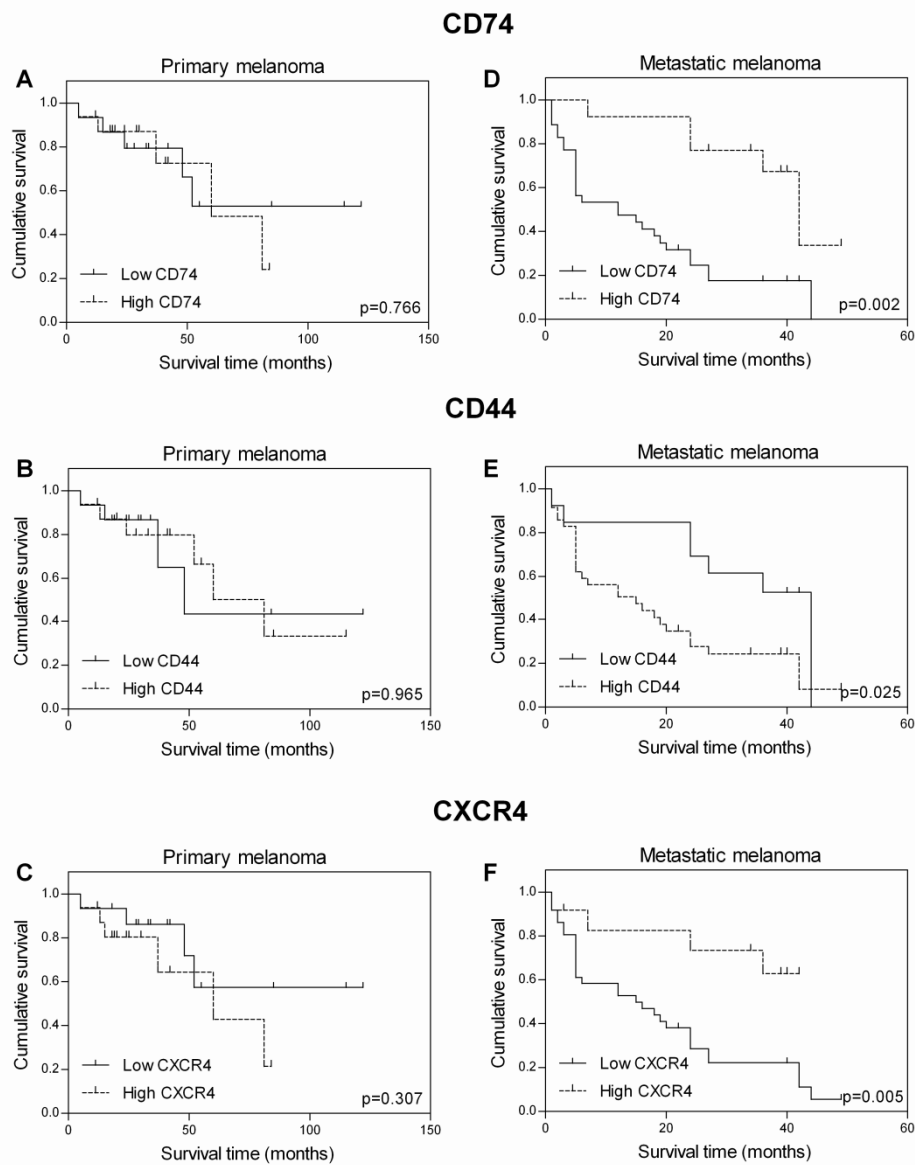


**Figure 3.5 – CD74, CD44 and CXCR4 expression and survival in primary and metastatic melanoma clinical samples using GEO dataset GSE8401.** Kaplan-Meier survival curves were generated based on association between the survival data of 52 patients with metastatic melanoma or 31 patients with primary melanoma and the level of CD74, CD44 and CXCR4 expression. No difference in disease-specific survival was measured between high and low expressors for any of the receptors analysed (A-C) for the cases of primary melanoma. Metastatic melanoma patients expressing high CD44 (dotted line, upper 50%) showed significantly poorer outcome ( $p = 0.025$ ) compared to the low CD44 expression patients (solid line) (E). Conversely, high expression CD74 and CXCR4 was associated with significantly better survival in metastatic disease ( $p = 0.002$  and  $0.005$ , respectively) (D and F).

### 3.3 Discussion

Melanoma is a cancer with high cure rates if the disease is recognised early and surgically removed. However, as described in Chapter 1, melanoma has the propensity to metastasise early and in a small proportion of cases the primary tumour is never found. Once this tumour escapes its boundaries it is almost universally fatal. As a result, a vast body of work has been undertaken to define the pathophysiological factors for melanoma that dictate outcome. These factors include both tumour-related and patient-related variables that are integrated into the staging scheme and known prognostic variables (see Section 1.1.4). However, comparing melanoma to other widely studied cancers, for example breast cancer, there is a lack of molecular characteristics that are useful as biomarkers. Mutation of BRAF has emerged over the last decade but it is clear that melanoma tumours are driven by a range of signalling pathways. Given the focus of this thesis on the potential roles of MIF in melanoma, it was the objective of this Chapter to further investigate the expression of MIF in melanomas *in situ* and to determine whether MIF expression was at all prognostic.

In the present study, *in silico* analysis of publically available expression microarray data was performed comparing the relative transcript levels of *MIF* in different stages of melanoma and normal skin and naevi (Figure 3.1; GEO data set GSE4587 (199)). This analysis showed that *MIF* expression is higher in metastatic melanoma compared to normal skin, naevi and *in situ* melanoma. This finding was then confirmed using IHC to assess MIF protein expression in *ex vivo* melanoma sections, and we similarly observed that MIF is strongly expressed in metastatic melanoma but significantly less, or not at all, in primary tumours (Table 3.1). Noticeably, MIF protein was found not only in the cytoplasm but also in the nucleus of tumour cells, in agreement with previous works that also showed cytoplasmic and nuclear staining in melanoma cell lines (98) and tissue sections (112). MIF protein expression has only been investigated in a single study looking at skin lesions, including benign and atypical naevi, melanoma and melanoma metastases. In these lesions, MIF expression and sub-cellular location was also different in

benign naevi versus atypical and malignant tumours (112). The heterogeneous MIF staining suggests that MIF could have different effects depending both on the cellular context and on its intracellular compartmentalization, although the biological significance of MIF sub-cellular localisation is still unclear. In that respect, it is pertinent to reflect upon the notion proposed by Verjans and colleagues in breast cancer where MIF was suggested to be pro-tumourigenic when secreted but anti-tumourigenic when retained by cells (133). The observation that MIF is also found in the cell nucleus opens up further possible roles for this molecule. These roles can only be addressed by better understanding of the molecular interactions and biochemistry of MIF. Localization of other cytokines in the cell nucleus has been previously described. Ligand-induced endocytosis of cytokine-receptor complexes and nuclear translocation has been suggested for several cytokines, including insulin, IFN-gamma, IL-1, IL-5, growth hormone and members of the FGF family (224, 225). Interestingly, CD44, one of the components of the MIF receptor complex, has recently been shown to be translocated to the nucleus where it has a role regulating transcription. The translocation of MIF and CD44 to the cell nucleus could indicate a novel mechanism for MIF signalling and this point is further considered in Chapter 5.

Despite the evidence that MIF levels are variable and often increased in malignant disease, there has been no investigation as to whether the expression levels of MIF have any prognostic significance for outcomes in melanoma patients. The IHC analysis undertaken, although small, served the purpose of validating the expression patterns of MIF previously reported. No clinical outcome data was available for the samples analysed here and at the time of this work the resources were not available for extending the IHC study to investigate the prognostic significance of MIF protein expression levels in melanoma. Consequently, *in silico* analysis of microarray data with associated clinical outcome was also performed. In the GEO dataset GSE8401 there was an indication that *MIF* expression levels may not be important for outcome when primary tumours were analysed. This was not the case for metastatic melanoma where high level of MIF was shown to be predictive of shorter disease-specific survival. Analysis of another two datasets involving only metastatic cases (GSE22153 and GSE22154) showed

that at least one of the (GSE22154) evoked the same trend. The same could not be observed for GSE22153 dataset, possibly because all cases exhibited fast progression to death. While statistical significance was only reached for GSE8401 dataset, rather than negating the findings, it should be considered encouraging that the analysis show any differences at all since these are all metastatic cases with almost invariably poor outcomes. What the results suggest is that the expression level of *MIF* mRNA associates with the rate of progression and death. This observation also provides important questions as to why this occurs and also how. If the assumption is made that more *MIF* mRNA equates to more MIF protein, and this is supported by the studies of Miracco *et al.* (112), understanding the impact of MIF on the biology of melanoma is key to defining the prognostic significance of MIF.

MIF is secreted by several tumours and is thought to act as an autocrine growth factor. As reviewed in Section 1.2.4, melanoma cells use autocrine mechanisms to control their proliferation and survival. In one of the few works investigating MIF's involvement in melanoma, anti-MIF neutralizing antibody significantly inhibited tumour-induced angiogenesis in tumour-bearing mice, supporting an autocrine function for MIF in melanoma (98). Extracellular MIF can activate intracellular signalling cascades by binding to the receptor complex CD74/CD44 or to the chemokine receptor CXCR4 (2, 116, 122). Interestingly, expression of these components of MIF signalling has also been shown to be associated with the progress of several malignancies (128, 130, 180, 190, 226-228). Therefore, it is reasonable to consider that autocrine MIF could affect melanoma progression through one or more of these receptors. To investigate this hypothesis, the level of expression of transcripts encoding these receptors was determined from dataset GSE4587. For this dataset, the analysis showed that, as for *MIF*, *CXCR4* was also expressed at higher levels in "advanced-stage" melanoma samples, compared to the "early-stage" (Figure 3.1B). *CD74* and *CD44* expression was not significantly different across the samples (Figure 3.1C and D) and *CXCR2* expression was either very low or absent (data not shown).

Next, transcripts encoding MIF receptor expression (CD74, CD44 and CXCR4) were evaluated within dataset GSE8404 (for which follow-up data of patient survival was available) and levels of expression were associated with clinical outcome. In the case of primary melanoma tumours, none of the MIF receptors showed prognostic significance (Figure 3.5A-C). Surprisingly, patients with metastatic melanoma expressing high levels of *CD74* presented better disease-specific survival compared with patients whose tumours expressed low levels of *CD74*, clearly differing from what was observed for *MIF* (Figure 3.5D). *CD74* expression has been associated with tumour development and progression for several forms of cancer, and poor prognosis in solid tumours (105, 123, 127-133, 226). Surface *CD74* has been identified in primary melanoma but not in benign melanocytes (134, 135). The specific role of surface *CD74* in melanoma remains to be elucidated, and although *CD74* is predictive of poor prognosis for several different cancers, until now, there was no study associating *CD74* expression with melanoma patient outcome. These observations suggest that *CD74* may have different roles in melanoma, independent of MIF signalling. Indeed, *CD74* was initially characterized for its role in regulating antigen presentation via HLA-DR molecules (see Section 1.4). HLA-DR have been of historical interest to melanoma, since together with leukemia, cutaneous melanoma is one of the most successful targets for cancer immunotherapy and represents a model disease to investigate tumour immunobiology (229, 230). Even though there are no reports on *CD74* expression levels associating with clinical outcome in melanoma, the expression of HLA-DR antigen has been extensively investigated in melanoma, but a consensus on whether it can predict survival has not been reached (231-235).

On the other hand, analysis of co-receptor *CD44* expression showed that high levels of *CD44* expression were associated with of significantly worse disease-specific survival for metastatic melanoma patients (Figure 3.5E). High *CD44* levels have been shown to be prognostic in other cancers before, in particular the levels of specific variant isoforms, such as *CD44v3* and *v6*. For example, in colorectal carcinoma, patients with higher *CD44s*, *CD44v3* and *CD44v6* expression level in tumour epithelium had lower cancer-related survival and shorter

recurrence-free survival than patients who had low expression levels (228). Another report in breast cancer also showed that women with CD44v6-positive breast carcinoma had poorer prognosis than those with CD44v6-negative breast carcinoma (227). However, in the context of melanoma, reports on the relationship between CD44 expression and prognosis are contradictory and limited to patients with primary melanoma. A report by Dietrich *et al.* showed that high level of CD44 expression in 92 patients with primary melanoma was associated with increased metastatic risk and reduced survival (236). The opposite was found by Karjalainen *et al.*, whose report described that decreased levels of CD44 predicts shorter recurrence free survival for primary melanoma patients (237). Other authors have investigated the role of specific variant isoforms in primary melanoma. In one of the reports, it was found that expression of CD44v3 and CD44v6 appeared to be absent in melanoma, and, in agreement with our own results for primary melanoma, CD44s expression level was not predictive of overall survival (238). Conversely, a more recent report using tissue microarray to compare protein expression of CD44v3 with primary melanoma clinical outcome showed that patients whose tumours were CD44v3 negative had a significantly higher probability of poor outcome than those with CD44v3 positive tumours. Furthermore, levels of expression were also significantly associated with outcome, with stronger expression of CD44v3 associated with better prognosis (239). Some of these results might appear contradictory but as described in Chapter 1 (Section 1.5) the biology of CD44 and its multiple splice variants and isoforms is exceedingly complex. It is also possible that some of these conflicting reports occur because of technical differences. This can ultimately only be addressed if a comprehensive study is undertaken but this would require substantial resources.

With respect to other MIF receptor transcripts, the analysis of the GEO8401 dataset also showed that metastatic melanoma patients with tumours expressing low levels of *CXCR4* mRNA have poorer outcome compared to patients with tumours presenting high *CXCR4* expression (Figure 3.5E), even though *CXCR4* expression appears to increase with melanoma progression as suggested by the *in silico* analysis of dataset GSE4587 (Figure 3.1B). This result

contradicts those of other clinical studies showing a significant association between high CXCR4 expression and poor prognosis (189, 191, 240). Nevertheless, such discrepancies might again be explained by different experimental approaches used, since the vast majority of the studies in melanoma evaluated CXCR4 protein expression by immunohistochemistry in a limited number of samples, while here mRNA expression data was used from a relatively large dataset. While mRNA and protein levels can exhibit positive correlations for individual genes, several factors can lead to significant differences and in fact, most reports on mRNA and protein abundances find only a weak positive correlation (221, 222, 241). Several biological factors can influence this, including, but not limited to, postranscriptional mechanisms controlling protein translation rate (242) and half-lives of specific proteins or mRNAs (243). Therefore, based on the results presented here and the literature, CXCR4 association with melanoma outcome is inconclusive and further research needs to be performed, ideally with larger clinical datasets and comparing mRNA and protein expression in matched samples.

Taken together, the results presented in this Chapter showed that increased *MIF* mRNA and protein expression may be associated with metastatic spread and poorer patient outcome. Within the limitations of such studies undertaken in melanoma where the majority of metastatic cases cause death, these data do suggest that higher levels of *MIF* expression in metastases is associated with faster progression to death. The present work further implicates MIF expression in tumour aggressiveness and suggests that MIF merits to be evaluated further to determine whether it could serve as a target for melanoma treatment.

## **Chapter 4**

**MIF knockdown inhibits growth and  
modulates Akt signalling in melanoma cells  
*in vitro***

## 4.1 Introduction

MIF was the first cytokine discovered where it was described as the product of T lymphocytes (244, 245). It is now known that a variety of other cells types produce MIF, including other immune cells, endocrine, endothelial and epithelial cells (91, 246). It is also considered to be atypical of the conventional classes of cytokines with known functions extended to roles as both a hormone and enzyme (90, 91). MIF is stored in pre-formed, cytoplasmic pools and is rapidly released in response to stimuli such as microbial products, proliferative signals, and hypoxia (91, 247, 248). Its release from cells occurs via a nonconventional protein secretion pathway, and depending on cellular context and stimulus status, MIF can bind to different extracellular receptor proteins (CD74/CD44, CXCR4 and CXCR2) and trigger different signalling pathways (91). Binding of MIF to these cell surface receptors can lead to activation of survival pathways including ERK and Akt pathways (107, 113, 249). MIF has also been shown to bind intracellularly to Jab1 (Jun-activation domain-binding protein-1) and inhibit its functions, such as activation of JNK, p27<sup>kip1</sup> degradation and activation of transcription factor AP-1 (250). Therefore, via this intracellular mechanism, MIF inhibits enhanced AP-1 activity and antagonizes Jab-1 dependent cell-cycle regulation through stabilization of p27<sup>kip1</sup> protein (250). Although there is no evidence of direct regulation of Akt signalling by Jab-1, it has been reported that Jab-1 can act as a regulator of MIF secretion, retaining MIF in the cytosol and thus interfering with the autocrine MIF loop and activation of Akt (107). On this basis it is believed that engagement by MIF of this critical pro-survival signalling pathway is involved in the development and progression of several cancers, for example breast, gastric and colon cancer (107, 249, 251).

A further consideration in understanding the signalling properties of MIF involves reflection upon previously published work, particularly studies that have utilised recombinant

MIF (rMIF) produced in bacteria. Uncertainties have been raised concerning endotoxin contamination present in recombinant protein preparations and care should therefore be taken in interpreting experiments undertaken with rMIF. Indeed, cellular studies of cytokine activities undertaken with bacterially expressed rMIF have produced controversial results (252, 253). Some researchers have adopted protocols designed to eliminate endotoxin (254, 255) but the relatively high concentrations of MIF typically used (100ng/mL) and ill-defined endotoxin levels in commercial preparations warrants caution in using bacterial rMIF. Since there was no recombinant MIF with defined levels of endotoxin commercially available, an attempt to produce recombinant MIF using the *Pichia pastoris* yeast system (256, 257) was carried out as part of the current project. The yeast system has the advantage of producing recombinant proteins inherently free of endotoxin. Unfortunately, this aspect of the project was very labour intensive, and as detailed in Appendix 1, failed to produce sufficient yield or purity to perform *in vitro* experiments. Consequently, the exercise was abandoned and the analysis of MIF function pursued by alternative means as described below.

In the previous Chapter it was shown that MIF expression increased with melanoma progression and was associated with poorer survival in patients with metastatic melanoma. The implication of this finding is that high MIF expression may be serving to drive the proliferation and/or survival of melanoma cells. Therefore, in order to investigate this hypothesis, the present Chapter aimed to characterise the role of endogenous MIF *in vitro* using a panel of melanoma cell lines. Considering the difficulties imposed by the use of recombinant MIF, the strategy adopted to examine the function of endogenous MIF expression in melanoma cells was the use of siRNA to deplete MIF levels within the cells. This approach was used in combination with a battery of functional cell assays designed to evaluate the role of MIF expression in melanoma cells.

## **4.2 Results**

### **4.2.1 Characterisation of MIF expression and MIF receptors in human melanoma cell lines**

To determine the expression patterns of MIF and its known receptors, a panel of 20 melanoma cell lines was utilised. The origin of these cell lines is described in Section 2.1. Total cell lysates were prepared from each cell line and equal amounts of protein were subjected to Western blotting against MIF, CD74 and its signalling co-receptor CD44 according to standard methods outlined in Section 2.4-7. The results shown in Figure 4.1A indicate that all melanoma cells ubiquitously express MIF, albeit at variable levels in each cell line. Similarly, all melanoma cells expressed variable levels of CD44 but these did not appear to be associated with the levels of MIF. Exactly half of the 20 cell lines also expressed detectable protein levels of CD74 (Figure 4.1A). To confirm these results, the cell surface expression of CD44 and CD74 was also examined by flow cytometry in all 20 cell lines using the methods described in Section 2.9. The results of this analysis were entirely concordant with the Western blotting data. Representative results are illustrated in Figure 4.1B and C.

To determine if melanoma cell lines also express alternative MIF chemokine receptors, all melanoma lines in the panel were also stained with anti-CXCR2 or anti-CXCR4 antibodies and the expression analysed by flow cytometry. The results showed that all 20 cell lines analysed were negative for CXCR2 expression, whereas all lines examined showed positive surface expression of CXCR4. Representative staining of 6 of the 20 cell lines is shown in Figure 4.2 A and B.

Collectively the results show that MIF, together with at least one of its known receptors, is expressed in all melanoma cell lines analysed, indicating that melanomas may possess the signalling components required to respond to MIF.

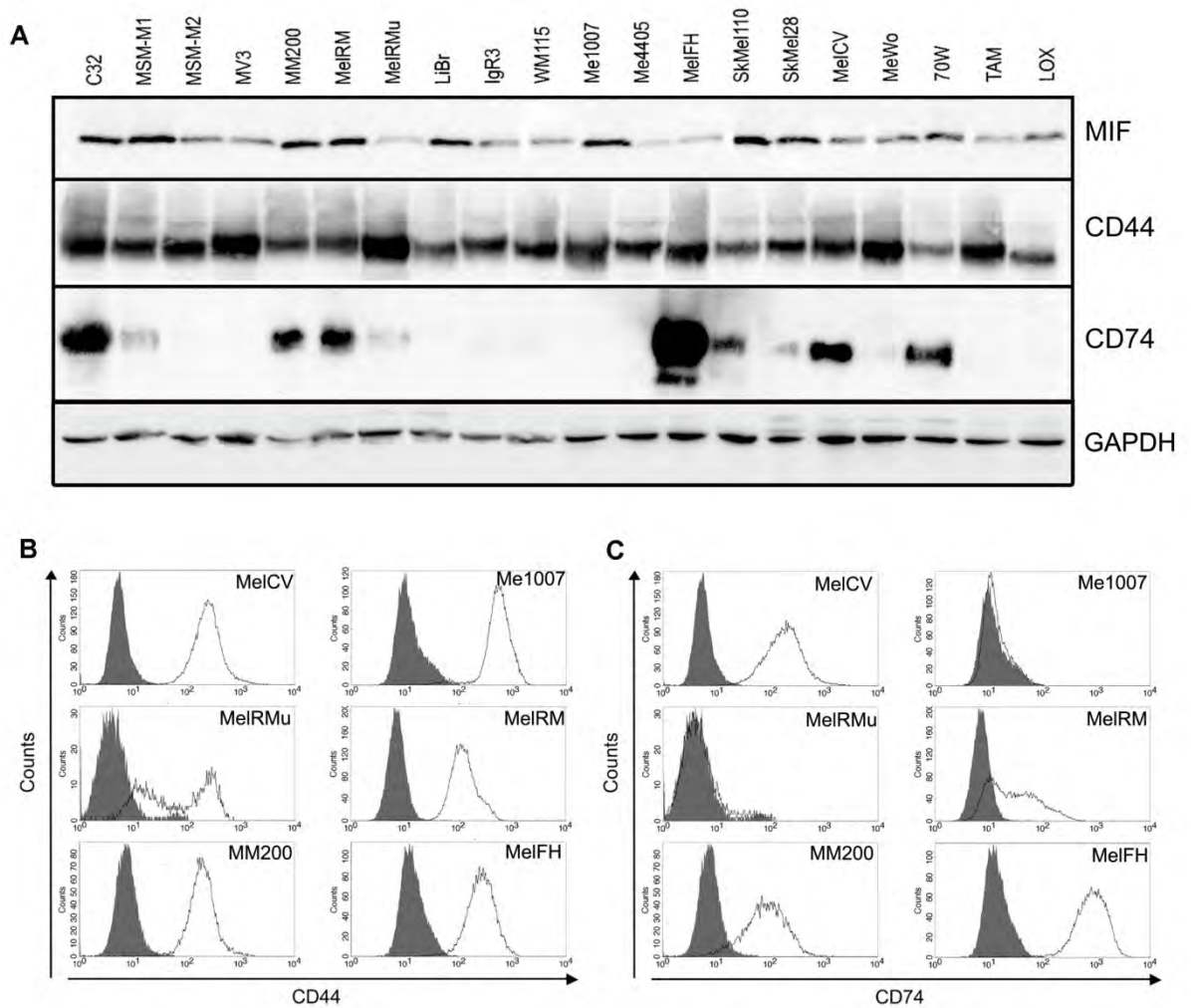


**Figure 4.1– MIF and MIF receptor expression in the human melanoma cell line panel. (A)** Representative Western blots showing MIF (~12.5KDa), CD44 (~85-150KDa), CD74 (~34KDa) and GAPDH (~36Kda) immunoreactive bands for all cell lines used throughout this study. MIF receptor, CD74, was detected in 10 out of 20 cell lines, while the co-receptor CD44 was ubiquitously expressed. Receptor expression was confirmed by cell surface staining and flow cytometry analysis (B and C). Specific antibody staining (open histogram) is shown overlaid over staining using a control antibody (solid histogram). (B) Consistent with the Western blotting results, all the cell lines stained positively for CD44. (C) CD74 was present at the surface of 10 out of 20 cells analysed (6 representative cell lines are displayed for the flow cytometric analyses).

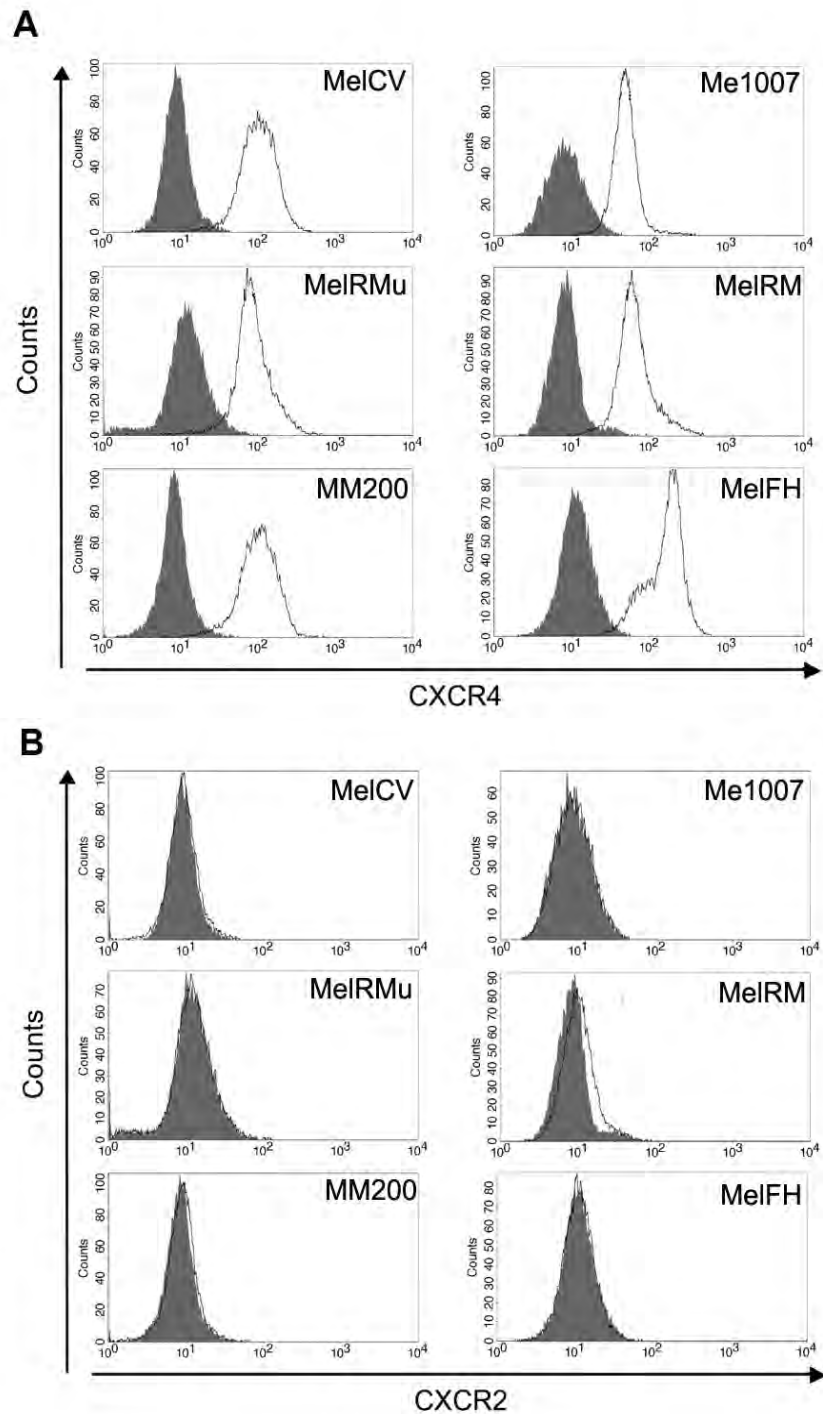


**Figure 4.2– Chemokine receptor expression in the human melanoma cell line panel.** CXCR4 and CXCR2 expression was assessed by cell surface staining and flow cytometry analysis. The cells were stained with specific antibodies compared to control antibodies (open histogram versus solid histogram respectively). (A) CXCR4 was present in all the cell lines analysed while (B) CXCR2 expression was absent in all the 20 cell lines (6 representative cell lines shown for each analysis).

#### **4.2.2 Small interfering RNA knockdown of MIF decreases melanoma cell proliferation and viability**

To determine the function of endogenous MIF in melanoma cells, transfection with siRNA to knockdown MIF protein levels was employed. Towards this approach, the ability of three siRNA oligonucleotide duplexes targeting MIF to reduce both mRNA and protein was assessed using qPCR and Western blotting, respectively. A total of 5 siRNA sequences were tested (Table 2.2). Of these, two sequences (MIF-21 and MIF-25) were the most effective in reducing MIF levels in melanoma cell lines (90-100% of endogenous expression). Thereafter, MIF-21 and/or MIF-25 were used for all subsequent studies to deplete cells of MIF protein.

To determine the effects of MIF knockdown on melanoma cell growth, both total cell number and cell viability were measured each day over a five day time course experiment by using an automated cell counter that measures viability and cell number using the propidium iodide exclusion method (Section 2.11). From the original cell line panel, two cell lines were first chosen to be studied in detail, Me1007 and MeICV, in order to test the effects of MIF in cells expressing CD74 (MeICV) or not (Me1007). Transfection of MIF (siMIF) or negative control (siNC) siRNA into MeICV and Me1007 melanoma cells confirmed a substantial reduction in the total MIF protein detected in cell lysates when measured over 1-5 days (Figure 4.3A and B, respectively). Compared to the control knockdown cells, the number of cells was significantly decreased after 3 days of MIF knockdown for both cell lines (Figure 4.3C and D) and this was accompanied with a significant decrease in cell viability (Figure 4.3E and F). Both effective siRNA duplexes (MIF-21 and MIF-25) promoted identical biological responses either as single agents or as pooled reagents indicating that depletion of endogenous MIF can significantly decrease the proliferative capacity and viability of melanoma cells in culture.

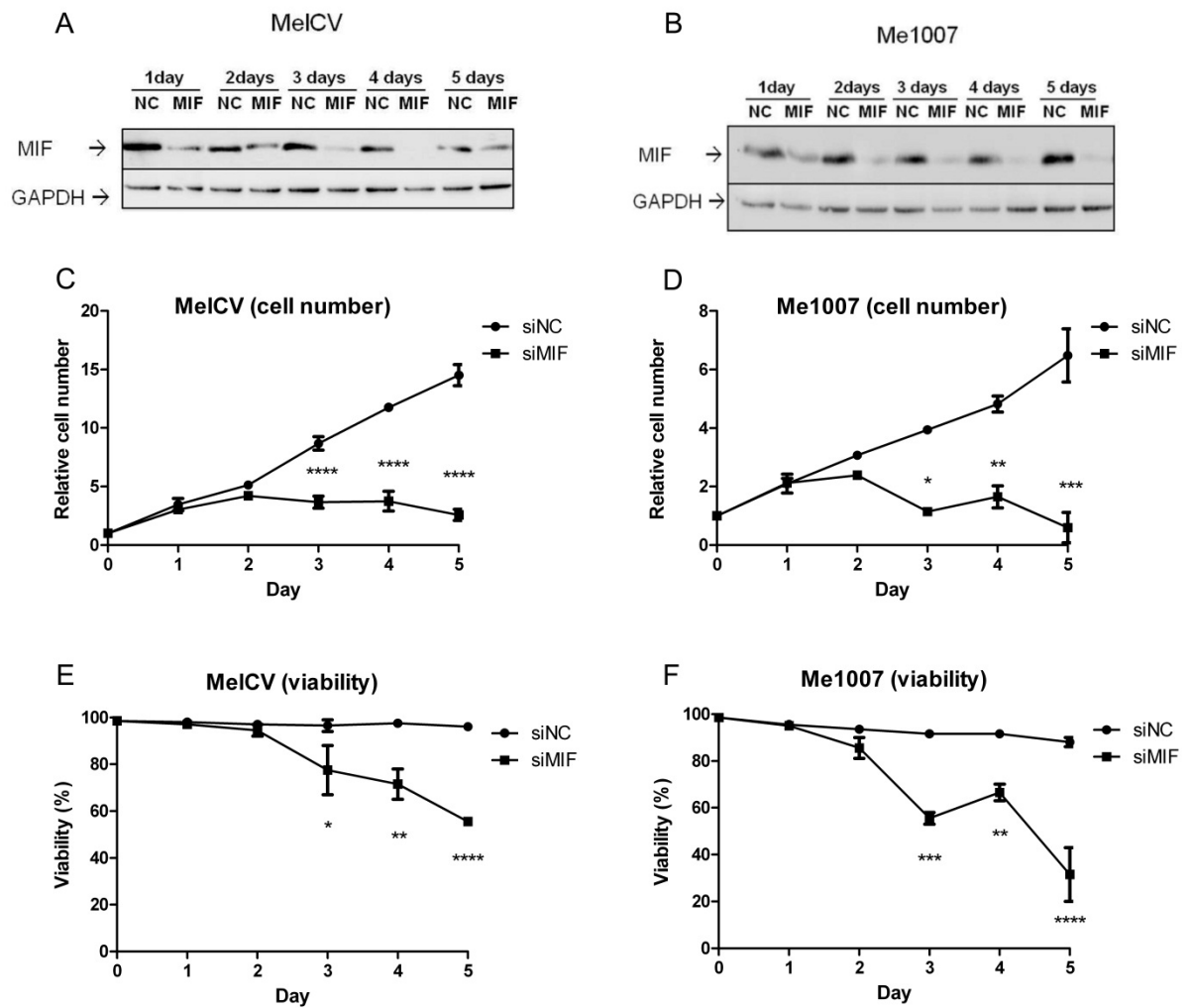


**Figure 4.3 – Small interfering RNA (siRNA) knockdown of MIF decreases melanoma cell proliferation and viability.** The indicated melanoma cell lines were transfected with MIF siRNA (siMIF; 50nM), and the knockdown was confirmed by Western blotting against MIF (~12.5KDa) or GAPDH(~36KDa) as a loading control. As a transfection control, a scrambled siRNA was used at the same concentration (siNC). MIF protein expression was reduced 1 day after transfection, and the knockdown was sustained for 5 days in both (A) Me1CV and (B) Me1007 cell lines. The cell number and viability were determined using an automated cell counter using the propidium iodide (PI) exclusion method. (C, D) The results for both Me1CV and Me1007 showed a significant reduction in the cell number starting from day 3 after transfection (E, F) and the viability was also reduced in a time-dependent manner. Values are mean + SEM of 3 experiments performed in triplicate (t-test, n=3, compared to siNC transfected cells. \*\*\*\* p<0.0001; \*\*\* p<0.001; \*\*p<0.01; \*p<0.05)

To better understand the effects of MIF knockdown on the proliferative capacity of melanoma cells, the Click-iT™ EdU flow cytometry assay was used that is similar in principle to the BrdU (Bromodeoxyuridine) incorporation assay. Cells are incubated with EdU, a nucleoside analogue of thymidine that is incorporated into DNA during replicative synthesis of DNA occurring in the S-phase of the cell cycle. Used together with the DNA-intercalating dye 7AAD to determine relative DNA content, this assay allows accurate quantitation of cells entering S-phase in a defined period of time. Compared to the individual counting of cultures used in the previous section it is also less laborious permitting an expansion of the analysis. A subset of six melanoma cell lines was therefore chosen for this task, including MelCV and Me1007 cells. These lines are shown in Table 4.1 with the rationale being that the cells were selected to include different levels of CD74 expression and also *BRAF* mutation status, since the latter has particular significance to the biology of melanoma as discussed in Section 1.2.1.

Control and MIF-siRNA treated melanoma cells were first analysed by the ClickIT™ technique as shown in Figure 4.4. Analysis of MelCV and Me1007 cells treated with MIF siRNA showed a clear reduction in cells entering S-phase compared to negative control siRNA (Figure 4.4 A and B). The results averaged over 5 independent experiments show that inhibition of MIF expression significantly reduces the percentage of cells in S phase compared to negative control siRNA transfection for both the MelCV and Me1007 melanoma cell lines (Figure 4.4C and D, respectively). Repeating the assay on the remaining cell lines showed that, to varying extents, MIF depletion significantly reduced the number of cells entering S-phase for 4 of the 6 melanoma cell lines examined (Figure 4.4E). The three most sensitive cell lines, MelCV, Me1007 and MelRMu, showed a decrease of more than 50% in cells entering S-phase. Mel-FH was also sensitive to MIF knockdown but to a lesser extent, showing ~40% reduction in cells entering S phase. Although there was a slight reduction, there was no significant effect of MIF depletion on MelRM and MM200 cells. Notably, sensitivity to MIF depletion was both independent of both CD74 expression and *BRAF* mutational status (compare Table 4.1 with Figure 4.4).

**Table 4.1** – MIF receptor expression levels and BRAF mutation status for cell lines selected for MIF functional studies

<b>Cell Line</b>	<b>MIF</b>	<b>CD74</b>	<b>CD44*</b>	<b>CXCR4*</b>	<b>BRAF<sup>V600E</sup></b>
<b>MeICV</b>	Medium	High	✓	✓	✓
<b>Me1007</b>	High	Not expressed	✓	✓	✗
<b>MeIRMu</b>	Low	Very low	✓	✓	✓
<b>MeIRM</b>	High	Medium	✓	✓	✗
<b>MM200</b>	High	Medium	✓	✓	✓
<b>MeIFH</b>	Low	Very High	✓	✓	✗

\*Levels of CD44 and CXCR4 expression were relatively homogenous for all the cell lines. There may be variations, for example variant isoforms of CD44, but these were not assessed.

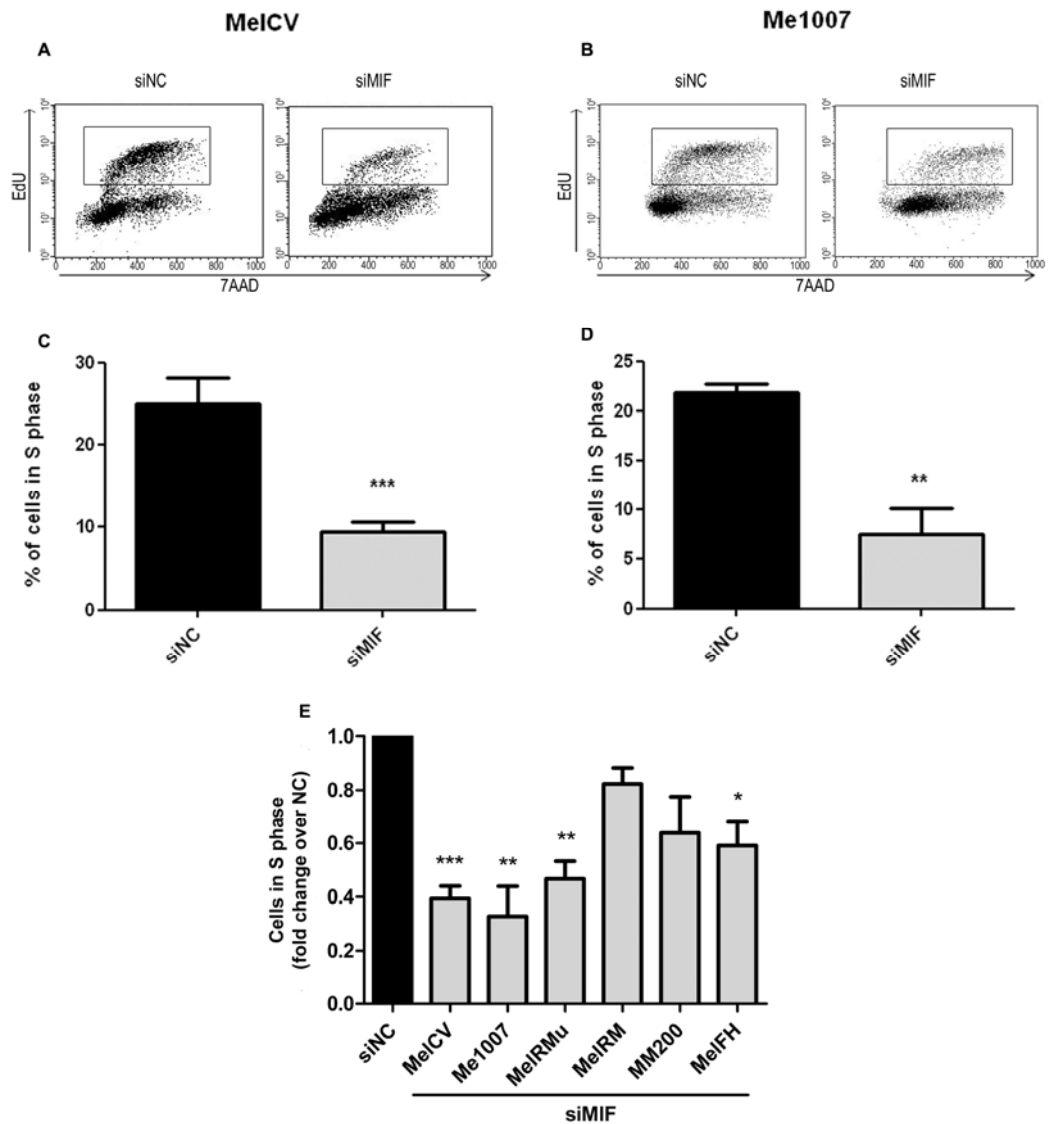


**Figure 4.4– Effects of MIF knockdown on the proportion of melanoma cells in S phase analysed using the Click-IT assay.** Cell proliferation was determined using Click-iT™ EdU flow cytometry assay as described in Section 2.11. Briefly, cells were transfected with MIF and NC siRNA and after 3 days, 10nM EdU was added to the media for 3h. Analysis of the samples was then conducted on a FACS Calibur flow cytometer. (A, B) Analysis of MeICV and Me1007 cells using the Click-iT™ assay allows accurate determination of the populations of cells entering S phase (box). The results show a clear reduction of number of cells in S phase after MIF knockdown for both MeICV and Me1007 cell lines. (C, D) The bar graphs show the percentage of cells in S phase after MIF knockdown. (E) The analysis was repeated for additional melanoma cell lines and MIF expression significantly reduced the number of cells entering S-phase for 4/6 cell lines. Values are means + SEM (t-test, n = 5, compared to siNC transfected cells. \*\*\* p<0.001 \*\*p<0.01 \*p<0.05).

#### **4.2.4 MIF knockdown decreases anchorage-independent colony formation**

Anchorage-independent cell growth is a hallmark of tumour progression and *in vitro* colony formation in soft agar is often used as a proxy of this characteristic of cell transformation. In order to explore the potential involvement of MIF in anchorage-independent tumour growth, cells were transfected with MIF siRNA or NC siRNA, and after 3 days, they were counted and re-plated into soft agar media. After 3-4 weeks of culture the resulting colonies were stained and random fields photographed for analysis. Colonies were analysed for both number and size according to Section 2.12.

Representative micrographs showing colony formation in MeICV and Me1007 colonies subjected to control or MIF knockdown are shown in Figure 4.5A and B respectively, with the insets showing individual colonies in detail. Quantitative analysis of these experiments show that both melanoma cell lines transfected with MIF siRNA formed significantly less colonies than cells transfected with control siRNA (Figure 4.5C and D). The colonies formed after MIF knockdown were also significantly smaller than controls (Figure 4.5E and F). These results suggest that MIF may function to enhance the soft agar growth capacity of melanoma cells.

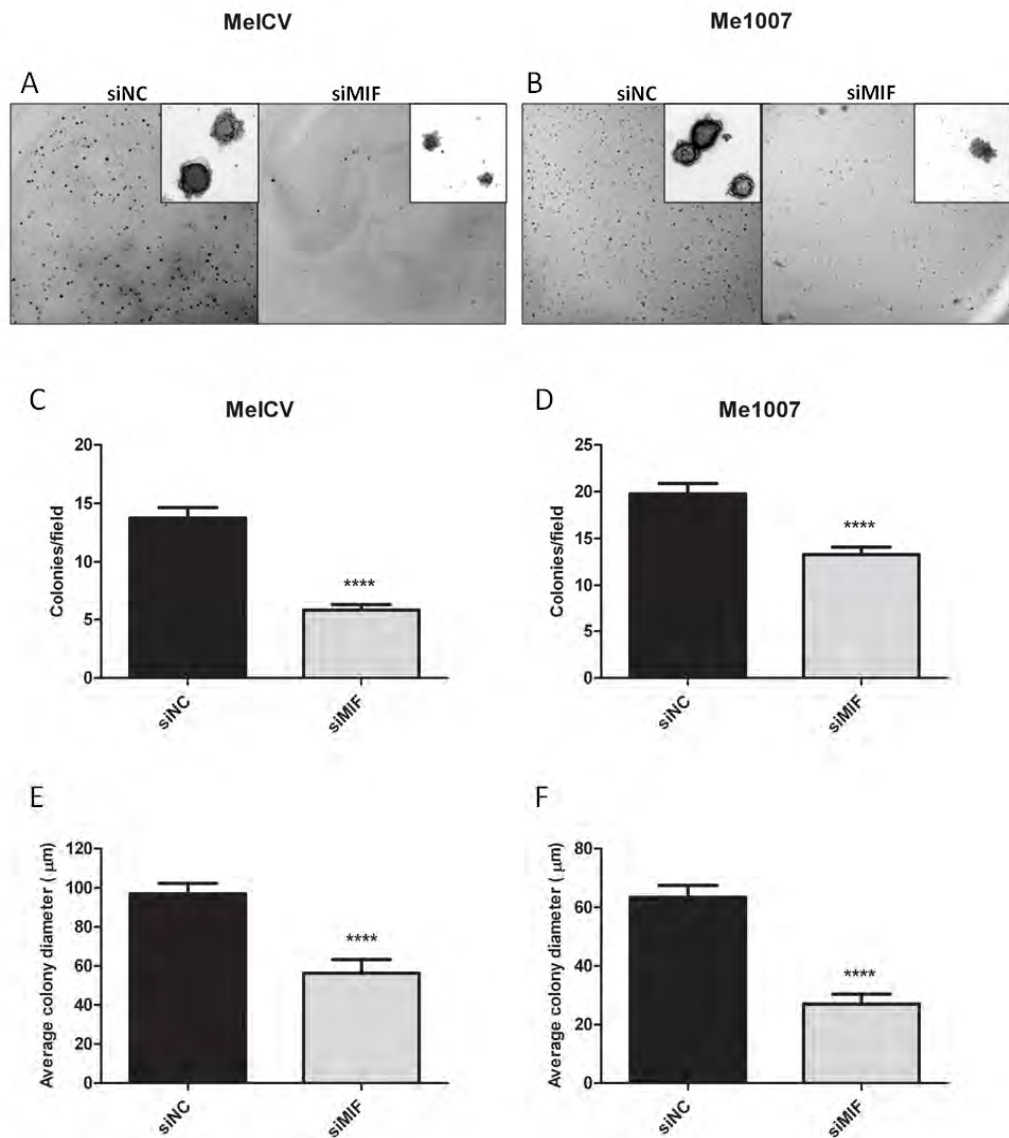


**Figure 4.5- MIF knockdown decreases anchorage-independent colony formation.** Three days after MIF knockdown, the indicated melanoma cells were harvested and seeded in plates within soft agar. Cells were allowed to grow and form colonies for 3-4 weeks. (A, B) Colonies were stained with Crystal Violet. Photos show a representative field from one of the wells at 5X magnification and the insets show the colonies in detail seen under 40X magnification. (C-F) Colonies from 10 different fields in were counted and 25 colonies measured for each experiment using the Axiovision software package. Analysis showed there was a significant reduction in colony numbers and size after MIF knockdown for both MeICV and Me1007. Values are means + SEM of 3 experiments performed in triplicate (t-test, n = 3, compared to siNC transfected cells. \*\*\*\* p<0.0001)

#### 4.2.5 MIF expression modulates Akt signalling pathway in melanoma cell lines

Signalling through the Akt pathway is well established to play an important role in melanoma progression (73, 74, 258). As prior studies have shown that MIF can activate the Akt pathway by binding either of its known receptors, CD74 (154) and CXCR4 (179), the effects of MIF knockdown on Akt-signalling in melanoma cells was examined by Western blotting.

From Figure 4.6 it was observed that proliferative capacity of four melanoma cell lines tested was sensitive to MIF depletion (MeICV, Me1007, MeIRMu and to a lesser extent MeIFH) and the other two (MeIRM and MM200) were comparatively resistant. All six melanoma cell lines were subjected to treatment with MIF siRNA, with knockdown of MIF protein after three days of transfection confirmed relative to controls using Western blotting (Figure 4.6A). Analysis of Akt status in the same cell lysates indicated that Akt phosphorylation was most strongly reduced (~40-70%) in MeICV, Me1007 and MeIRMu cells and to a lesser extent (~20%) in MeIFH, MM200 and MeIRM cell lines as a consequence of MIF knockdown (Figure 4.6B). Further analysis of the downstream cell cycle modulators known to be influenced by Akt signalling was also undertaken. CDK4 and Cyclin D1 involved in G1/S transition also showed some level of inhibition across the 6 cell lines (Figure 4.6C). Cyclin D1 showed a reduction of 15-35% after MIF depletion and CDK4 was reduced in ~10-30% across all the cell lines. The expression of Cyclin-dependent kinase inhibitor, p27 was increased in most of the cell lines following MIF depletion (20-40%), except MM200, for which there was no apparent change in p27 levels (Figure 4.6C). On balance these results support the notion that Akt-signalling is down regulated in response to MIF knockdown with the degree of sensitivity to MIF depletion commensurate with the inhibitory effects observed on the Akt pathway.

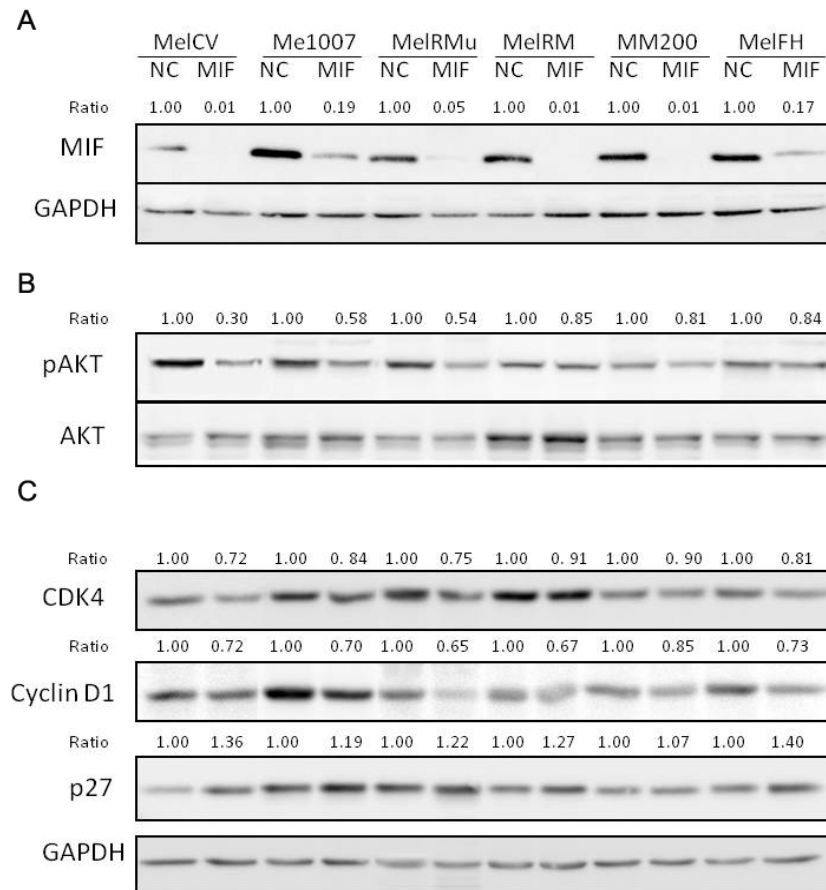


**Figure 4.6 - MIF expression modulates Akt signalling in melanoma cell lines.**

Representative Western blots showing specific immunoreactive bands for MIF, Akt and key cell cycle regulators in the 6 indicated melanoma cell lines. Cells were transfected with MIF and NC siRNA and after 3 days, cells were lysed and submitted to Western blotting. (A) Inhibition of MIF expression 3 days after knockdown was confirmed for all the cell lines analysed. The normalised ratio of expression comparing MIF to control NC knockdown was determined by dividing the optical density of the MIF specific band (~12.5KDa) by GAPDH(~36KDa) using the Multi Gauge software package, as described in Section 2.8. (B) Phosphorylation of Akt (Ser 473) was reduced with MIF knockdown in different levels across the cell lines. In this case, the ratio shows the optical density of the phospho-Akt (~60KDa) band divided by the total Akt (~60KDa). (C) Cell cycle regulators Cyclin D1 (~37KDa) and CDK4 (~34KDa) were also reduced after MIF knockdown in all cell lines, while the cyclin-dependent kinase inhibitor p27 (27KDa) was also increased in most cell lines. The ratio was determined by dividing the optical density of the specific band by that of GAPDH. The ratios shown are the means of 3 independent experiments.

#### **4.2.6 MIF expression is upregulated under hypoxic conditions in melanoma cell lines**

The melanoma cells lines analysed in the present Chapter contain variable levels of MIF protein. Several cancer studies outside of melanoma report that MIF expression closely correlates with tumour aggressiveness and metastatic potential, suggesting an important contribution to disease severity and survival (206, 259). MIF expression in malignant cells has also been suggested to contribute towards adaptation to the tumour microenvironment. One important characteristic often associated with the tumour micro-environment is hypoxia. Moreover, hypoxic conditions have been found to induce expression of specific patterns of genes in tumours which confer a survival advantage on cancer cells, allowing tumour growth and spread in this environment (260). MIF has recently been shown to contribute to tumoral hypoxic adaptation by promoting hypoxia-induced HIF-1 $\alpha$  stabilisation. In addition, hypoxia is a strong regulator of MIF expression and secretion (261). To find out if MIF expression is regulated by hypoxic conditions in melanoma, two different cell lines, MeICV and Me1007, were submitted to hypoxic conditions for 3 days and then MIF expression was compared to cells kept under normoxia using Western blotting. These results showed that MIF protein was significantly up-regulated in both cell lines under hypoxia conditions (Figure 4.7). These findings are consistent with the idea that induced expression of MIF in melanoma may contribute to tumoral hypoxic adaptation.

To further examine if MIF upregulation under hypoxic conditions does confer a survival advantage to melanoma cells, MIF was depleted using siRNA and the cells placed under normoxic or hypoxic conditions. Cell viability was measured by MTS reduction as detailed in Section 2.14. As expected, MIF knockdown under standard (normoxic) conditions reduced viability in both cell lines consistent with previous results. Exposure to hypoxic conditions had a deleterious effect on Me1007 cell viability but it had no significant effect on MeICV cells. For Me1007 cells, inhibition of MIF did not further decrease the toxic effects of hypoxia, since no significant difference was observed compared to siNC treated cells under hypoxic conditions (Figure 4.8). Likewise, MeICV cells depleted of MIF gave similar viability measurements irrespective of whether the cells were cultured under normoxic or hypoxic conditions.

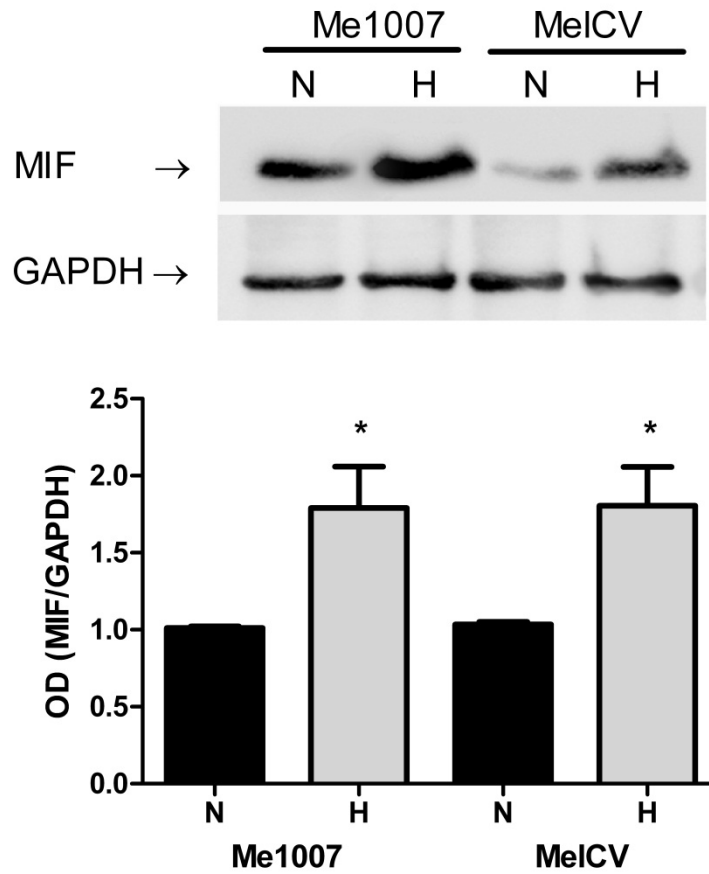


**Figure 4.7 - MIF is upregulated in melanoma cell lines under hypoxia.** Representative Western blot showing MIF immunoreactive bands (~12.5KDa) for Me1007 and MelCV cell lines after 3 days under normoxia (N; atmospheric O<sub>2</sub> and 5% CO<sub>2</sub>) or hypoxia (H; 0.1% O<sub>2</sub> and 5% CO<sub>2</sub>). The bar graph reports the optical density (OD) values of MIF relative to GAPDH (~36KDa) with data normalised to control cells kept under normoxic conditions. Values are mean + SEM (t-test, n=3, compared to normoxia; \*p<0.05).

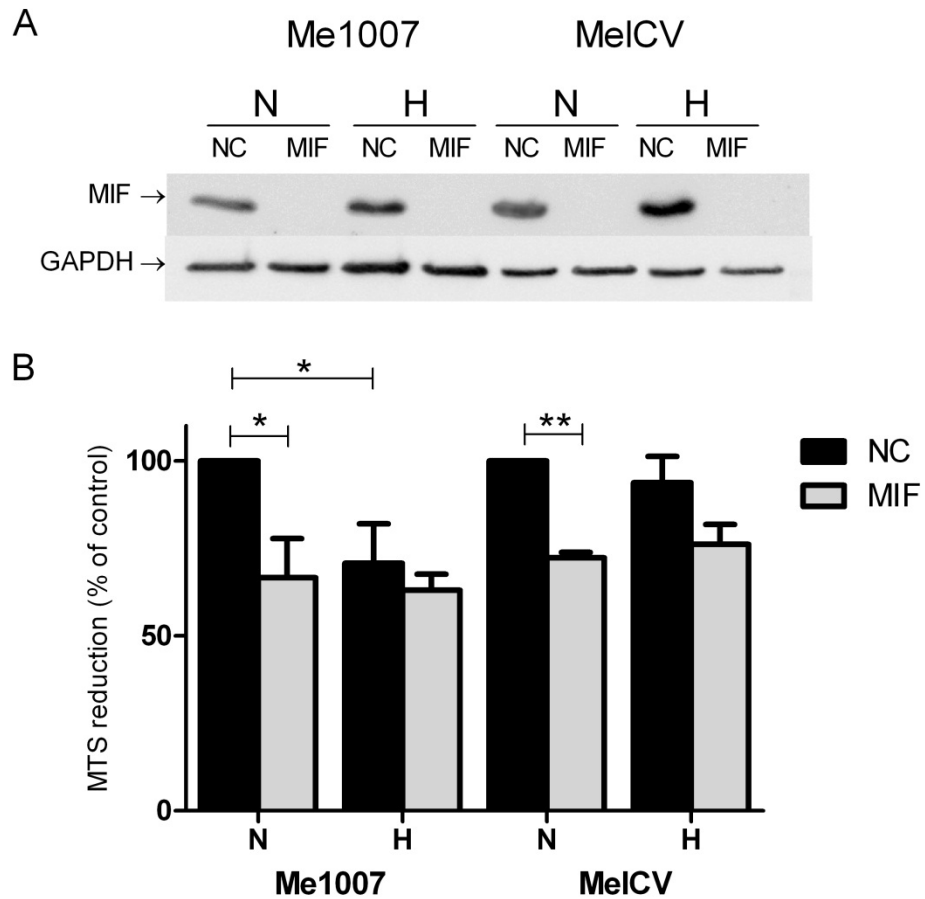


**Figure 4.8 – Effects of MIF depletion on melanoma cell viability under conditions of hypoxia.** (A) Representative Western blot showing MIF immunoreactive bands (~12.5KDa) and GAPDH (~36KDa) for Me1007 and MeICV cell lines 3 days after transfection with MIF or NC siRNA under normoxia (N) or hypoxia (H). (B) Cell viability measured by MTS reduction represented as percentage of cells transfected with NC siRNA under normoxia for each cell line. Values are mean + SEM (t-test, n=3, compared to normoxia; \*p<0.05 and \*\*p<0.01).

### 4.3 Discussion

Although MIF was first described as a proinflammatory cytokine, it has been shown by many authors to play a role in the development and progression of cancer, acting as an extracellular, protumorigenic factor (92-94). The aim of this Chapter was to investigate in more detail the functional role of MIF in human melanoma cells. Considering that many of the biological roles ascribed to MIF in the literature have been controversial because of uncertainties in endotoxin contamination present in preparations of rMIF (252, 253), an alternative strategy to examine the function of endogenous MIF expression in melanoma cells was adopted, primarily using siRNA to knockdown MIF levels. The two different siRNA sequences for MIF (MIF-21 and MIF-25) effectively reduced MIF levels while scrambled control siRNA sequence had no effect on MIF expression. In all experiments the reduction of MIF levels observed was at least 75% but mostly >95%, which is in the acceptable range for siRNA experiments. In MelCV and Me1007 cell lines, MIF knockdown resulted in significantly reduced cell number and viability over 6 days (Figure 4.3), indicating that endogenous MIF expression could be generally required for the growth of melanoma cells.

These experiments were in part instigated because MIF involvement in cell cycle regulation has been shown before in different cancer cells (108, 113, 249). In the context of melanoma, little work has been previously done apart from two small studies. Shimizu *et al.* (1999) demonstrated that inhibition of MIF expression resulted in inhibition of proliferation, migration and tumour-induced angiogenesis (98). In a second study using a single murine melanoma cell line (B16-F10), Culp *et al.* (2007) showed that MIF inhibition significantly delayed tumour establishment when injected into mice (111). While these results are supportive of the current work, that indicates MIF involvement in cancer cell growth, they are both single cell line studies and also rely on the effects of high concentrations of bacterially produced recombinant

MIF. Representing a more comprehensive approach, this Chapter utilised 6 independent human melanoma cell lines expressing different levels of CD74 with or without *BRAF* mutation (Table 4.1).

To better understand the role of MIF expression in melanoma cells, further quantitative assays were employed on all 6 melanoma cell lines. Cell proliferation after MIF knockdown was further explored using the Click-iT™ assay, a sensitive and quantitative assay which measures the number of cells entering S-phase. This analysis showed that MIF knockdown significantly reduced cells transitioning to the S-phase in 4 of the 6 melanoma cell lines (Figure 4.4E), suggesting the proliferative capacity of the majority of the melanoma cell lines studied have some degree of reliance on MIF expression. At least for the MelCV and Me1007 lines examined in detail, MIF depletion compromised their viability (Figure 4.3). However, over the time course of 5 days, the major effect observed was the failure of cells to proliferate and this finding was complemented by the Click-iT™ analysis of cells entering S-phase. This suggests that MIF knockdown has primarily cytostatic effects on melanoma cells and by itself is not effective in promoting high levels of cell death. The inhibitory action of MIF depletion also occurred independently of *BRAF* mutation status and this similarly has important implications should targeting of MIF be considered as a treatment for melanoma (see Chapter 6).

To further explore MIF effects in melanoma cells, its role in anchorage-independent growth was also considered, this being one of the recognised hallmarks of cancer. Colony formation in soft agar is a 3D proliferation assay that is intimately linked to tumorigenicity. This assay also verified the involvement of MIF in anchorage-independent tumour growth with the results showing that *MIF* siRNA transfection significantly reduced the number of colonies formed by both MelCV and Me1007 melanoma cell lines. The colonies formed were also smaller after *MIF* knockdown compared to control cells (Figure 4.5). These results indicate that MIF may function to enhance the anchorage-independent growth capacity of melanoma cells and its depletion can significantly compromise this capacity, at least in cell culture models.

A further question to be addressed is how MIF and its associated signalling pathways may be achieving these effects in melanoma. As described, the receptor mechanisms and signal transduction pathways involved in MIF-mediated cell activation have only partially been unravelled. MIF signalling can be achieved either by binding to the CD74/CD44 receptor complex or by binding to the chemokine receptors CXCR2 or CXCR4 (2, 116). In order to further investigate this, the expression of known MIF receptors was characterized in a panel of human melanoma cell lines. A relatively large panel of 20 cell lines was used to account for the known heterogeneity of the disease. The expression of the components of MIF signalling in melanoma has been previously shown by different groups (98, 112, 134, 148, 186), but most of the *in vitro* studies have been limited to a few cell lines. This is the first study comprising a large panel of human melanoma cell lines.

Here, the results show that MIF was expressed in all 20 cells lines tested, albeit at variable levels. CD74 is expressed in half of the cell lines, while its co-receptor CD44 is expressed in all the cell lines. The chemokine receptor CXCR4 was expressed in all the cell lines analysed, however CXCR2 was not expressed at detectable levels in any cell line (Figure 4.2). These data therefore suggests that melanoma cells possess at least one of the signalling receptors required to respond to MIF. Although, it is notable that while CD44 was expressed by all the cell lines, CD74 was only expressed in 10/20 cell lines. The growth promoting effects of MIF appeared to be independent of CD74, since they were also observed in cell lines not expressing this receptor, for example the Me1007 melanoma cell line. Consistent with our findings, CD74 has been shown to be expressed in melanoma by others (134, 135), but MIF effects appear to be independent of this receptor's expression (111). All the cells lines express CXCR4 but not CXCR2, suggesting that MIF signalling in melanoma is more likely to occur through CXCR4 binding if there is a single common mechanism employed by melanoma cells involving the known MIF receptors. In that respect, CD44 is also known to act as a signalling co-receptor for other receptors, e.g. ErbB4 (3), and its involvement cannot be totally discounted.

MIF's role in tumourigenesis has been suggested to involve autocrine MIF activity and it has been established that MIF promotes activation of Akt by an autocrine loop (107, 248). Furthermore, the addition of neutralising antibodies to tumour (G361 cell line)-bearing mice significantly suppressed tumour-induced angiogenesis (98) supporting an autocrine role for MIF in melanoma. However, in addition to its extracellular role, MIF may have additional regulatory functions within the cell. For example, Kleemann *et al.* (2000) reported that MIF signalling might involve a mechanism that bypasses the need for a cell-surface receptor. As mentioned before, after endocytosis, MIF can bind directly to the cytoplasmic protein Jab-1 (250). By binding Jab-1, MIF can inhibit its functions and regulate cell growth and gene expression by modulating phosphorylation of c-Jun and AP-1 activity. Jab-1 also binds and promotes the degradation of p27<sup>Kip1</sup>, a protein that inhibits the cell division cycle (262). In addition, Jab-1 has been reported to act as a regulator of MIF secretion, retaining MIF in the cytosol. This could interfere with MIF autocrine function and activation of Akt (107). MIF has been shown to promote tumour cell survival by activating the Akt pathway (107, 249) and members of the PI3K and Akt signalling cascades have been implicated in initiation, progression and invasive phenotypes of melanoma (73, 74, 258) as reviewed in Chapter 1. Because of these functional associations between MIF and Akt, the Akt signalling pathway became a focus for the study.

Akt activation can stimulate proliferation through multiple downstream targets affecting cell-cycle regulation (263). For examples, Akt can phosphorylate p27<sup>Kip1</sup> cyclin-dependent kinase inhibitor, which prevents its localisation to the nucleus attenuating its cell-cycle inhibitory effects (264-266). In addition, Akt can also phosphorylate GSK3, which in turn phosphorylates G1 cyclins, such as Cyclin D and Cyclin E, targeting them for proteasomal degradation (267, 268). Therefore, phosphorylation and inhibition of GSK3 by Akt enhances the stability of these proteins. In the current study, MIF knockdown resulted in a decrease of Akt phosphorylation in the 6 selected cell lines, and this effect was accompanied by a reduction in expression of Cyclin D1 and Cyclin dependent kinase 1 (CDK1), and an increased expression of p27<sup>Kip1</sup> (Figure 4.6). Quantitation of these results confirmed that the degree of Akt activation and effects on its

signalling components was largely consistent with the functional effects of MIF knockdown. For example, the MeICV cell line that was shown to be highly sensitive to MIF depletion (proliferation, viability, cloning efficiency) also had prominent down-regulation of pAkt. In contrast, the MeIRM cell line that was only marginally affected by MIF knockdown had the least disturbances in Akt signalling components. Collectively this suggests that activation of the Akt pathway is one of the mechanisms by which MIF regulates the cell cycle.

Another angle of investigation involved the potential of MIF to allow melanoma cells to survive conditions of hypoxia. It is well recognised that the tumour microenvironment is quite dissimilar to normal tissues and one key difference is the lack of oxygenation in poorly vascularised tumours (reviewed in (269, 270)). HIF-1 $\alpha$  is one of the key transcription factors identified to be activated by hypoxia (269, 270) and MIF plays a role in hypoxic adaptation by promoting hypoxia-induced HIF-1 $\alpha$  stabilization (261). Stable HIF-1 $\alpha$  translocates to the nucleus where it dimerises with the constitutively expressed HIF1 $\beta$  subunit, forming the active HIF1 complex. This complex then binds to the hypoxia-responsive element (HRE) and induces upregulation of a variety of genes, promoting tumour vascularisation and modulating adaptive metabolic changes that allow continuing biosynthesis and tumour growth in low oxygen conditions (269, 270). Hypoxia is also a strong regulator of MIF expression and secretion (261) and this was confirmed here, as illustrated in Figure 4.7, where MIF was shown to be upregulated under hypoxic conditions. Overexpression of MIF induced by a hypoxic environment could confer a survival advantage to melanoma cells, to promote tumour growth under low oxygen situations.

To address the role of MIF induction by hypoxia in our experimental model, MIF was depleted using siRNA in hypoxic and normoxic conditions, and cell viability was measured. The results showed that MIF depletion decreased cell viability of both cell lines under normoxia, and exposing the cells to hypoxic conditions had a negative effect on viability on only one of the cell lines (Me1007). No significant difference was seen after MIF depletion comparing normoxia with

hypoxia for either cell line (Figure 4.8). For the hypoxia sensitive Me1007 cells, it might have been expected that cell viability would be greatly compromised when MIF was depleted. Rather, as stated, MIF siRNA treatment resulted in no additional reduction in cell viability beyond that produced by hypoxia alone. Therefore, hypoxia induces MIF levels, but loss of MIF does not compromise cell survival under hypoxic conditions (Figure 4.8), which may suggest that MIF does not influence cell survival under the conditions examined. Moreover, it is important to consider that the experimental conditions used here, consisting of cells growing in a monolayer, do not properly mimic the 3D environment of physiological conditions. The best way to study effects of microenvironment in cancer progression would be to use conditions closer to the physiological situation such as 3D cultures that mimic more closely the tumour tissue or ideally, experimental *in vivo* models of melanoma.

In conclusion, the results presented in this Chapter implicate MIF in melanoma proliferation and survival. In addition, MIF expression was implicated in anchorage-independent growth and upregulated under hypoxic conditions. It was also shown that a role of MIF in melanoma cells is likely to be through Akt signalling, since MIF knockdown reduced Akt activation and modulated the expression of downstream cell-cycle regulators.

# **Chapter 5**

**Subcellular distribution of MIF and CD44 in  
melanoma cell lines**

## 5.1 Introduction

Following on from the work of the previous Chapters, the next directive of this thesis was to investigate the mechanisms of MIF signal transduction complexes in melanoma. Our laboratory has a longstanding involvement in the signalling role of CD44 in cancer and indeed it was that interest that promoted MIF as a subject for study. CD44 is believed to be universally expressed in all cases of melanoma and in this project all twenty cell lines examined expressed abundant levels of CD44 (Figure 4.1). As mentioned previously in Chapter 1 (Section 1.5.1), CD44 itself lacks intrinsic kinase activity and must engage signalling pathways through specific interactions with other signalling components. In particular, our laboratory and others have shown that the cytoplasmic tail of CD44 can physically bind to members of the Src family kinases that in turn activate the Akt signalling cascade (reviewed in (3)). The general importance of the Akt pathway to the growth and survival of melanoma cells is well known (refer to Section 1.2.2) and in Chapter 4, a strong functional association was revealed between MIF and the Akt pathway in most melanoma cell lines. If it could be established that CD44 acts as MIF co-receptor in this setting, then this would provide a better mechanistic understanding of how MIF signals are transmitted and processed in melanoma cells. Such knowledge may be important in developing new treatments against melanoma that utilise strategies for antagonising MIF signalling.

In Chapter 3, the cellular localisation of MIF was studied in melanocytic tumours ranging from naevi through to metastases of melanoma. This showed that MIF immunoreactivity could be found in both the cytoplasm of melanoma cells together with the cell nucleus. As discussed in Chapter 4, MIF is somewhat unusual for a cytokine because it is stored in cytoplasmic pools and is released through a mechanism involving the action of Jab1 (Section 4.1). On the other hand, while the occurrence of MIF in the cell nucleus is known (98, 112), its role in this location

is yet to be elucidated. CD44 was already known to be endocytosed and transported to the nucleus, either in an intact full-length form, or a cleaved product as described in Section 1.5.2. Together, these observations were highly reminiscent of reports concerning the signalling activities of other growth factors and their receptors, as discussed in Section 3.3. The hypothesis was formed that intact FL-CD44 as part of MIF-receptor complex was responsible for the delivery of MIF to the cell nucleus, a location that appears to have special significance since MIF is located there in the majority of melanoma cells, less frequently in naevi and not at all in precursor melanocytes (112).

In order to develop this concept further, both at a spatial and temporal level, experiments were undertaken to survey the localisation of MIF and CD44 in melanoma cell lines. This analysis would provide the basis for further functional studies to define exactly how the important cellular functions of MIF identified in Chapter 4 are executed.

## 5.2 Results

### 5.2.1 The subcellular localisation of MIF in cultured melanoma cells

To begin an investigation of the role of MIF and MIF receptors in melanoma, it was first examined where the MIF protein was localised in cultured melanoma cells. The cohort of 6 melanoma cell lines used extensively in the previous Chapter (Table 4.1) were grown on glass coverslips and processed for intracellular staining by permeabilization using Triton X-100 according to the methods described in Section 2.16. After indirect immunofluorescent staining against MIF, the cells were counterstained with DAPI to decorate nuclear DNA. Optical sectioning was then employed to determine if MIF staining was co-incident with DAPI staining as this would indicate the presence of MIF in the cell nucleus. The results of this analysis are presented in Figure 5.1.

Consistent with the results of Chapter 3 and previous reports, significant amounts of intracellular MIF was observed throughout the cytosol of all of the cell lines examined. In all cell lines the cytoplasmic staining appeared to be quite punctuate but the staining was not associated with clearly identifiable cytosolic compartments. Another feature of the staining was the apparent presence of MIF staining in the nucleus of cells, again consistent with results in the *in vivo* setting. Although microscopy is fundamentally a qualitative method, close analysis of the relative amounts of MIF present in the cytosol versus nucleus displayed an intriguing trend. Those cell lines deemed to be most sensitive to MIF depletion (Me1007, MeICV and MeIRMu) tended to have more protein expression of nuclear MIF than those that were relatively resistant (MM200, MeIRM and MeIFH). This observation promoted the idea that the growth promoting effects of MIF were associated with its presence and presumably its function in the cell nucleus.

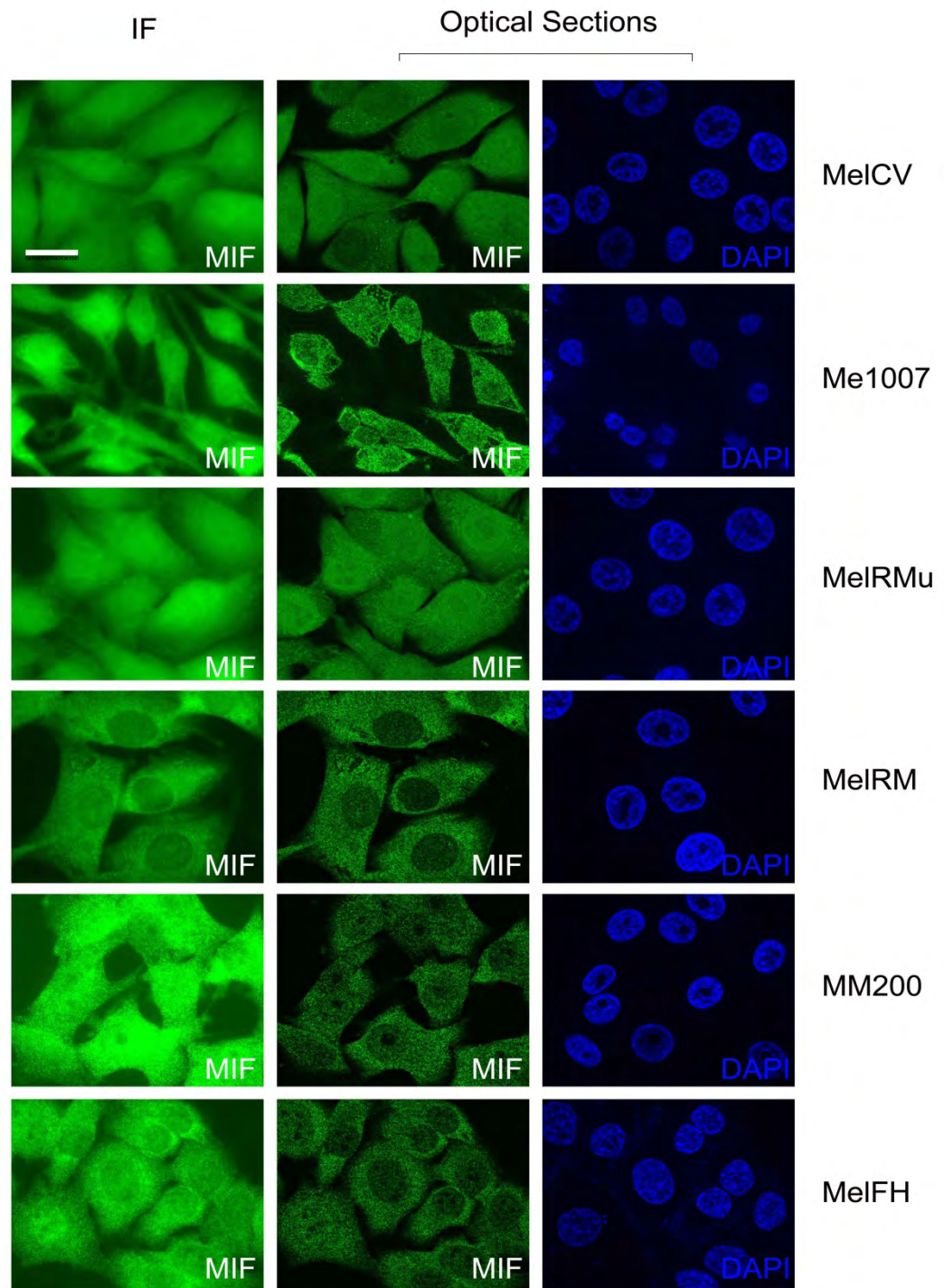


**Figure 5.1 – Cellular distribution of MIF in human melanoma cell lines.** The indicated cell lines were grown on glass coverslips, fixed, permeabilised and immunostained with MIF mAb antibody and a fluorescent secondary conjugate (Alexa488 anti-mouse IgG). The cells were imaged using epifluorescence microscopy. The left panels are standard immunofluorescence (IF) microphotographs whereas the middle and right panels are optical sections of cells showing MIF staining or the nuclear marker DAPI as indicated. Scale bar = 20µm

### **5.2.2 The cellular distribution of CD44 in cultured human melanoma cells**

Using the methods employed to examine the localisation of MIF, the distribution of CD44 was also examined in melanoma cell lines. In this case the Hermes-3 mAb, directed against the extracellular domain of CD44, was employed. The results of this analysis are presented in Figure 5.2.

Staining for CD44 in all 6 melanoma cell lines showed it to be a cell surface protein that was highly abundant, consistent with both the flow cytometric analysis and the Western blot analysis (Figure 4.1) Specific CD44 signals were observed on apical and basolateral surfaces but these were not strictly homogenous. Staining was often enriched in cell extremities and in microvilli located on the apical surface of cells. The strong membrane staining of CD44 provided some difficulty in assessing whether any CD44 was present in the cell nucleus. Therefore, optical sectioning was required to examine these samples. Comparison of CD44 staining with DAPI in the cell nucleus showed that no CD44 signals were present in the cell nucleus. All detectable CD44 signals in this analysis were confined to the cell membrane of all 6 melanoma cell lines.

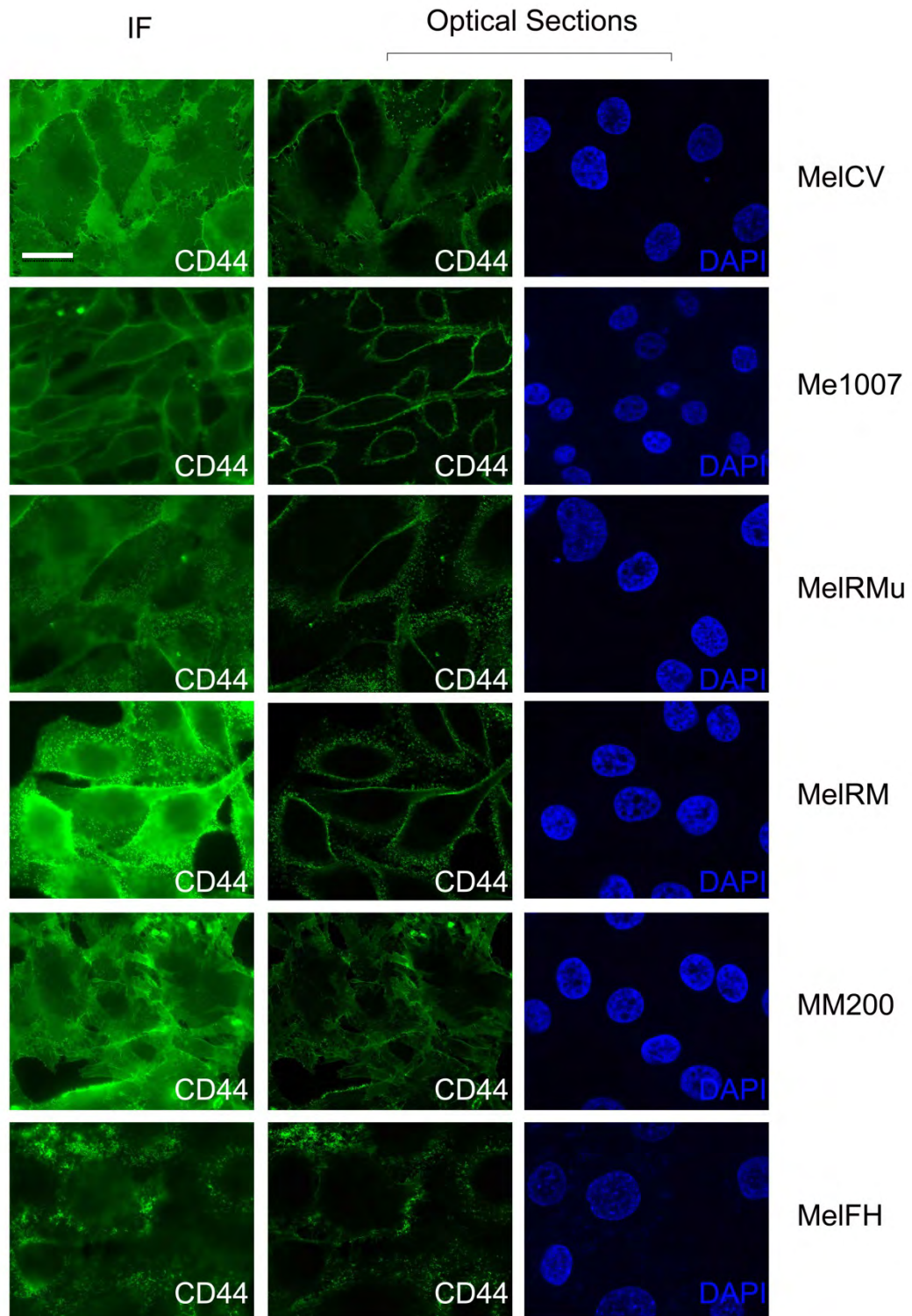


**Figure 5.2– Cellular distribution of CD44 in human melanoma cell lines.** The indicated cell lines grown on glass coverslips were fixed, permeabilised and immunostained with CD44 mAb antibody (Hermes3) and a fluorescent secondary conjugate (Alexa488 anti-mouse IgG). The left panels are immunofluorescence (IF) microphotographs whereas the middle and the right panels are optical sections of cells showing CD44 staining or the nuclear marker DAPI as indicated. Scale bar = 20µm.

### 5.2.3 Characterization of CD44 sub-cellular localization in HT-29 and MCF10A cells

In the preceding Section no evidence could be observed for the presence of intact CD44 in the nucleus of 6 different melanoma cell lines (Figure 5.2). Since the phenomenon of intact CD44 in the cell nucleus had not been previously described for melanoma cells, it was important to confirm the veracity of this finding by establishing the validity of the methods used. Two main reports have used immunofluorescence staining to visualise intact full-length CD44 in the cell nucleus, one using the HT-29 colon and H1299 lung carcinoma cells (171), and the other showed full-length CD44 localizes to the nucleus of several cell types, including prostate carcinoma (PC3), foetal fibroblasts (MRC5) and mammary epithelial cells (MCF10A) (170).

The HT-29 cell line was readily available in the laboratory together with a large panel of monoclonal antibodies directed against the extracellular domain of CD44. HT-29 cells were grown under standard conditions and allowed to adhere to glass coverslips prior to immunostaining with a panel of 8 anti-CD44 mAbs. The resulting samples were processed for confocal microscopy with optical sections that transect the nucleus of the cells taken. The results are shown in Figure 5.3. No specific staining was observed with the detection reagents alone. Moreover, as observed in the previous Section, Hermes-3 staining decorated the plasma membrane of the cells but no staining of the cell nucleus was evident. Moreover none of the other 7 anti-CD44 clones produced any hint of nuclear staining despite exquisite staining of the plasma membrane. The chance that epitopes detecting one mAb was somehow masked seemed possible, but that 8/8 independent clones failed to identify intact CD44 in the nucleus was perplexing, given the recent findings published in high profile journals (170, 171).

One possibility was that the in-house HT-29 cells were different to those published, or that the growth conditions employed were inappropriate for the translocation of CD44 to the cell nucleus. To further investigate, studies were next undertaken in MCF10A mammary epithelial cells, that had also been reported to have the intact CD44 molecule present in the cell nucleus

(170). One feature of these cells is the great morphological differences observed in cells cultured at low density (mesenchymal), high density (epithelial) and within matrigel (acini) (271).

It is known that different culture conditions can affect the expression of adhesion molecules like CD44 (272), therefore the internalization and nuclear translocation could also be affected by cell density and culture conditions. For that reason, 3 different cell culture conditions were compared: low density and high density adherent cell culture, and 3D cell culture. As before, cells were permeabilised and immunostained with extracellular antibodies against CD44, in this case E1/2 that provides the highest signal to noise of all the available anti-CD44 mAb (Figure 5.3). These results are shown in Figure 5.4A with the analysis showing that CD44 staining again exhibited exclusively membrane staining. There was no co-localization of CD44 staining with nuclear marker, DAPI, and the different culture conditions employed had no influence on the results.

To further confirm this finding, the analysis was extended using different cellular markers. To visualise a larger number of cells, Figure 5.4B shows a low magnification field of MCF10A cells, and in addition to the nuclear marker DAPI, staining with the filamentous actin probe Alexa488 phalloidin was also performed. Again CD44 staining was strongly present at the cell surface and the merged images show that there was no co-localization of CD44 and the nuclear marker for any of the cells in the field. Closer details of the staining of CD44 are shown in Figure 5.4C. MCF10A cells were stained with an antibody against the mitochondrial marker Cytochrome C, in addition to the antibody against CD44 and the nuclear marker DAPI. In this instance the visualisation of mitochondria is useful in delineating the cytosolic space of individual cells. Again there is strong localisation of CD44 to the cell membrane. This high resolution image shows some intracellular CD44 staining, but this was confined to the cytosol (mostly large vesicles), with no significant signal present in the cell nucleus.

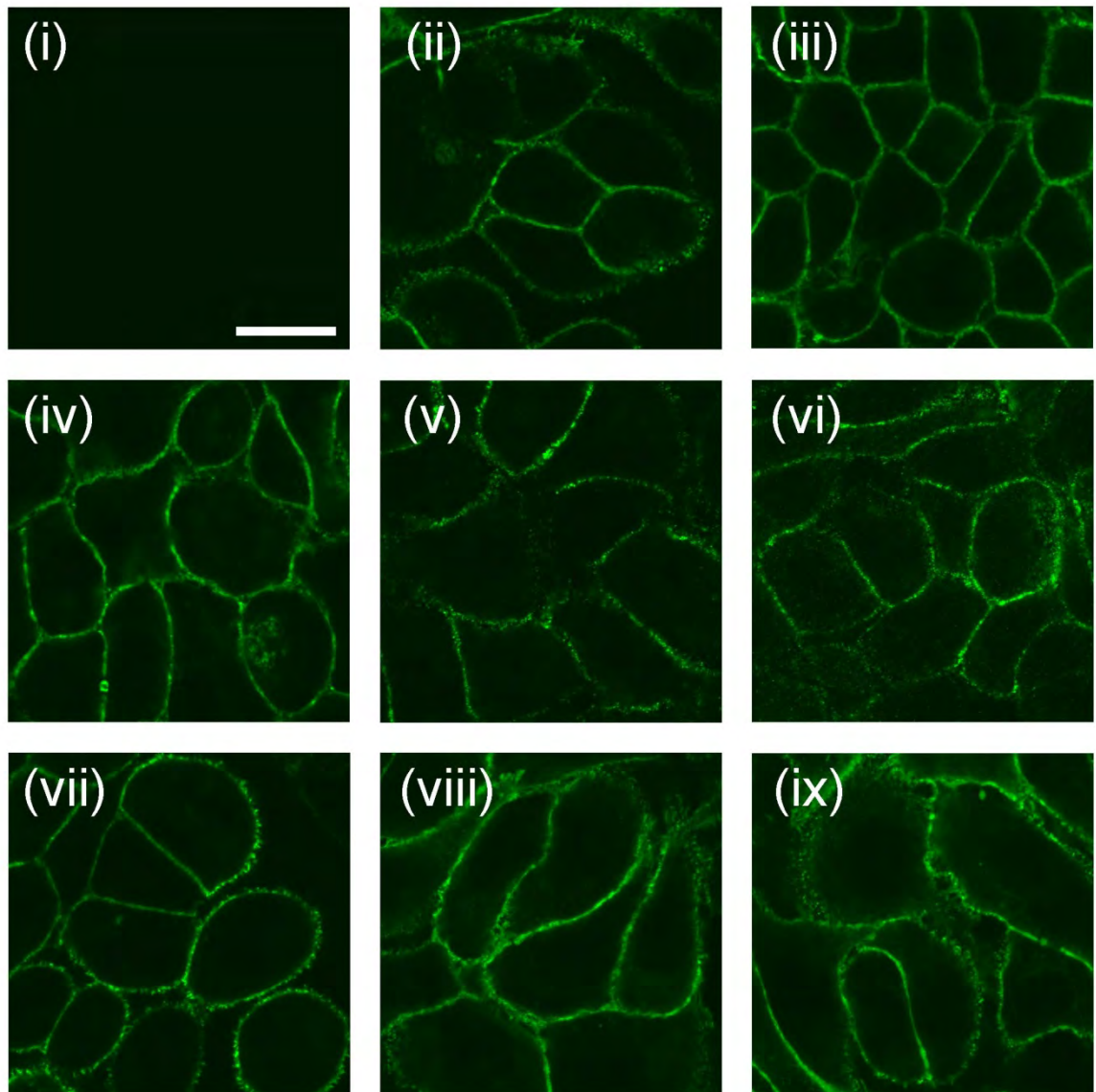


**Figure 5.3- Distribution of CD44 in HT-29 cells.** Cells grown on glass coverslips were fixed, permeabilised and immunostained with (i) detection reagents alone (anti-mouse IgG Alexa488 conjugate) or (ii - ix) mAb directed against the extracellular domain of CD44. The clones used were: (ii) Hermes-3 (in house); (iii) E1/2 (in house); (iv) Bu52 (Serotec); (v) F10-44-2 (SouthernBiothech); (vi) 2F10 (RD); (vii) 3E8 (in house); (viii) 5F12 (NeoMarkers); (ix) Bu52 (AnceCell). The cells were analysed using confocal microscopy. The images are optical sections of cells stained with each CD44 antibody against the extracellular domain in combination with a fluorescent secondary conjugate (Alexa488 anti-mouse IgG). Scale bar = 20µm

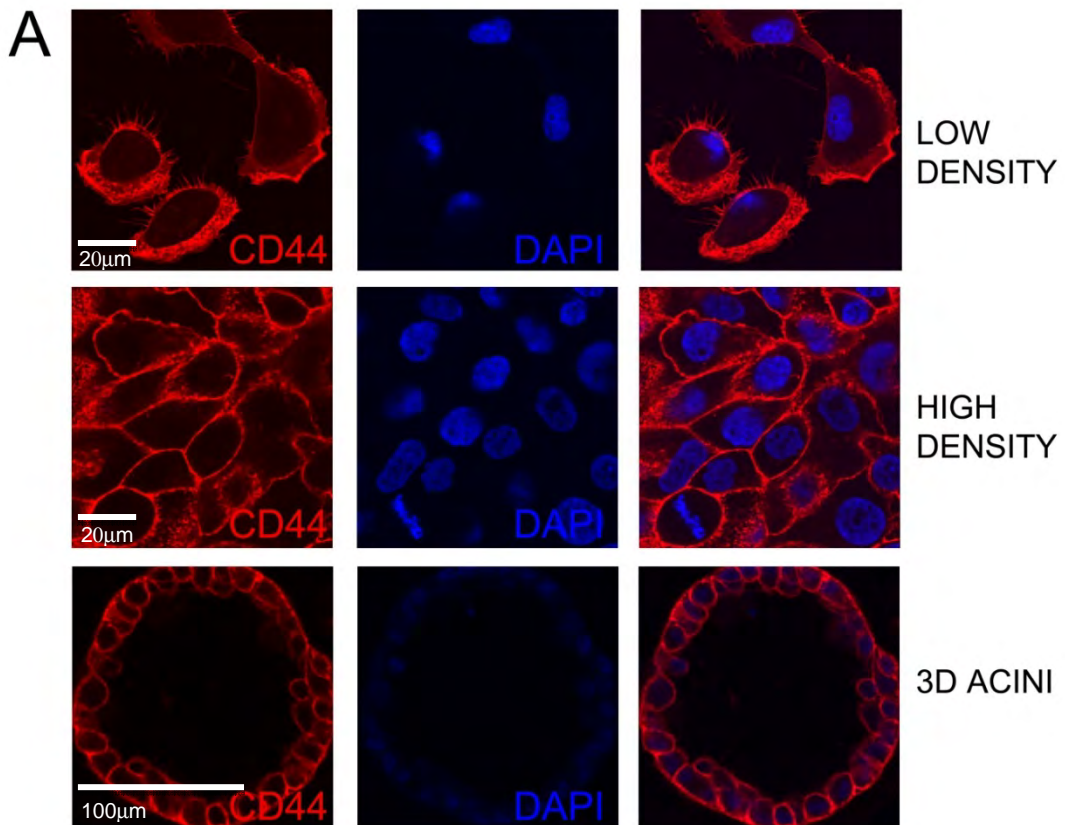
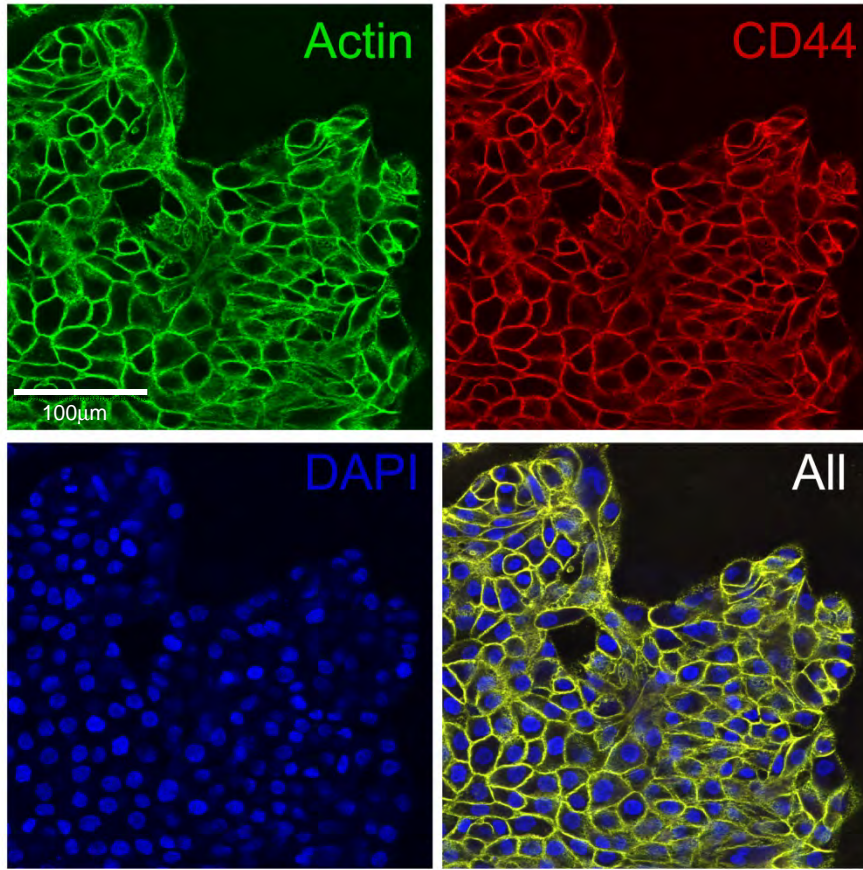
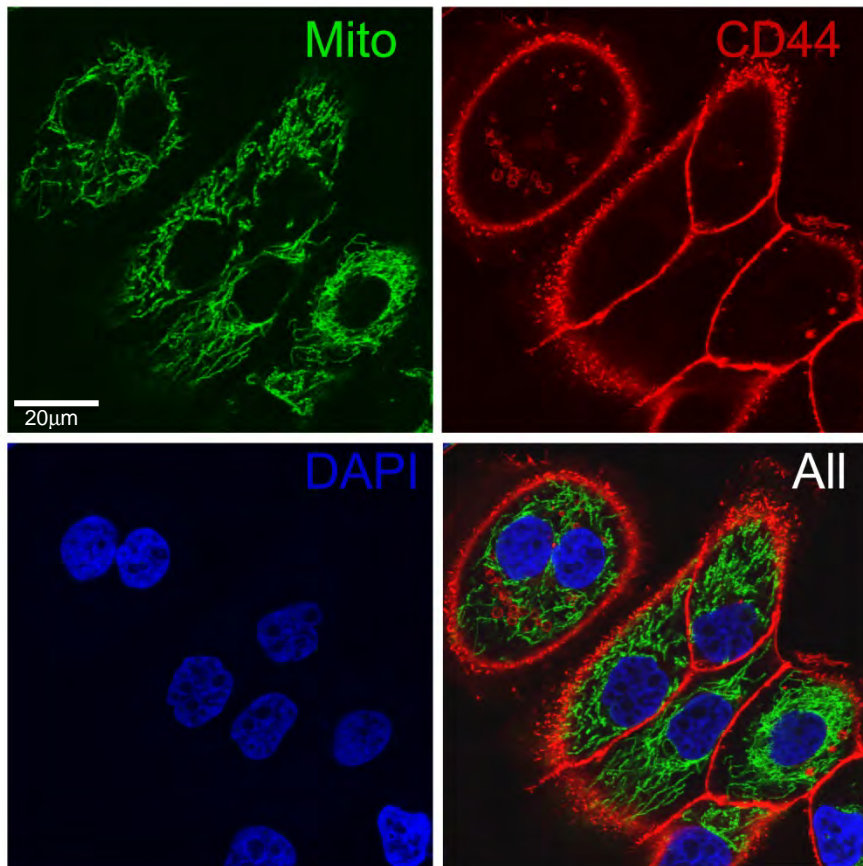


**Figure 5.4 – Immunofluorescence analysis showing the distribution of CD44 in MCF10A cells.** The photomicrographs represent optical sections of cells stained with the CD44 antibody (clone E1/2) against the extracellular domain in combination with the secondary antibody Alexa555<sup>®</sup> anti-mouse IgG or other indicated markers. Cell nuclei were counterstained using DAPI. (A) Immunofluorescence analysis of MCF10A cultured under different conditions (low density, high density and acini) showing CD44 staining (red; left panel), nuclear staining by DAPI (blue; middle panel) and the merged images (right panel). No co-localization of CD44 and the nuclear marker is observed. (B; next page) Immunofluorescence analysis of MCF10A cells under low magnification showing filamentous actin staining (Green; Top left panel) using Alexa488<sup>®</sup> phalloidin probe (Life Technologies); CD44 staining (Red; Top right panel); DAPI nuclear staining (Blue; Bottom left panel) and the merged images (Bottom right panel). A large number of cells can be observed in the small magnification images but no co-localization of CD44 and the nuclear marker is observed. (C, next page) MCF10A cells stained with anti-cytochrome C antibody as a mitochondrial marker (Green; top left panel), CD44 staining (Red; top right panel), DAPI (Blue, bottom left panel) or the merged images (bottom right panel). The Zenon<sup>®</sup> labelling kit was used to prepare direct fluorophore labelled-primary antibodies as described in Section 2.16 Some intracellular CD44 appears withing the cytosol but no CD44 is seen in the cell nucleus.

**B**



**C**



#### **5.2.4 Characterisation of antibodies against the extracellular and intracellular domain of CD44 in Western blotting**

Since CD44 could not be detected in the nucleus of any of the cell lines tested by immunofluorescence staining, to eliminate the possibility of technical problems that could conceivably be at play, the Western blot technique was also employed in order to further investigate the subcellular localization of full length CD44, and its cleaved cytoplasmic tail (ICD). First, it was necessary to characterise the blotting characteristics of antibodies against the extracellular domain of CD44 together with the CD44 ICD. For reasons described above, this work was undertaken in HT-29 cells that have been described to translocate the intact CD44 receptor to the cell nucleus (171). The HT-29 cells were transfected with siRNA against CD44 (siCD44) or scrambled control siRNA (siNC), and 3 days after transfection, cells were lysed and subjected to Western blotting.

Figure 5.5A shows the detection of CD44 using the Hermes-3 antibody, which recognizes the extracellular domain of CD44 (273). The bands represent the standard full length molecule (~90kDa) and the larger splice variants (100-150kDa), possibly V3 and V6 that have previously been reported in these cells (274, 275). It is clearly shown that the intensity of detected bands is decreased in cells transfected with siRNA against CD44. Although this represents partial knock-down of the receptor, it confirms the specificity of the antibody against the major reactive bands. The same samples were subjected to Western blot using CD44 ICD antibody, a commercial polyclonal antibody that recognizes the intracellular domain. This antibody detects, in addition to the full length molecule (90-100kDa), one band at 25kDa, which corresponds to the membrane bound cleaved CD44 containing the cytoplasmic domain (CD44 CTF), and a ~16kDa band, which corresponds to the CD44 ICD fragment. To further confirm the validity of this antibody, cells were treated with PMA (phorbol myristate acetate), which is known to induce CD44 cleavage (276). The detection of CD44 ICD was increased after PMA treatment in a concentration-dependant manner. GAPDH expression under the same treatment conditions remained unchanged (Figure 5.5C). Therefore, the major reactive bands identified by the antibody detecting CD44 cytoplasmic domain were also confirmed to be specific.

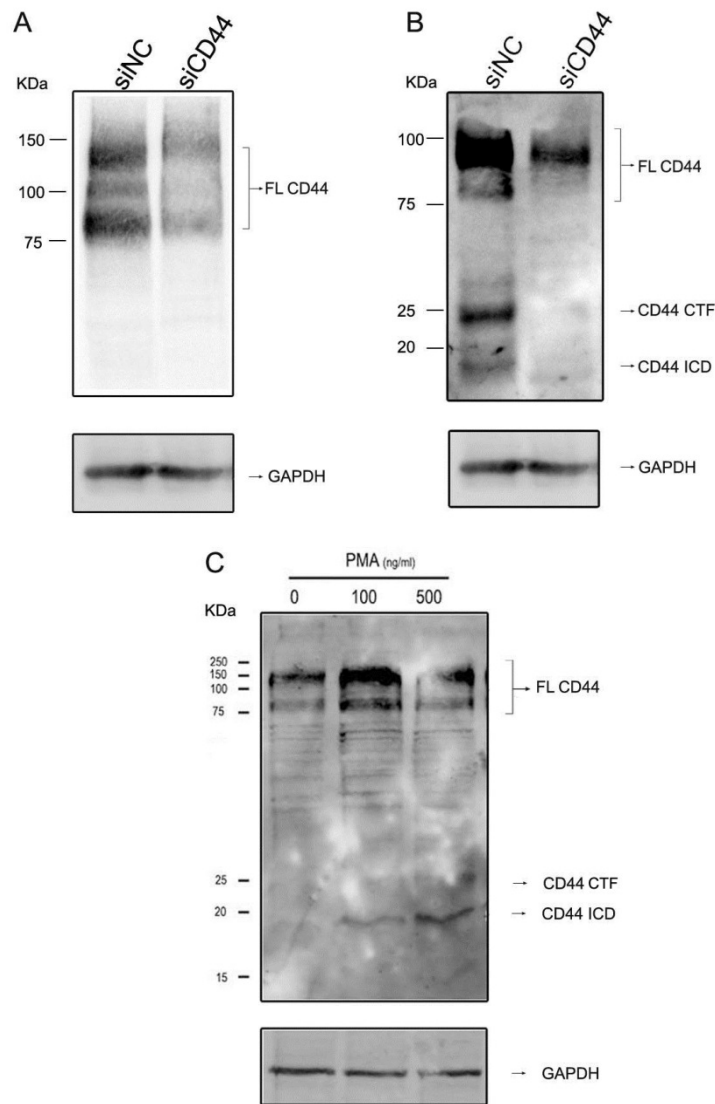


**Figure 5.5– Detection of CD44 by Western blotting using antibodies against extracellular and intracellular domain.** (A) HT-29 cells were transfected with siRNA against CD44 (siCD44) or scrambled siRNA (siNC) and after 3 days, were harvested and submitted to Western blotting with an antibody against the extracellular domain of CD44 (Hermes-3). The immunoreactive bands detected correspond to the different isoforms of CD44 with molecular weights ranging from ~90-150kDa (FL CD44). (B) Blotting with an antibody against the cytoplasmic tail of CD44 (CD44 ICD). Besides the full length molecule (90kDa), two additional specific bands were observed. The 25KDa band corresponds to the membrane bound cleaved CD44 containing the cytoplasmic domain (CD44 CTF). The CD44 intracytoplasmic domain (ICD) was also detected (~16kDa). (C) HT-29 cells were treated with 100 or 500ng/mL of PMA for 30 minutes. PMA treatment caused the appearance of bands at ~25 and ~16kDa representing the cleavage products of CD44. Note that different percentages of acrylamide were used to optimally detect FL CD44 (7.5%, A) and the cleaved products (12%, B and C) and therefore the migration patterns of markers appear different.

### **5.2.5 Biochemical determination of the subcellular localization of CD44 using a detergent-based lysis method**

After verifying the specificity of the anti-CD44 blotting reagents, the next step was to further investigate CD44 subcellular localization. HT-29 cells were lysed using detergent-based lysis, and the nuclear fraction was collected by centrifugation at 5,000 x g for 15 minutes. The supernatant was also kept and represents the cytosolic/cell membrane fraction. Both nuclear and cytosolic fractions were then submitted to Western blotting and probed with CD44 antibodies against the extracellular or intracellular domain. The results show that full length CD44 detected by Hermes-3 antibody is strongly present in the cytoplasmic/membrane fraction, consistent with results obtained with the whole cell lysates (compare Figures 5.5A and 5.6A). Examination of the nuclear fraction also showed a faint band of identical size and appearance as the main CD44 immunoreactive band in lysates (Figure 5.6A). Therefore, some intact CD44 can be found in a biochemical fractionation that enriches the cell nucleus.

The same nuclear and cytosolic fractions were also subjected to analysis using the CD44-ICD antibody. As shown in Figure 5.6B, the full length molecule was again strongly detected in the cytoplasmic/membrane fraction, as well as the membrane bound CD44-CTF (25kDa). The CD44 ICD fragment (~16kDa) was also detected, but only in the nuclear fraction, consistent with the known nuclear transportation of the ICD fragment after cleavage.

In order to better understand these results, further analyses were performed to understand the composition of these fractions. GAPDH antibody was used as a cytoplasmic marker, and Figure 5.6C shows that, although the strongest band is in the cytoplasmic fraction, some GAPDH was also detected in the nuclear fraction. Conversely, a nuclear marker, Lamin A/C, could also be detected in small amounts in the cytoplasmic fraction (Figure 5.6D). Furthermore, using an antibody against CD9, a cell-surface protein which is a member of the

tetraspanin family, analysis showed that most of the CD9 protein was detected in the cytoplasmic/membrane fraction although a faint band can still be seen in the nuclear fraction (Figure 5.6E). Collectively these results suggest that the method employed greatly enriches the presence of nuclear proteins in the nuclear fraction and cytosolic and transmembrane proteins in the cytosolic fraction. These observations are consistent with the notion that these fractionations represent enrichments rather than purifications. The presence of small amounts of intact CD44 in the cell nucleus in this context may therefore not provide irrefutable evidence of CD44 translocation to the cell nucleus.

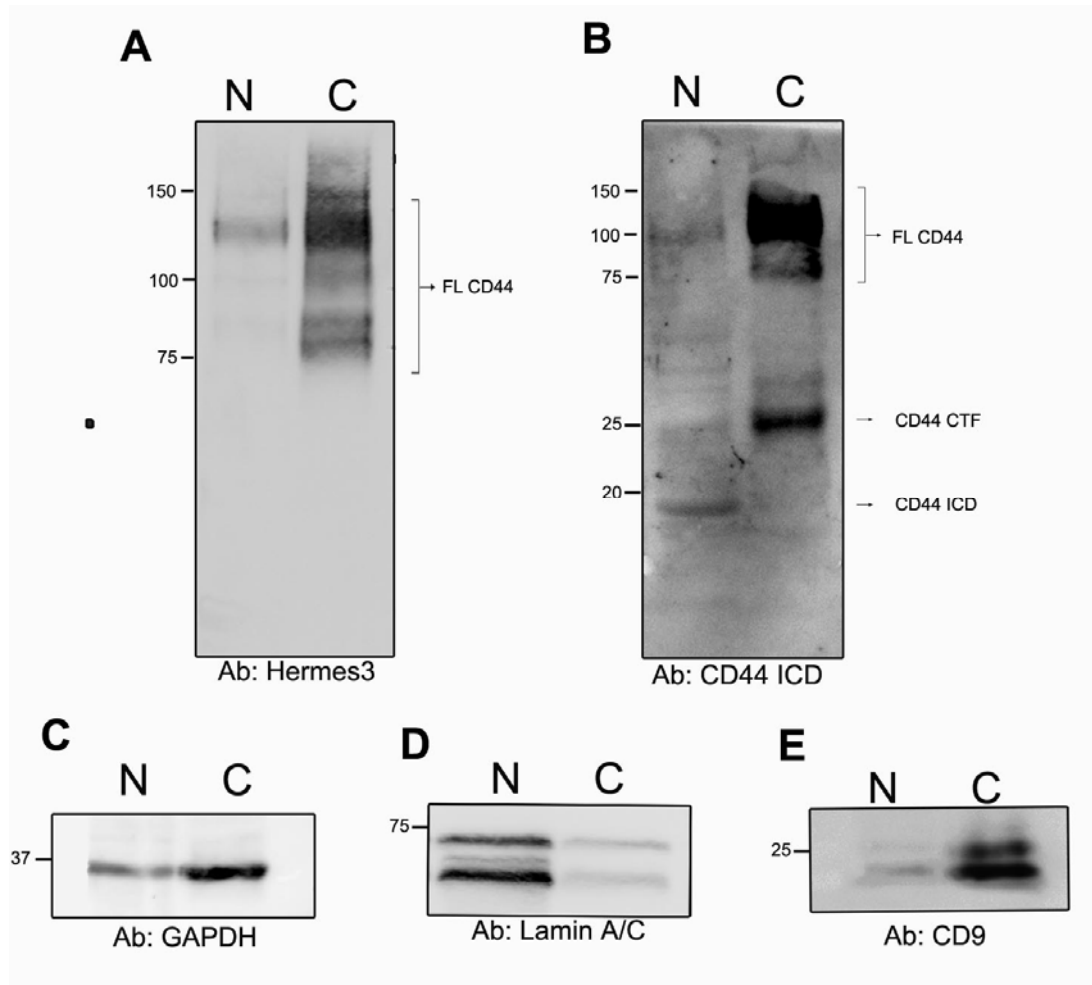


**Figure 5.6 - Subcellular localization of CD44 after cell fractionation using detergent-based lysis.** Nuclear and cytoplasmic fractions prepared from the HT-29 cell line were analysed by Western blotting using antibodies against CD44 extracellular domain (Hermes-3; A); CD44 ICD (B); GAPDH (C); Lamin A/C (D) and CD9 (E). Specific CD44 bands are highlighted as per Figure 5.3: full-length CD44 (FL CD44), intracytoplasmic domain (CD44 ICD) and membrane-bound C-terminal fragment (CD44-CTF). Numbers on the left are Molecular Weights (kDa).

### **5.2.6 Determination of CD44 sub-cellular localization using nitrogen decompression lysis and fractionation by differential centrifugation**

In the previous Section, subcellular fractionation using a detergent-based method failed to provide convincing evidence that the full length CD44 molecule could translocate to the cell nucleus. Indeed, together with the results of immunofluorescent staining, some doubt was cast upon as to whether this occurs at all. As further verification, an alternative “non-detergent” method was employed.

Cell disruption by nitrogen decompression from a pressurized vessel is a rapid and effective way to homogenize cells and tissues, to release intact organelles, and to prepare cell membranes. HT-29 cells were lysed by nitrogen decompression and cell fractions were separated by differential centrifugation (277, 278) as described in Chapter 2. Four fractions were collected: fraction 1 is a nuclei enriched fraction pelleted at 1,000 x g; fraction 2 is mitochondria enriched fraction, pelleted at 20,000 x g; fraction 3 is the light membrane enriched fraction pelleted at 100,000 x g; finally the supernatant containing cytosolic proteins is fraction 4. The different fractions were then submitted to Western blotting and probed with CD44 antibody Hermes-3 and specific markers: GAPDH for cytosolic fraction, Lamin A/C for nuclear fraction and CD9 for membrane fractions respectively.

The results show that although the majority of CD44 was present in the membrane fraction as expected, some level of the receptor was also detected in the mitochondria- and nuclear-enriched fractions, as well as in the cytosol. Nevertheless, GAPDH, which is a cytosolic protein, was also detected at a lower level in all the other fractions; Lamin A/C, the nuclear marker, was also present in the mitochondria-enriched fraction and at lower levels in the membrane fraction; CD9, a cell-surface protein, was detected in both mitochondrial and nuclear fractions in addition to the cell membrane fraction. These results again suggest that these cellular fractions are not pure but only enriched. Taken together, the most logical interpretation is that these fractionation procedures have the inherent limitation of small amounts of cross-contamination between fractions.

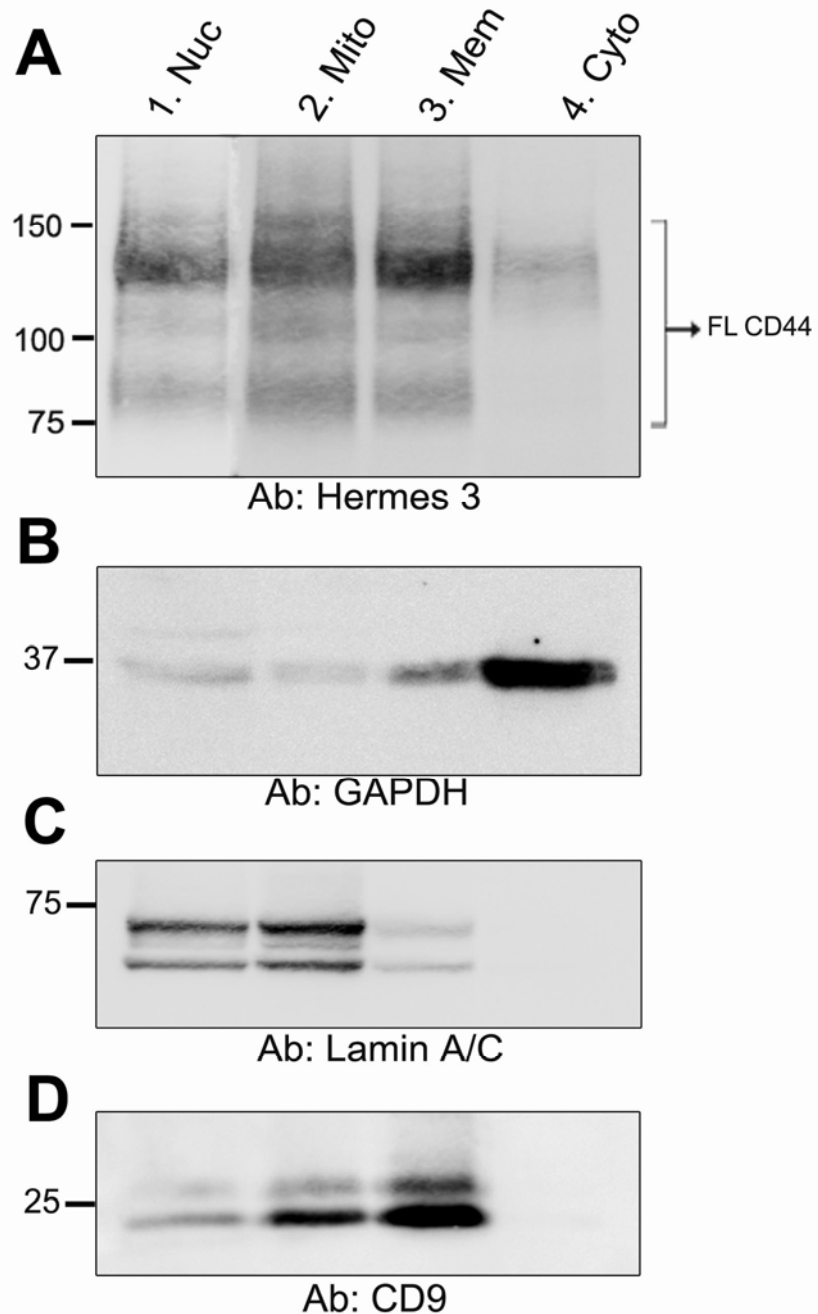


**Figure 5.7- Sub-cellular localization of CD44 in HT-29 cells after nitrogen decompression lysis and cell fractionation.** Cells were disrupted by nitrogen decompression and the subcellular fractions were separated by differential centrifugation. Fraction 1 is the nuclear fraction (Nuc), pelleted at 1000 x g; fraction 2 is the mitochondrial fraction (Mito) pelleted at 20,000 x g; Fraction 3 contains light cell membranes (Mem) pelleted at 100,000 x g and the supernatant is the cytosolic fraction (Cyto; fraction 4). The different fractions were analysed by Western blotting using antibodies against CD44 extracellular domain (Hermes-3; A); GAPDH (B); Lamin A/C (C) or CD9 (D).

### 5.3 Discussion

Consistent with the Western blotting data presented in Figure 4.1, an analysis of 6 melanoma cell lines using indirect immunofluorescence staining for MIF showed abundant MIF protein present within all of the melanoma cells both in the cytoplasm and cell nucleus (Figure 5.1). Cell lines that had more nuclear MIF staining were those most sensitive to the effects of MIF depletion using siRNA. The converse was also true, those with relatively less MIF in the cell nucleus were not as sensitive to the inhibition of proliferation that occurred as a result of MIF depletion. This result provided an indication that the significant functions of MIF, with respect to antagonising MIF and inhibiting melanoma cell growth, may occur within the cell nucleus.

For reasons described in the Introduction to this Chapter, it was considered that CD44 was a strong candidate for being involved in the delivery of MIF to the cell nucleus. The possibility of direct nuclear translocation of cell surface receptors has been known for many years, but with limited acceptance due to lack of knowledge of how such receptors might travel into the nucleus (279). One of the first full-length receptors reported to traffic to the nucleus was EGFR (epidermal growth factor receptor), and since then, other reports have shown different examples of receptor nuclear-translocation, like ErbB2, FDFR1, c-Met and IGF-1R (reviewed in (280, 281)) but the mechanistic basis of these findings remains hidden. Different mechanisms have been proposed for nuclear translocation, including classical nuclear localization signal (NLS) binding to the importin  $\alpha/\beta$  complex (281), association of non-NLS containing receptors to an NLS-containing cytosolic binding partner (280), or by covalent binding of the small-ubiquitin-like modifier-1 (SUMO-1; SUMOylation) (282). In the case of CD44, a nuclear localization signal (NLS) was mapped to the cytoplasmic tail, and it was thought to mediate its nuclear translocation through interaction with the carrier transportin-1 (170, 171).

The immunofluorescence analysis of CD44 expression in melanoma cells showed strong cell surface staining for this receptor, but no detection was observed in the cell nucleus

(Figure 5.2). Using the same methodology, two different nuclear proteins could be readily recognised using both monoclonal and polyclonal antibody reagents (Appendix 3) indicating that the cell nucleus was permeabilised and nuclear proteins were readily accessible to staining. To confirm the veracity of this finding, the distribution of this receptor was further studied by immunofluorescent staining using HT-29 and MCF10A, cells which have been shown to contain nuclear FL-CD44 (170), using a panel of 8 mAb against the extracellular domain of CD44, and different culture conditions. Again, the staining pattern for immunoreactive CD44 indicated an exclusive membrane localization of CD44 with no co-localization was observed with the nuclear marker DAPI. Notably this assessment also included the exact antibody clone (Hermes-3) used to detect nuclear FL-CD44 in previous studies (170) indicating that the failure of our experiments was not due to epitope masking.

Further analyses were performed using biochemical techniques to eliminate the possibility of technical problems. Antibodies against the extracellular or intracellular domain were validated by using siRNA mediated knockdown of CD44, after which the intensity of CD44 immunoreactive bands was diminished (Figure 5.5). Detection of CD44-ICD was further confirmed by treatment with PMA, which is known to induce cleavage of the receptor (276) (Figure 5.5C). The same antibodies were then used to detect CD44 in different cell fractions prepared using different techniques. The first method used here was a detergent-based lysis followed by low speed centrifugation, in order to pellet the nucleus. The results show that full-length CD44 detected by the extracellular domain antibody was strongly present in the cytoplasmic/cell membrane fraction and a less intense band could also be detected in the nuclear fraction. The CD44 ICD was only detected in the nuclear fraction (Figure 5.6). As an alternative method, cell disruption by nitrogen decompression from a pressurized vessel was used to homogenize the cells and 4 different fractions were separated by differential centrifugation. In this case, full length CD44 was strongly detected at the membrane fraction, but some level of the protein was also detected in the mitochondrial, nuclear and cytosolic fractions (Figure 5.7).

It is essential to stress that with traditional sub-cellular fractionation procedures like the ones used here, complete purification is almost impossible but rather favours the enrichment of particular fractions. Therefore, it is important to assess the fractions quality and purity by analysing a set of sub-cellular marker proteins (283). GAPDH, a cytoplasmic glycolytic enzyme, was used as a cytoplasmic marker, and independently of the fractionation method used, this enzyme was detectable in all fractions, although more strongly in the cytoplasmic fraction (Figure 5.6 and 5.7). Lamin A/C are nuclear membrane structural components commonly used as nuclear markers. In the present work, Lamin A/C was present in the nuclear fraction, but was also detected in other fractions.

To better understand the observed CD44 distribution in these experiments, another cell membrane protein, CD9, was also used as a control. CD9 was a cell-surface protein which is a member of the tetraspanin family. The results clearly show that CD9 is strongly present in the membrane fractions, but also detected in the nuclear fractions, as was the case for FL-CD44. Taken together, the distribution of markers across the different fractions confirms the presence of cross-fraction contamination, thus the presence of FL-CD44 in the nuclear fraction cannot support the conclusion that the molecule is internalized and translocated to the nucleus. Thus, despite two reports in high profile journals showing evidence of nuclear translocation of CD44, the results presented in this Chapter suggests that only a fragment of CD44 is translocated to the nucleus and full-length molecule is found exclusively at cell surface level. This does not invalidate the finding that nuclear MIF is important, and indeed this intriguing finding warrants further investigation.

# **Chapter 6**

## **General Conclusions and Future Directions**

## 6.1 General Conclusions

### 6.1.1 Recent facts on melanoma

Melanoma is considered Australia's national cancer since our continent has the highest incidence of this disease in the world. As reviewed in Chapter 1, melanoma rates in Australia have doubled in the 20 years from 1986-2006, and are still on the rise, with an estimated 392 extra cases per year. Especially among young Australians (15-44 years-old), melanoma is the most common cancer and among 20–34 year-olds, melanoma kills more young Australians than any other single cancer (4, 5). The statistics are alarming, and in response prevention campaigns have been implemented, with strategies involving sun avoidance, sun protection and also regular skin checks. However, in a large number of cases melanoma is not detectable in early stages, and it is not always related to sun exposure.

Since current approaches to prevent melanoma have not been able to reduce the incidence rates, efforts have been directed to improve early detection and to develop more effective melanoma therapeutics. When detected early, melanoma is highly curable by surgical excision. However, melanoma is an insidious disease that has the propensity to metastasize early. Current treatments for disseminated disease are highly inefficient and once the tumour spreads beyond the primary site, melanoma is almost universally fatal. Despite intensive research into better ways to treat malignant melanoma, it remains refractory to conventional therapy. In fact, when surgery is not an available option, enrolment in a clinical trial is the recommended course of action, highlighting the desperate situation faced by sufferers of this disease (22, 36, 37) .

The clinical management of melanoma remains a significant challenge, however discoveries made in recent years have substantially changed the outlook for melanoma therapies. Scientists like Professor Richard Marais changed the course of melanoma research with the finding that *BRAF* mutation was critical in a large proportion of melanomas (78). In

2002, the discovery of BRAF mutations in more than half of melanoma cases was a breakthrough in melanoma research and opened the doors to significant therapeutic advances against malignant melanoma (41). This discovery created the opportunity to develop a highly specific oncogene-directed therapy in a relatively short timeframe. In 2004, the Marais group was the first to solve the crystal structure of the BRAF protein, a discovery that allowed the development of PLX4032 (now referred to as vemurafenib), which is a specific inhibitor of the mutated BRAF protein (284, 285). A few years later (2011), orally available vemurafenib was approved by the FDA for the treatment of BRAF mutant metastatic melanoma. Treatment with vemurafenib shows a high response rate and survival advantage in comparison with standard chemotherapy. Disappointingly, the clinical benefit for most patients is limited and the great majority eventually exhibit disease progression due to acquired resistance to treatment. The mechanisms of resistance to BRAF inhibition are under intensive research and clinical programs attempting to abrogate resistance are already being pursued (286, 287). Although not a cure, uncovering the importance of BRAF was a crucial step toward developing new treatments for melanoma. However, melanoma is a heterogeneous disease, and the potential benefits brought by selective mutant BRAF inhibitors are only applicable to around 60% of melanoma patients. Thus while the melanoma landscape has now substantially changed, for those patients not presenting BRAF mutation, finding other targets is still urgent.

The thinking for some time has been that the solution to the problem of melanoma lies with a better understanding of the alterations in melanoma signalling pathways. This idea comes about because the inherent resistance of melanoma to treatment is thought to be in large part due to the hyperactivation of survival signalling pathways. Virtually all melanomas display constitutive activation of the ERK/MAPK and Akt pathways and this is thought to be one of the earliest events in melanoma development as well as being essential in its progression (49, 69, 85). The hyperactivation of these pathways is primarily achieved by mutations in upstream proteins, including BRAF, NRAS and PTEN (6) and some of the resistance mechanisms to BRAF inhibitor treatment involves the “reactivation” of these enzymes through alternative pathways (61-63). In that context, it is important to emphasize that tumours that do

not contain any activating mutation on the above mentioned genes still present constitutive activation of ERK and Akt pathways and in such cases, the activation could be achieved by aberrant autocrine production of growth factors (86, 88). The work presented in this thesis focused on the role of one such growth factor, MIF. MIF had previously been observed to act as the autocrine factor driving activation of survival pathways. In the context of cancer, these properties of MIF are thought to contribute to uncontrolled proliferation and tumour aggressiveness. In melanoma, however, these proposed functions have not been explored in detail.

### **6.1.2 MIF expression in melanoma progression**

The study presented in Chapter 3 used a combination of *in silico* analyses of relative MIF mRNA expression together with immunohistochemistry of tissue biopsies to show that MIF expression is higher in metastatic melanoma compared to normal skin, naevi or primary melanoma. The availability of microarray datasets with associated clinical follow-up data made possible further investigation to associate MIF transcript levels with patient survival. Although MIF expression has been shown to associate with cancer prognosis for a variety of human cancers like lung, prostate, colorectal, and gastric cancer (206, 208, 259, 288-291), there were no previous reports associating MIF expression with melanoma outcome. Here it was shown for the first time that high expression of *MIF* is associated reduced disease-free survival of patients with metastatic melanoma (Figure 3.3) implicating it in tumour aggressiveness. This is particularly significant for metastatic melanoma, since the majority of cases cause death, and there is a lack of molecular characteristics that are useful as biomarkers.

Moreover, to verify if transcripts encoding MIF signalling receptors were also indicative of poor disease outcome, *in silico* analyses were also conducted for *CD74*, *CD44* and *CXCR4* expression. From this analysis, only *CD44* showed an association of high expression with worse prognosis. Surprisingly, *CD74* and *CXCR4* showed the opposite relationship, with lower expression being associated with worse disease-free survival (Figure 3.5). High *CXCR4* in particular had been previously reported as a poor prognostic indicator in a range of cancers

including melanoma (189, 191, 240). The fact that *CD74* and *CXCR4* expression levels were differently associated with patient prognosis could indicate that these receptors have different roles in melanoma, independent of MIF signalling. Although CD44 has not been shown to directly bind MIF, the finding that both *MIF* and *CD44* higher expression levels are associated with faster disease progression raised the hypothesis that MIF and CD44 could have associated roles in melanoma progression. This notion was further addressed in Chapter 5, where the nuclear localization of MIF and CD44 were examined.

### **6.1.3 The functional role of MIF in melanoma cell lines**

Having shown that MIF expression was associated with poor prognosis for patients with metastatic melanoma, the next step was to investigate the mechanisms of MIF signalling in these tumours. The approach taken in Chapter 4 was to investigate the effects of MIF expression on melanoma cell proliferation and survival *in vitro*, including the analysis of downstream signalling.

MIF has previously been implicated in many aspects of tumour progression, including cell proliferation, invasion, and angiogenesis (94, 103, 104, 113), but very little was known about the function of MIF in melanoma cells. Here, the MIF protein was first found to be ubiquitously expressed in a large panel of 20 melanoma cell lines, confirming their suitability to examine the function of MIF. Thereafter, siRNA was used to inhibit MIF expression in 6 different cell lines selected to include different combinations of CD74 expression levels and *BRAF* mutation status (Chapter 4, Table 4.1). These experiments showed that MIF inhibition significantly decreased the ability of cells to proliferate in 4 out of the 6 cell lines analysed (Figure 4.4). Specifically, the depletion of MIF reduced the number of cells entering S-phase of the cell cycle, suppression of cell growth and the reduction of cell viability beginning 3 days after MIF knockdown. Additional experiments also showed that MIF depletion also impaired anchorage-independent cell growth in two human melanoma cell lines (Figure 4.5). Collectively these results promoted the notion that the proliferative capacity of the majority of melanoma cells is reliant upon their endogenous expression of the MIF protein.

An association was then established between MIF expression in melanoma and the Akt signalling pathway. MIF knock-down resulted in a decrease of Akt phosphorylation in several melanoma cell lines, and this effect was accompanied by a reduction in expression of Cyclin D1 and Cyclin dependent kinase 1 (CDK1), and increased expression of p27 (Figure 4.6). In addition, the degree of MIF knockdown influence on Akt activation for each cell line was largely correlative with the functional effects of MIF expression, suggesting that MIF regulates cell-cycle by activating Akt pathway in melanoma cells.

MIF signalling can act through both CXCR4 and CD74 receptors, the latter requiring CD44 to act as a co-receptor to permit signal transduction. Western blotting and flow cytometry analysis showed that although all 20 melanoma cell lines analysed expressed CD44 and the chemokine receptor CXCR4, only expressed CD74 (Figure 4.1 and 4.2). Although the complex formed by CD74 and CD44 was the first proposed membrane receptor complex for MIF, here it was shown that the effects of MIF on melanoma cell lines were independent of CD74, since no association was seen between CD74 expression and the sensitivity of cells to MIF depletion. Although not presented in the thesis, further experiments were undertaken to examine the participation of these receptors in MIF signalling and melanoma proliferation. SiRNA mediated knockdown was also performed for each of the receptors, using at least 3 different siRNA sequences, followed by proliferation analysis by the ClickIT™ assay. If MIF's role in melanoma cell lines was dependent on one of the receptors, it would be expected that the receptor depletion would have the same effect as MIF depletion. However, the siRNA sequences used here to knockdown CD44, CD74 and CXCR4 were unable to completely deplete expression, with only 40-60% reduction in protein levels observed (data not shown). No significant difference was observed in the proliferation analyses, which could be in part due to incomplete knockdown, but it also suggests that MIF could function independently of these known MIF receptors.

A large panel of melanoma cell lines was used for *in vitro* studies, in an attempt to account for the vast heterogeneity that is a characteristic of malignant melanoma. In this

context, recent advances in melanoma treatment using specific BRAF<sup>V600E</sup> inhibitors were considered. Most importantly, the sensitivity of individual melanoma cell lines to MIF depletion was not associated with *BRAF* mutational status. Therefore, MIF presents as a potential target for an alternative treatment for melanoma, particularly for patients that do not have mutated *BRAF*, or for the cases that develop resistance to BRAF inhibitor treatment.

#### **6.1.4 CD44 translocation to the nucleus: a potential mechanism for delivering the MIF signal?**

As mentioned in the previous section, siRNA inhibition studies were performed to directly examine the contribution of known MIF receptor expression to MIF signalling in melanoma. However, these experiments were confounded by technical issues. With respect to understanding how MIF functions in melanoma cells, another area of interest concerned the results of Chapter 3, where it was shown that in addition to its cytoplasmic pool, MIF was also present in the nucleus of melanoma cells. Considering that ligand-induced endocytosis of cytokine-receptor complexes and nuclear translocation have been suggested for several cytokines (224, 225) and that CD44 has recently been shown by two independent reports to be translocated to the nucleus (170, 171), we hypothesised that if CD44 was involved in the translocation of MIF to the nucleus of melanoma cells, this could indicate a novel mechanism for MIF signalling in melanoma.

Accordingly, in Chapter 5 it was investigated whether MIF and CD44 co-localized in the nucleus of melanoma cells and this would provide preliminary evidence of the proposed mechanism. The presence of MIF was confirmed in the nucleus of melanoma cell lines by immunofluorescence staining (Figure 5.1). Interestingly the cell lines that presented higher expression of MIF in the nucleus were also the most sensitive to MIF depletion, suggesting that the effects of MIF in melanoma cell lines could be associated with its presence and function in the cell nucleus. The same analysis was repeated for CD44 expression, but unexpectedly,

CD44 could only be detected at the cell surface of the melanoma cell lines examined (Figure 5.2). This negative result provided a conundrum, since on the basis of recent publications, it was anticipated that the intact CD44 molecule would be found in the nucleus of melanoma cells. It was suspected that the inability to visualise intact CD44 in the nucleus could have occurred because of methodological issues, for example, by the epitope recognised by our mAb being masked. Consequently, it was decided to verify the method against other cells known to have intact CD44 in the nucleus, like the colon cancer cell line, HT-29 (171) and the human epithelial cell line, MCF10A (170) and also to evaluate a panel of anti-CD44 mAbs. For this purpose, different techniques were employed, including different methods of cell fractionation and immunostaining with confocal microscopy analysis, using antibodies against the extracellular region of CD44 to confirm the presence of the full length molecule in the nucleus. Subcellular fractionation is a technique commonly used to investigate nuclear localization of proteins, and we showed here that although FL-CD44 can be detected in the nuclear fractions, this was almost certainly due to cross-fraction contamination, as shown by the use of nuclear, cytoplasmic and membrane markers. Therefore, these methods should be used with caution, since the cellular fractions resulting from these processes are only enriched but not pure, potentially giving misleading conclusions.

Probably the most convincing published evidence for the presence of FL-CD44 in the nucleus comes from the technique of immunofluorescence staining combined with confocal microscopy. Surprisingly, exhaustive use of this technique showed no staining for CD44 in the nucleus in a variety of settings. Collectively with the biochemical evidence the results presented in Chapter 5 do not support the initial hypothesis that CD44 could be involved in the translocation of MIF to the nucleus in melanoma cells. Nevertheless, this is important since the functional consequences of CD44 signalling are highly relevant to a great number of cancers. The results however do support the well established paradigm of sequential cleavage and transport of the CD44-ICD to the cell nucleus. Therefore, it will be important to publish this work to allow a proper re-evaluation of this process.

## 6.2 Future Directions

The targeting of components of cell survival pathways has been successfully employed in the treatment of several cancers. In melanoma, the development of selective BRAF<sup>V600E</sup> inhibitors in the last decade has brought hope of an efficient treatment for metastatic disease. While this has arguably produced the most spectacular results, the approach has not occurred in isolation and inhibitors of survival pathways have met with their own success in the other forms of cancer. In lung cancer, for instance, current targeted therapy includes the use of inhibitors of EGFR and drugs targeting EML4-ALK, which is an aberrant fusion gene product with constitutive kinase activity. In chronic myelogenous leukemia (CML), the tyrosine kinase enzyme ABL (V-abl Abelson murine leukemia viral oncogene homolog 1) in white blood cells is locked in its activated form, and imatinib, a drug used to treat this cancer, inhibits the tyrosine kinase activity of ABL. Breast cancer patients with tumours overexpressing ErB-2 (human epidermal growth factor receptor 2) are also treated with trastuzumab, a FDA approved monoclonal antibody targeting ErB-2.

No matter how effective single anti-cancer agents have become, all too frequently they fail to eradicate disease. The development of drug resistance, involving secondary mutations or other aberrant signalling activations, circumvents the cytotoxic effects of both targeted and non-targeted treatments. It is now apparent for many cancers that multiple redundant aberrant signalling pathways are at play, and this circumstance requires the use of combined targeted approaches to achieve a cure for these malignancies. Indeed, new therapeutic strategies trying to address drug resistance mechanisms have been using combined therapy in an attempt to overcome this problem (292-295). Where then does this place the major findings of this thesis?

First, being able to associate high MIF expression with faster disease progression in melanoma highlights the general importance of MIF to this disease. Therefore, this observation places MIF as a *bona fide* target in melanoma. Secondly, the targeting of MIF is

likely to be effective for patients independent of *BRAF* mutational status and indeed may be applicable to the majority of patients. A further important question then arises as to how practically to achieve the targeting of MIF *in vivo*. Towards this, it is encouraging that such work is already underway.

MIF is known to have tautomerase activity and although the relationship between the catalytic activity and biological function of MIF is not fully understood, targeting MIF tautomerase activity using small-molecule inhibitors has emerged as an attractive therapeutic strategy (296, 297). To date, various classes of small molecule MIF inhibitors have been produced and MIF inhibition has proven beneficial in a number of disease models. However, most of the inhibitors available are not ideal for pharmaceutical development. For example, ISO-1, the most well characterized MIF inhibitor, displays only micromolar potency with respect to MIF inhibition, raising concerns about low potency and off-target effects. Recently, a great deal of work has been done to accelerate the development of clinically relevant MIF inhibitors, and superior performance inhibitors as compared to the prototypical ISO-1 have already been described (298). The new generations of MIF inhibitors could be of potential therapeutic benefit for treatment of melanoma, by itself or combined with *BRAF*<sup>V600E</sup> inhibitors and/or other drugs.

Moreover, the present work used small interfering RNA (siRNA) to target MIF, and this has been shown to be very efficient in completely depleting MIF from melanoma cells and greatly reducing melanoma growth. Over the last decade, many research groups and pharmaceutical companies have been working on strategies to be able to efficiently use siRNA in cancer therapeutics. Significant advances in this field have been made so far, but several obstacles remain to be overcome, including effective tumour-specific siRNA delivery (299-303). One process where we hope to participate is by means of a recent collaboration in the development of dual compounds called aptamers that are able to both target cancer cells and simultaneously deliver siRNA. Should these be successful, this could represent an efficient strategy for inhibiting MIF function in melanoma.

## **Appendix 1**

Production of recombinant MIF in *Pichia pastoris*

## 1 *Pichia pastoris* system

As discussed in Chapter 4, the use of commercial recombinant MIF (rMIF) raises the potential problem of undefined endotoxin contamination since all available are prepared in bacterial systems. To circumvent this serious drawback, an alternative method to produce recombinant MIF using yeast was undertaken. The system used for this purpose was the *Pichia pastoris* yeast system (256, 257, 304-306) which would potentially allow the production of bioactive endotoxin-free recombinant MIF. In addition, as a eukaryote, *Pichia pastoris* has many other advantages common of higher eukaryotic expression system. Unlike bacteria, the intracellular environment of these yeast undertake many of the post-translational protein processing events occurring in higher eukaryotes, while being relatively easy to manipulate (307). Post-translational modifications can also be a disadvantage, but this needs to be assessed on a case-by-case basis.

*Pichia pastoris* can only poorly ferment sugars or other carbon sources. As a methylotrophic yeast, *P. pastoris* is capable of metabolizing methanol as its sole carbon source. Like many alternative carbon source pathways, growth on methanol requires the induction of a specific set of metabolic enzymes. The first step in the metabolism of methanol is the oxidation of methanol to formaldehyde using molecular oxygen by the enzyme alcohol oxidase. Alcohol oxidase has a poor affinity of O<sub>2</sub>, and *Pichia pastoris* compensates by generating large amounts of the enzyme. The promoter regulating the production of alcohol oxidase is the one used to drive heterologous protein expression in *Pichia*. Two genes in *Pichia* code for alcohol oxidase, *AOX1* and *AOX2*, but the majority of alcohol oxidase activity in the cell is attributable to the product of the *AOX1* gene. Expression of *AOX1* is tightly regulated and induced by methanol to very high levels. The gene has been isolated and a plasmid-borne version of the *AOX1* promoter is used to drive expression of the gene of interest, encoding the desired heterologous protein (308-310). Expression of the *AOX1* gene is controlled at the level of transcription. In addition, growth on glucose represses transcription, even in the presence of the inducer

methanol. For this reason, growth on glycerol is recommended for optimal induction with methanol (309, 311).

There are three phenotypes of *P. pastoris* host strains with regard to methanol utilization. The Mut<sup>+</sup> or methanol utilization plus phenotype, grow on methanol at the wild-type rate and require high feeding rates of methanol in large-scale fermentation (312). The Mut<sup>S</sup> (methanol utilization slow phenotype) have a disruption in the *AOX1* gene. Since the cells must then rely on the weaker *AOX2* for methanol metabolism, a slower growing and slower methanol utilization strain is produced. The Mut<sup>-</sup> (methanol utilization minus phenotype) are unable to grow on methanol, since these strains have both *AOX* genes deleted. One of the advantages of this phenotype is that low growth rates may be desirable for production of certain recombinant products (313).

The expression of foreign gene product in *P. pastoris* comprises four principal steps. The first step is to insert the gene into an expression vector, which can be for intracellular expression or for secreted expression. Once the gene is successfully cloned behind the *AOX1* promoter, the plasmid is linearized to stimulate recombination when it is transformed into *P. pastoris* host. It is advisable to transform both Mut<sup>+</sup> and Mut<sup>S</sup>, since one phenotype may favour better expression of some proteins than the other. The third step is to test the expression of both Mut<sup>+</sup> and Mut<sup>S</sup> recombinants in a small scale, using different time-points. Expression can be assessed by SDS-PAGE followed by Coomassie staining and/or Western blot. The *Pichia* recombinant strain which best expresses the protein of interest should then be used for further optimization and expression scale-up. The last step is purification of the recombinant protein using appropriate methods (256, 312, 313). To facilitate this step, affinity tags such as the poly-histidine tag are frequently used. Since MIF had never been produced in this system, three synthetic constructs were designed and outsourced for synthesis (Table 1.1). These comprised a wild-type MIF with no affinity tags (MIF-WT), MIF containing a poly-histidine tag (MIF-6HIS), and MIF with mutation on potential glycosylation sites to avoid hyperglycosylation by yeast (MIF-NG).

## 2 Methods

Production of recombinant MIF was performed using the EasySelect™ *Pichia* Expression Kit, from Invitrogen (#K1740-01). The composition of all growth media used was according to the protocols recommended by the supplier.

### 2.1 *Pichia pastoris* Strains

The kit included three different strains of *P. pastoris*. X-33 and GS115 are Mut<sup>+</sup> strains while KM71H is Mut<sup>S</sup> strain. X-33 is a wild-type strain that is useful for selection on Zeocin™ and large-scale growth. It will grow in Yeast Extract Peptone Dextrose Medium (YPD) and in minimal media. The *Pichia* strain GS115 has a mutation in the histidinol dehydrogenase gene (*his4*) that prevents it from synthesizing histidine. GS115 will grow on complex medium such as YPD, and on minimal media supplemented with histidine. The KM71H strain has a mutation in the argininosuccinate lyase gene (*arg4*) that prevents it from growing in the absence of arginine. *Pichia pastoris* grow in temperatures between 28-30°C in liquid cultures or plates. Growth above 32°C during induction can be detrimental to protein expression and can even lead to cell death.

### 2.2 Storage of *Pichia* strains

Glycerol stocks were prepared for each *Pichia pastoris* strain. Briefly, a single colony of each strain was grown overnight in YPD. The cells were harvested and resuspended in YPD containing 15% glycerol at a final OD<sub>600</sub> of 50-100 (approximately 1.5-5 x 10<sup>9</sup> cells/mL). Cells were then frozen in liquid nitrogen and stored at -80°C.

### 2.3 *Pichia* expression vector

Two expression vectors were used, one to express MIF intracellularly (pPICZA) and one for secreted expression (pPICZ $\alpha$ ). The vectors maps are illustrated in Figure A1.1.

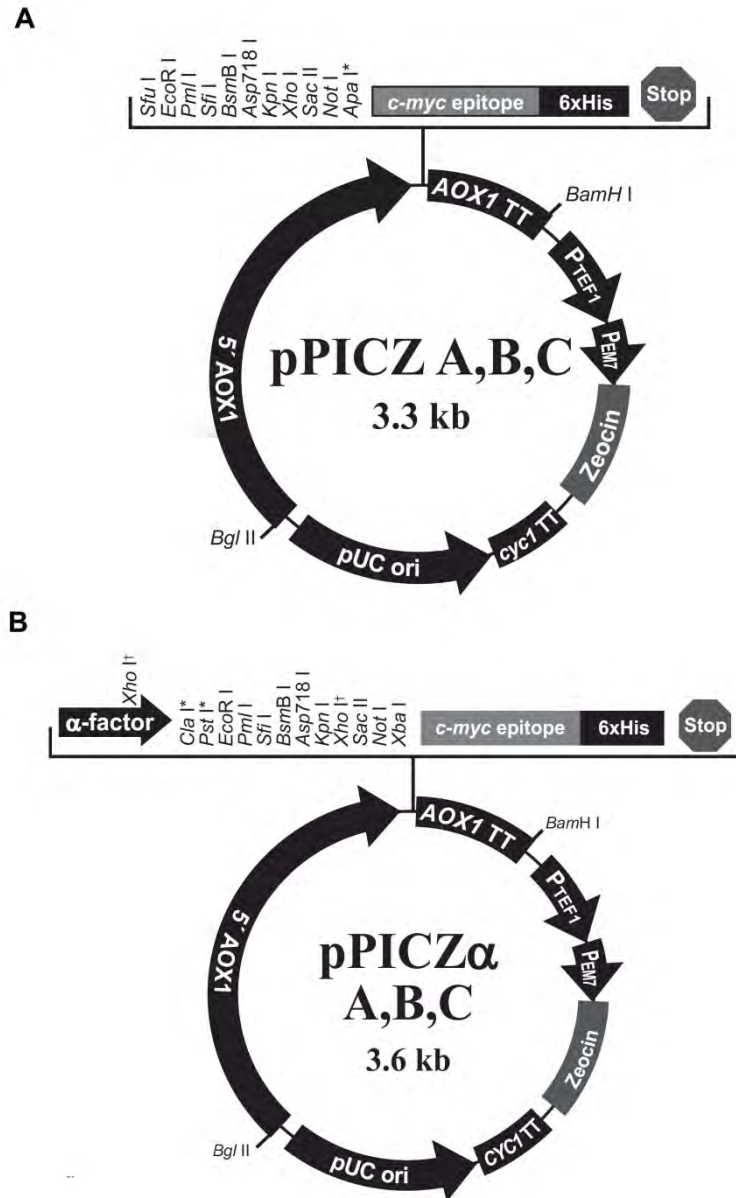


**Figure A1.1 – Maps of pPICZ and pPICZ $\alpha$  vectors.** The figure summarizes the features of the pPICZ (A) and pPICZ $\alpha$  (B) vectors. Reproduced from EasySelect™ *Pichia* Expression Kit Manual (Invitrogen, MAN0000042).

## 2.4 Cloning MIF constructs into pPICZA vector and transformation into *E. coli*

The vectors were first digested with *EcoRI* and *XhoI* and to prevent religation, a reaction with calf intestinal alkaline phosphatase (CIAP) was performed. This enzyme dephosphorylates the 5'-phosphorylated ends of DNA. Three different MIF constructs (Table A1.1) were ligated to the linearized vector, namely wild-type MIF (MIF-WT), MIF containing poly-histidine tag to assist purification (MIF-6HIS) and MIF with mutated glycosylation sites (MIF-NG). The ligation mixtures were then transformed into *E. coli* (*DH5α*) which were grown in Low Salt LB Medium (for Zeocin™ to be active, the salt concentration of the medium must remain low) containing 25µg/mL Zeocin™. Ten Zeocin™-resistant transformants were picked and grown in 2mL Low Salt LB medium with Zeocin™. Plasmid DNA was then isolated by miniprep for restriction analysis and automated sequencing performed to confirm that the coding sequence was in frame. Glycerol stocks of the purified clones were prepared and stored as described above.



## 2.5 Electroporation of *Pichia pastoris*

Plasmids identified above as containing *MIF* inserts were linearized using the *PmeI* restriction enzyme, and purified with PureLink PCR Micro Kit (Invitrogen, K310050). Each *P. pastoris* strain was grown in 5mL of YPD in a 50mL conical tube at 30°C overnight. Then, 500mL of fresh medium was inoculated with 0.5mL of the overnight culture in a 2L flask and grown overnight again to an  $OD_{600} = 1.3-1.5$ . Cells were centrifuged at 1500 x g for 5 minutes at 4°C and the pellet resuspended with 500mL of ice-cold sterile water. Cells were centrifuged again and resuspended with 250mL of ice cold sterile water. After the third centrifugation, cells were resuspended in 20mL of ice-cold sterile 1M sorbitol. Then the cells were centrifuged one more time and the pellet was resuspended in 1mL ice-cold sorbitol for a final volume of approximately 1.5mL.

For electroporation, 80µL of the cell suspension above was mixed with 5-10µg of linearized DNA, transferred to an ice-cold 0.2cm electroporation cuvette and incubated on ice for 5 minutes. An electric pulse was applied to the cell suspension (1500V, 2000Ohm, 25µF) and 1mL of ice-cold 1M sorbitol was immediately added to the cuvette. The contents of the cuvette were transferred to a sterile 15mL tube and incubated at 30°C without shaking for 2h. Different volumes of the suspension (10µL, 50µL or 100µL) were spread on YPDS plates containing 100µg/mL Zeocin<sup>TM</sup> and incubated for 3-10 days at 30°C until colonies formed. Colonies from X33 and GS115 strains were then tested for Mut phenotype by plating the Zeocin<sup>TM</sup>-resistant transformants on MDH (Minimal Dextrose with Histidine) and MMH (Minimal Methanol with Histidine) plate and incubating then at 28-30°C for 2 days. Mut<sup>+</sup> was supposed to grow on both plates while Mut<sup>S</sup> would grow better on MDH plate, but show little or no grow on the MMH plate. Only Mut<sup>+</sup> phenotypes were selected from both strains for rMIF expression. Since the KM71H strain is Mut<sup>S</sup>, it did not need to be tested for Mut phenotype. The presence of the insert was confirmed by PCR for all the transformants (data not shown).

## 2.6 Expression analysis of recombinant *Pichia* strains and purification of rMIF

Zeocin<sup>TM</sup>-resistant recombinant strains containing one of the MIF inserts (WT or 6HIS) were grown, first in a small scale to determine the optimal method and conditions for expression. Each recombinant strain was inoculated in 7mL BMGY media (Buffered Glycerol-complex Medium) and grown overnight at 30°C shaking constantly. Then, cells were pelleted by centrifugation at 3000 x g and resuspended in 5mL of BMMY (Buffered Methanol-complex Medium). 1mL of cells were collected at different time points (0h, 5h, 10h, 24h and 48h), pelleted by centrifugation and kept at -80°C for later analysis.

Expression of MIF was verified by SDS-PAGE (as described in Chapter 2) followed by Western blot and/or Coomassie blue staining. Scale-up of expression was performed for the recombinant strains that successfully expressed rMIF. Cells were lysed in Yeast Breaking Buffer (YBB; 50mM sodium phosphate, pH 7.4, 1mM PMSF, 1mM EDTA, 5% glycerol). Briefly, cells were pelleted by centrifugation and washed in YBB. After washing, the cells were pelleted again and resuspended to an OD600 of 50-100 in YBB. An equal volume of acid-washed glass beads (0.5mm) was added and the mixture was vortexed for 30 seconds and incubated on ice for 30 seconds. Alternated vortex and cooling steps were repeated 7 times. The lysate was then centrifuged for 10 minutes at 12,000 x g and clear supernatant transferred to a new tube. Purification of rMIF as detailed here was performed using two different methods. The first was using TALON Metal Affinity Resins (Clontech Laboratories) and the second was using the His SpinTrap Kit (GE Healthcare). Varying concentrations of imidazole for elution were used as indicated.

### 3 Small-scale expression in recombinant *Pichia* strains

To determine the optimal method and conditions for expression of rMIF, one of each *Pichia* strain (X33, GS116 and KM71H) containing each MIF insert was grown in BMGY medium and then induced in BMMY medium for 48 hours. A fraction of the culture was collected at different time-points. Cell pellets were lysed and submitted to Western blotting to verify MIF expression.

MIF protein expression was not detected for any of *Pichia* strains containing the MIF-NG insert. *Pichia* strain X33 containing MIF-WT insert and the GS116 strain containing MIF-6HIS insert also did not show rMIF at detectable levels (data not shown). However, both the X33 strain containing MIF-6HIS insert and GS116 with MIF-WT insert produced a reactive band with a molecular weight of ~100kDa (Figure A1.2A and B), which is far in excess of the predicted MIF molecular weight of 12.5kDa. Since the band is detected by a specific MIF antibody and its intensity increases with time, it is probably MIF-related. The high molecular weight could possibly be due to abnormal hyperglycosylation or formation of multimers.

Further analysis of the KM71H strain containing MIF-WT also showed expression of the high molecular weight product (Figure A1.2C). However, more encouraging results were obtained using the transformant containing MIF-6HIS, since a band at the predicted MIF molecular weight (~12.5kDa) was detected. Although a single band was detected in the cells induced up to 10 hours, after 24 hours, an additional lower molecular weight band was also detected (Figure A1.2D), which could possibly represent a cleavage product after lengthy induction. Based on these results, the KM71H strain containing MIF-6HIS was selected for scale-up of expression but with methanol induction limited to 6 hours, to avoid the occurrence of the cleavage product.

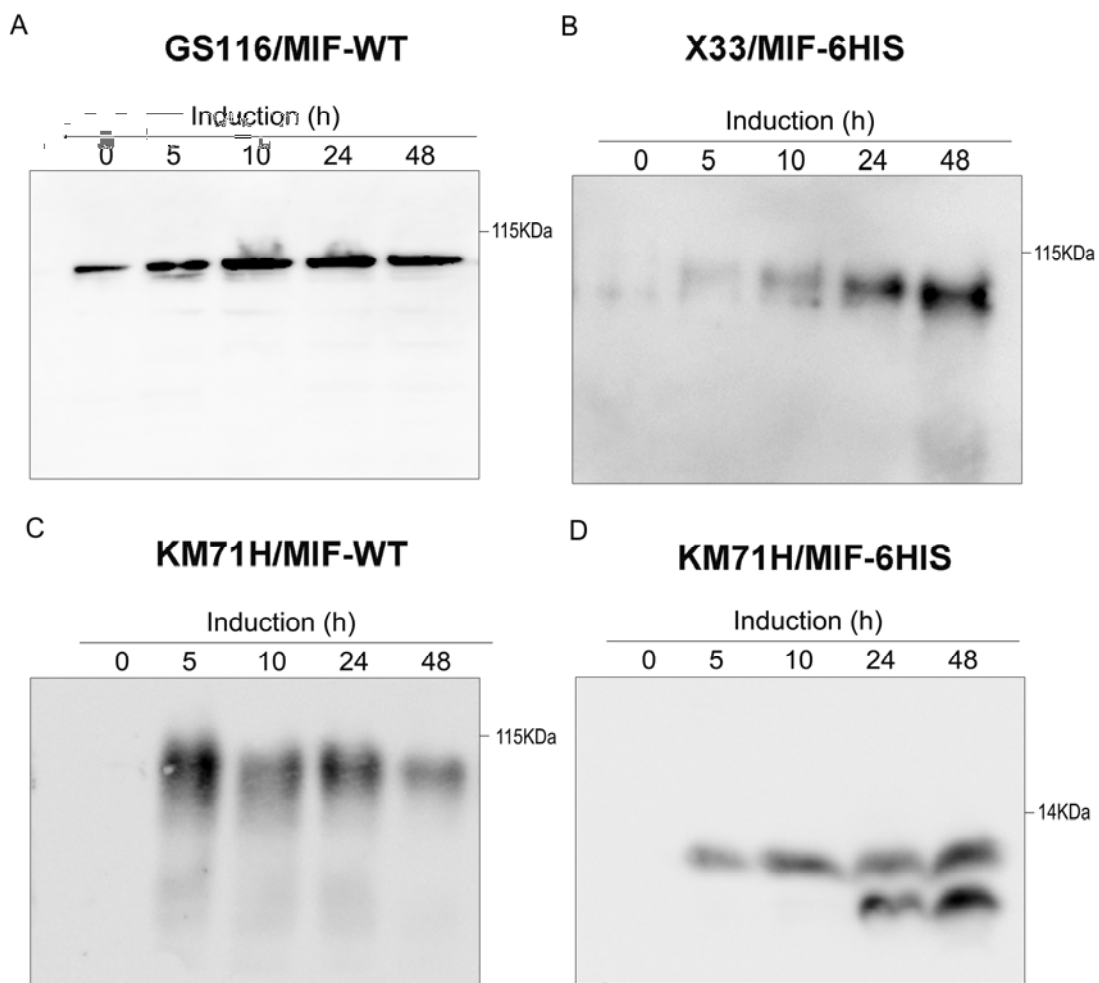


**Figure A1.2 – Induction of rMIF expression in different transformed strains of *P. pastoris*.** The three different strains containing MIF-WT or MIF-6HIS insert were grown in media containing methanol for the indicated times. The cells were lysed and the homogenates were subjected to Western blotting using MIF monoclonal antibody. GS116 containing MIF-WT (A) and X33 containing MIF-6HIS (B) showed a band at ~100kDa and the expression increased with time. A similar high molecular weight band was also observed for the strain KM71H with MIF-WT, but the intensity of the bands was not time-related (C). The only transformant to produce a protein at the anticipated molecular weight predicted for MIF (12.5kDa) was KM71H transformed with MIF-6HIS (D).

## 4 Large-scale rMIF expression and purification

The *Pichia* strain KM71H containing MIF-6HIS insert was inoculated in 25mL BMGY media and grown overnight until an OD<sub>600</sub> 1.7 was reached. The cells were then pelleted, resuspended in 200mL of induction media (BMMY) and were induced for 6 hours at 30°C under constant shaking. Proteins were then extracted as described in Section 2.6, and submitted to purification.

### 4.1 Purification of rMIF-6HIS using Talon Metal Affinity resin

Talon Metal Affinity resin is a durable immobilized metal affinity chromatography (IMAC) resin, charged with cobalt, which has a high affinity and specificity for his-tagged proteins. To purify rMIF using Talon Metal Affinity resin, the lysates were 5X diluted in washing buffer (50mM sodium phosphate, pH 7.0, 300mM NaCl) and incubated with the resin for 20min at room temperature. After washing the resin, the elution was performed using gravity-flow columns and 5mL of 150mM imidazole in washing buffer. The eluate was collected in 500µL fractions, run in a Tris-tricine gel and submitted to Western blotting as described in Chapter 2. Analysis showed that although a strong band for rMIF can be detected in the lysate before purification, MIF was not detected in any of the elution fractions, except for a very faint band in fraction 8. A very weak band is also detected in the flow through fractions (the lysate supernatant collected after binding with the resin) (Figure A1.3A). This result likely indicates that most of the protein bound to the resin, but was not successfully eluted. Higher concentrations of imidazole up to 500mM were used in attempt to elute rMIF from the column, but no improvement in elution was observed (Figure A1.3B).

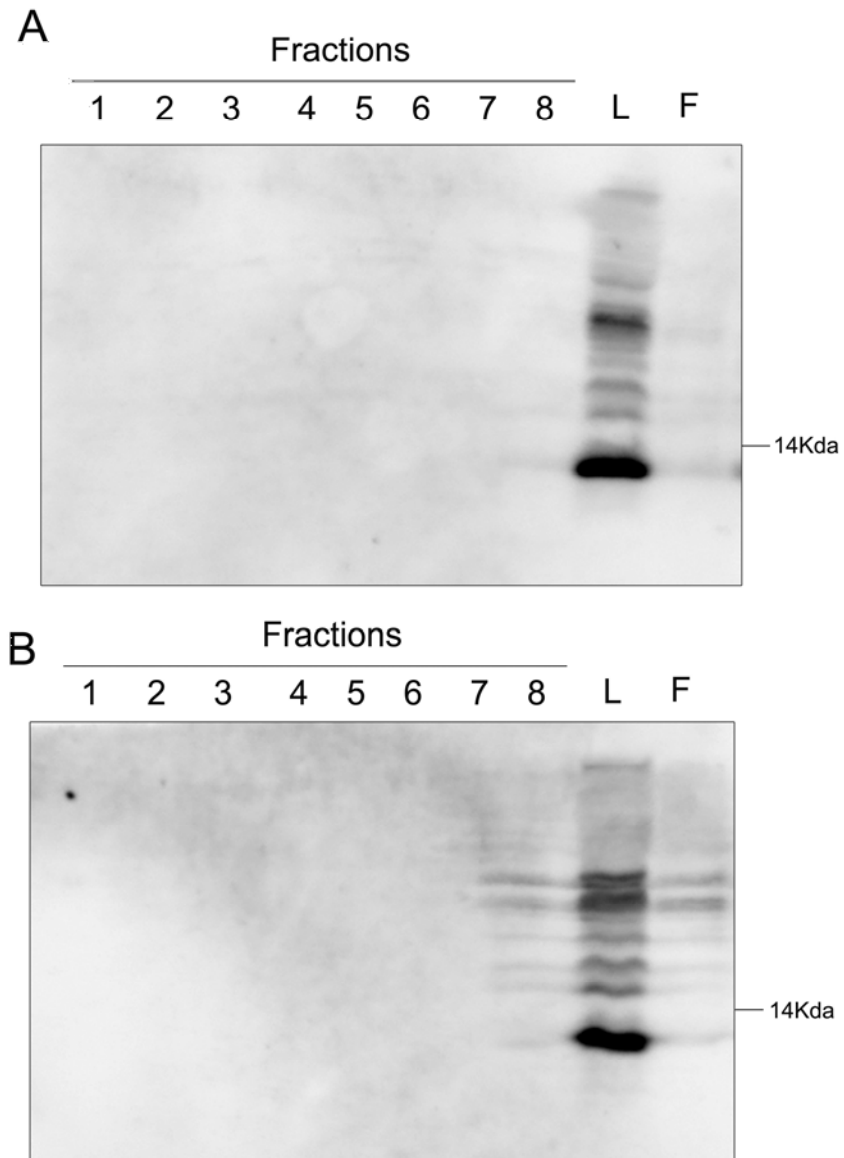


**Figure A1.3 – Purification of rMIF-6HIS using Talon Metal Affinity resin.** The KM71H strain containing MIF-6HIS was induced with methanol for 6 hours, and the lysates submitted to purification by IMAC using Talon resin. Eluate was collected in 8 fractions of 500uL, which were then submitted to Western blot for MIF detection. Different concentrations of imidazole were used in the elution buffer namely 150mM (A) or 500mM (B) with no significant elution of rMIF observed. L = Lysate; F = Flow through.

#### 4.2 Purification of rMIF-6HIS using His SpinTrap Kit

Since the attempt to purify rMIF using the Talon Metal Affinity resin was not successful, an alternative IMAC chemistry was used. His SpinTrap Kit consists of a single-use spin column charged with nickel for purifying histidine-tagged proteins. To purify rMIF using the His SpinTrap Kit, the column was equilibrated with binding buffer provided with the kit and the sample was added for binding. After the recommended washes, rMIF was eluted with different concentrations of imidazole ranging from 5mM to 1M and the eluates were submitted to electrophoresis, followed by either Coomassie gel staining or Western blotting. The Western blotting analysis shows that rMIF is only detected in the eluate when imidazole concentrations were 500mM or above (Figure A1.4A). Although a strong band was detected by Western blotting, rMIF was not visible in the Coomassie stained gel, but significant contaminant proteins were present in all the elutions (Figure A1.4B). Coomassie stain is able to detect as little as 100ng of protein, while Western analysis can detect as little as 1pg of protein. Since rMIF was not detected in the Coomassie stained gel, this result suggests that the purification failed to yield more than 100ng of rMIF.

Another attempt was made to improve the yield by generating more biomass before induction. KM71H containing *MIF-6HIS* insert was inoculated in a larger volume (250mL) of BMGY media in a 2L flask and grown for two days instead of overnight. The cells were then pelleted, resuspended in 200mL of induction media (BMMY) and were induced for 6 hours at 30°C under constant shaking. Protein purification was performed as before, but this time, using 2M imidazole for elution in 3 consecutive 200µL elution steps. Western blot analysis showed that the larger amount of MIF was eluted in the first fraction (Figure A1.4C), and this time a very faint band could be observed in the Coomassie stained gel (Figure A1.4D), but many other contaminant protein bands were also observed.

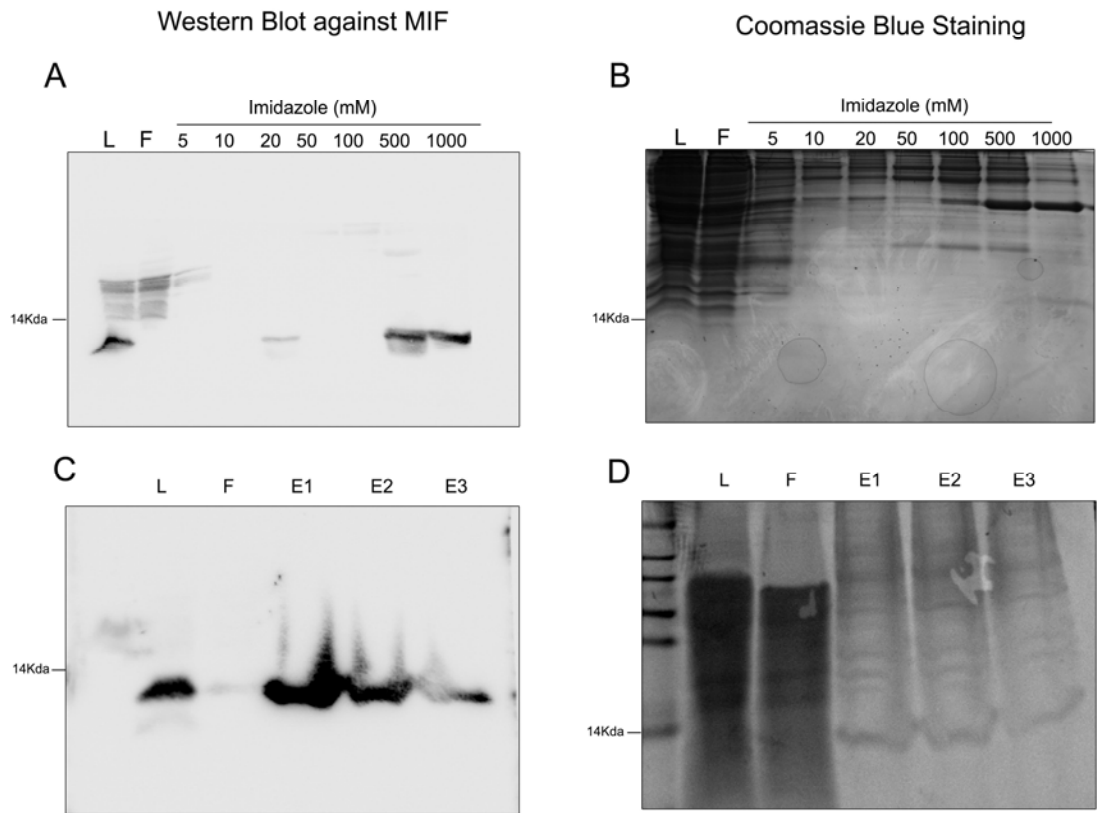


**Figure A1.4 – Purification of rMIF-6HIS using His SpinTrap Kit.** The KM71H strain containing MIF-6HIS was induced with methanol for 6 hours, and lysates submitted to purification by IMAC using His SpinTrap kit. Different concentrations of imidazole were used in the elution buffer (5-1000mM), and eluates were submitted to electrophoresis followed by Western blot or Coomassie staining. (A) The Western blot shows that rMIF was present in the lysate [L], and was bound to the column, since no MIF is detected in the flow-through fraction [F]. The elution of MIF was successful at 500mM and 1M imidazole concentration. (B) The Coomassie-stained gel did not show any band at the molecular weight of MIF in the eluates. (C-D) Modifications to the method were attempted in order to produce more biomass and increase yield. This time, elution was done in three steps with 2M imidazole denoted E1, E2 and E3 respectively.

## 5 Conclusions

In order to study effects of MIF *in vitro*, the addition of recombinant MIF to cells in culture is commonly the method of choice. For that purpose, the best option would be to use rMIF produced in yeast to overcome the problem raised by the presence of endotoxins, which can themselves elicit significant biological responses when applied to cells. Significant difficulties were encountered, with some constructs failing to transform into yeast and even when successful, the rMIF protein produced appeared to be abnormally large. Only one construct (MIF-6HIS) in one yeast strain (KM71H) looked hopeful and although rMIF was successfully induced, it failed to be purified in sufficient quantities and purity to perform the intended *in vitro* experiments.

Moreover, in addition to the work described here, alternative protocols were also attempted. For example, repeated transformations were performed to obtain multiple-copy recombinants and increase expression levels. Purification by using zinc-based columns was also attempted, and although these provided better purity, they also failed to provide enough yield to perform the intended *in vitro* experiments. As mentioned in the Methods, the production of secreted MIF using the pPICZ $\alpha$  secretion vector was also attempted. If successful, this would have possibly negated the need for additional purification, as the yeast secrete few other proteins. However, only low amounts of the high molecular weight expression product was detected in the culture supernatant of induced yeast (data not shown). The optimization attempts to prepare rMIF were very time consuming and labour intensive, but ultimately, the use of *Pichia pastoris* system was abandoned and the analysis of MIF function pursued by alternative means, as described in Chapter 4.

## **Appendix 2**

Cut-Point determination for Survival Analysis in

Chapter 3

## Cut-point determination for survival analysis

In clinical research the assessment of prognostic factors is often based on the division of the patients into two groups: a high risk and a low risk group. A common strategy is to select an optimal cut-off value in the prognostic factor which defines the two groups. The effect is then measured as difference between the groups. In the absence of any a priori clinical information regarding the prognostic relationship between a continuous covariate and outcome, the appropriateness of a cut-point model must be determined empirically (314-316). In the present thesis, outcome-based methods were used to allow an optimal cut-point to be estimated; the optimal cut-point being defined as that threshold value of the continuous covariate distribution which best separates low and high risk patients with respect to disease-specific survival (314, 317).

To determine the appropriated cut-point for the expression of the genes of interest, the largest clinical dataset available was used (GSE8401). First, frequency distribution histograms were used in order to visualise if any natural cut-point is suggested by data distribution (Figure A2.1). While most of the transcript expression levels showed nothing of particular interest, the distribution of expression values for CD74 looked slightly bimodal, which could suggest a natural cut-point for “high-expressors” and “low expressors”.

Next, expression of each gene was divided into quartiles and Kaplan-Meier survival curves were generated for patients with primary melanoma and metastatic melanoma (Figure A2.2). Although the transcripts analysed were not prognostic in the primary tumour (Figure A2.2A-D), they appear to be in the melanoma metastasis and a separation of low and high risk patients with respect to outcome can be visualised. Using the quartiles as a starting point, the optimized cut-points were determined and utilized in the survival curves presented in Chapter 3. For MIF survival analysis, it appears to be a separation between the 50% upper expression levels compared to the lower 50% in regard to outcome (Figure A2.2E). Therefore, a median cut-point was used for MIF transcript expression in all later analysis. For CXCR4 and CD74,

higher 25% cut-point was used given that, as seen in Figure A2.2F and H, these groups comprise patients with lower risk in regard to outcome compared to the lower quartile groups. Conversely, for CD44 the lower 25% quartile seemed to represent the lower risk group in regard to outcome, therefore this was the optimized cut-point for CD44 transcript expression. These optimized cut off points defined here were used for all datasets analysed in Chapter 3.

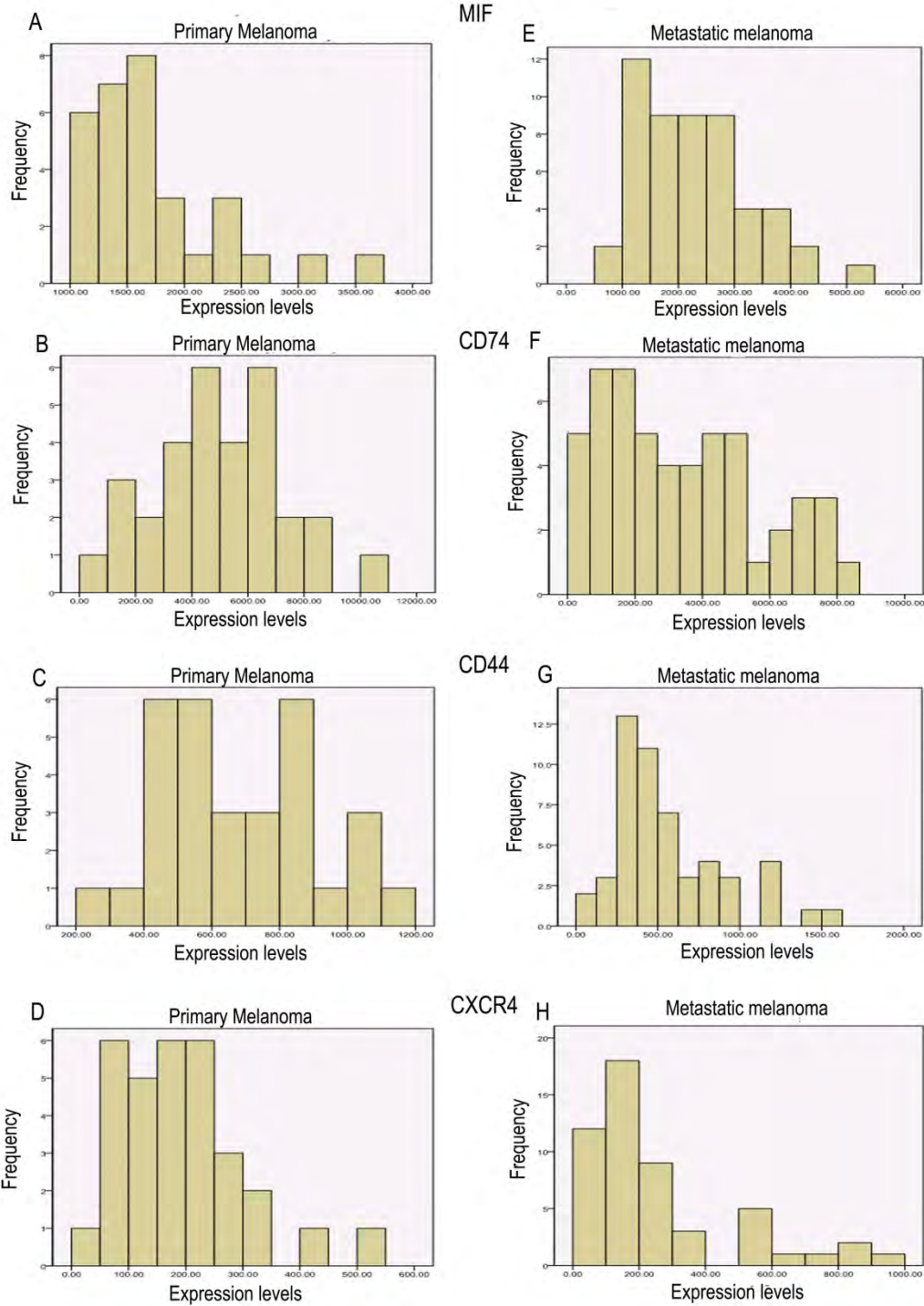


**Figure A2.1 – Frequency distribution histograms of MIF and receptors transcripts in patients with Primary or Metastatic melanoma.** The bar graphs show the relative expression level of each indicated transcript versus the frequency among the patients with primary melanoma (A-D) or metastatic melanoma (E-H).

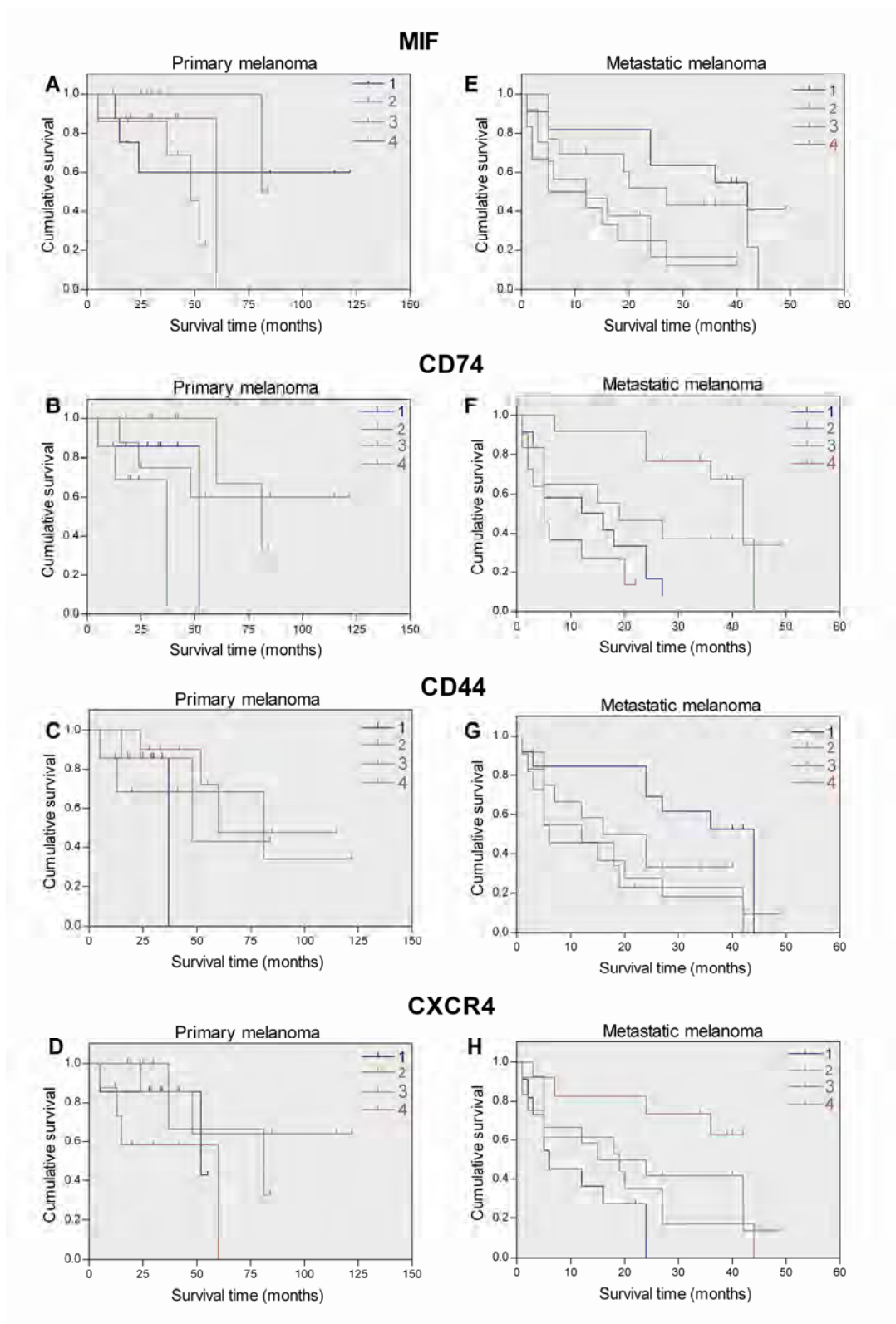


**Figure A2.2 – Survival analysis of MIF and receptors expression in primary and metastatic melanoma clinical samples using GEO dataset GSE8401.** Kaplan-Meier survival curves were generated for patients with primary melanoma (A-D; n=31) and metastatic melanoma (E-H; n=52) based on quartiles of the relative expression of MIF (A and E), CD74 (B and F), CD44 (C and G) and CXCR4 (D and H) transcripts.

## **Appendix 3**

Validation of immunofluorescence methods used  
to analyse proteins located in the nucleus

## **Rationale and results**

This thesis aimed to characterise the subcellular distribution of MIF and CD44 in melanoma cell lines, particularly their presence in the cell nucleus where translocation of intact CD44 had previously been observed. In Chapter 5 there was no evidence that intact CD44 was present in the nucleus, even in cells where this has previously been identified.

Therefore in order to confirm that the methods used were appropriate to detect nuclear proteins, experiments with nuclear control proteins were undertaken. Melanoma cell lines were grown on glass coverslips and processed for intracellular staining by permeabilization using Triton X-100 exactly according to the methods described in Section 2.16. The cells were then immunostained for CREAP (rabbit anti-CREAP, a gift of Dr. Kristy Shipman), a transcription factor found in the nucleus (318), and SC-35 (also known as Splicing factor SC35 and Splicing factor, arginine/serine-rich 2). This protein is found in bodies in the nucleus that are highly enriched in poly(A) RNA. These nuclear bodies are referred to as speckles, SC 35 domains, or splicing factor compartments (SFCs) (319).

After indirect immunofluorescent staining the cells were counterstained with DAPI to decorate nuclear DNA. Optical sectioning was then employed to determine if the nuclear proteins could be detected and were co-incident with DAPI staining. The results of this analysis are presented in Figure A3.1 and clearly show the presence of both CREAP and SC-35 in the cell nucleus, co-localizing with DAPI staining. These results illustrate that proteins found in the nucleus are readily stained using the methods employed. The failure of the experiments in Chapter 5 to detect intact CD44 in the cell nucleus cannot be attributed to the inability of the reagents to permeabilize the nucleus.

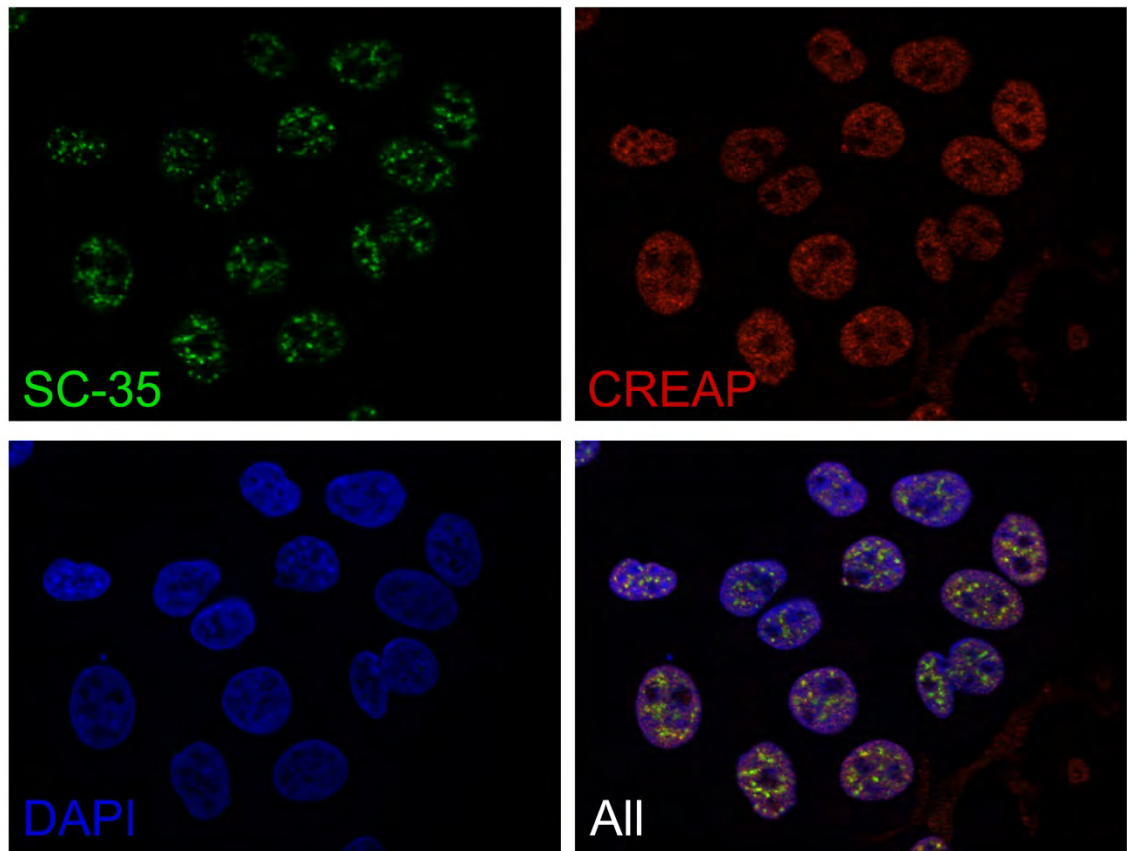


**Figure A3.1 - Immunofluorescence analysis showing the staining of nuclear proteins CREAP and SC-35.** The photomicrographs represent optical sections of cells stained with the anti-SC-35 (green; top left panel), or anti-CREAP (red; top right panel) antibody in combination with the secondary antibody Alexa488® anti-mouse IgG and Alexa549® anti-rabbit IgG respectively. Cell nuclei were counterstained using DAPI (blue, bottom left panel). The merged images (bottom right panel) show co-localization of CREAP, SC-35 and the nuclear marker.

## References

1. Martegani MP, Del Prete F, Gasbarri A, Natali PG, Bartolazzi A. Structural variability of CD44v molecules and reliability of immunodetection of CD44 isoforms using mAbs specific for CD44 variant exon products. *Am J Pathol.* 1999;154(1):291-300. Epub 1999/01/23.
2. Shi X, Leng L, Wang T, Wang W, Du X, Li J, et al. CD44 is the signaling component of the macrophage migration inhibitory factor-CD74 receptor complex. *Immunity.* 2006;25(4):595-606. Epub 2006/10/19.
3. Thorne RF, Legg JW, Isacke CM. The role of the CD44 transmembrane and cytoplasmic domains in co-ordinating adhesive and signalling events. *J Cell Sci.* 2004;117(Pt 3):373-80. Epub 2004/01/02.
4. Cancer in adolescents and young adults in Australia. Australian Institute of Health and Welfare., 2011 Cat. no. CAN 59. Contract No.: no. 62.
5. Cancer in Australia: an overview, 2010 Australian Institute of Health and Welfare & Australasian Association of Cancer Registries. , 2010 Contract No.: Cat. no. CAN 56.
6. Hocker TL, Singh MK, Tsao H. Melanoma genetics and therapeutic approaches in the 21st century: moving from the benchside to the bedside. *J Invest Dermatol.* 2008;128(11):2575-95. Epub 2008/10/18.
7. Chin L. The genetics of malignant melanoma: lessons from mouse and man. *Nat Rev Cancer.* 2003;3(8):559-70. Epub 2003/08/02.
8. Shih ST, Carter R, Sinclair C, Mihalopoulos C, Vos T. Economic evaluation of skin cancer prevention in Australia. *Prev Med.* 2009;49(5):449-53. Epub 2009/09/15.
9. Godar DE. Worldwide increasing incidences of cutaneous malignant melanoma. *J Skin Cancer.* 2011;2011:858425. Epub 2011/10/19.
10. Tracey E, Kerr T, Dobrovic A, Currow D. Cancer In NSW: Incidence and Mortality Report 2008. Sydney: Cancer Institute NSW. , 2010 Aug. Report No.
11. Jemal A, Siegel R, Ward E, Hao Y, Xu J, Murray T, et al. Cancer statistics, 2008. *CA Cancer J Clin.* 2008;58(2):71-96. Epub 2008/02/22.
12. Tuong W, Cheng LS, Armstrong AW. Melanoma: epidemiology, diagnosis, treatment, and outcomes. *Dermatol Clin.* 2012;30(1):113-24. Epub 2011/11/29.
13. Hansson J. Familial cutaneous melanoma. *Adv Exp Med Biol.* 2010;685:134-45. Epub 2010/08/07.

14. Udayakumar D, Mahato B, Gabree M, Tsao H. Genetic determinants of cutaneous melanoma predisposition. *Semin Cutan Med Surg.* 2010;29(3):190-5. Epub 2010/11/06.
15. Pho L, Grossman D, Leachman SA. Melanoma genetics: a review of genetic factors and clinical phenotypes in familial melanoma. *Curr Opin Oncol.* 2006;18(2):173-9. Epub 2006/02/08.
16. Lin J, Hocker TL, Singh M, Tsao H. Genetics of melanoma predisposition. *Br J Dermatol.* 2008;159(2):286-91. Epub 2008/06/13.
17. Sharpless E, Chin L. The INK4a/ARF locus and melanoma. *Oncogene.* 2003;22(20):3092-8. Epub 2003/06/06.
18. Piccinin S, Doglioni C, Maestro R, Vukosavljevic T, Gasparotto D, D'Orazi C, et al. p16/CDKN2 and CDK4 gene mutations in sporadic melanoma development and progression. *Int J Cancer.* 1997;74(1):26-30. Epub 1997/02/20.
19. Goldstein AM, Struewing JP, Chidambaram A, Fraser MC, Tucker MA. Genotype-phenotype relationships in U.S. melanoma-prone families with CDKN2A and CDK4 mutations. *J Natl Cancer Inst.* 2000;92(12):1006-10. Epub 2000/06/22.
20. Meyskens FL, Jr., Farmer PJ, Anton-Culver H. Etiologic pathogenesis of melanoma: a unifying hypothesis for the missing attributable risk. *Clin Cancer Res.* 2004;10(8):2581-3. Epub 2004/04/23.
21. Kanavy HE, Gerstenblith MR. Ultraviolet radiation and melanoma. *Semin Cutan Med Surg.* 2011;30(4):222-8. Epub 2011/11/30.
22. Miller AJ, Mihm MC, Jr. Melanoma. *N Engl J Med.* 2006;355(1):51-65. Epub 2006/07/11.
23. Clark WH. Tumour progression and the nature of cancer. *Br J Cancer.* 1991;64(4):631-44. Epub 1991/10/01.
24. Braig M, Schmitt CA. Oncogene-induced senescence: putting the brakes on tumor development. *Cancer Res.* 2006;66(6):2881-4. Epub 2006/03/17.
25. Bandarchi B, Ma L, Navab R, Seth A, Rasty G. From melanocyte to metastatic malignant melanoma. *Dermatol Res Pract.* 2010;2010. Epub 2010/10/12.
26. Thirlwell C, Nathan P. Melanoma--part 2: management. *Bmj.* 2008;337:a2488. Epub 2008/12/03.
27. Thompson JF, Scolyer RA, Kefford RF. Cutaneous melanoma. *Lancet.* 2005;365(9460):687-701. Epub 2005/02/22.
28. Sampson JH, Carter JH, Jr., Friedman AH, Seigler HF. Demographics, prognosis, and therapy in 702 patients with brain metastases from malignant melanoma. *J Neurosurg.* 1998;88(1):11-20. Epub 1998/01/07.
29. Patel JK, Didolkar MS, Pickren JW, Moore RH. Metastatic pattern of malignant melanoma. A study of 216 autopsy cases. *Am J Surg.* 1978;135(6):807-10. Epub 1978/06/01.

30. Patnana M, Bronstein Y, Szklaruk J, Bedi DG, Hwu WJ, Gershenwald JE, et al. Multimethod imaging, staging, and spectrum of manifestations of metastatic melanoma. *Clin Radiol*. 2011;66(3):224-36. Epub 2011/02/08.
31. Balch CM, Gershenwald JE, Soong SJ, Thompson JF, Atkins MB, Byrd DR, et al. Final version of 2009 AJCC melanoma staging and classification. *J Clin Oncol*. 2009;27(36):6199-206. Epub 2009/11/18.
32. Balch CM, Gershenwald JE, Soong SJ, Thompson JF. Update on the melanoma staging system: the importance of sentinel node staging and primary tumor mitotic rate. *J Surg Oncol*. 2011;104(4):379-85. Epub 2011/08/23.
33. Garbe C, Eigentler TK, Keilholz U, Hauschild A, Kirkwood JM. Systematic review of medical treatment in melanoma: current status and future prospects. *Oncologist*. 2011;16(1):5-24. Epub 2011/01/08.
34. Testori A, Rutkowski P, Marsden J, Bastholt L, Chiarion-Sileni V, Hauschild A, et al. Surgery and radiotherapy in the treatment of cutaneous melanoma. *Ann Oncol*. 2009;20 Suppl 6:vi22-9. Epub 2009/07/28.
35. Hamid O, Boasberg PD, Rosenthal K, O'Day SJ. Systemic treatment of metastatic melanoma: new approaches. *J Surg Oncol*. 2011;104(4):425-9. Epub 2011/08/23.
36. Bhatia S, Tykodi SS, Thompson JA. Treatment of metastatic melanoma: an overview. *Oncology (Williston Park)*. 2009;23(6):488-96. Epub 2009/06/24.
37. Blank CU, Hooijkaas AI, Haanen JB, Schumacher TN. Combination of targeted therapy and immunotherapy in melanoma. *Cancer Immunol Immunother*. 2011;60(10):1359-71. Epub 2011/08/19.
38. Bartkova J, Lukas J, Guldberg P, Alsner J, Kirkin AF, Zeuthen J, et al. The p16-cyclin D/Cdk4-pRb pathway as a functional unit frequently altered in melanoma pathogenesis. *Cancer Res*. 1996;56(23):5475-83. Epub 1996/12/01.
39. Hanahan D, Weinberg RA. The hallmarks of cancer. *Cell*. 2000;100(1):57-70. Epub 2000/01/27.
40. Pollock PM, Harper UL, Hansen KS, Yudt LM, Stark M, Robbins CM, et al. High frequency of BRAF mutations in nevi. *Nat Genet*. 2003;33(1):19-20. Epub 2002/11/26.
41. Davies H, Bignell GR, Cox C, Stephens P, Edkins S, Clegg S, et al. Mutations of the BRAF gene in human cancer. *Nature*. 2002;417(6892):949-54. Epub 2002/06/18.
42. Da Forno PD, Saldanha GS. Molecular aspects of melanoma. *Clin Lab Med*. 2011;31(2):331-43. Epub 2011/05/10.
43. Michaloglou C, Vredeveld LC, Soengas MS, Denoyelle C, Kuilman T, van der Horst CM, et al. BRAFE600-associated senescence-like cell cycle arrest of human naevi. *Nature*. 2005;436(7051):720-4. Epub 2005/08/05.
44. Kuphal S, Bosserhoff A. Recent progress in understanding the pathology of malignant melanoma. *J Pathol*. 2009;219(4):400-9. Epub 2009/09/23.

45. Cohen C, Zavala-Pompa A, Sequeira JH, Shoji M, Sexton DG, Cotsonis G, et al. Mitogen-activated protein kinase activation is an early event in melanoma progression. *Clin Cancer Res.* 2002;8(12):3728-33. Epub 2002/12/11.
46. Zhuang L, Lee CS, Scolyer RA, McCarthy SW, Palmer AA, Zhang XD, et al. Activation of the extracellular signal regulated kinase (ERK) pathway in human melanoma. *J Clin Pathol.* 2005;58(11):1163-9. Epub 2005/10/29.
47. Kolch W. Coordinating ERK/MAPK signalling through scaffolds and inhibitors. *Nat Rev Mol Cell Biol.* 2005;6(11):827-37. Epub 2005/10/18.
48. Packer LM, East P, Reis-Filho JS, Marais R. Identification of direct transcriptional targets of (V600E)BRAF/MEK signalling in melanoma. *Pigment Cell Melanoma Res.* 2009;22(6):785-98. Epub 2009/08/18.
49. Winner M, Koong AC, Rendon BE, Zundel W, Mitchell RA. Amplification of tumor hypoxic responses by macrophage migration inhibitory factor-dependent hypoxia-inducible factor stabilization. *Cancer Res.* 2007;67(1):186-93. Epub 2007/01/11.
50. Sullivan RJ, Flaherty KT. BRAF in Melanoma: Pathogenesis, Diagnosis, Inhibition, and Resistance. *J Skin Cancer.* 2011;2011:423239. Epub 2011/12/17.
51. Nikolaou VA, Stratigos AJ, Flaherty KT, Tsao H. Melanoma: New Insights and New Therapies. *J Invest Dermatol.* 2012. Epub 2012/01/06.
52. Ades F, Metzger-Filho O. Targeting the Cellular Signaling: BRAF Inhibition and Beyond for the Treatment of Metastatic Malignant Melanoma. *Dermatol Res Pract.* 2012;2012:259170. Epub 2012/01/05.
53. Eisen T, Ahmad T, Flaherty KT, Gore M, Kaye S, Marais R, et al. Sorafenib in advanced melanoma: a Phase II randomised discontinuation trial analysis. *Br J Cancer.* 2006;95(5):581-6. Epub 2006/08/02.
54. McDermott DF, Sosman JA, Gonzalez R, Hodi FS, Linette GP, Richards J, et al. Double-blind randomized phase II study of the combination of sorafenib and dacarbazine in patients with advanced melanoma: a report from the 11715 Study Group. *J Clin Oncol.* 2008;26(13):2178-85. Epub 2008/05/01.
55. Amaravadi RK, Schuchter LM, McDermott DF, Kramer A, Giles L, Gramlich K, et al. Phase II Trial of Temozolomide and Sorafenib in Advanced Melanoma Patients with or without Brain Metastases. *Clin Cancer Res.* 2009;15(24):7711-8. Epub 2009/12/10.
56. Hauschild A, Agarwala SS, Trefzer U, Hogg D, Robert C, Hersey P, et al. Results of a phase III, randomized, placebo-controlled study of sorafenib in combination with carboplatin and paclitaxel as second-line treatment in patients with unresectable stage III or stage IV melanoma. *J Clin Oncol.* 2009;27(17):2823-30. Epub 2009/04/08.
57. Margolin KA, Moon J, Flaherty LE, Lao CD, Akerley WL, 3rd, Othus M, et al. Randomized Phase II Trial of Sorafenib with Temsirolimus or Tipifarnib in Untreated Metastatic Melanoma (SWOG S0438). *Clin Cancer Res.* 2012. Epub 2012/01/10.
58. Flaherty KT, Puzanov I, Kim KB, Ribas A, McArthur GA, Sosman JA, et al. Inhibition of mutated, activated BRAF in metastatic melanoma. *N Engl J Med.* 2010;363(9):809-19. Epub 2010/09/08.

59. Luke JJ, Hodi FS. Vemurafenib and BRAF Inhibition: A New Class of Treatment for Metastatic Melanoma. *Clin Cancer Res.* 2012;18(1):9-14. Epub 2011/11/16.
60. Chapman PB, Hauschild A, Robert C, Haanen JB, Ascierto P, Larkin J, et al. Improved survival with vemurafenib in melanoma with BRAF V600E mutation. *N Engl J Med.* 2011;364(26):2507-16. Epub 2011/06/07.
61. Nazarian R, Shi H, Wang Q, Kong X, Koya RC, Lee H, et al. Melanomas acquire resistance to B-RAF(V600E) inhibition by RTK or N-RAS upregulation. *Nature.* 2010;468(7326):973-7. Epub 2010/11/26.
62. Johannessen CM, Boehm JS, Kim SY, Thomas SR, Wardwell L, Johnson LA, et al. COT drives resistance to RAF inhibition through MAP kinase pathway reactivation. *Nature.* 2010;468(7326):968-72. Epub 2010/11/26.
63. Wagle N, Emery C, Berger MF, Davis MJ, Sawyer A, Pochanard P, et al. Dissecting therapeutic resistance to RAF inhibition in melanoma by tumor genomic profiling. *J Clin Oncol.* 2011;29(22):3085-96. Epub 2011/03/09.
64. Wu H, Goel V, Haluska FG. PTEN signaling pathways in melanoma. *Oncogene.* 2003;22(20):3113-22. Epub 2003/06/06.
65. Aguisa-Toure AH, Li G. Genetic alterations of PTEN in human melanoma. *Cell Mol Life Sci.* 2011. Epub 2011/11/15.
66. Parsons R, Simpson L. PTEN and cancer. *Methods Mol Biol.* 2003;222:147-66. Epub 2003/04/25.
67. Sale EM, Sale GJ. Protein kinase B: signalling roles and therapeutic targeting. *Cell Mol Life Sci.* 2008;65(1):113-27. Epub 2007/10/24.
68. Scheid MP, Woodgett JR. Unravelling the activation mechanisms of protein kinase B/Akt. *FEBS Lett.* 2003;546(1):108-12. Epub 2003/06/28.
69. Dhawan P, Singh AB, Ellis DL, Richmond A. Constitutive activation of Akt/protein kinase B in melanoma leads to up-regulation of nuclear factor-kappaB and tumor progression. *Cancer Res.* 2002;62(24):7335-42. Epub 2002/12/25.
70. Nicholson KM, Anderson NG. The protein kinase B/Akt signalling pathway in human malignancy. *Cell Signal.* 2002;14(5):381-95. Epub 2002/03/08.
71. Steelman LS, Stadelman KM, Chappell WH, Horn S, Basecke J, Cervello M, et al. Akt as a therapeutic target in cancer. *Expert Opin Ther Targets.* 2008;12(9):1139-65. Epub 2008/08/13.
72. Brazil DP, Park J, Hemmings BA. PKB binding proteins. Getting in on the Akt. *Cell.* 2002;111(3):293-303. Epub 2002/11/07.
73. Stahl JM, Sharma A, Cheung M, Zimmerman M, Cheng JQ, Bosenberg MW, et al. Deregulated Akt3 activity promotes development of malignant melanoma. *Cancer Res.* 2004;64(19):7002-10. Epub 2004/10/07.

74. Madhunapantula SV, Robertson GP. The PTEN-AKT3 signaling cascade as a therapeutic target in melanoma. *Pigment Cell Melanoma Res.* 2009;22(4):400-19. Epub 2009/06/06.
75. Dankort D, Curley DP, Cartlidge RA, Nelson B, Karnezis AN, Damsky WE, Jr., et al. Braf(V600E) cooperates with Pten loss to induce metastatic melanoma. *Nat Genet.* 2009;41(5):544-52. Epub 2009/03/14.
76. Sekulic A, Haluska P, Jr., Miller AJ, Genebriera De Lamo J, Ejadi S, Pulido JS, et al. Malignant melanoma in the 21st century: the emerging molecular landscape. *Mayo Clin Proc.* 2008;83(7):825-46. Epub 2008/07/11.
77. Curtin JA, Fridlyand J, Kageshita T, Patel HN, Busam KJ, Kutzner H, et al. Distinct sets of genetic alterations in melanoma. *N Engl J Med.* 2005;353(20):2135-47. Epub 2005/11/18.
78. Garnett MJ, Marais R. Guilty as charged: B-RAF is a human oncogene. *Cancer Cell.* 2004;6(4):313-9. Epub 2004/10/19.
79. Tsao H, Zhang X, Fowlkes K, Haluska FG. Relative reciprocity of NRAS and PTEN/MMAC1 alterations in cutaneous melanoma cell lines. *Cancer Res.* 2000;60(7):1800-4. Epub 2000/04/15.
80. Gorden A, Osman I, Gai W, He D, Huang W, Davidson A, et al. Analysis of BRAF and N-RAS mutations in metastatic melanoma tissues. *Cancer Res.* 2003;63(14):3955-7. Epub 2003/07/23.
81. Ellerhorst JA, Greene VR, Ekmekcioglu S, Warneke CL, Johnson MM, Cooke CP, et al. Clinical correlates of NRAS and BRAF mutations in primary human melanoma. *Clin Cancer Res.* 2011;17(2):229-35. Epub 2010/10/27.
82. Kumar R, Angelini S, Hemminki K. Activating BRAF and N-Ras mutations in sporadic primary melanomas: an inverse association with allelic loss on chromosome 9. *Oncogene.* 2003;22(58):9217-24. Epub 2003/12/19.
83. Sensi M, Nicolini G, Petti C, Bersani I, Lozupone F, Molla A, et al. Mutually exclusive NRASQ61R and BRAFV600E mutations at the single-cell level in the same human melanoma. *Oncogene.* 2006;25(24):3357-64. Epub 2006/02/08.
84. Goel VK, Lazar AJ, Warneke CL, Redston MS, Haluska FG. Examination of mutations in BRAF, NRAS, and PTEN in primary cutaneous melanoma. *J Invest Dermatol.* 2006;126(1):154-60. Epub 2006/01/19.
85. Babchia N, Calipel A, Mouriaux F, Faussat AM, Mascarelli F. The PI3K/Akt and mTOR/P70S6K signaling pathways in human uveal melanoma cells: interaction with B-Raf/ERK. *Invest Ophthalmol Vis Sci.* 2010;51(1):421-9. Epub 2009/08/08.
86. Satyamoorthy K, Li G, Gerrero MR, Brose MS, Volpe P, Weber BL, et al. Constitutive mitogen-activated protein kinase activation in melanoma is mediated by both BRAF mutations and autocrine growth factor stimulation. *Cancer Res.* 2003;63(4):756-9. Epub 2003/02/20.
87. Ivanov VN, Hei TK. Combined treatment with EGFR inhibitors and arsenite upregulated apoptosis in human EGFR-positive melanomas: a role of suppression of the PI3K-AKT pathway. *Oncogene.* 2005;24(4):616-26. Epub 2004/12/08.

88. Lazar-Molnar E, Hegyesi H, Toth S, Falus A. Autocrine and paracrine regulation by cytokines and growth factors in melanoma. *Cytokine*. 2000;12(6):547-54. Epub 2000/06/14.
89. Bloom BR, Bennett B. Mechanism of a reaction in vitro associated with delayed-type hypersensitivity. *Science*. 1966;153(731):80-2. Epub 1966/07/01.
90. Swope MD, Lolis E. Macrophage migration inhibitory factor: cytokine, hormone, or enzyme? *Rev Physiol Biochem Pharmacol*. 1999;139:1-32. Epub 1999/08/24.
91. Baugh JA, Bucala R. Macrophage migration inhibitory factor. *Crit Care Med*. 2002;30(1 Supp):S27-S35. Epub 2002/03/14.
92. Dumitru CA, Gholaman H, Trelakis S, Bruderek K, Dominas N, Gu X, et al. Tumor-derived macrophage migration inhibitory factor modulates the biology of head and neck cancer cells via neutrophil activation. *Int J Cancer*. 2011;129(4):859-69. Epub 2011/02/18.
93. Yasasever V, Camlica H, Duranyildiz D, Oguz H, Tas F, Dalay N. Macrophage migration inhibitory factor in cancer. *Cancer Invest*. 2007;25(8):715-9. Epub 2007/12/07.
94. Xiao DZ, Dai B, Chen J, Luo Q, Liu XY, Lin QX, et al. Loss of macrophage migration inhibitory factor impairs the growth properties of human HeLa cervical cancer cells. *Cell Prolif*. 2011;44(6):582-90. Epub 2011/10/14.
95. Bach JP, Deuster O, Balzer-Geldsetzer M, Meyer B, Dodel R, Bacher M. The role of macrophage inhibitory factor in tumorigenesis and central nervous system tumors. *Cancer*. 2009;115(10):2031-40. Epub 2009/03/28.
96. Grieb G, Merk M, Bernhagen J, Bucala R. Macrophage migration inhibitory factor (MIF): a promising biomarker. *Drug News Perspect*. 2010;23(4):257-64. Epub 2010/06/04.
97. Mitchell RA, Bucala R. Tumor growth-promoting properties of macrophage migration inhibitory factor (MIF). *Semin Cancer Biol*. 2000;10(5):359-66. Epub 2000/12/02.
98. Shimizu T, Abe R, Nakamura H, Ohkawara A, Suzuki M, Nishihira J. High expression of macrophage migration inhibitory factor in human melanoma cells and its role in tumor cell growth and angiogenesis. *Biochem Biophys Res Commun*. 1999;264(3):751-8. Epub 1999/11/02.
99. Morrison H, Sherman LS, Legg J, Banine F, Isacke C, Haipek CA, et al. The NF2 tumor suppressor gene product, merlin, mediates contact inhibition of growth through interactions with CD44. *Genes Dev*. 2001;15(8):968-80. Epub 2001/04/24.
100. Takahashi N, Nishihira J, Sato Y, Kondo M, Ogawa H, Ohshima T, et al. Involvement of macrophage migration inhibitory factor (MIF) in the mechanism of tumor cell growth. *Mol Med*. 1998;4(11):707-14. Epub 1999/02/05.
101. Fingerle-Rowson G, Petrenko O, Metz CN, Forsthuber TG, Mitchell R, Huss R, et al. The p53-dependent effects of macrophage migration inhibitory factor revealed by gene targeting. *Proc Natl Acad Sci U S A*. 2003;100(16):9354-9. Epub 2003/07/25.
102. Chesney J, Metz C, Bacher M, Peng T, Meinhardt A, Bucala R. An essential role for macrophage migration inhibitory factor (MIF) in angiogenesis and the growth of a murine lymphoma. *Mol Med*. 1999;5(3):181-91. Epub 1999/07/15.

103. Baron N, Deuster O, Noelker C, Stuer C, Strik H, Schaller C, et al. Role of macrophage migration inhibitory factor in primary glioblastoma multiforme cells. *J Neurosci Res*. 2011;89(5):711-7. Epub 2011/03/02.
104. Liao B, Zhong BL, Li Z, Tian XY, Li Y, Li B. Macrophage migration inhibitory factor contributes angiogenesis by up-regulating IL-8 and correlates with poor prognosis of patients with primary nasopharyngeal carcinoma. *J Surg Oncol*. 2010;102(7):844-51. Epub 2010/09/28.
105. Meyer-Siegler KL, Iczkowski KA, Leng L, Bucala R, Vera PL. Inhibition of macrophage migration inhibitory factor or its receptor (CD74) attenuates growth and invasion of DU-145 prostate cancer cells. *J Immunol*. 2006;177(12):8730-9. Epub 2006/12/05.
106. Meyer-Siegler KL, Leifheit EC, Vera PL. Inhibition of macrophage migration inhibitory factor decreases proliferation and cytokine expression in bladder cancer cells. *BMC Cancer*. 2004;4:34. Epub 2004/07/14.
107. Lue H, Thiele M, Franz J, Dahl E, Speckgens S, Leng L, et al. Macrophage migration inhibitory factor (MIF) promotes cell survival by activation of the Akt pathway and role for CSN5/JAB1 in the control of autocrine MIF activity. *Oncogene*. 2007;26(35):5046-59. Epub 2007/02/22.
108. Denz A, Pilarsky C, Muth D, Ruckert F, Saeger HD, Grutzmann R. Inhibition of MIF leads to cell cycle arrest and apoptosis in pancreatic cancer cells. *J Surg Res*. 2010;160(1):29-34. Epub 2009/09/04.
109. Repp AC, Mayhew ES, Apte S, Niederkorn JY. Human uveal melanoma cells produce macrophage migration-inhibitory factor to prevent lysis by NK cells. *J Immunol*. 2000;165(2):710-5. Epub 2000/07/06.
110. Rumpler G, Becker B, Hafner C, McClelland M, Stolz W, Landthaler M, et al. Identification of differentially expressed genes in models of melanoma progression by cDNA array analysis: SPARC, MIF and a novel cathepsin protease characterize aggressive phenotypes. *Exp Dermatol*. 2003;12(6):761-71. Epub 2004/01/13.
111. Culp WD, Tsagozis P, Burgio M, Russell P, Pisa P, Garland D. Interference of macrophage migration inhibitory factor expression in a mouse melanoma inhibits tumor establishment by up-regulating thrombospondin-1. *Mol Cancer Res*. 2007;5(12):1225-31. Epub 2008/01/04.
112. Miracco C, De Nisi MC, Arcuri F, Cosci E, Pacenti L, Toscano M, et al. Macrophage migration inhibitory factor protein and mRNA expression in cutaneous melanocytic tumours. *Int J Oncol*. 2006;28(2):345-52. Epub 2006/01/05.
113. Bifulco C, McDaniel K, Leng L, Bucala R. Tumor growth-promoting properties of macrophage migration inhibitory factor. *Curr Pharm Des*. 2008;14(36):3790-801. Epub 2009/01/09.
114. Leng L, Metz CN, Fang Y, Xu J, Donnelly S, Baugh J, et al. MIF signal transduction initiated by binding to CD74. *J Exp Med*. 2003;197(11):1467-76. Epub 2003/06/05.
115. Starlets D, Gore Y, Binsky I, Haran M, Harpaz N, Shvidel L, et al. Cell-surface CD74 initiates a signaling cascade leading to cell proliferation and survival. *Blood*. 2006;107(12):4807-16. Epub 2006/02/18.

116. Bernhagen J, Krohn R, Lue H, Gregory JL, Zerneck A, Koenen RR, et al. MIF is a noncognate ligand of CXC chemokine receptors in inflammatory and atherogenic cell recruitment. *Nat Med.* 2007;13(5):587-96. Epub 2007/04/17.
117. Stumptner-Cuvelette P, Benaroch P. Multiple roles of the invariant chain in MHC class II function. *Biochim Biophys Acta.* 2002;1542(1-3):1-13. Epub 2002/02/21.
118. Barrera CA, Beswick EJ, Sierra JC, Bland D, Espejo R, Mifflin R, et al. Polarized expression of CD74 by gastric epithelial cells. *J Histochem Cytochem.* 2005;53(12):1481-9. Epub 2005/06/01.
119. Henne C, Schwenk F, Koch N, Moller P. Surface expression of the invariant chain (CD74) is independent of concomitant expression of major histocompatibility complex class II antigens. *Immunology.* 1995;84(2):177-82. Epub 1995/02/01.
120. Anderson HA, Bergstralh DT, Kawamura T, Blauvelt A, Roche PA. Phosphorylation of the invariant chain by protein kinase C regulates MHC class II trafficking to antigen-processing compartments. *J Immunol.* 1999;163(10):5435-43. Epub 1999/11/24.
121. Matza D, Kerem A, Medvedovsky H, Lantner F, Shachar I. Invariant chain-induced B cell differentiation requires intramembrane proteolytic release of the cytosolic domain. *Immunity.* 2002;17(5):549-60. Epub 2002/11/16.
122. Naujokas MF, Morin M, Anderson MS, Peterson M, Miller J. The chondroitin sulfate form of invariant chain can enhance stimulation of T cell responses through interaction with CD44. *Cell.* 1993;74(2):257-68. Epub 1993/07/30.
123. Binsky I, Haran M, Starlets D, Gore Y, Lantner F, Harpaz N, et al. IL-8 secreted in a macrophage migration-inhibitory factor- and CD74-dependent manner regulates B cell chronic lymphocytic leukemia survival. *Proc Natl Acad Sci U S A.* 2007;104(33):13408-13. Epub 2007/08/10.
124. Lue H, Kapurniotu A, Fingerle-Rowson G, Roger T, Leng L, Thiele M, et al. Rapid and transient activation of the ERK MAPK signalling pathway by macrophage migration inhibitory factor (MIF) and dependence on JAB1/CSN5 and Src kinase activity. *Cell Signal.* 2006;18(5):688-703. Epub 2005/08/27.
125. Koch N, Moldenhauer G, Hofmann WJ, Moller P. Rapid intracellular pathway gives rise to cell surface expression of the MHC class II-associated invariant chain (CD74). *J Immunol.* 1991;147(8):2643-51. Epub 1991/10/15.
126. Roche PA, Teletski CL, Stang E, Bakke O, Long EO. Cell surface HLA-DR-invariant chain complexes are targeted to endosomes by rapid internalization. *Proc Natl Acad Sci U S A.* 1993;90(18):8581-5. Epub 1993/09/15.
127. Ishigami S, Natsugoe S, Tokuda K, Nakajo A, Iwashige H, Aridome K, et al. Invariant chain expression in gastric cancer. *Cancer Lett.* 2001;168(1):87-91. Epub 2001/05/23.
128. Nagata S, Jin YF, Yoshizato K, Tomoeda M, Song M, Iizuka N, et al. CD74 is a novel prognostic factor for patients with pancreatic cancer receiving multimodal therapy. *Ann Surg Oncol.* 2009;16(9):2531-8. Epub 2009/06/06.

129. Burton JD, Ely S, Reddy PK, Stein R, Gold DV, Cardillo TM, et al. CD74 is expressed by multiple myeloma and is a promising target for therapy. *Clin Cancer Res.* 2004;10(19):6606-11. Epub 2004/10/12.
130. Borghese F, Clanchy FI. CD74: an emerging opportunity as a therapeutic target in cancer and autoimmune disease. *Expert Opin Ther Targets.* 2011;15(3):237-51. Epub 2011/01/07.
131. Greenwood C, Metodieva G, Al-Janabi K, Lausen B, Alldridge L, Leng L, et al. Stat1 and CD74 overexpression is co-dependent and linked to increased invasion and lymph node metastasis in triple-negative breast cancer. *J Proteomics.* 2011. Epub 2011/12/20.
132. McClelland M, Zhao L, Carskadon S, Arenberg D. Expression of CD74, the receptor for macrophage migration inhibitory factor, in non-small cell lung cancer. *Am J Pathol.* 2009;174(2):638-46. Epub 2009/01/10.
133. Verjans E, Noetzel E, Bektas N, Schutz AK, Lue H, Lennartz B, et al. Dual role of macrophage migration inhibitory factor (MIF) in human breast cancer. *BMC Cancer.* 2009;9:230. Epub 2009/07/16.
134. Ong GL, Goldenberg DM, Hansen HJ, Mattes MJ. Cell surface expression and metabolism of major histocompatibility complex class II invariant chain (CD74) by diverse cell lines. *Immunology.* 1999;98(2):296-302. Epub 1999/12/14.
135. Weeraratna AT, Becker D, Carr KM, Duray PH, Rosenblatt KP, Yang S, et al. Generation and analysis of melanoma SAGE libraries: SAGE advice on the melanoma transcriptome. *Oncogene.* 2004;23(12):2264-74. Epub 2004/02/03.
136. Aruffo A, Stamenkovic I, Melnick M, Underhill CB, Seed B. CD44 is the principal cell surface receptor for hyaluronate. *Cell.* 1990;61(7):1303-13. Epub 1990/06/29.
137. Lesley J, Hyman R, Kincade PW. CD44 and its interaction with extracellular matrix. *Adv Immunol.* 1993;54:271-335. Epub 1993/01/01.
138. Orian-Rousseau V. CD44, a therapeutic target for metastasising tumours. *Eur J Cancer.* 2010;46(7):1271-7. Epub 2010/03/23.
139. Underhill C. CD44: the hyaluronan receptor. *J Cell Sci.* 1992;103 ( Pt 2):293-8. Epub 1992/10/01.
140. Mackay CR, Terpe HJ, Stauder R, Marston WL, Stark H, Gunthert U. Expression and modulation of CD44 variant isoforms in humans. *J Cell Biol.* 1994;124(1-2):71-82. Epub 1994/01/01.
141. Sreaton GR, Bell MV, Jackson DG, Cornelis FB, Gerth U, Bell JI. Genomic structure of DNA encoding the lymphocyte homing receptor CD44 reveals at least 12 alternatively spliced exons. *Proc Natl Acad Sci U S A.* 1992;89(24):12160-4. Epub 1992/12/15.
142. Faassen AE, Schrage JA, Klein DJ, Oegema TR, Couchman JR, McCarthy JB. A cell surface chondroitin sulfate proteoglycan, immunologically related to CD44, is involved in type I collagen-mediated melanoma cell motility and invasion. *J Cell Biol.* 1992;116(2):521-31. Epub 1992/01/01.

143. Ponta H, Sherman L, Herrlich PA. CD44: from adhesion molecules to signalling regulators. *Nat Rev Mol Cell Biol.* 2003;4(1):33-45. Epub 2003/01/04.
144. Gunthert U, Hofmann M, Rudy W, Reber S, Zoller M, Haussmann I, et al. A new variant of glycoprotein CD44 confers metastatic potential to rat carcinoma cells. *Cell.* 1991;65(1):13-24. Epub 1991/04/05.
145. Naor D, Wallach-Dayana SB, Zahalka MA, Sionov RV. Involvement of CD44, a molecule with a thousand faces, in cancer dissemination. *Semin Cancer Biol.* 2008;18(4):260-7. Epub 2008/05/10.
146. Ratajczak MZ. Cancer stem cells--normal stem cells "Jedi" that went over to the "dark side". *Folia Histochem Cytobiol.* 2005;43(4):175-81. Epub 2005/12/31.
147. Zoller M. CD44: can a cancer-initiating cell profit from an abundantly expressed molecule? *Nat Rev Cancer.* 2011;11(4):254-67. Epub 2011/03/11.
148. Ahrens T, Assmann V, Fieber C, Termeer C, Herrlich P, Hofmann M, et al. CD44 is the principal mediator of hyaluronic-acid-induced melanoma cell proliferation. *J Invest Dermatol.* 2001;116(1):93-101. Epub 2001/02/13.
149. Birch M, Mitchell S, Hart IR. Isolation and characterization of human melanoma cell variants expressing high and low levels of CD44. *Cancer Res.* 1991;51(24):6660-7. Epub 1991/12/15.
150. Schaidt H, Soyer HP, Heider KH, Hofmann-Wellenhof R, Zatloukal K, Smolle J, et al. CD44 and variants in melanocytic skin neoplasms. *J Cutan Pathol.* 1998;25(4):199-203. Epub 1998/06/03.
151. Shiras A, Bhosale A, Patekar A, Shepal V, Shastry P. Differential expression of CD44(S) and variant isoforms v3, v10 in three-dimensional cultures of mouse melanoma cell lines. *Clin Exp Metastasis.* 2002;19(5):445-55. Epub 2002/08/30.
152. Foger N, Marhaba R, Zoller M. Involvement of CD44 in cytoskeleton rearrangement and raft reorganization in T cells. *J Cell Sci.* 2001;114(Pt 6):1169-78. Epub 2001/03/03.
153. Tzircotis G, Thorne RF, Isacke CM. Directional sensing of a phorbol ester gradient requires CD44 and is regulated by CD44 phosphorylation. *Oncogene.* 2006;25(56):7401-10. Epub 2006/06/21.
154. Gore Y, Starlets D, Maharshak N, Becker-Herman S, Kaneyuki U, Leng L, et al. Macrophage migration inhibitory factor induces B cell survival by activation of a CD74-CD44 receptor complex. *J Biol Chem.* 2008;283(5):2784-92. Epub 2007/12/07.
155. Veillat V, Carli C, Metz CN, Al-Abed Y, Naccache PH, Akoum A. Macrophage migration inhibitory factor elicits an angiogenic phenotype in human ectopic endometrial cells and triggers the production of major angiogenic factors via CD44, CD74, and MAPK signaling pathways. *J Clin Endocrinol Metab.* 2010;95(12):E403-12. Epub 2010/09/11.
156. Nagano O, Saya H. Mechanism and biological significance of CD44 cleavage. *Cancer Sci.* 2004;95(12):930-5. Epub 2004/12/15.

157. Okamoto I, Kawano Y, Tsuiki H, Sasaki J, Nakao M, Matsumoto M, et al. CD44 cleavage induced by a membrane-associated metalloprotease plays a critical role in tumor cell migration. *Oncogene*. 1999;18(7):1435-46. Epub 1999/03/02.
158. Murakami D, Okamoto I, Nagano O, Kawano Y, Tomita T, Iwatsubo T, et al. Presenilin-dependent gamma-secretase activity mediates the intramembranous cleavage of CD44. *Oncogene*. 2003;22(10):1511-6. Epub 2003/03/12.
159. Goebeler M, Kaufmann D, Brocker EB, Klein CE. Migration of highly aggressive melanoma cells on hyaluronic acid is associated with functional changes, increased turnover and shedding of CD44 receptors. *J Cell Sci*. 1996;109 ( Pt 7):1957-64. Epub 1996/07/01.
160. Okamoto I, Tsuiki H, Kenyon LC, Godwin AK, Emler DR, Holgado-Madruga M, et al. Proteolytic cleavage of the CD44 adhesion molecule in multiple human tumors. *Am J Pathol*. 2002;160(2):441-7. Epub 2002/02/13.
161. Perez-Encinas M, Villamayor M, Campos A, Gonzalez S, Bello JL. Tumor burden and serum level of soluble CD25, CD8, CD23, CD54 and CD44 in non-Hodgkin's lymphoma. *Haematologica*. 1998;83(8):752-4. Epub 1998/10/30.
162. Guo YJ, Liu G, Wang X, Jin D, Wu M, Ma J, et al. Potential use of soluble CD44 in serum as indicator of tumor burden and metastasis in patients with gastric or colon cancer. *Cancer Res*. 1994;54(2):422-6. Epub 1994/01/15.
163. Kawano Y, Okamoto I, Murakami D, Itoh H, Yoshida M, Ueda S, et al. Ras oncoprotein induces CD44 cleavage through phosphoinositide 3-OH kinase and the rho family of small G proteins. *J Biol Chem*. 2000;275(38):29628-35. Epub 2000/07/18.
164. Okamoto I, Kawano Y, Matsumoto M, Suga M, Kaibuchi K, Ando M, et al. Regulated CD44 cleavage under the control of protein kinase C, calcium influx, and the Rho family of small G proteins. *J Biol Chem*. 1999;274(36):25525-34. Epub 1999/08/28.
165. Anderegg U, Eichenberg T, Parthaune T, Haiduk C, Saalbach A, Milkova L, et al. ADAM10 is the constitutive functional sheddase of CD44 in human melanoma cells. *J Invest Dermatol*. 2009;129(6):1471-82. Epub 2008/10/31.
166. De Strooper B, Iwatsubo T, Wolfe MS. Presenilins and gamma-Secretase: Structure, Function, and Role in Alzheimer Disease. *Cold Spring Harb Perspect Med*. 2012;2(1):a006304. Epub 2012/02/09.
167. Cichy J, Pure E. The liberation of CD44. *J Cell Biol*. 2003;161(5):839-43. Epub 2003/06/11.
168. Okamoto I, Kawano Y, Murakami D, Sasayama T, Araki N, Miki T, et al. Proteolytic release of CD44 intracellular domain and its role in the CD44 signaling pathway. *J Cell Biol*. 2001;155(5):755-62. Epub 2001/11/21.
169. Pelletier L, Guillaumot P, Freche B, Luquain C, Christiansen D, Brugiere S, et al. Gamma-secretase-dependent proteolysis of CD44 promotes neoplastic transformation of rat fibroblastic cells. *Cancer Res*. 2006;66(7):3681-7. Epub 2006/04/06.
170. Janiszewska M, De Vito C, Le Bitoux MA, Fusco C, Stamenkovic I. Transportin regulates nuclear import of CD44. *J Biol Chem*. 2010;285(40):30548-57. Epub 2010/07/29.

171. Lee JL, Wang MJ, Chen JY. Acetylation and activation of STAT3 mediated by nuclear translocation of CD44. *J Cell Biol.* 2009;185(6):949-57. Epub 2009/06/10.
172. Kakinuma T, Hwang ST. Chemokines, chemokine receptors, and cancer metastasis. *J Leukoc Biol.* 2006;79(4):639-51. Epub 2006/02/16.
173. Zernecke A, Bernhagen J, Weber C. Macrophage migration inhibitory factor in cardiovascular disease. *Circulation.* 2008;117(12):1594-602. Epub 2008/03/26.
174. Conroy H, Mawhinney L, Donnelly SC. Inflammation and cancer: macrophage migration inhibitory factor (MIF)--the potential missing link. *Qjm.* 2010;103(11):831-6. Epub 2010/09/02.
175. Vera PL, Iczkowski KA, Wang X, Meyer-Siegler KL. Cyclophosphamide-induced cystitis increases bladder CXCR4 expression and CXCR4-macrophage migration inhibitory factor association. *PLoS One.* 2008;3(12):e3898. Epub 2008/12/11.
176. Moore JP, Trkola A, Dragic T. Co-receptors for HIV-1 entry. *Curr Opin Immunol.* 1997;9(4):551-62. Epub 1997/08/01.
177. Luker KE, Luker GD. Functions of CXCL12 and CXCR4 in breast cancer. *Cancer Lett.* 2006;238(1):30-41. Epub 2005/07/28.
178. Fulton AM. The chemokine receptors CXCR4 and CXCR3 in cancer. *Curr Oncol Rep.* 2009;11(2):125-31. Epub 2009/02/17.
179. Tarnowski M, Grymula K, Liu R, Tarnowska J, Drukala J, Ratajczak J, et al. Macrophage migration inhibitory factor is secreted by rhabdomyosarcoma cells, modulates tumor metastasis by binding to CXCR4 and CXCR7 receptors and inhibits recruitment of cancer-associated fibroblasts. *Mol Cancer Res.* 2010;8(10):1328-43. Epub 2010/09/24.
180. Sakai N, Yoshidome H, Shida T, Kimura F, Shimizu H, Ohtsuka M, et al. CXCR4/CXCL12 expression profile is associated with tumor microenvironment and clinical outcome of liver metastases of colorectal cancer. *Clin Exp Metastasis.* 2011. Epub 2011/11/15.
181. Wang L, Li CL, Yu WB, Yin HP, Zhang GY, Zhang LF, et al. Influence of CXCR4/SDF-1 axis on E-cadherin/beta-catenin complex expression in HT29 colon cancer cells. *World J Gastroenterol.* 2011;17(5):625-32. Epub 2011/02/26.
182. Yu T, Wu Y, Huang Y, Yan C, Liu Y, Wang Z, et al. RNAi Targeting CXCR4 Inhibits Tumor Growth Through Inducing Cell Cycle Arrest and Apoptosis. *Mol Ther.* 2011. Epub 2011/11/24.
183. Schwartz V, Lue H, Kraemer S, Korbil J, Krohn R, Ohl K, et al. A functional heteromeric MIF receptor formed by CD74 and CXCR4. *FEBS Lett.* 2009;583(17):2749-57. Epub 2009/08/12.
184. Schwartz V, Kruttgen A, Weis J, Weber C, Ostendorf T, Lue H, et al. Role for CD74 and CXCR4 in clathrin-dependent endocytosis of the cytokine MIF. *Eur J Cell Biol.* 2011. Epub 2011/10/22.
185. Dessein AF, Stechly L, Jonckheere N, Dumont P, Monte D, Leteurtre E, et al. Autocrine induction of invasive and metastatic phenotypes by the MIF-CXCR4 axis in drug-resistant human colon cancer cells. *Cancer Res.* 2010;70(11):4644-54. Epub 2010/05/13.

186. Kim M, Koh YJ, Kim KE, Koh BI, Nam DH, Alitalo K, et al. CXCR4 signaling regulates metastasis of chemoresistant melanoma cells by a lymphatic metastatic niche. *Cancer Res.* 2010;70(24):10411-21. Epub 2010/11/09.
187. Murakami T, Maki W, Cardones AR, Fang H, Tun Kyi A, Nestle FO, et al. Expression of CXC chemokine receptor-4 enhances the pulmonary metastatic potential of murine B16 melanoma cells. *Cancer Res.* 2002;62(24):7328-34. Epub 2002/12/25.
188. Scala S, Giuliano P, Ascierto PA, Ierano C, Franco R, Napolitano M, et al. Human melanoma metastases express functional CXCR4. *Clin Cancer Res.* 2006;12(8):2427-33. Epub 2006/04/28.
189. Franco R, Cantile M, Scala S, Catalano E, Cerrone M, Scognamiglio G, et al. Histomorphologic parameters and CXCR4 mRNA and protein expression in sentinel node melanoma metastasis are correlated to clinical outcome. *Cancer Biol Ther.* 2010;9(6):423-9. Epub 2010/01/12.
190. Kim J, Mori T, Chen SL, Amersi FF, Martinez SR, Kuo C, et al. Chemokine receptor CXCR4 expression in patients with melanoma and colorectal cancer liver metastases and the association with disease outcome. *Ann Surg.* 2006;244(1):113-20. Epub 2006/06/24.
191. Scala S, Ottaiano A, Ascierto PA, Cavalli M, Simeone E, Giuliano P, et al. Expression of CXCR4 predicts poor prognosis in patients with malignant melanoma. *Clin Cancer Res.* 2005;11(5):1835-41. Epub 2005/03/10.
192. Zhang XD, Franco A, Myers K, Gray C, Nguyen T, Hersey P. Relation of TNF-related apoptosis-inducing ligand (TRAIL) receptor and FLICE-inhibitory protein expression to TRAIL-induced apoptosis of melanoma. *Cancer Res.* 1999;59(11):2747-53. Epub 1999/06/11.
193. Mitchell MS, Kan-Mitchell J, Morrow PR, Darrach D, Jones VE, Mescher MF. Phase I trial of large multivalent immunogen derived from melanoma lysates in patients with disseminated melanoma. *Clin Cancer Res.* 2004;10(1 Pt 1):76-83. Epub 2004/01/22.
194. Fodstad O, Aamdal S, McMenamin M, Nesland JM, Pihl A. A new experimental metastasis model in athymic nude mice, the human malignant melanoma LOX. *Int J Cancer.* 1988;41(3):442-9. Epub 1988/03/15.
195. Ishikawa M, Fernandez B, Kerbel RS. Highly pigmented human melanoma variant which metastasizes widely in nude mice, including to skin and brain. *Cancer Res.* 1988;48(17):4897-903. Epub 1988/09/01.
196. van Muijen GN, Jansen KF, Cornelissen IM, Smeets DF, Beck JL, Ruiter DJ. Establishment and characterization of a human melanoma cell line (MV3) which is highly metastatic in nude mice. *Int J Cancer.* 1991;48(1):85-91. Epub 1991/04/22.
197. Carey TE, Takahashi T, Resnick LA, Oettgen HF, Old LJ. Cell surface antigens of human malignant melanoma: mixed hemadsorption assays for humoral immunity to cultured autologous melanoma cells. *Proc Natl Acad Sci U S A.* 1976;73(9):3278-82. Epub 1976/09/01.
198. Coates AS, Crawford M. Growth of human melanoma in nude mice: suppression by T-lymphocytes from the tumor donor: brief communication. *J Natl Cancer Inst.* 1977;59(4):1325-9. Epub 1977/10/01.

199. Smith AP, Hoek K, Becker D. Whole-genome expression profiling of the melanoma progression pathway reveals marked molecular differences between nevi/melanoma in situ and advanced-stage melanomas. *Cancer Biol Ther.* 2005;4(9):1018-29. Epub 2005/10/28.
200. Beckman IG, Bradley J, Brooks D, Zola H. Delineation of serologically distinct monomorphic determinants of human MHC class II antigens: evidence of heterogeneity in their topographical distribution. *Mol Immunol.* 1984;21(3):205-14. Epub 1984/03/01.
201. Simpson RJ. Disruption of cultured cells by nitrogen cavitation. *Cold Spring Harb Protoc.* 2010;2010(11):pdb prot5513. Epub 2010/11/03.
202. Sadeqzadeh E, de Bock CE, Zhang XD, Shipman KL, Scott NM, Song C, et al. Dual processing of FAT1 cadherin protein by human melanoma cells generates distinct protein products. *J Biol Chem.* 2011;286(32):28181-91. Epub 2011/06/18.
203. Thorne RF, Zhang X, Song C, Jin B, Burns GF. Novel immunoblotting monoclonal antibodies against human and rat CD36/fat used to identify an isoform of CD36 in rat muscle. *DNA and cell biology.* 2006;25(5):302-11. Epub 2006/05/24.
204. Mhaidat NM, Thorne RF, de Bock CE, Zhang XD, Hersey P. Melanoma cell sensitivity to Docetaxel-induced apoptosis is determined by class III beta-tubulin levels. *FEBS letters.* 2008;582(2):267-72. Epub 2007/12/19.
205. Bach JP, Rinn B, Meyer B, Dodel R, Bacher M. Role of MIF in inflammation and tumorigenesis. *Oncology (Williston Park).* 2008;75(3-4):127-33. Epub 2008/09/16.
206. Meyer-Siegler KL, Bellino MA, Tannenbaum M. Macrophage migration inhibitory factor evaluation compared with prostate specific antigen as a biomarker in patients with prostate carcinoma. *Cancer.* 2002;94(5):1449-56. Epub 2002/03/29.
207. Yu DS, Lin JC, Hsieh DS, Chang SY, Lee CF. Modulation of MDR-1 gene by MIF and GSTpi with drug resistance generation in hormone independent prostate cancer. *Arch Androl.* 2006;52(4):283-91. Epub 2006/05/27.
208. Legendre H, Decaestecker C, Nagy N, Hendlisz A, Schuring MP, Salmon I, et al. Prognostic values of galectin-3 and the macrophage migration inhibitory factor (MIF) in human colorectal cancers. *Mod Pathol.* 2003;16(5):491-504. Epub 2003/05/16.
209. Meyer-Siegler KL, Iczkowski KA, Vera PL. Further evidence for increased macrophage migration inhibitory factor expression in prostate cancer. *BMC Cancer.* 2005;5:73. Epub 2005/07/08.
210. Muramaki M, Miyake H, Yamada Y, Hara I. Clinical utility of serum macrophage migration inhibitory factor in men with prostate cancer as a novel biomarker of detection and disease progression. *Oncol Rep.* 2006;15(1):253-7. Epub 2005/12/06.
211. Ren Y, Law S, Huang X, Lee PY, Bacher M, Srivastava G, et al. Macrophage migration inhibitory factor stimulates angiogenic factor expression and correlates with differentiation and lymph node status in patients with esophageal squamous cell carcinoma. *Ann Surg.* 2005;242(1):55-63. Epub 2005/06/24.
212. Camlica H, Duranyildiz D, Oguz H, Oral EN, Yasasever V. The diagnostic value of macrophage migration inhibitory factor (MIF) in gastric cancer. *Pathol Oncol Res.* 2008;14(1):79-83. Epub 2008/03/19.

213. Mohri Y, Mohri T, Wei W, Qi YJ, Martin A, Miki C, et al. Identification of macrophage migration inhibitory factor and human neutrophil peptides 1-3 as potential biomarkers for gastric cancer. *Br J Cancer*. 2009;101(2):295-302. Epub 2009/06/25.
214. Shun CT, Lin JT, Huang SP, Lin MT, Wu MS. Expression of macrophage migration inhibitory factor is associated with enhanced angiogenesis and advanced stage in gastric carcinomas. *World J Gastroenterol*. 2005;11(24):3767-71. Epub 2005/06/22.
215. Agarwal R, Whang DH, Alvero AB, Visintin I, Lai Y, Segal EA, et al. Macrophage migration inhibitory factor expression in ovarian cancer. *Am J Obstet Gynecol*. 2007;196(4):348 e1-5. Epub 2007/04/04.
216. Kim K, Visintin I, Alvero AB, Mor G. Development and validation of a protein-based signature for the detection of ovarian cancer. *Clin Lab Med*. 2009;29(1):47-55. Epub 2009/04/25.
217. Mor G, Visintin I, Lai Y, Zhao H, Schwartz P, Rutherford T, et al. Serum protein markers for early detection of ovarian cancer. *Proc Natl Acad Sci U S A*. 2005;102(21):7677-82. Epub 2005/05/14.
218. Jesneck JL, Mukherjee S, Yurkovetsky Z, Clyde M, Marks JR, Lokshin AE, et al. Do serum biomarkers really measure breast cancer? *BMC Cancer*. 2009;9:164. Epub 2009/05/30.
219. Bando H, Matsumoto G, Bando M, Muta M, Ogawa T, Funata N, et al. Expression of macrophage migration inhibitory factor in human breast cancer: association with nodal spread. *Jpn J Cancer Res*. 2002;93(4):389-96. Epub 2002/05/03.
220. Xu X, Wang B, Ye C, Yao C, Lin Y, Huang X, et al. Overexpression of macrophage migration inhibitory factor induces angiogenesis in human breast cancer. *Cancer Lett*. 2008;261(2):147-57. Epub 2008/01/04.
221. Chen G, Gharib TG, Huang CC, Taylor JM, Misek DE, Kardia SL, et al. Discordant protein and mRNA expression in lung adenocarcinomas. *Mol Cell Proteomics*. 2002;1(4):304-13. Epub 2002/07/04.
222. Gygi SP, Rochon Y, Franz BR, Aebersold R. Correlation between protein and mRNA abundance in yeast. *Mol Cell Biol*. 1999;19(3):1720-30. Epub 1999/02/18.
223. Xu L, Shen SS, Hoshida Y, Subramanian A, Ross K, Brunet JP, et al. Gene expression changes in an animal melanoma model correlate with aggressiveness of human melanoma metastases. *Mol Cancer Res*. 2008;6(5):760-9. Epub 2008/05/29.
224. Jans DA, Hassan G. Nuclear targeting by growth factors, cytokines, and their receptors: a role in signaling? *Bioessays*. 1998;20(5):400-11. Epub 1998/07/22.
225. Johnson HM, Torres BA, Green MM, Szente BE, Siler KI, Larkin J, 3rd, et al. Cytokine-receptor complexes as chaperones for nuclear translocation of signal transducers. *Biochem Biophys Res Commun*. 1998;244(3):607-14. Epub 1998/04/16.
226. Shachar I, Haran M. The secret second life of an innocent chaperone: the story of CD74 and B cell/chronic lymphocytic leukemia cell survival. *Leuk Lymphoma*. 2011;52(8):1446-54. Epub 2011/03/23.

227. Ma W, Deng Y, Zhou L. The prognostic value of adhesion molecule CD44v6 in women with primary breast carcinoma: a clinicopathologic study. *Clin Oncol (R Coll Radiol)*. 2005;17(4):258-63. Epub 2005/07/07.
228. Ropponen KM, Eskelinen MJ, Lipponen PK, Alhava E, Kosma VM. Expression of CD44 and variant proteins in human colorectal cancer and its relevance for prognosis. *Scand J Gastroenterol*. 1998;33(3):301-9. Epub 1998/04/21.
229. Altomonte M, Fonsatti E, Visintin A, Maio M. Targeted therapy of solid malignancies via HLA class II antigens: a new biotherapeutic approach? *Oncogene*. 2003;22(42):6564-9. Epub 2003/10/07.
230. Marsman M, Jordens I, Griekspoor A, Neefjes J. Chaperoning antigen presentation by MHC class II molecules and their role in oncogenesis. *Adv Cancer Res*. 2005;93:129-58. Epub 2005/03/31.
231. Bernsen MR, Hakansson L, Gustafsson B, Krysanter L, Rettrup B, Ruiter D, et al. On the biological relevance of MHC class II and B7 expression by tumour cells in melanoma metastases. *Br J Cancer*. 2003;88(3):424-31. Epub 2003/02/06.
232. Ostmeier H, Fuchs B, Otto F, Mawick R, Lippold A, Krieg V, et al. Can immunohistochemical markers and mitotic rate improve prognostic precision in patients with primary melanoma? *Cancer*. 1999;85(11):2391-9. Epub 1999/06/05.
233. Ricaniadis N, Kataki A, Agnantis N, Androulakis G, Karakousis CP. Long-term prognostic significance of HSP-70, c-myc and HLA-DR expression in patients with malignant melanoma. *Eur J Surg Oncol*. 2001;27(1):88-93. Epub 2001/03/10.
234. Si Z, Hersey P. Expression of the neuroglandular antigen and analogues in melanoma. CD9 expression appears inversely related to metastatic potential of melanoma. *Int J Cancer*. 1993;54(1):37-43. Epub 1993/04/22.
235. van Duinen SG, Ruiter DJ, Broecker EB, van der Velde EA, Sorg C, Welvaart K, et al. Level of HLA antigens in locoregional metastases and clinical course of the disease in patients with melanoma. *Cancer Res*. 1988;48(4):1019-25. Epub 1988/02/15.
236. Dietrich A, Tanczos E, Vanscheidt W, Schopf E, Simon JC. High CD44 surface expression on primary tumours of malignant melanoma correlates with increased metastatic risk and reduced survival. *Eur J Cancer*. 1997;33(6):926-30. Epub 1997/05/01.
237. Karjalainen JM, Tammi RH, Tammi MI, Eskelinen MJ, Agren UM, Parkkinen JJ, et al. Reduced level of CD44 and hyaluronan associated with unfavorable prognosis in clinical stage I cutaneous melanoma. *Am J Pathol*. 2000;157(3):957-65. Epub 2000/09/12.
238. Ranuncolo SM, Ladeda V, Gorostidy S, Morandi A, Varela M, Lastiri J, et al. Expression of CD44s and CD44 splice variants in human melanoma. *Oncol Rep*. 2002;9(1):51-6. Epub 2001/12/19.
239. Pacifico MD, Grover R, Richman PI, Daley FM, Buffa F, Wilson GD. CD44v3 levels in primary cutaneous melanoma are predictive of prognosis: assessment by the use of tissue microarray. *Int J Cancer*. 2006;118(6):1460-4. Epub 2005/09/28.

240. Tucci MG, Lucarini G, Brancorsini D, Zizzi A, Pugnali A, Giacchetti A, et al. Involvement of E-cadherin, beta-catenin, Cdc42 and CXCR4 in the progression and prognosis of cutaneous melanoma. *Br J Dermatol*. 2007;157(6):1212-6. Epub 2007/11/01.
241. Maier T, Guell M, Serrano L. Correlation of mRNA and protein in complex biological samples. *FEBS Lett*. 2009;583(24):3966-73. Epub 2009/10/24.
242. Pascale A, Govoni S. The complex world of post-transcriptional mechanisms: is their deregulation a common link for diseases? Focus on ELAV-like RNA-binding proteins. *Cell Mol Life Sci*. 2012;69(4):501-17. Epub 2011/09/13.
243. Varshavsky A. The N-end rule: functions, mysteries, uses. *Proc Natl Acad Sci U S A*. 1996;93(22):12142-9. Epub 1996/10/29.
244. Bloom BR, Bennett B. Mechanism of a reaction in vitro associated with delayed-type hypersensitivity. *Science*. 1966;153(3731):80-2. Epub 1966/07/01.
245. David JR. Delayed hypersensitivity in vitro: its mediation by cell-free substances formed by lymphoid cell-antigen interaction. *Proc Natl Acad Sci U S A*. 1966;56(1):72-7. Epub 1966/07/01.
246. Calandra T, Roger T. Macrophage migration inhibitory factor: a regulator of innate immunity. *Nat Rev Immunol*. 2003;3(10):791-800. Epub 2003/09/23.
247. Calandra T, Bernhagen J, Mitchell RA, Bucala R. The macrophage is an important and previously unrecognized source of macrophage migration inhibitory factor. *J Exp Med*. 1994;179(6):1895-902. Epub 1994/06/01.
248. Mitchell RA, Metz CN, Peng T, Bucala R. Sustained mitogen-activated protein kinase (MAPK) and cytoplasmic phospholipase A2 activation by macrophage migration inhibitory factor (MIF). Regulatory role in cell proliferation and glucocorticoid action. *J Biol Chem*. 1999;274(25):18100-6. Epub 1999/06/11.
249. Li GQ, Xie J, Lei XY, Zhang L. Macrophage migration inhibitory factor regulates proliferation of gastric cancer cells via the PI3K/Akt pathway. *World J Gastroenterol*. 2009;15(44):5541-8. Epub 2009/11/26.
250. Kleemann R, Hausser A, Geiger G, Mischke R, Burger-Kentischer A, Flieger O, et al. Intracellular action of the cytokine MIF to modulate AP-1 activity and the cell cycle through Jab1. *Nature*. 2000;408(6809):211-6. Epub 2000/11/23.
251. Maharshak N, Cohen S, Lantner F, Hart G, Leng L, Bucala R, et al. CD74 is a survival receptor on colon epithelial cells. *World J Gastroenterol*. 2010;16(26):3258-66. Epub 2010/07/09.
252. Calandra T, Bernhagen J, Metz CN, Spiegel LA, Bacher M, Donnelly T, et al. MIF as a glucocorticoid-induced modulator of cytokine production. *Nature*. 1995;377(6544):68-71. Epub 1995/09/07.
253. Bernhagen J, Mitchell RA, Calandra T, Voelter W, Cerami A, Bucala R. Purification, bioactivity, and secondary structure analysis of mouse and human macrophage migration inhibitory factor (MIF). *Biochemistry*. 1994;33(47):14144-55. Epub 1994/11/29.

254. Kudrin A, Scott M, Martin S, Chung CW, Donn R, McMaster A, et al. Human macrophage migration inhibitory factor: a proven immunomodulatory cytokine? *J Biol Chem.* 2006;281(40):29641-51. Epub 2006/08/09.
255. Lubetsky JB, Dios A, Han J, Aljabari B, Ruzsicska B, Mitchell R, et al. The tautomerase active site of macrophage migration inhibitory factor is a potential target for discovery of novel anti-inflammatory agents. *J Biol Chem.* 2002;277(28):24976-82. Epub 2002/05/09.
256. Cregg JM, Tolstorukov I, Kusari A, Sunga J, Madden K, Chappell T. Expression in the yeast *Pichia pastoris*. *Methods Enzymol.* 2009;463:169-89. Epub 2009/11/07.
257. Lin Cereghino GP, Sunga AJ, Lin Cereghino J, Cregg JM. Expression of foreign genes in the yeast *Pichia pastoris*. *Genet Eng (N Y).* 2001;23:157-69. Epub 2001/09/26.
258. Madhunapantula SV, Robertson GP. Therapeutic Implications of Targeting AKT Signaling in Melanoma. *Enzyme Res.* 2011;2011:327923. Epub 2011/04/05.
259. del Vecchio MT, Tripodi SA, Arcuri F, Pergola L, Hako L, Vatti R, et al. Macrophage migration inhibitory factor in prostatic adenocarcinoma: correlation with tumor grading and combination endocrine treatment-related changes. *Prostate.* 2000;45(1):51-7. Epub 2000/08/29.
260. Finger EC, Giaccia AJ. Hypoxia, inflammation, and the tumor microenvironment in metastatic disease. *Cancer Metastasis Rev.* 2010;29(2):285-93. Epub 2010/04/16.
261. Rendon BE, Willer SS, Zundel W, Mitchell RA. Mechanisms of macrophage migration inhibitory factor (MIF)-dependent tumor microenvironmental adaptation. *Exp Mol Pathol.* 2009;86(3):180-5. Epub 2009/02/03.
262. Tomoda K, Kubota Y, Kato J. Degradation of the cyclin-dependent-kinase inhibitor p27Kip1 is instigated by Jab1. *Nature.* 1999;398(6723):160-5. Epub 1999/03/23.
263. Manning BD, Cantley LC. AKT/PKB signaling: navigating downstream. *Cell.* 2007;129(7):1261-74. Epub 2007/07/03.
264. Liang J, Zubovitz J, Petrocelli T, Kotchetkov R, Connor MK, Han K, et al. PKB/Akt phosphorylates p27, impairs nuclear import of p27 and opposes p27-mediated G1 arrest. *Nat Med.* 2002;8(10):1153-60. Epub 2002/09/24.
265. Shin I, Yakes FM, Rojo F, Shin NY, Bakin AV, Baselga J, et al. PKB/Akt mediates cell-cycle progression by phosphorylation of p27(Kip1) at threonine 157 and modulation of its cellular localization. *Nat Med.* 2002;8(10):1145-52. Epub 2002/09/24.
266. Viglietto G, Motti ML, Bruni P, Melillo RM, D'Alessio A, Califano D, et al. Cytoplasmic relocalization and inhibition of the cyclin-dependent kinase inhibitor p27(Kip1) by PKB/Akt-mediated phosphorylation in breast cancer. *Nat Med.* 2002;8(10):1136-44. Epub 2002/09/24.
267. Diehl JA, Cheng M, Roussel MF, Sherr CJ. Glycogen synthase kinase-3beta regulates cyclin D1 proteolysis and subcellular localization. *Genes Dev.* 1998;12(22):3499-511. Epub 1998/12/01.
268. Welcker M, Singer J, Loeb KR, Grim J, Bloecher A, Gurien-West M, et al. Multisite phosphorylation by Cdk2 and GSK3 controls cyclin E degradation. *Mol Cell.* 2003;12(2):381-92. Epub 2003/10/11.

269. Evans CE, Branco-Price C, Johnson RS. HIF-mediated endothelial response during cancer progression. *Int J Hematol*. 2012;95(5):471-7. Epub 2012/05/09.
270. Mucaj V, Shay JE, Simon MC. Effects of hypoxia and HIFs on cancer metabolism. *Int J Hematol*. 2012;95(5):464-70. Epub 2012/04/28.
271. Debnath J, Muthuswamy SK, Brugge JS. Morphogenesis and oncogenesis of MCF-10A mammary epithelial acini grown in three-dimensional basement membrane cultures. *Methods*. 2003;30(3):256-68. Epub 2003/06/12.
272. Zhou J, Haggerty JG, Milstone LM. Growth and differentiation regulate CD44 expression on human keratinocytes. *In Vitro Cell Dev Biol Anim*. 1999;35(4):228-35. Epub 1999/09/09.
273. Jalkanen S, Bargatze RF, de los Toyos J, Butcher EC. Lymphocyte recognition of high endothelium: antibodies to distinct epitopes of an 85-95-kD glycoprotein antigen differentially inhibit lymphocyte binding to lymph node, mucosal, or synovial endothelial cells. *J Cell Biol*. 1987;105(2):983-90. Epub 1987/08/01.
274. Reeder JA, Gotley DC, Walsh MD, Fawcett J, Antalis TM. Expression of antisense CD44 variant 6 inhibits colorectal tumor metastasis and tumor growth in a wound environment. *Cancer Res*. 1998;58(16):3719-26. Epub 1998/08/29.
275. Macdonald DC, Leir SH, Brooks C, Sanders E, Lackie P, Rosenberg W. CD44 isoform expression on colonic epithelium mediates lamina propria lymphocyte adhesion and is controlled by Th1 and Th2 cytokines. *Eur J Gastroenterol Hepatol*. 2003;15(10):1101-10. Epub 2003/09/23.
276. Gasbarri A, Del Prete F, Girnita L, Martegani MP, Natali PG, Bartolazzi A. CD44s adhesive function spontaneous and PMA-inducible CD44 cleavage are regulated at post-translational level in cells of melanocytic lineage. *Melanoma Res*. 2003;13(4):325-37. Epub 2003/07/29.
277. Cox B, Emili A. Tissue subcellular fractionation and protein extraction for use in mass-spectrometry-based proteomics. *Nat Protoc*. 2006;1(4):1872-8. Epub 2007/05/10.
278. Lambowitz AM. Preparation and analysis of mitochondrial ribosomes. *Methods Enzymol*. 1979;59:421-33. Epub 1979/01/01.
279. Wells A, Marti U. Signalling shortcuts: cell-surface receptors in the nucleus? *Nat Rev Mol Cell Biol*. 2002;3(9):697-702. Epub 2002/09/05.
280. Bryant DM, Stow JL. Nuclear translocation of cell-surface receptors: lessons from fibroblast growth factor. *Traffic*. 2005;6(10):947-54. Epub 2005/09/06.
281. Wang YN, Yamaguchi H, Hsu JM, Hung MC. Nuclear trafficking of the epidermal growth factor receptor family membrane proteins. *Oncogene*. 2010;29(28):3997-4006. Epub 2010/05/18.
282. Sehat B, Tofigh A, Lin Y, Trocme E, Liljedahl U, Lagergren J, et al. SUMOylation mediates the nuclear translocation and signaling of the IGF-1 receptor. *Sci Signal*. 2010;3(108):ra10. Epub 2010/02/11.

283. Rosner M, Hengstschlager M. Detection of cytoplasmic and nuclear functions of mTOR by fractionation. *Methods Mol Biol.* 2012;821:105-24. Epub 2011/11/30.
284. Sala E, Mologni L, Truffa S, Gaetano C, Bollag GE, Gambacorti-Passerini C. BRAF silencing by short hairpin RNA or chemical blockade by PLX4032 leads to different responses in melanoma and thyroid carcinoma cells. *Mol Cancer Res.* 2008;6(5):751-9. Epub 2008/05/07.
285. Wan PT, Garnett MJ, Roe SM, Lee S, Niculescu-Duvaz D, Good VM, et al. Mechanism of activation of the RAF-ERK signaling pathway by oncogenic mutations of B-RAF. *Cell.* 2004;116(6):855-67. Epub 2004/03/24.
286. Bollag G, Tsai J, Zhang J, Zhang C, Ibrahim P, Nolop K, et al. Vemurafenib: the first drug approved for BRAF-mutant cancer. *Nat Rev Drug Discov.* 2012. Epub 2012/10/13.
287. Jordan EJ, Kelly CM. Vemurafenib for the treatment of melanoma. *Expert Opin Pharmacother.* 2012. Epub 2012/10/26.
288. Han I, Lee MR, Nam KW, Oh JH, Moon KC, Kim HS. Expression of macrophage migration inhibitory factor relates to survival in high-grade osteosarcoma. *Clin Orthop Relat Res.* 2008;466(9):2107-13. Epub 2008/06/20.
289. Kamimura A, Kamachi M, Nishihira J, Ogura S, Isobe H, Dosaka-Akita H, et al. Intracellular distribution of macrophage migration inhibitory factor predicts the prognosis of patients with adenocarcinoma of the lung. *Cancer.* 2000;89(2):334-41. Epub 2000/08/05.
290. Hira E, Ono T, Dhar DK, El-Assal ON, Hishikawa Y, Yamanoi A, et al. Overexpression of macrophage migration inhibitory factor induces angiogenesis and deteriorates prognosis after radical resection for hepatocellular carcinoma. *Cancer.* 2005;103(3):588-98. Epub 2004/12/22.
291. Xia HH, Yang Y, Chu KM, Gu Q, Zhang YY, He H, et al. Serum macrophage migration-inhibitory factor as a diagnostic and prognostic biomarker for gastric cancer. *Cancer.* 2009;115(23):5441-9. Epub 2009/08/18.
292. Flaherty KT, Infante JR, Daud A, Gonzalez R, Kefford RF, Sosman J, et al. Combined BRAF and MEK inhibition in melanoma with BRAF V600 mutations. *N Engl J Med.* 2012;367(18):1694-703. Epub 2012/10/02.
293. Gajria D, Chandarlapaty S. HER2-amplified breast cancer: mechanisms of trastuzumab resistance and novel targeted therapies. *Expert Rev Anticancer Ther.* 2011;11(2):263-75. Epub 2011/02/24.
294. Luu T, Chung C, Somlo G. Combining emerging agents in advanced breast cancer. *Oncologist.* 2011;16(6):760-71. Epub 2011/05/06.
295. Rodon J, Perez J, Kurzrock R. Combining targeted therapies: practical issues to consider at the bench and bedside. *Oncologist.* 2010;15(1):37-50. Epub 2010/01/19.
296. Al-Abed Y, VanPatten S. MIF as a disease target: ISO-1 as a proof-of-concept therapeutic. *Future Med Chem.* 2011;3(1):45-63. Epub 2011/03/25.
297. Ouertatani-Sakouhi H, El-Turk F, Fauvet B, Cho MK, Pinar Karpinar D, Le Roy D, et al. Identification and characterization of novel classes of macrophage migration inhibitory factor

(MIF) inhibitors with distinct mechanisms of action. *J Biol Chem*. 2010;285(34):26581-98. Epub 2010/06/03.

298. Bai F, Asojo OA, Cirillo P, Ciustea M, Ledizet M, Aristoff PA, et al. A novel allosteric inhibitor of macrophage migration inhibitory factor (MIF). *J Biol Chem*. 2012;287(36):30653-63. Epub 2012/07/12.

299. Fang B, Jiang L, Zhang M, Ren FZ. A novel cell-penetrating peptide TAT-A1 delivers siRNA into tumor cells selectively. *Biochimie*. 2012. Epub 2012/09/27.

300. Karagiannis ED, Alabi CA, Anderson DG. Rationally designed tumor-penetrating nanocomplexes. *ACS Nano*. 2012;6(10):8484-7. Epub 2012/10/24.

301. Khatri N, Misra A. Development of siRNA lipoplexes for intracellular delivery in lung cancer cells. *J Pharm Bioallied Sci*. 2012;4(Suppl 1):S1-3. Epub 2012/10/16.

302. Wang X, Liu P, Liu H, Yang W, Liu Z, Zhuo Z, et al. Delivery of interferons and siRNA targeting STAT3 using lentiviral vectors suppresses the growth of murine melanoma. *Cancer Gene Ther*. 2012. Epub 2012/09/29.

303. Yang Y, Li J, Liu F, Huang L. Systemic delivery of siRNA via LCP nanoparticle efficiently inhibits lung metastasis. *Mol Ther*. 2012;20(3):609-15. Epub 2011/12/22.

304. Cregg JM, Vedvick TS, Raschke WC. Recent advances in the expression of foreign genes in *Pichia pastoris*. *Biotechnology (N Y)*. 1993;11(8):905-10. Epub 1993/08/01.

305. Sreekrishna K, Potenz RH, Cruze JA, McCombie WR, Parker KA, Nelles L, et al. High level expression of heterologous proteins in methylotrophic yeast *Pichia pastoris*. *J Basic Microbiol*. 1988;28(4):265-78. Epub 1988/01/01.

306. Wegner GH. Emerging applications of the methylotrophic yeasts. *FEMS Microbiol Rev*. 1990;7(3-4):279-83. Epub 1990/12/01.

307. Cregg JM. Introduction: distinctions between *Pichia pastoris* and other expression systems. *Methods Mol Biol*. 2007;389:1-10. Epub 2007/10/24.

308. Ellis SB, Brust PF, Koutz PJ, Waters AF, Harpold MM, Gingeras TR. Isolation of alcohol oxidase and two other methanol regulatable genes from the yeast *Pichia pastoris*. *Mol Cell Biol*. 1985;5(5):1111-21. Epub 1985/05/01.

309. Koutz P, Davis GR, Stillman C, Barringer K, Cregg J, Thill G. Structural comparison of the *Pichia pastoris* alcohol oxidase genes. *Yeast*. 1989;5(3):167-77. Epub 1989/05/01.

310. Tschopp JF, Brust PF, Cregg JM, Stillman CA, Gingeras TR. Expression of the lacZ gene from two methanol-regulated promoters in *Pichia pastoris*. *Nucleic Acids Res*. 1987;15(9):3859-76. Epub 1987/05/11.

311. Cregg JM, Madden KR, Barringer KJ, Thill GP, Stillman CA. Functional characterization of the two alcohol oxidase genes from the yeast *Pichia pastoris*. *Mol Cell Biol*. 1989;9(3):1316-23. Epub 1989/03/01.

312. Cereghino JL, Cregg JM. Heterologous protein expression in the methylotrophic yeast *Pichia pastoris*. *FEMS Microbiol Rev*. 2000;24(1):45-66. Epub 2000/01/21.

313. Macauley-Patrick S, Fazenda ML, McNeil B, Harvey LM. Heterologous protein production using the *Pichia pastoris* expression system. *Yeast*. 2005;22(4):249-70. Epub 2005/02/11.
314. Mazumdar M, Glassman JR. Categorizing a prognostic variable: review of methods, code for easy implementation and applications to decision-making about cancer treatments. *Statistics in medicine*. 2000;19(1):113-32. Epub 2000/01/07.
315. Buettner P, Garbe C, Guggenmoos-Holzmann I. Problems in defining cutoff points of continuous prognostic factors: example of tumor thickness in primary cutaneous melanoma. *Journal of clinical epidemiology*. 1997;50(11):1201-10. Epub 1997/12/11.
316. Hill C. [Prognostic value of a continuous variable and an optimal cutoff point]. *Bulletin du cancer*. 1993;80(8):649-52. Epub 1993/08/01. Valeur pronostique d'une variable continue et point de cesure optimal.
317. Mazumdar M, Smith A, Bacik J. Methods for categorizing a prognostic variable in a multivariable setting. *Statistics in medicine*. 2003;22(4):559-71. Epub 2003/02/19.
318. Shipman KL, Robinson PJ, King BR, Smith R, Nicholson RC. Identification of a family of DNA-binding proteins with homology to RNA splicing factors. *Biochemistry and cell biology = Biochimie et biologie cellulaire*. 2006;84(1):9-19. Epub 2006/02/08.
319. Fu XD, Maniatis T. Factor required for mammalian spliceosome assembly is localized to discrete regions in the nucleus. *Nature*. 1990;343(6257):437-41. Epub 1990/02/01.